

## INFORMATION TO USERS

This manuscript has been reproduced from the microfilm master. UMI films the text directly from the original or copy submitted. Thus, some thesis and dissertation copies are in typewriter face, while others may be from any type of computer printer.

**The quality of this reproduction is dependent upon the quality of the copy submitted.** Broken or indistinct print, colored or poor quality illustrations and photographs, print bleedthrough, substandard margins, and improper alignment can adversely affect reproduction.

In the unlikely event that the author did not send UMI a complete manuscript and there are missing pages, these will be noted. Also, if unauthorized copyright material had to be removed, a note will indicate the deletion.

Oversize materials (e.g., maps, drawings, charts) are reproduced by sectioning the original, beginning at the upper left-hand corner and continuing from left to right in equal sections with small overlaps.

ProQuest Information and Learning  
300 North Zeeb Road, Ann Arbor, MI 48106-1346 USA  
800-521-0600

UMI<sup>®</sup>



University of Alberta

**Genetic Analysis During Mouse Mammary Gland Post-Natal  
Development**

By

Brian David Maciejko



A thesis submitted to the Faculty of Graduate Studies and Research in partial fulfillment  
of the requirements for the degree of Master of Science

in

Molecular Biology and Genetics

Department of Biological Sciences

Edmonton, Alberta

Fall 2005



Library and  
Archives Canada

Bibliothèque et  
Archives Canada

0-494-09231-9

Published Heritage  
Branch

Direction du  
Patrimoine de l'édition

395 Wellington Street  
Ottawa ON K1A 0N4  
Canada

395, rue Wellington  
Ottawa ON K1A 0N4  
Canada

*Your file* *Votre référence*

*ISBN:*

*Our file* *Notre référence*

*ISBN:*

**NOTICE:**

The author has granted a non-exclusive license allowing Library and Archives Canada to reproduce, publish, archive, preserve, conserve, communicate to the public by telecommunication or on the Internet, loan, distribute and sell theses worldwide, for commercial or non-commercial purposes, in microform, paper, electronic and/or any other formats.

The author retains copyright ownership and moral rights in this thesis. Neither the thesis nor substantial extracts from it may be printed or otherwise reproduced without the author's permission.

**AVIS:**

L'auteur a accordé une licence non exclusive permettant à la Bibliothèque et Archives Canada de reproduire, publier, archiver, sauvegarder, conserver, transmettre au public par télécommunication ou par l'Internet, prêter, distribuer et vendre des thèses partout dans le monde, à des fins commerciales ou autres, sur support microforme, papier, électronique et/ou autres formats.

L'auteur conserve la propriété du droit d'auteur et des droits moraux qui protègent cette thèse. Ni la thèse ni des extraits substantiels de celle-ci ne doivent être imprimés ou autrement reproduits sans son autorisation.

---

In compliance with the Canadian Privacy Act some supporting forms may have been removed from this thesis.

Conformément à la loi canadienne sur la protection de la vie privée, quelques formulaires secondaires ont été enlevés de cette thèse.

While these forms may be included in the document page count, their removal does not represent any loss of content from the thesis.

Bien que ces formulaires aient inclus dans la pagination, il n'y aura aucun contenu manquant.

  
**Canada**

## Abstract

The mouse mammary gland (MG) is capable of undergoing numerous cycles of post-natal differentiation involving the switch from massive cell proliferation to controlled cell death. This switch encompasses the switch from lactation to involution. By screening the first day after weaning of the pups, different subsets of genes were found to be differentially regulated over the course of MG post natal development. 2 groups of genes (iron metabolism and the calycin superfamily) were subjected to northern analysis due to functional commonalities. A second method of examining genetic expression at the switch was executed by observing the northern, western and *in situ* localization of a transcriptional co-activator, *cited2*, which was previously identified in another stressed degeneration model (light induced retinal degeneration). Together *cited2*, the calycin superfamily and genes related to iron metabolism were found to be associated through a potential transcriptional regulatory pathway: PPAR mediated transcription.

## TABLE OF CONTENTS

Page Number

<b>CHAPTER 1 – INTRODUCTION</b>		
		1
1.1	INTRODUCTION	1
1.2	THE MODEL SYSTEM	1
1.3	POST NATAL DEVELOPMENT OF THE MAMMARY GLAND	1
1.4	MAMMARY GLAND APOPTOSIS	7
1.5	GENE EXPRESSION	10
1.6	THESIS PROPOSAL	11
1.7	SUMMARY	11
<b>CHAPTER 2 – MATERIALS AND METHODS</b>		
		14
2.1	MG TISSUES	14
2.2	RNA EXTRACTION	14
2.2.1.	Total RNA Extraction	14
2.2.2	Isolation of the mRNA	14
2.2.3	Prepping the Streptavidin Paramagnetic Particles	15
2.2.4	Isolating the mRNA-SA-PMPs	15
2.2.5	Elution of the mRNA	16
2.3	cDNA LIBRARY SYNTHESIS AND MAKING OF MACROARRAY	17
2.3.1	cDNA - First Strand Synthesis	17
2.3.2	cDNA Second Strand Synthesis	17
2.3.3	Blunting the cDNA	17
2.3.4	Ligating the EcoRI Adapters	17
2.3.5	Phosphorylating the EcoRI Ends	18
2.3.6	Digestion with Xho	18
2.3.7	Size Fractionation	18
2.3.8	Processing the cDNA Fractions	18
2.3.9	Ligating the cDNA into the Uni-ZAP XR Vector	19
2.3.10	Preparation of the Host Bacteria and Titrating the Library	19
2.3.11	Isolation of the Plaques	20
2.3.12	Phagemid Extraction	20

2.4	I1 MOUSE MG MACROARRAY ANALYSIS	21
2.4.1	Creation of the Macroarrays	21
2.4.2	Amplification of cDNA for Labelling	21
2.4.3	Hybridization of Radioactively Labelled cDNA to Macroarrays	22
2.5	SEQUENCING, SEQUENCE ANALYSIS AND BIOINFORMATICS	22
2.5.1	Sequencing	22
2.6	ANALYSIS OF THE IDENTIFIED GENES	23
2.6.1	Examining RNA Expression	23
2.6.1.1	Northern Analysis	23
2.6.1.1a	Sample Preparation	23
2.6.1.1b	Gel Electrophoresis of Total RNA	23
2.6.1.1c	Northern Transfer	24
2.6.1.1d	Hybridization of Radiolabelled PCR Products to Northern	24
2.6.1.1e	Detection of Expression and Normalization of the Exposures	24
2.6.1.2	In situ Hybridization	24
2.6.1.2a	Fluorescent In situ Hybridization	24
2.6.1.2a1	Preparation of Sections Samples	24
2.6.1.2a2	Hybridization of DIG Labelled PCR Product	25
2.6.1.2a3	Posthybridization	25
2.6.1.2a4	Detection of Fluorescence and mRNA Localization	25
2.6.1.2b	Radioactive in situ Hybridization	26
2.6.1.2b1	Preparation of Sections	26
2.6.1.2b2	Hybridization of Sections	26
2.6.1.2b3	Posthybridization	27
2.6.1.2b4	Detection of Radioactivity and Probe Localization	27
2.6.2	Examining Protein Expression	28
2.6.2.1	Western Transfer Analysis.	28
2.6.2.1a	Protein Isolation	28
2.6.2.2b	Sample Preparation	28
2.6.2.2c	SDS PAGE of Protein Samples	28
2.6.2.2d	Western Transfer	28
2.6.2.2e	Antibody Production	29
2.6.2.2f	Antibody Detection	29
2.6.2.3	Antibody Competition Assay	30

2.7	PROBE PREPARATION	30
2.7.1	Random Primer Labelling of Probes for Northern and Macroarray Analysis	30
2.7.2	DIG Labelling of PCR product	31
2.7.3	Radioactive <i>in situ</i> Hybridization Riboprobe	32
	<b>CHAPTER 3 – I1 cDNA LIBRARY ANALYSIS</b>	<b>34</b>
3.1	INTRODUCTION	34
3.2	RESULTS	36
3.2.1	Quality Control of Total RNA	36
3.2.2	Differential Screening of the I1 Involution Library	36
3.2.3	Validity of Genes Isolated from the Mammary Gland	45
3.2.4.	Expression	45
3.3	DISCUSSION	55
3.3.1	Effectiveness of the 5 Way Differential Screen	55
3.3.2	Gene expression	57
3.3.3	Gene Profiling	58
3.3.4	Conclusions	59
	<b>CHAPTER 4 – THE CALYGIN SUPERFAMILY AND IRON METABOLISM GENES</b>	<b>61</b>
4.1	INTRODUCTION	61
4.1.1	The Iron Binding Proteins	62
4.1.2	The Calycin Superfamily	64
4.2	RESULTS	68
4.2.1	Northern Analysis	68
4.2.2	Northern Analysis of Clones Relating to Iron Metabolism	68
4.2.2.1	Transferrin	68
4.2.2.2	Lactotransferrin	68
4.2.2.3	Ferritin Light Chain	71
4.2.2.4	Ferritin Heavy Chain	71
4.2.3	Northern Analysis of the Calycin Superfamily	74
4.2.3.1	Fatty Acid Binding Protein 4	74
4.2.3.2	Fatty Acid Binding Protein 3	74
4.2.3.3	Orosomuroid 1	77
4.2.3.4	Lipocalin 2	77
4.2.4	Multi Tissue Bioinformatic Analysis	80

4.2.5.	Association with PPAR Mediated Transcription	80
4.2.5.1	Promoter Analysis for Evidence of a Potential PPAR Interaction	83
4.2.5.2	Iron Binding Proteins and PPAR Mediated Transcription	85
4.2.5.3	The Calycin Superfamily and PPAR Mediated Transcription	86
4.3	DISCUSSION	87
	<b>CHAPTER 5 – CHARACTERIZATION OF <i>CITED2</i> EXPRESSION IN MAMMARY GLAND INVOLUTION</b>	93
5.1	INTRODUCTION	93
5.2	RESULTS	99
5.2.1	mRNA Analysis	99
5.2.1.1	<i>Cited2</i> Northern Analysis	99
5.2.1.2	<i>Vegfa</i> Northern Analysis	99
5.2.1.3	Fluorescent <i>in situ</i> Analysis of <i>cited2</i>	102
5.2.1.4	Radioactive <i>in situ</i> Hybridization	102
5.2.2	Protein Analysis of <i>cited2</i>	107
5.2.2.1	Competition Assay	107
5.2.2.2	Western Analysis	107
5.2.3	<i>Cited2</i> and a Possible Role in PPAR Mediated Transcription	110
5.2.4	Isolation of PPRE in Upstream Sequence of Factors Involved with <i>cited2</i>	110
5.3	DISCUSSION	112
	<b>CHAPTER 6 – CONCLUSIONS</b>	117
	<b>CITATIONS</b>	122
	<b>APPENDICES</b>	136
	Sequences and Blast identities of clones	136
	Recipes	161

## LIST OF TABLES

<b>Table Number</b>		<b>Page Number</b>
3.1	Difference in Densitometry Values Between L10 and I1 for Known Clones	52
4.1	Table 4.1 Genes Relating to Iron Metabolism or the Calycin Superfamily	61
4.2	Multi-tissue Bioinformatic Characterization of Clones Related to Iron Metabolism and the Calycin Superfamily	81
6.1	Contributions to Published Manuscripts or Abstracts	118

## LIST OF FIGURES

Figure Number		Page Number
1.1:	Alveolar Structure	3
1.2:	Development of the MG Through Pregnancy	5
1.3:	Cellular Interactions in the Alveolus	9
1.4:	Experimental Flow Chart	13
3.1:	cDNA Library Synthesis and Validation	38
3.2:	Distribution of Clones Isolated From the MacroArray Screen	40
3.3:	Macroarray Screen	43
3.4:	<i>WAP</i> Northern Analysis	47
3.5:	Known Clone Northern Analysis	48-49
3.6:	Unknown Northern Analysis	50-51
3.7:	Observing Common Profiles Among the Clones Placed on Northern	54
4.1:	Fenton Reaction	63
4.2:	Beta Barrel Protein Structure	65
4.3:	<i>trf</i> and <i>lrf</i> Northern Analysis	70
4.4:	<i>fth</i> and <i>ftl</i> Northern Analysis	73
4.5:	<i>fabp3</i> and <i>fabp4</i> Northern Analysis	76
4.6:	<i>orm1</i> and <i>lcn2</i> Northern Analysis	79
4.7:	Identification of Putative PPRE in the Promoter Region of Genes Related to Iron Metabolism and the Calycin Superfamily	84

4.8:	Expression Trends for the Calycin Superfamily and Genes Related to Iron Metabolism	89
5.1:	<i>cited2</i> Gene and Protein Structure	94
5.2:	<i>cited2</i> Sequence Alignments:	97
5.3:	<i>cited2</i> Northern Expression in the Mammary Gland	101
5.4:	<i>vegfa</i> Northern Expression in the Mammary Gland	104
5.5:	<i>In situ</i> Analysis	106
5.6:	<i>cited2</i> Antibody Competition Assay	108
5.7:	Western Analysis of <i>cited2/Mrg1</i> .	109
5.8:	Identification of PPRE in the Promoter Region of Genes Involved With <i>cited2</i>	111
5.9:	<i>vegfa</i> and <i>cited2</i> mRNA Comparison	114
6.1:	A Hypothetical Model	121

## **ABBREVIATIONS**

Ab	Antibody	MGI	Mouse Genome Informatics
BLAST	Basic Local Alignment Search Tool	min	minute
BM	Basement membrane	mRNA	Messenger RNA
PCD	programmed cell death	MRF	minus restriction
bp	Nucleotide base pair	NCBI	National Centre for Biotechnology Information
cDNA	Complementary DNA	NIH	National Institute of Health
CDS	coding sequence	nr	non redundant
Ci	curries	OD600	absorbance at wavelength 600nm
cpm	Counts per minute	P	pregnant
DAPI	4',6-diamidino-2-phenylindole	PBS	Phosphate buffered saline
dATP	2-deoxyadenosine 5-triphosphate	PCR	Polymerase chain reaction
dCTP	2-deoxycytosine 5-triphosphate	RNA	Ribonucleic acid
dH <sub>2</sub> O	distilled water	ROS	Reactive oxygen species
ddH <sub>2</sub> O	Distilled deionized water	rpm	Revolutions per minute
DEPC	Diethylpyrocarbonate	rRNA	Ribosomal RNA
dGTP	2-deoxyguanosine 5-triphosphate	SSC	sodium chloride sodium citrate
DIG	Digoxigenin	SDS-PAGE	Denaturing polyacrylamide gel electrophoresis
DMSO	dimethyl sulfoxide	sec	Second
DNA	Deoxyribonucleic acid	TEA	tetraethylammonium
dNTP	deoxynucleotide triphosphate	TEB	Terminal end bud
dpi	dots per inch (resolution)	V	Virgin
DTT	1,4-Dithio-DL-threitol	v/v	Volume per volume
dTTP	2-deoxythymidine 5-triphosphate		
EBI	European Bioinformatics Institute		
ECL	Electrochemoluminescence		
ECM	Extracellular matrix		
EMBL	European Molecular Biology Laboratory		
EtBr	ethidium bromide		
EtOH	ethanol		
g	gram		
I	involution		
L	lactation		
l	litre		
M	molar		
mA	milli ampere		
m/v	Mass per volume		
MEC	Mammary epithelial cell		
MG	Mammary gland		

## **CHAPTER 1 - INTRODUCTION**

### **1.1 INTRODUCTION**

A major research interest in our lab is to understand the role of cellular stress over the course of tissue involution. The progression of involution is reflective of a distortion in the balance of active cell death (apoptosis) and cell survival processes, which favours death. A consistent goal in the lab is to identify genes that might help define an “involution” phenotype. Although many groups have studied the roles of very specific genes involved in the involution process, very few groups have taken a more global approach to define the molecular phenotype. For my studies I focused on identifying changes in gene expression over the course of mouse mammary gland (MG) involution. My goals were to characterize genes that show altered expression over the course of mouse MG involution.

### **1.2 THE MODEL SYSTEM**

The fully developed MG consists of highly organized networks of ducts that make and secrete milk. At a structural level the MG is quite complex despite the fact it is composed only of three major cell types, the luminal epithelial cells which form the lining of the alveolus, the myoepithelial cells which lie between the epithelial cells and the basement membrane and stromal cells which provide structure to the MG (Figure 1.1). The stromal cells are most prominent in the virgin and virgin like states of the MG. The myoepithelial cells act as a muscle layer to contract the alveolus and force milk down the duct work and out the nipple. The third cell and most metabolically active is the epithelial cell, which is most developed in the lactating animal and is responsible for producing milk (Mather and Keenan, 1998). Other cells such as macrophages, blood cells, and adipocytes are also present in the MG.

### **1.3 POST NATAL DEVELOPMENT OF THE MAMMARY GLAND**

The MG of a mature female rat undergoes a full developmental cycle of pregnancy, lactation, involution, and reversion to a virgin-like state each time the Dam becomes pregnant (reviewed in Figure 1.2). The fully developed MG evolves from a virgin or virgin-like state consisting mainly of stromal cells with adipocytes present throughout the

**Figure 1.1: Alveolar Structure:** The MG alveolus is comprised of two major cell types, the epithelial and myoepithelial cells. The Epithelial cells create the lobular structure and line the lumen of the alveolus. The myoepithelial cells lie in between the epithelial cells and the basement membrane. Upon stimulation by oxytocin the myoepithelial cells contract and force the milk out of the lumen into the duct. The arrows indicate the direction of milk flow. The top image was taken from <http://classes.aces.uiuc.edu/AnSci308/mamorganize.html>.

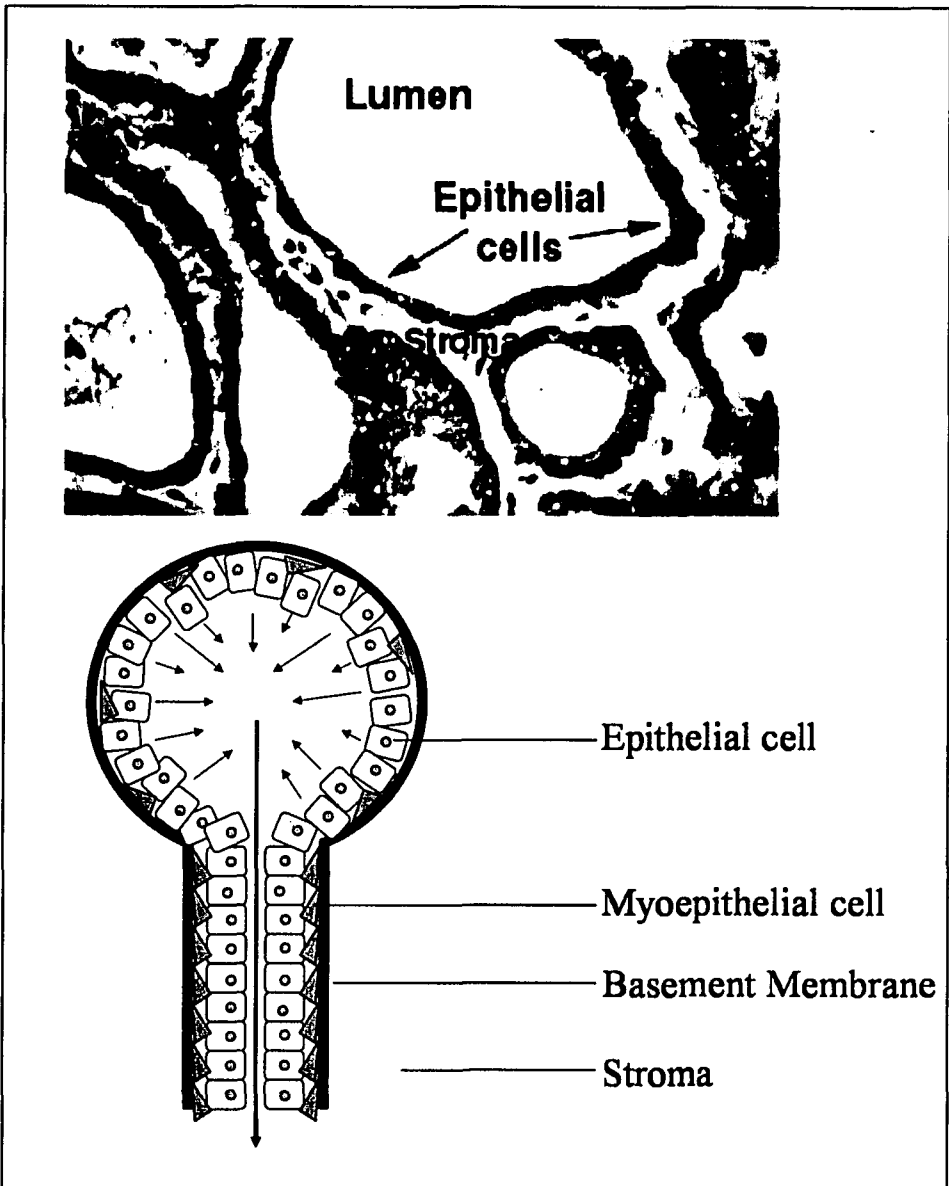
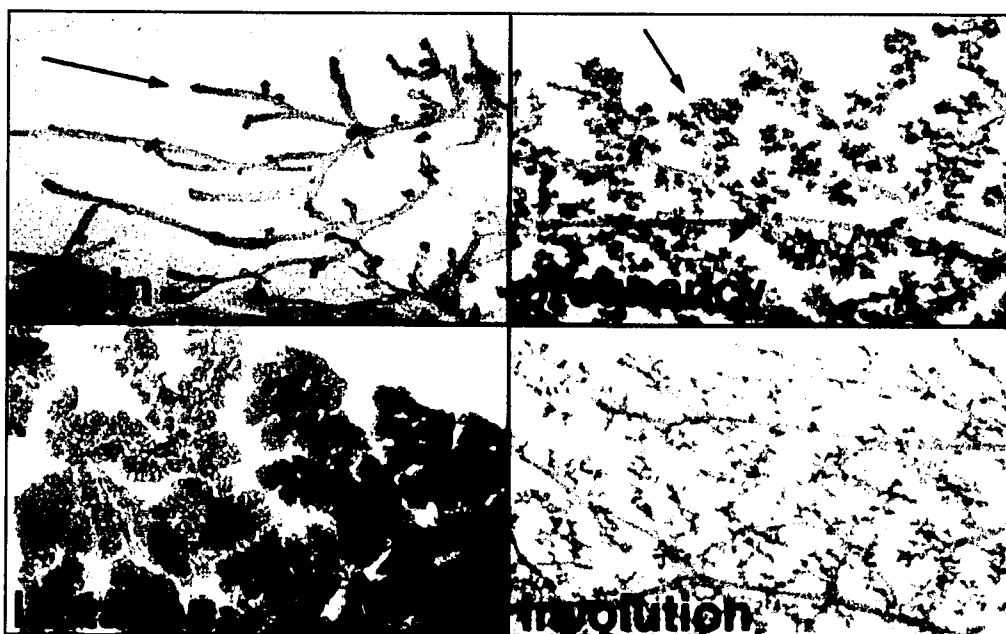


**Figure 1.2: Development of the MG Through Pregnancy:** The MG follows a cyclical development post-natally once the female mouse has been impregnated. After fertilization the MG begins to differentiate into a complex network of ducts and alveoli. During Lactation the MG becomes very active in milk production and the alveoli swell. Once the pups have been removed from the Dam, the MG begins to regress as is seen in the involution panel above and begins to mirror the virgin like state. At the end of involution some alveoli remain. Arrows point to terminal end buds (TEB) that differentiate into alveoli. Figure obtained from Dierisseau and Hennighausen. <http://mammary.nih.gov/atlas/wholemounds/normal/index.html>



fat pad of the MG. The virgin state is produced by a simple duct work that invades the fat pad comprising the majority of the MG. Upon pregnancy the MG responds to a number of hormonal signals such as growth hormone and estrogen, factors responsible for regulating the development of the ductal system (Hovey, Trott and Vonderhaar, 2002). Numerous branches extend from the original duct work and the terminal end buds (TEB), the very tips of each of the ducts, multiply in number and eventually develop into the alveolus when the system receives prolactin and progesterone signals (Briskin, 2002). The MG during pregnancy is therefore characterized by a large proliferation of alveolar structures. The lobular structure of the alveolus is only able to take form if a scaffold is present to grow into; in the MG the stromal cells provide this. The interaction of the stromal cells, myoepithelial and mammary epithelial cells (MEC) allow for the production of the basement membrane (Jin *et al.*, 2000). This basement membrane is responsible for the structure that mediates physical stress signaling to the epithelial cells and also provides tensile strength of the MG that prevents rupturing of the alveolus. Once these alveolar structures have been established and the system receives signals from hormones such as progesterone, placental lactogen and corticosteroid, the alveoli begin production of milk protein such as the caseins, whey acidic protein and alpha-lactalbumin. These milk proteins are secreted into the lumen of the alveolus via micelles and expelled down the ductwork to the nipple upon stimulation of oxytocin (Lefcourt and Akers, 1983).

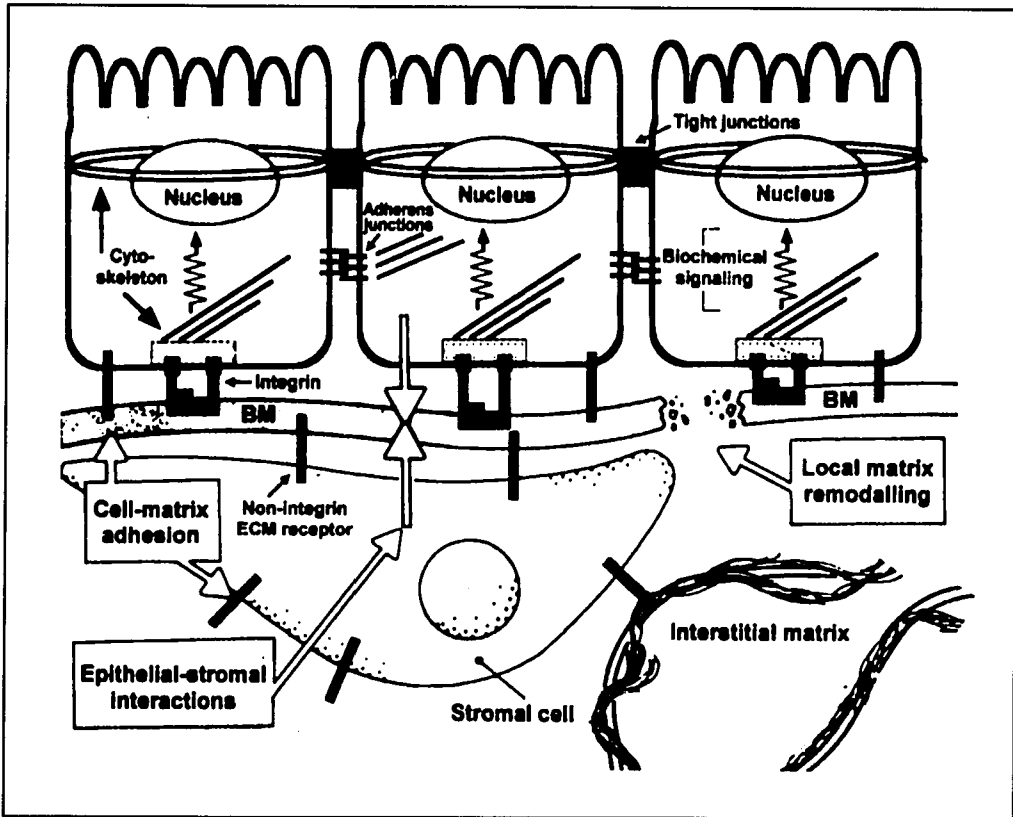
The presence of prolactin and the physical suckling of the pups maintain a state of lactation, once these factors are removed a physical buildup of milk in the MG lumen leads to engorgement, and we get the progression into involution. Thus in the lab setting we can induce involution in Dams by removing the pups (weaning). The physical stress of the strained alveolus on the basement membrane upon weaning signals for apoptosis to occur in the epithelial cells and causes the induction of the inflammatory response or the acute phase response (the first set of genes transcribed and translated after insult or injury) (Stein *et al.*, 2004). The epithelial cells are connected to the basement membrane through various mechanisms, including integrin-extracellular matrix interactions, the distortion of these interactions due to the physical stress on the alveolus from milk build-

up can lead to an alteration in genetic transcription (Jones and Walker, 1999). It is believed that the disruption of this connection due to mechanical stress induced by an engorged alveolus is a primary event in the initiation of MG involution though the exact mechanism of involution initiation is not known. A physical remodeling of the alveolar structures and an eventual proliferation of stromal tissue then follow this. Restructuring leads to a virgin-like state where the organ has now reset itself and is now ready for another cycle. Postnatal MG development is therefore a highly complex process. For the purposes of this thesis the stages of MG development are summarized in figure 1.2. The important stage with respect to my studies has involved the transition from a lactating gland to an involuting gland.

#### **1.4 MAMMARY GLAND APOPTOSIS**

The death of epithelial cells over the course of MG involution is mediated by an apoptotic mechanism (Kumar *et al.*, 2000). Although the complete mechanism is not yet known, several studies demonstrate that MG epithelial cell death involve DNA fragmentation, apoptotic body formation and macrophage invasion and can be induced by tumour necrosis factor (TNF) and transforming growth factor beta 3 (TGF $\beta$ 3) (Thompson, 1955; Quarrie Addey and Wilde, 1995). Overall, MG involution can be broken down into two stages; reversible or proteinase independent involution and irreversible or proteinase dependent involution (Lund *et al.*, 1996). The proteinase independent involution in mice is defined by the first 2 days after weaning of the pups, or day 2 involution (I2), and is characterized by a small number of isolated epithelial cells undergoing apoptosis due to the engorgement of the alveolus and removal of oxytocin stimulation (Liu *et al.*, 1995). The presence of prolactin and the physical suckling of the pups maintain a lactation phase, but once these factors are removed a physical buildup of milk in the MG lumen leads to engorgement. The physical stress on the alveolus from milk build-up causes a distortion of the interactions between the epithelial cells and the basement membrane that leads to an alteration in genetic transcription (figure 1.3) (Jones and Walker, 1999). It is believed that the disruption of this connection due to mechanical stress induced by an engorged alveolus is a primary event in the initiation of MG involution, though the exact mechanism of the process is not well understood. Even

**Figure 1.3: Cellular Interactions in the Alveolus:** The epithelial cells are connected to the basement membrane which provides a rigid structure to the alveolus and prevents rupturing of the alveolus and maintains the milk in the lumen of the alveolus. The epithelial cells interact with the basement membrane through integrins and other various receptors. When the basement membrane becomes distorted or damaged, the integrins relay signals to the epithelial cells. These signals can activate a response in the epithelial cells to initiate programmed cell death. Through connections between epithelial cells, signals are also transmitted to neighboring cells in a response to stress in the environment. This image was taken from Hagions *et al.* (1998) *Philos Trans R Soc Lond B Biol Sci* 353:857-870



though apoptosis occurs at this point, the entire process can be reverted to the metabolically active lactogenic state by reintroducing prolactin and oxytocin or by reintroducing a suckling stimulus to the Dam (Li *et al.*, 1997).

During the second stage of involution (days 2-10 after weaning), proteolytic enzymes such as matrix metalloproteinases (MMP), for example stromelysin-1, stromelysin-3 and gelatinase, are produced and mediate a structural remodelling of the gland (Furth, 1999). The disruption of the basement membrane can cause an alteration of normal integrin signalling resulting in the induction of *ICE* and the caspase apoptotic pathway in the remaining epithelial cells (Prince *et al.*, 2002). The highest levels of apoptosis occur 2-4 days after weaning (2-4 days into the involution stage, I2-I4) and are largely restricted to epithelial and myoepithelial cells (Lund *et al.*, 1966). At about 4 days after weaning (I4) the alveoli collapse and adipocytes become more prevalent. The stroma begins to infiltrate the regressing areas once encompassed by the alveoli and the adipocytes become prominent by the late stages of involution (I9). The ductwork in the gland becomes less complex and the numbers of alveoli have decreased dramatically. There is still the presence of apoptotic bodies by 10 days after weaning (I10) though the numbers are far lower. At the end of involution the gland is similar in structure to the virgin, but there are scattered alveoli still present with a mildly more complex ductal structure.

## 1.5 GENE EXPRESSION

With respect to MG development most studies have focused on changes in gene expression that marks a stage of active lactation (milk production) or the transition between early and late involution (apoptosis). Until recently, the approach most studies have taken to define the developing MG was to examine the expression of a single gene over the course of development. A large majority of the studies have focused on specific groups of genes involved with milk synthesis (caseins and whey acidic protein, ferritin), proteolysis (TIMPs, gelatinase, metalloproteinases), apoptosis related events (clusterin, *ICE*, *bcl-x*, *bax*, *tgf $\beta$* , *IGFBP5*) and a long list of transcription factors or mediators (*Stat3*, *IRF-1*, *p53*, *Smad3*, *Nf-kB*, *Stat5*, *AP-1*, *Esx*, *Msx*, *Oct-1*, *Nf-1*) ( Kane *et al.*, 2000; Hebbard *et al.*, 2000; Marti *et al.*, 1999; Marti *et al.*, 1994; Neve *et al.*, 1998; Lee *et al.*

2000; Baik *et al.*, 1998; Breton-Gorius, 1980; Paape *et al.*, 1996; Wright *et al.*, 1990; Miyake, 2003; Furth, 1999; Watson *et al.*, 2003; Satoh *et al.*, 2004; Zhao *et al.*, 2004). With the advent of microarray technology a number of groups have attempted to take a more global analysis of gene expression over the course of MG development, a topic that will be further discussed in chapter 3.

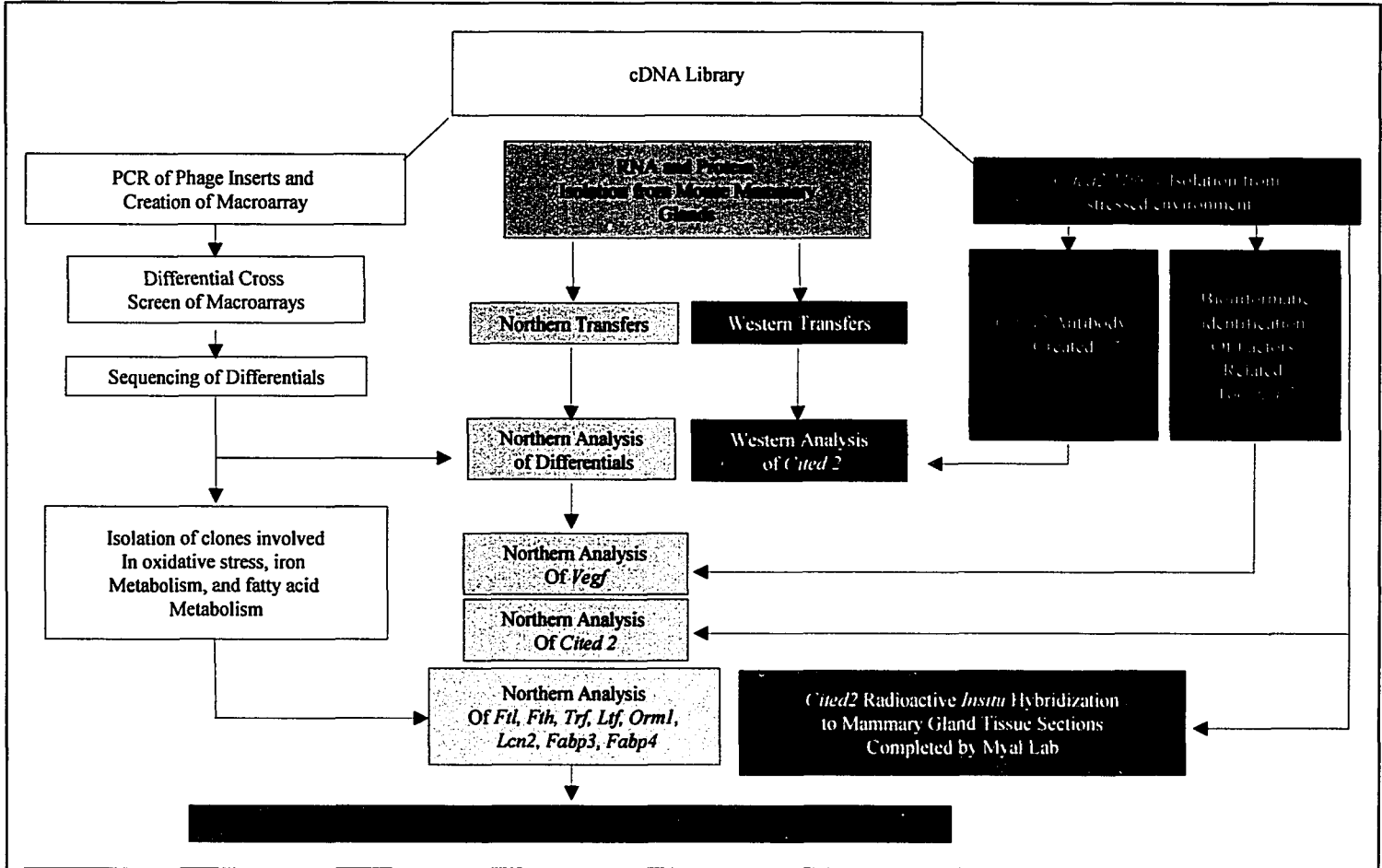
## 1.6 THESIS PROPOSAL

At the time of my thesis proposal there had been no concerted effort to definitively characterize the gene expression that marks the transition from a lactating MG to an involuting state at a global level (Day 1 after weaning (I1)). *Tgfb3* causes local apoptosis without structural remodeling of the MG and its up-regulation at both the mRNA and protein levels one day after weaning makes this developmental time point very relevant in understanding the transition of a lactating gland to an involuting gland (Nguyen and Pollard, 2000). Characterization of gene expression at this developmental time point (I1) will lead to insights into the process of early MG involution. I hypothesize that differences in the expression of specific subsets of genes may define the change in the tissue environment at this developmental interval.

## 1.7 SUMMARY

I have identified genes that are differentially expressed during early involution through a differential macroscreen of cDNA clones taken from a MG cDNA library created from cDNA derived from mRNA isolated from MG tissue taken one day after weaning (I1) (Chapter 3) and by northern analysis of genes known to be involved in involution of other model systems (*cited2*, Chapter 5). The expression profile of select genes identified from my screen that belong to specific gene families (iron binding proteins or the calycin superfamily of genes) are discussed in Chapter 4. Bioinformatic analysis of these genes (*cited2*, iron binding proteins, and calycin genes) led to the common link of a transcriptional regulation pathway mediated by peroxisome proliferator activated receptors (PPAR) (Chapter 4 and 5). The sequence of experimental events can be observed in figure 1.4.

**Figure 1.4: Experimental Flow Chart:** Outlined above are the series of experiments executed to analyse the onset of involution in the mammary gland. 2 methods of screening were used to examine genetic expression in the MG; on the left macroarray analysis lead to the discovery of differential clones; on the right, selection of a gene isolated from a stressed environment and examined in the mammary gland.



## CHAPTER 2 - MATERIALS AND METHODS

### 2.1 MG TISSUES

Tissues were isolated from female mice at different stages over the course of the MG development cycle representative of the first parturition: 15 week virgin (virgin 15 weeks, V15), virgin 20 weeks (V20), 2 days into pregnancy (pregnancy 2 days, P2), pregnancy 13 days (P13), 3 days into the lactation period (lactation 3 days, L3), lactation 10 days, L10), 0.08 days after weaning, the induction of involution (involution 2 hours/0.08 days, I0.08), involution 1-10 days (I1-10). MG involution was induced by removal of the pups (forced weaning) at L10, and all involution time points are measured with reference to this event. The tissues were procured using standard protocols in the Myal laboratory (Dr. Y. Myal, Dept of Pathology, University of Manitoba). All protocols used are in accordance with the interdisciplinary principles and guidelines for the use of animals in research, testing, and education issued by the New York Academy of Sciences' Ad Hoc Committee on Animal Research.

### 2.2. RNA EXTRACTION

#### 2.2.1. Total RNA Extraction.

Total RNA was isolated using the Chomczynski and Sacchi method (as described in Life Technologies-TRIZOL extraction, Invitrogen, Carlsbad, CA), from the isolated tissues. Frozen tissues were wrapped in tinfoil and placed on dry ice to be fragmented with a blunt object. Pieces were transferred to previously weighed falcon tubes from VWR (West Chester, PA, USA) and weighed to obtain the tissue mass. Keeping the tissue samples on dry ice, 1.5 ml of TRIZOL was added to each tissue in the tubes. The tissues were then subjected to homogenization utilizing a polytron. Each tissue was subjected to 3-15 second (sec) periods with an approximately 30 sec incubation on ice in between runs. After homogenization, TRIZOL was added until a final volume was obtained that corresponded to a ratio of 2ml TRIZOL for every 100mg of tissue. 0.2 ml of chloroform per 2ml of homogenate was added and the sample was shaken vigorously for approximately 15 seconds (secs). The samples were then aliquoted into individual 1.5ml centrifuge tubes and centrifuged at 13000rpm at 4°C for 15 minutes (mins). The aqueous

layer containing the RNA was removed (not exceeding 700 $\mu$ l) and transferred to new 1.5ml tubes to which an equal volume of cold isopropanol was added. Samples were mixed and left at room temperature for 10 mins. They were centrifuged at 13000rpm at 4°C for 10 mins and the supernatant was subsequently decanted. To wash the resulting RNA pellet, 1ml of cold reagent grade alcohol was then added to each tube and re-centrifuged for 5 mins. The alcohol was decanted and the RNA pellets left to air dry for 5-15 mins. Depending on the size of the pellet, re-suspension was executed with DEPC treated water ranging from 10-60 $\mu$ l. 3  $\mu$ l were removed to be run on a denaturing agarose (FMC BioProducts, Rockland Maine; Seakem, Cambrex, East Rutherford, NJ) gel and the remaining sample was placed on dry ice and stored at -70°C.

### **2.2.2 Isolation of the mRNA.**

150 $\mu$ g of total RNA was used in the isolation of mRNA using the small scale Promega (Madison, WI) PolyATtract mRNA Isolation System. Brought to a final volume of 500 $\mu$ l, the RNA sample was heated for 10 mins at 65°C. The samples were removed and at room temperature 3 $\mu$ l of the biotinylated-oligo (dT) probe and 13 $\mu$ l of 20XSSC were added to the RNA sample. The samples sat at room temperature for approximately 10 mins until the samples reached room temperature. During this time 0.5XSSC and 0.1XSSC were made. This was accomplished by adding 30 $\mu$ l of 20XSSC to 1.170ml of RNase free water to make 0.5XSSC and by adding 7 $\mu$ l of 20XSSC to 1.393 ml of RNase free water.

### **2.2.3 Prepping the Streptavidin Paramagnetic Particles.**

For each sample, one tube of Streptavidin-Paramagnetic Particles (SA-PMPs) was re-suspended until all particles were evenly distributed in the solution. The tubes were then placed in the magnetic rack for approximately 30 secs until the magnetic beads had settled on the side. The supernatant was carefully removed using a 1ml pipette, followed by a 200 $\mu$ l pipette to remove the remaining solution. To wash these particles three successive washes were completed with 300 $\mu$ l of 0.5XSSC removing the supernatant

each time as described above. After the third wash the pellets were re-suspended in 100 $\mu$ l of 0.5XSSC.

#### **2.2.4 Isolating the mRNA-SA-PMPs.**

The contents of each RNA mix were added to an individual SA-PMP tube. The samples were allowed to incubate at room temperature for 10 mins with a gentle inversion every couple minutes to prevent sedimentation. The supernatant was then removed as described above by placing the tubes in the magnetic rack. The mRNA-SA-PMP now should be collected along the side of the tube. To wash these samples 100 $\mu$ l of 0.1XSSC was added to each tube and mixed by gentle flicking. This was repeated 3 more times.

#### **2.2.5 Elution of the mRNA.**

After the last wash the mRNA-SA-PMP were collected on the side of the tube as described above and the supernatant carefully removed. To elute the mRNA from the beads 100 $\mu$ l of RNase free water was added to each tube and gently flicked. The beads were collected on the side of the tube. The supernatant was removed carefully and placed in an RNase free tube. To increase the elution from the beads a second wash was done with 150 $\mu$ l of RNase free water. Removing the supernatant was repeated as above and the 150 $\mu$ l supernatant was added to the initial elution. Based on the generalization that mRNA constitutes approximately 1-3% of total RNA we assumed that we obtained maximum 5 $\mu$ g of mRNA. To concentrate this mRNA we added 0.1 volume (25 $\mu$ l) of 3M sodium acetate and 1.0 volume (250 $\mu$ l) isopropanol to the samples and let them precipitate overnight at  $-20^{\circ}\text{C}$ . The next day we centrifuged the samples at 13000rpm for 10 min. This was followed by a wash in 70% ethanol and a second centrifugation as above. The pellet was dried in a vacuum chamber for approximately 15 min and re-suspended in 30 $\mu$ l RNase free water.

### **2.3 cDNA LIBRARY SYNTHESIS AND MAKING OF MACROARRAY**

A cDNA library was created from cDNA derived from the purified mRNA isolated from mouse MG excised from dams 1 day after weaning (I1), UniZAP-XR cDNA Library Synthesis Kit and ZAP-cDNA Gigapack Gold Cloning kit (Stratagene, La Jolla, CA). All

buffers, enzymes, primers, and reagents were supplied by the kit and all concentrations, volumes and protocols utilized followed the recommendations of the provided protocol. cDNA was synthesized using a cDNA Synthesis Kit (Stratagene, La Jolla, CA).

### **2.3.1 cDNA - First Strand Synthesis.**

Synthesis of the first strand was completed using Stratascript reverse transcriptase which is based on the Moloney murine leukemia virus reverse transcriptase (MMLV-RT) that lacks any detectable RNase H activity. This was engineered by a point mutation in the RNase H region of the gene, which subsequently inactivates any function in that region. Taking a third of the isolated mRNA, the first strand of cDNA was synthesized with a linker-primer that would complement the poly A-tail of mRNA and contained an *XhoI* endonuclease restriction site. 5 $\mu$ l was removed and transferred to a tube containing 0.5 $\mu$ l of [ $\alpha$ -<sup>32</sup>P] dATP (800 Ci/mmol) as a first strand synthesis control reaction.

### **2.3.2 cDNA Second Strand Synthesis.**

At 16°C RNase H and DNA PolII were added to the first strand mix along with [ $\alpha$ -<sup>32</sup>P] dATP (800 Ci/mmol) and the required reagents. RNase H was to degrade the original mRNA template which would now act as numerous primers for elongation by DNA PolII. This reaction was executed at 16°C to eliminate hairpin formation of the template. The radioactive nucleotide was added as a method of detection when the sample is run through the sepharose column.

### **2.3.3 Blunting the cDNA.**

*Pfu* DNA polymerase was added with the corresponding reagents to the second strand mix and incubated at 72°C for 30 mins. Following phenol/chloroform purification of the cDNA, the sample was precipitated using sodium acetate and ethanol overnight at -20°C. After precipitating the cDNA and the supernatant carefully removed, the pellet was air dried and re-suspended in 9 $\mu$ l of *EcoRI* adapters at 4°C for 30 mins.

### **2.3.4 Ligating the EcoRI Adapters.**

T4 DNA ligase was added to the second strand sample and incubated for 2 days at 4°C in the respective buffer and rATP. The reaction was stopped by incubating the sample at 70°C for 30 mins.

### **2.3.5 Phosphorylating the EcoRI Ends.**

Once the sample had cooled to room temperature T4 polynucleotide kinase was added to the mix with the respective buffers and rATP. The reaction was carried out at 37°C for 30 mins. The reaction was inactivated by incubating the sample at 70°C for 30 mins.

### **2.3.6 Digestion with XhoI.**

*XhoI* was added to the mix with the respective buffer and allowed to incubate at 37°C for 1.5 hours. To stop and precipitate the reaction STE was added followed by 100% ethanol. The samples were precipitated overnight at -20°C and centrifuged the following morning for approximately 60min. The pellet was re-suspended in 14µl STE buffer and 3.5µl of column loading dye was added. Following these steps the cDNA fragment should have an *EcoRI* site at the 3' end and an *XhoI* site at the 5' end allowing for directed insertion into the UniZAP-XR vector.

### **2.3.7 Size Fractionation.**

The column was created out of a 1ml pipette, 10ml syringe, cotton plug from the pipette and rubber tubing. Sepharose Cl-2B was added to the column by first filling the column with STE and allowing the sepharose to pool at the bottom. Once the sample has been added to the column, the dye will mark the area of cDNA fractionation that will be recovered after size fractionation through the column. The column should separate complete cDNA molecules from smaller fragmented samples, and unincorporated nucleotides. Fractions were obtained from the leading edge of the dye in 3 drop samples to the lagging edge of the dye. Using the scintillation counter two peaks were observed at the leading edge and used for further steps.

### **2.3.8 Processing the cDNA Fractions**

The samples were purified using phenol/chloroform extraction and the cDNA in the aqueous layer was precipitated via ethanol overnight at  $-20^{\circ}\text{C}$ . After centrifugation as above for cDNA precipitation the pellet was checked for radioactivity and the supernatant decanted. The pellet was washed in ethanol, dried and re-suspended in  $5\mu\text{l}$  of sterile water.

### **2.3.9 Ligating the cDNA into the UniZAP XR Vector**

A portion of the cDNA was added to UniZAP XR vector and T4 DNA ligase containing the respective buffer for T4 DNA ligase. The reactions were incubated at  $4^{\circ}\text{C}$  for 2 days. The final product should contain a complete UniZAP XR fragment with the cDNA cloned into the MCS with the poly A tail of the cDNA at the T3 end of the vector.

### **2.3.10 Preparation of the Host Bacteria and Titrating the Library**

*E.coli* XLI-Blue MRF' cells were grown up in a 25ml liquid culture containing 10mM  $\text{MgSO}_4$  and 0.2% Maltose. XLI-Blue cells were used due to their *RecA*' genotype which prevents recombination in the cell. The cells were grown to  $\text{OD}_{600}$  1.0 centrifuged down, and re-suspended in 10mM  $\text{MgSO}_4$  to an  $\text{OD}_{600}$  of 0.5. To  $200\mu\text{l}$  of these cells,  $1\mu\text{l}$  of the library was added and incubated at  $37^{\circ}\text{C}$  for 15 mins. This was then added to 8ml of NZY top agarose melted and cooled to approximately  $47^{\circ}\text{C}$ . The mix was gently but quickly mixed and added to the surface of pre-warmed NZY agar plates. The plates were allowed to sit for 10 mins to allow the top agarose to solidify and then incubated overnight at  $37^{\circ}\text{C}$ . This was completed with multiple plates to obtain a wide array of clones for isolation. To amplify the library for storage, three samples were created with an overabundance of library to promote clearing of the lawn. Plating was executed as above and after incubation overnight 8-10ml of SM buffer was added to the surface of each plate and let stand overnight at  $4^{\circ}\text{C}$ . The next day the SM buffer was collected and the plates were rinsed with an additional 2ml SM buffer. Chloroform was added to each tube to a final volume of 5%; the tubes were thoroughly mixed and incubated at room temperature for 15 mins. The cellular debris was removed by centrifuging the tubes at

500xg for 10 mins. The supernatant was decanted into a sterile polypropylene tube and chloroform was added to a final concentration of 0.3%. Aliquots were then made with a DMSO concentration of 7 % (v/v) and stored at  $-80^{\circ}\text{C}$ . The library constructed represented a mouse mammary gland cDNA library representative of the tissue one day into involution (I1).

### **2.3.11 Isolation of the Plaques**

Plaques were recovered from the unamplified cDNA library plated above and stored individually in approximately 300 $\mu\text{l}$  SM buffer. An aliquot of each phage clone was PCR amplified as follows using standard T3 and T7 primers that flanked the cloning site. An initial denaturation of  $94^{\circ}\text{C}$  was carried out for 5 mins followed by a 30 cycles of annealing the primers at  $50^{\circ}\text{C}$  for 2min with an extension period of 3 mins at  $72^{\circ}\text{C}$  by taq DNA polymerase and a denaturation of 1 min at  $94^{\circ}\text{C}$ . The presence of PCR products was confirmed by gel electrophoresis on 1% agarose gels stained with ethidium bromide (EtBr) run in 0.5xTBE buffer.

### **2.3.12 Phagemid Extraction**

XLI-Blue MRF' and SOLR cells were grown in an overnight liquid culture to a final  $\text{OD}_{600}$  of 1.0. From the cored stocks obtained above, 250 $\mu\text{l}$  was added to 200 $\mu\text{l}$  of XLI-Blue MRF' cells with the addition of 1 $\mu\text{l}$  of ExAssist Helper phage provided by the kit. The mixes were incubated at  $37^{\circ}\text{C}$  for 15 mins. After the initial incubation, 3ml of LB broth was added to each sample and incubated for 2-3 hours at  $37^{\circ}\text{C}$  in a shaking incubator. To stop the reaction the samples were heated to  $65^{\circ}\text{C}$  for 20 mins and then spun down at 1000xg for 15 mins to remove any bacterial components. We then decanted the supernatant into sterile polypropylene tubes; this supernatant now contained our filamentous pBluescript phagemid with insert. To grow the phagemid, we then added 100 $\mu\text{l}$  of the phagemid supernatant to 200 $\mu\text{l}$  of SOLR cells, and 10 $\mu\text{l}$  of the phagemid to another tube with 200 $\mu\text{l}$  SOLR cells. The tubes were then incubated at  $37^{\circ}\text{C}$  for 15 mins and 200 $\mu\text{l}$  of each mix was spread on LB-Amp (50 $\mu\text{g}/\text{ml}$ ) plates for selection. The plates were then incubated overnight at  $37^{\circ}\text{C}$ . The next day colonies were picked and added to a

tube containing LB-Amp broth for overnight growth at 37°C. These cultures were then prepared into small glycerol stocks for long term storage at -80°C.

## **2.4 II MOUSE MG MACROARRAY ANALYSIS**

### **2.4.1 Creation of the Macroarrays**

The PCR products obtained as described above, that consisted of a single band greater than 500 base pairs in length when run on an agarose gel, were selected for inclusion on custom-made macroarrays. Multiple copies of the macroarrays were made by spotting the PCR products onto nylon membranes in triplicate using a 96-pin arraying device (V&P Scientific, San Diego, CA). Approximately 1  $\mu$ l of each PCR product was spotted onto the macroarrays. The arrays were then soaked for 2 mins in 0.4 M NaOH to denature the DNA. To neutralize the denaturation the macroarrays were then soaked in 1 M Tris-HCl, pH 7.5 for 2 mins. Once the arrays dried to the point that there was no more solution on the surface of the membranes, the DNA was UV cross-linked to the nylon membrane with 1200 j of UV light.

### **2.4.2 Amplification of cDNA for Labelling**

The following protocol is a derivation from Clontech's SMART cDNA synthesis protocol. The first strand was created by adding 3  $\mu$ l of the RNA sample to 1  $\mu$ l of the CDS oligo (10  $\mu$ M) and 1 ml SMART II oligo (10  $\mu$ M). These were incubated for 2 mins at 72°C and then cooled on ice for 2 mins. To the tube 2  $\mu$ l 5X first strand buffer was added with 1  $\mu$ l DTT (20mM) 1  $\mu$ l 10mM dNTPs and 1  $\mu$ l Powerscript reverse transcriptase. The reaction was let incubate for 1 hour at 42°C. To create the second strand 66.4  $\mu$ l ddH<sub>2</sub>O was added to the reaction with 10  $\mu$ l 10XPCR buffer, 10  $\mu$ l CDS amplification oligo (10  $\mu$ M) 1.6  $\mu$ l dNTPs (25mM) and 2  $\mu$ l Qiagen taq. The reactions were then carried out in a thermocycler using the following protocol.

95 C for 5 mins

1 cycle of

60 C for 30 secs

72 C for 4.5 mins

Amplification was carried out by adding 71.4  $\mu$ l ddH<sub>2</sub>O, 10  $\mu$ l 10X PCR buffer, 10  $\mu$ l CDS amplification oligos (20  $\mu$ M), 1.6  $\mu$ l dNTP (25mM each), 2  $\mu$ l Qiagen tag, and 5  $\mu$ l second strand product from above to a new tube. The reaction was then subjected to 23 cycles of:

95 C for 30 secs

60 C for 30 secs

72 C for 4.5 mins

Final cycle 72 C for 4.5 mins

The reaction was purified using a Qiaquick PCR purification kit according to the manufacturer's protocol.

### **2.4.3 Hybridization of Radioactively Labelled cDNA to Macroarrays**

Differential expression levels were detected via labelling cDNA isolated from tissues V15, P13, L10, I1, and I3 as described in the probe section above. The arrays were pre-hybridized with Hybrisol II solution (Serologicals Corporation, Norcross, GA) at 68°C for 1.5 hours. The probes were boiled at 95°C for 5 min and then cooled on ice for 5 mins before they were added to the hybrisol. Hybridization in the presence of the denatured probes and Hybrisol II took place overnight at 68°C. Minimum activity used per hybridization was  $1.6 \times 10^6$  CPM/ml of hybridization buffer. The next day the membranes were washed 3 times for 0.5 hour each with 2X SSC / 0.1% SDS, then twice for 15 mins each with 0.1X SSC / 0.1% SDS. Film was exposed to the macroarrays and exposures were taken of the samples ranging from 3 hours to 24 hours. The resulting autorads were scanned into the computer at a resolution of 600dpi.

## **2.5 SEQUENCING, SEQUENCE ANALYSIS AND BIOINFORMATICS.**

### **2.5.1 Sequencing**

Clones corresponding to differentially expressed genes identified by autoradiography from the macroarray screen were selected for sequencing. Sequencing was done using a Dyanamic ET Terminator Cycle Sequencing kit (Amersham-Pharmacia Biotech, Uppsala, Sweden) as per the manufacturer's protocol. The sequencing protocol I used is as follows. Denaturation of the double strands was completed at 95°C for 20 secs

followed by an annealing period of 15 secs at 45°C. Elongation of the reaction was carried out at 60°C for 1 min. This cycle was repeated 25 times with a final hold at 4°C to prevent potential degradation of the DNA sequence. The sequenced DNA fragments were then precipitated with 3mM sodium acetate and ethanol. The samples were then washed with 500µl 70% ethanol and then pelleted by centrifugation at 13000rpm for 10 mins at 4°C. The pellets were then air dried for sequencing for approximately 5 mins and submitted to MBSU (molecular biology service unit) to be sequenced. To determine the identity of the 11 mouse MG cDNA clones and their human orthologues, sequences were submitted to a BLAST search against the GenBank database at NCBI ([www.ncbi.nih.gov](http://www.ncbi.nih.gov)). The BLAST searches were executed using the default parameters for the non-redundant (nr) database.

## **2.6 ANALYSIS OF THE IDENTIFIED GENES**

### **2.6.1 Examining RNA Expression**

#### **2.6.1.1 Northern Analysis**

##### **2.6.1.1a *Sample Preparation***

9.5 µg of Total RNA isolated from the MG tissues was added to a loading mix composed of 4µl 10X MOPS, 7µl formaldehyde, 20µl deionized formaldehyde, and 1µl EtBr (1mg/ml), for a final volume of 41µl. Each sample was heated to 55°C for 15 mins and immediately cooled on ice. To each sample 8µl of 6X loading buffer (0.25% bromophenol blue, 0.25% xylene cyanol FF, 15% Ficoll (Type 400, Pharmacia) in water) was added. The samples sat on ice until the gel was ready to be loaded.

##### **2.6.1.1b *Gel Electrophoresis of Total RNA***

Total MG RNA from animals representing our developmental profile as well as a 0.24-9.5 kb RNA size ladder (Invitrogen, Carlsbad, CA) were electrophoresed on a 1% agarose / 18% formaldehyde / 10% MOPS gels (Wong et al., 1993; Sambrook et al., 1989). Gels were run initially at 120 volts for approximately 20 mins and then either lowered to 25 volts for an overnight run, or raised to 200 volts for a 1-2 hour run.

### **2.6.1.1c Northern Transfer**

After electrophoresis the 18S and 28S ribosomal bands were visualized with UV light. Overnight the RNA on the gel was passively transferred to BioDyne-B nylon membrane (Pall Corporation, Port Washington, NY) using 10X SSC as a transfer medium. Transferred RNA was UV cross-linked to the nylon membrane using a Stratalinker (Stratagene, La Jolla, CA). Transfers were kept in Whatman (Rose Scientific Ltd. Edmonton, Canada) paper in a dry location until later use.

### **2.6.1.1d Hybridization of Radiolabelled PCR Products to Northern**

Gel purified PCR products derived from a single clone as described below served as templates for random primer radiolabelling (as stated in 2.7.1). The hybridization and wash conditions were identical to those described above for the array analysis in 2.4.3 except hybridization was carried out at 65°C.

### **2.6.1.1e Detection of Expression and Normalization of the Exposures**

Depending on the amount of radioactivity detected with the Geiger counter, exposures were completed on X-ray film from a matter of minutes to 3 week exposures. The autoradiograms were digitally scanned at 600dpi and then analysed by densitometry using the histogram function in Adobe Photoshop v7. The autoradiography results of the Northern hybridization were normalized to the 18S band of each blot's corresponding RNA gel prior to transfer (Correa-Rotter et al., 1992). The process quantifies the net intensity of each band on the Northern autoradiograph relative to one another while correcting for variation in RNA loading between each lane. Normalized intensity values were calculated using the following formula. (bg = background)

$$\frac{(\text{Mean intensity subject band} - \text{mean bg intensity}) * (\text{pixel number})}{(\text{Mean intensity 18s rRNA} - \text{mean bg intensity}) * (\text{pixel number}) / (\text{lowest net value})}$$

### **2.6.1.2 In situ Hybridization**

#### **2.6.1.2a Fluorescent In situ Hybridization**

**2.6.1.2a1 Preparation of Sections** Samples were obtained from the Myal lab at the University of Manitoba already embedded in paraffin. 5-8µm sections were made and were placed on Fisherbrand Superfrost/Plus Slides (Fisher Scientific, Hampton, NH).

They were incubated at 37°C overnight and then placed in slide holders with Drierite (W.A. Hammond Drierite Company, Xenia, OH) as a desiccant. To remove the paraffin from the slides they were treated 2X10 min with xylene. The sections were rehydrated through a series of 2 mins washes in various percentages of reagent grade ethanol as follows; 100%, 100%, 95%, 80%, 70%, 50%, ddH<sub>2</sub>O (DEPC treated) 1XPBS for 5 mins. I then treated the sections with a 0.02M HCl solution for 10 mins followed by a 2 min wash in 1XPBS. To fix the sections a 4% paraformaldehyde wash was executed for 10 mins. The sections were then subjected to a proteinase K digestion; I varied the concentrations initially to obtain the most suitable working concentration. The concentrations were 1µg/ml, 20 µg/ml, 100µg/ml and 1000ug/ml. The decided concentration to use in future experiments was 20 µg/ml. The slides were incubated at 37°C for one hour and subsequently washed with a 1XPBS solution with 2mg/ml glycine for 5 mins. A control slide was set aside for 100µg/ml RNase A digestion at 37°C for one hour. The slides were then washed 2X5 mins in 1XPBS. Some trials were then subjected to dehydration by repeating the rehydration steps (see above) in reverse order or air dried.

**2.6.1.2a2 Hybridization of DIG Labelled PCR Product.** Hybridization was carried out with Sigma Hybridization buffer for *in situ*'s. DIG labelled probes were made from purified PCR product as stated in section G-3. 10µl of the probe was boiled for 5 mins and then cooled on ice. 190ul of hyb buffer was then added to the 10ul sample. The complete 200µl was added to the sections by dropping the probe on the centre of the section. The sections were then covered with a Fisherbrand coverslip (Fisher Scientific, Hampton, NH) and sealed with rubber cement (Ross Adhesives, Toronto Can.). The slides were placed in a humid chamber at 42°C for hybridization overnight.

**2.6.1.2a3 Posthybridization.** The slides were soaked in 2XSSC at 42°C with a gentle shake to remove the coverslips. Once the coverslips were removed the slides were washed 3X5 mins in 2XSSC/50% formamide at 42°C. This was followed by 5X2 mins washes in 2XSSC at 42°C.

**2.6.1.2a4** *Detection of Fluorescence and mRNA Localization* The slides were incubated in blocking buffer (0.1% Triton X-100; 2% lamb's serum) or a nucleic acid hybridization blocking reagent in 1XPBS from Roche (F. Hoffmann-La Roche Ltd, Basel, Switzerland) for 30 mins at room temperature. The anti-DIG FITC antibody was diluted 1:1000 in hybridization buffer and 100µl placed on the slide, covered with a coverslip and sealed with rubber cement. The slides were incubated at 37°C for one hour and subsequently washed 2X5 mins in 4XSSC; 0.1% Tween 20 at 42°C. 50µl of DAPI (Sigma-Aldrich, St. Louis, MO) was added to each slide and let sit for 5 mins. After the DAPI stain, one drop of Antifade (Molecular Probes) was added and covered with a coverslip. Sections were viewed under a single photon confocal microscope.

**2.6.1.2b** *Radioactive in situ hybridization*

Protocol was completed by Anne Blanchard alongside Dr. Yvonne Myal at the University of Manitoba in Winnipeg, Manitoba, Canada. Sense and Anti sense probes of *cited2* were synthesized using the Promega (Madison, WI, USA) Riboprobe synthesis kit and corresponding protocol.

**2.6.1.2b1** *Preparation of Sections.* Tissues were sectioned and placed on slides as indicated above. Treatment of the slides with paraffin sections are as follows. Deparaffinization occurred with two washes of 2 mins each in xylene and was succeeded by a dehydration sequence as follows. 2x 2 min washes in 100% Ethanol, 2 min wash in 95% Ethanol, 2 min wash in 70% Ethanol and a 5 min wash in DEPC treated H<sub>2</sub>O followed by 2X5 min washes in 1XPBS. The sections were then treated with proteinase K (1µg/ml) in a solution of 100mM Tris pH 8.0; 50mM EDTA pH 8.0 for 30 mins at 37°C. The reaction was stopped by 2 successive washes in PBS for 2 mins. Fixation of the sections was complete via a 4% Paraformaldehyde; 1XPBS pH 7.4 incubation for one min. Next two 2 min washes were done in 1XPBS followed by an acetylation reaction as follows. 6.1ml TEA in dH<sub>2</sub>O pH 8.0 brought to a final volume of 500ml with dH<sub>2</sub>O. A presoak was done in 250ml of the above solution for 2 mins. The slides were then drained and placed in a dish containing acetic anhydride for a final percentage of 0.25% in 250ml (0.625ml/250ml). The dish was then filled with the remaining 250ml of TEA and the

slides were incubated for 10 mins at room temperature. The slides were then washed twice in 2XSSC for 2 mins each. Dehydration was completed as above and dried for a minimum of 1 hour to a maximum period of overnight.

**2.6.1.2b2** *Hybridization of Sections.* Probes synthesized as stated above were diluted to a final working concentration of 1X10cpm/ml. 5M DTT was added to the probe to obtain 150mM from 100mM. The probes were then vortexed, centrifuged and heated to 65°C for 10 mins. They were quickly centrifuged and stored on ice until ready for use. Under a fumehood the probes were applied to the sections ranging from 20-40µl sealed with a coverslip and rubber cement. The slides were then placed in a humid chamber overnight at 42°C.

**2.6.1.2b3** *Posthybridization.* The next day the hybridizations were stopped and coverslips removed by washing the slides in 4XSSC/10mM DTT for 30-45 mins. Once the coverslips came off the slides were then washed 2 more times in 4XSSC/10mM DTT for 15 mins each. Dehydration of the slides was repeated as above except this time containing 300mM Ammonium acetate. The slides were then incubated in a solution containing 20mM Tris/ 1mM EDTA/ 0.3M NaCl/ 10mM DTT/ 50% formamide for 10 mins at 55°C followed by 2 X 2 min washes in ice cold 2XSSC/10mM DTT. To remove any remaining background Riboprobes the slides were treated for 30min at 37°C in a solution containing 0.5M NaCl/ 10mM Tris/ 1mM EDTA with 10ug/ml RNaseA (5prime-3prime Inc, Boulder, CO). The slides were then washed with the previous solution lacking the RNaseA for 10 mins at 37°C. The final washes were completed at room temperature on a slow shaker as follows. 2x 5 min washes in 2XSSC; 1X15 mins in 1XSSC; 3X15 mins in 0.1XSSC. The slides were then dehydrated as above containing 300mM Ammonium acetate and dried overnight in a fumehood.

**2.6.1.2b4** *Detection of Radioactivity and Probe Localization.* For detection Kodak emulsion NBT-2 (Eastman Kodak Company, Rochester NY.) was used at 40°C. The emulsion was poured into a dip miser and allowed to sit for 15 mins. To remove potential bubbles, 3 blank slides were dipped in the solution. The sample slides were then carefully

dipped into the emulsion; the backs of the slides were wiped clean and then placed on a drying rack. The slides were dried in a humid chamber for one hour and then placed in light tight boxes with small bags of Drierite (W.A. Hammond Drierite Company, Xenia OH). 3 sets of duplicate slides were run in the process. The slides were then placed in a refrigerator in the light tight boxes and exposed at 2, 4 and 6 weeks. Development was executed as follows: 4 min incubation in Kodak D-19; 10 dips in dH<sub>2</sub>O; 5 min incubation in Kodak fixer; 2 X 5 min washes in dH<sub>2</sub>O. Slides were then stained with Lee's stain for 20-30 secs, dehydrated by dipping the slides 5-7 times in 70% ethanol, 15-20 times in 95% ethanol, and 2x 2 min soaks in 100%. The sections were finally cleared in xylene via 2x 2 min washes. The resulting signal from the probe on the sections was viewed using a Nikon E1000 Microscope and the ACT1 V.2.62 Nikon corporation software.

## **2.6.2 Examining Protein Expression**

### **2.6.2.1 Western transfer analysis.**

#### **2.6.2.1a *Protein Isolation***

Proteins were isolated from the organic layer that remained from the TRIzol protocol of RNA extraction. The proteins were then quantified using both the Bradford assay (10mg coomassie blue g-250, 5ml 95% EtOH, 10ml 85% orthophosphoric acid in a final volume of 100ml (ddH<sub>2</sub>O)) and the Bio-Rad DC protein quantification assay.

#### **2.6.2.2b *Sample Preparation***

Based on the stock protein sample with the lowest concentration, aliquots of each time point were made containing 6µg of protein in 10µl of 1% SDS. To each sample 10µl of 2XLaemelli buffer was added and the samples were boiled for 5 mins and put immediately on ice.

#### **2.6.2.2c *SDS PAGE of Protein Samples***

Samples were run in a 5.36% SDS stacking and 13.2% SDS polyacrylamide separating gel. The gel was run at 68 volts for approximately 30 mins and then raised to approximately 160 volts to complete the process. Markers used in the gel were Gibco

Benchmark pre-stained protein ladder (Invitrogen, Carlsbad, CA) and Bio-Rad Kaleidoscope Prestained Standard (Bio-Rad incorporated, Hercules, CA).

#### **2.6.2.2d Western Transfer**

Once the gel was run it was then electro-transferred to nitrocellulose membranes to produce a blot (Bio-Rad incorporated, Hercules, CA) using the BioRad Mini-Protean II wet transfer apparatus. Transfers were carried out at either 300mA for 1 hour or 100mA overnight in 1X transfer buffer (6.06g Tris-Base, 28.8g Glycine, 400ml Methanol, 1400ml water, pH to 8.3 and brought to a final volume of 2L). To determine the quality of the transfer the membranes were stained in Ponceau S for 90 secs and then washed in MilliQ water.

#### **2.6.2.2e Antibody Production**

*Cited2* antibody was made by Covance (Princeton, NJ) based on the peptide sequence used to create the antibody originally obtained from Shioda. The peptide sequence used was NQYFNHHPYPHNHYM and corresponds to amino acids 120-135 of the *cited2* protein. On day 0 of the test, the rabbits were pre-bled subsequently injected with 500µg of the immunogen in FCA (Freund's complete Adjuvant). 3 weeks after the initial injection, the rabbits were boosted with 250µg of the immunogen this time emulsified in FIA (Freund's incomplete adjuvant) and 10 days following the boost the rabbits were subjected to the first test bleed (5ml; Day 31). The next day the rabbits were boosted again with 250µg of the immunogen emulsified in FIA and the second test bleed was carried out 10 days after this point (5ml; Day 52). The third boost was injected 11 days after this again with 250µg of immunogen in FIA and 10 days after the boost the first production bleed was executed (20ml; Day 73). The rabbits were subjected to another boost as above and a second production bleed (20ml) was taken 21 days (Day 94) after the first production bleed. A final boost was given on Day 105 and a production bleed was taken 10 days after this (20ml, Day 115). To terminate the production a final bleed was carried out on day 118 and approximately 50ml of serum was extracted.

### **2.6.2.2f Antibody Detection**

The blots were blocked (200ml TBS, 100 $\mu$ l Tween20, 10g skim milk powder) for 1 hour at room temperature, then stained with the anti-MRG1 antibody (obtained from Shioda, and subsequently from the Windber Research Institute) diluted from 1:500 to 1:10000 in antibody buffer (NaCl 8.1g, Tris base 1.2g, Tween20 300 $\mu$ l, 1% Skim milk, final volume 1000ml (ddH<sub>2</sub>O)) for one hour. Secondary antibody (anti-rabbit) (Stressgen, Victoria, BC, Canada) labelled with horseradish peroxidase was prepared in a 1:2000 dilution in antibody buffer mentioned above and incubated for one hour at room temperature. In between antibody stains and after the final stain, the transfer was washed 3x20 min in antibody buffer. Detection was executed by ECL detection (Amersham Pharmacia Biotech) and exposures were taken on x-ray film at 5, 10, and 30 secs as well as 1, 5, and 10 mins.

### **2.6.2.3 Antibody Competition Assay**

Peptide that was used as an epitope to raise the *cited2* antibody was dissolved in water to a final concentration of 1 mg/ml. To block the antibody before western hybridization the 10 $\mu$ g of the peptide were incubated with the diluted antibody (1:5000) for one hour at room temperature. Another sample was treated with the same conditions, one hour incubation in 1X antibody buffer at room temperature, except without peptide as a control. The two samples were hybridized to western test strips of L10 total protein and incubated overnight at 4°C in a rotating hybridization oven. They were then washed for approximately 3x20 mins in 1X antibody buffer, 1% skim milk at room temperature and then immunohybridized with the secondary antibody (HRP labelled Goat anti-rabbit IgG; 1:5000) at room temperature for 1.5 hours in a rotating hybridization oven. The strips were then washed as above and treated with the ECL detection kit from Amersham Pharmacia Biotech. The strips were then exposed to x-ray film as described above.

## **2.7 PROBE PREPARATION**

### **2.7.1 Random Primer Labelling of Probes for Northern and Macroarray Analysis**

5 $\mu$ l of cDNA (or 5 $\mu$ l of insert PCR product) was diluted to a final volume of 34 $\mu$ l with ddH<sub>2</sub>O. To this 10 $\mu$ l of 5X random prime buffer (1M HEPES buffer (pH 6.6), hexa-

deoxyribonucleotides, 27 hexa-deoxyribonucleotides 27 OD<sub>270</sub>/ml, 0.1mM dATP dTTP dGTP, 50mM  $\beta$ -mercaptoethanol, 0.25M Tris-Cl pH 8.0, 25mM MgCl<sub>2</sub>) mix was added and heated at 95°C for 5 mins then immediately cooled on ice. At room temperature 1 $\mu$ l of klenow fragment (Invitrogen, Carlsbad, CA, USA) and 5 $\mu$ l of  $\alpha$ -P<sup>32</sup>-dCTP (Perkin Elmer, Boston, MA; Amersham Pharmacia, Buckinghamshire, England) was added and mixed thoroughly. The reaction was carried out for either 30-60 mins at 37°C or overnight at room temperature. Both methods were attempted to optimize the effectiveness of the reaction. No major difference was noted in the activity of the probe based on scintillation counting. Probes were purified using QIAquick PCR purification following the stepwise procedure outlined in the kit manual (Qiagen, Hilden, Germany). To stop the reaction I added 250 $\mu$ l of PB buffer (Qiagen) and then spun it through a QiaQuick spin column (Qiagen) for 15 secs. Then column was washed 2 times with 450 $\mu$ l of PE buffer (Qiagen), centrifuging for 15 secs at 14000rpm with each wash. To elute the probe I added 100 $\mu$ l of ddH<sub>2</sub>O to the column, let it sit for 1 min and then spun the column for 1 min to collect the probe. 1 $\mu$ l of the purified probe was to be counted for specific activity in the scintillation counter. The probe was then heated at 95°C for 5 mins then directly transferred to ice for 5 mins ready for use in the corresponding experiment.

Invitrogen's Random Primer Labelling Kit (Carlsbad, CA) was also used in varying labelling reactions. The protocol requires 25ng of DNA dissolved in 5-20 $\mu$ l of water. The diluted DNA is then boiled for 5 mins and cooled on ice. To the DNA sample, 2 $\mu$ l of dATP, dGTP and dTTP are added along with 15 $\mu$ l of the Random Primers Buffer Mixture (Invitrogen, Carlsbad, CA). The  $\alpha$ <sup>32</sup>P-dCTP is then added in 5 $\mu$ l quantities to each reaction. To optimize the final working concentrations the samples are brought to a final volume of 49 $\mu$ l with ddH<sub>2</sub>O and 1 $\mu$ l of klenow fragment is added. The reaction was carried out for a minimum of one hour at room temperature and purified as stated directly above (G-1).

### **2.7.2 DIG Labelling of PCR product**

To make the probe 3 $\mu$ g of PCR product in 15 $\mu$ l total water was boiled for 15 mins and promptly cooled on ice for approximately 5 mins. After a brief centrifugation in a table

top microcentrifuge, 2µl of hexanucleotide mix, 2µl of dNTP mix and 1µl of klenow from the Roche (F. Hoffmann-La Roche Ltd, Basel, Switzerland ) DNA DIG labelling kit was added to each sample and incubated at 37°C overnight. The reactions were stopped the next day by adding 2µl 0.2M EDTA pH 8.0, 2.5µl 4M LiCl, and 75µl cold ethanol to each reaction. The samples were precipitated at -20°C for 30 mins and centrifuged at 13000rpm for 25 mins at 4°C. The pellets were then washed with 1ml 70% ethanol, centrifuged for 15 mins at 13000rpm at 4°C. Post centrifugation the pellets were dried via vacuum centrifugation and subsequently dissolved in 50µl TE at 37°C. 1µl was taken for detection and quantification. The remainder of the sample was diluted with 551 µl TE, 5µl salmon sperm DNA (10mg/ml), 5µl tRNA (10mg/ml), and 61µl 3M Na-Ac pH 5.5. The mix was then split into 2 tubes (335µl each) and 840µl of cold ethanol was added to each tube before allowing the samples to precipitate on ice for 30 mins. After the incubation on ice, the samples were centrifuged at 13000rpm for 50 mins at 4°C. The pellets were dried in a speed vacuum for 5 mins and then re-suspended in 50µl of FSP (50% deionized formamide, 2XSSC, 50mM Na-P<sub>04</sub>) to be stored at -20°C until later use.

To detect the strength of the probes a dilution series was prepared for each probe as follows: 1/10; 1/100; 1/1000; 1/10000. The samples were compared to a dilution series of control DIG labelled DNA in the magnitude series as follows: 100pg/µl; 10pg/µl; 1pg/µl; 0.1pg/µl. 1ul from each tube was dotted onto a nylon membrane (Amersham Pharmacia Biotech, Uppsala, Sweden ) in a grid with proper identification of samples and control. The membrane was then fixed by baking the membrane for 2 hours at 80°C. The membrane was then treated as per the protocol provided with the Roche (F. Hoffmann-La Roche Ltd, Basel, Switzerland) NBT/BCIP detection kit.

### **2.7.3 Radioactive *insitu* Hybridization Riboprobe**

At room temperature an NTP mix was prepared by adding 1µl rATP, 1µl rCTP, 1µl rGTP and 1µl RNase free water to a tube. To individual tubes for sense and antisense probe synthesis add 4µl 5x transcription buffer, 0.5µl RNasin, 2.0µl 100mM DTT, 4.0µl of the rNTP mix made above, 1.0µl of 100µM UTP, 1µl of template DNA (1mg/ml), 10.0µl of dried down <sup>35</sup>S-UTP and 1µl of primer (Sp6, T7, or T3 depending on sense, antisense,

and plasmid). The mix was allowed to incubate at 37°C for 2 hours. Following the reaction 1 µl of DNase 1 was added to each reaction and incubated at 37°C for 15 mins. After removal of any DNA, 29 µl of RNase free water was added to each tube. 1 µl was removed for scintillation counting and the stock was stored at -70°C. Sephadex columns were inverted several times to re-suspend the sepharose beads. The columns were drained and then centrifuged at 1100xg for 2 mins to compact the column. The riboprobes were thawed on ice, heated at 65°C for 10 mins and then briefly spun down and applied to the centre of the sephadex column. The columns were placed in a collection tube and spun at 1100xg for 4 mins to collect the probes. The probes were then diluted to a total volume of 90 µl and 10 µl yeast tRNA (10mg/ml), 50 µl of 5M sodium acetate pH 5.5 and 300 µl of cold absolute alcohol was added to each tube. The samples were allowed to precipitate overnight at -20°C. The next day the probes were precipitated by centrifugation at 12500 rpm for 45 mins at 4°C. The ethanol was pipetted off and the probes were allowed to dry on ice for 30min with parafilm covering the tubes. Once the pellets were dry, 25 µl of DEPC treated water was added to each tube, heated to 65°C for 5 mins and placed on ice. Scintillation counts were done on 1 µl of probe and total counts were done on 2 µl of probe. Quantities of probe were calculated to have a final working value of 1X10 cpm/ml.

## CHAPTER 3 – I1 cDNA LIBRARY ANALYSIS

### 3.1 INTRODUCTION

To date there has been no concerted effort to definitively characterize the gene expression that marks the MG transition from a lactating gland to an involuting state at a global level (I1). Historically genes known to be expressed at this time point have represented factors associated with milk metabolism and lactation. More recently, *tgfb3* was found to be up-regulated with respect to mRNA and protein levels within the first day after weaning (Nguyen and Pollard, 2000). The significance of *tgfb3* expression is that it has been associated with apoptosis process (Nguyen and Pollard, 2000), suggesting that the process of MG involution is already active one day after weaning. In order to gain some insight into the molecular phenotype at this MG developmental time point I made and screened a cDNA library made with mRNA isolated from MG taken from Dams one day after weaning. As opposed to a conventional library screen I used clones isolated from this library to create a custom macroarray that was then differentially screened.

The macroarray or microarray screen is a tool that allows us to examine the expression of a large number of genes in a relatively short period of time. Conventional microarrays consist of gene specific oligonucleotides or cDNA inserts dotted onto a nylon membrane or a glass slide. In either case the array is screened with a cDNA derived probe. The macroarray I used was constructed by dotting purified PCR products of individual clones isolated from the I1 cDNA library onto a nylon membrane. In order to ensure reproducibility of the results each “clone” was dotted onto the same membrane in 3 different spots. A constant amount of PCR product for an individual clone is on each macroarray allowing for direct comparison between screens. The macroarrays were then probed with radiolabelled cDNA created from various conditions, in this case, cDNA was created from various time points during MG development (Virgin week 15 (V15); Pregnancy day 13 (P13); Lactation day 10 (L10); Involution day 1 (I1); Involution day 3 (I3) ). The results obtained depend on the amount of cDNA in each probe that is able to specifically hybridize to the PCR product of an individual clone on the macroarray. Therefore the varying levels of signal intensity from the autoradiographs of the macroarrays should be representative of the level of mRNA expression in the tissue that the cDNA was created from. By comparing intensities produced by the hybridization of

cDNA created from the different conditions, one can obtain an expression profile of a gene across the developmental time points in question.

In the last few years a number of studies have taken advantage of a global expression analysis that the macroarray/microarray screening allows. One group has taken to create their own limited cDNA clone array from cDNA libraries made from MG tissues taken from lactating animals and screening them with cDNA probes created from a broad spectrum of MG developmental tissues, including involuting MG (Lemkin *et al.*, 2000). Four published studies have screened affymetrix arrays, consisting of short gene specific oligonucleotides on a glass slide, for developmental time specific gene expression (Master *et al.*, 2002; Clarkson *et al.*, 2003; Clarkson and Watson, 2003; Rudolph *et al.*, 2003). The first approach has the advantage that the genes being screened are known lactating MG expressed genes, the limitation is the small size of the number of genes on the array (about 3000) and the fact that positive identified genes in the screen still need to be verified with respect to whether there is true expression during MG involution. The second approach has the advantage in that a very large number of genes can be screened; however each putative positive signal that results from the screen needs to be verified for MG involution expression before any conclusions can be made. Both approaches, however, give significant information that can be used to draw upon the types of cellular processes that are being augmented to define a specific transition from one developmental stage to the next stage in the course of MG development. The macroarray screen approach I utilize is different from the existing published microarray screens. First of all I started by generating my own gene array with clones taken from an I1 MG cDNA library derived from mRNA extracted from tissue at the exact developmental time point that I am interested in. This means that all the genes identified from the array constitute I1 MG expressed genes. For my work I wanted to obtain clones that had a high expression in I1 and had a varying expression pattern over the remainder of the MG developmental profile, representing the switch in genetic expression with the change in environmental pressures at this point.

## **3.2 RESULTS**

### **3.2.1 Quality Control of Total RNA**

Total RNA was isolated from the MG of a female mouse one day after weaning (I1) of the pups. The RNA was run on a 1% agarose denaturing gel to determine the quality of the RNA based on the integrity of the 18s rRNA band. Figure 3.1A shows the 18s and 28s rRNA bands of the MG at day 1, 2, and 3 of involution (I1, I2 and I3 respectively). The RNA used in the creation of the day 1 involution cDNA library (I1 MG cDNA library) is observed in the first lane (I1). The rRNA bands are well defined and there is little to no smearing above or below each band. This quality can be compared to the RNA in lane 2 (I2) where degradation is observed and characterized by bands that run lower on the gel and show smearing below the band. Lane 3 consists of I3 total RNA and does not appear to be degraded. The creation of the library using the total RNA from the first lane (I1) resulted in a phage library with a titer of  $1.27 \times 10^9$  plaques/ml. 2685 plaques produced from plating an aliquot of the library were isolated, PCR amplified, and the resulting products were run on a gel (figure 3.1B). The products that appeared to have a single band were used to create macroarrays. The bands amplified from the library ranged in size from approximately 400 bases to approximately 3kb.

### **3.2.2 Differential Screening of the I1 Involution Library**

Two sets of screens were completed through the course of my experiments (figure 3.2). Both screens involved cDNA libraries made from total RNA isolated from mouse MG tissue one day after weaning or involution day 1 (I1). The basic protocol was followed in both screens. Selection of clones with differential hybridization signals were identified and the clones were submitted for single pass sequencing to generate an expressed sequence tag that could be used for BLAST analysis and gene identification.

The first screen involved the isolation of highly expressed genes by screening plaque lifts made from an existing amplified I1 MG cDNA library with I1 MG cDNA. Unfortunately, because the MG is involved in the production of milk proteins during this period, a high number of clones representing milk associated proteins were isolated; 30/53 or 57%.

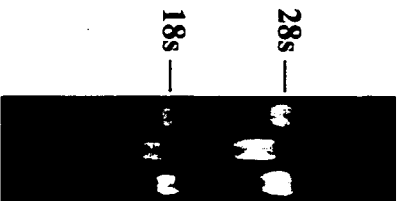
**Figure 3.1: cDNA library synthesis and validation:**

**A) Quality of RNA:** Total RNA was isolated from the MG of mice at different times during development. One day after weaning (Involution 1) is the focus of the study and the time point selected for creation of the cDNA library. After isolation, total RNA was run on a 1% agarose denaturing gel, stained with ethidium bromide and photographed. The corresponding 18s and 28s rRNA bands are indicated. RNA from the sample run in involution lane 1 was used to make a cDNA library in the Uni-ZAP XR phage vector system.

**B) Validation of the cDNA library:** Clones were isolated from the library and the cloned inserts were PCR amplified using primer sites adjacent to the cloning site. PCR amplified inserts were run on a 1% agarose gel and stained with ethidium bromide. The negative image of a representative gel is shown. The sizes of the inserts shown are representative of the clones isolated in general. Some PCR reactions did not produce any detectable insert (CG 200 bordered) but in general The cloned insert sizes ranged from 400 bp up to 3000 bp (\*). The standard marker used in these gels is Invitrogen's 1kb+ ladder. Those PCR products that displayed a single tight band were used in the creation of the macroarrays.

**A)**

**Involution 1  
Involution 2  
Involution 3**



**B)**

**PCR amplified inserts from isolated clones**

- Marker
- TL289T
- CG267
- TL266
- D151
- CG133
- D29
- CG146
- D181
- BL189
- BL136
- CG255
- BL191
- BL1350
- VL364
- BL182
- CG200**
- BL153
- D124
- BL155
- BL2584
- VL98
- D372
- D172
- CG78

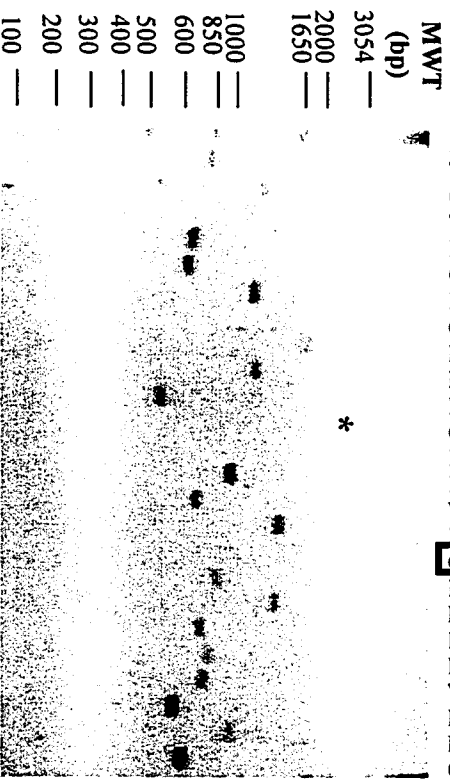


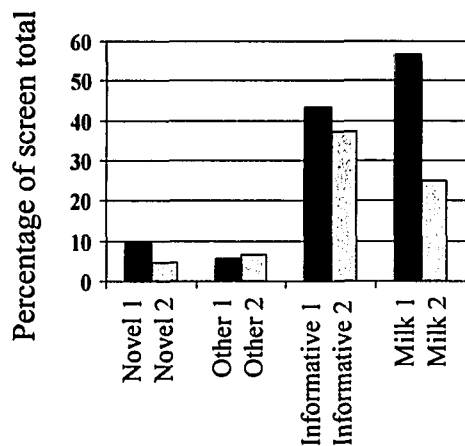
**Figure 3.2: Distribution of Clones Isolated From the MacroArray Screen:**

- A) All clones that were subjected to sequence analysis were grouped based on their biological function and common characteristics. Groups with 5 or more representative clones isolated from the screen were tabulated above. Groups with 4 or less representatives isolated from the screen were placed in the “other” category. Clone numbers are present from the first and second screens with the total number of representatives in the last column.
- B) A comparison was done between the two screens to identify the effectiveness of the selection process. The total number of clones representing one group was divided by the total number of clones identified in that screen. The subsequent values are compared to each other in graph B.
- C) The number of isolated clones was totaled for each group and divided by the total number of differentially expressed clones identified in the screen. The resulting percentage was graphed as above. Letters identifying each column (A....I) correspond to the respective group in the chart (A).

A

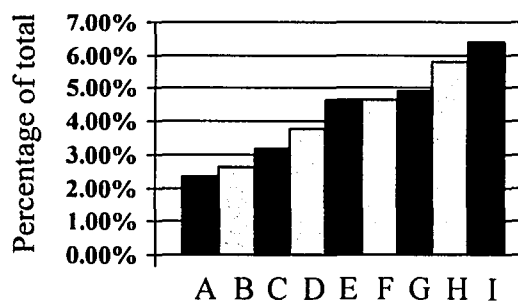
	Gene category according to Function	Screen 1	Screen 2	Total
A	Protease Inhibitors	2	6	8
B	Calycin Superfamily	4	5	9
C	Cell Adhesion	0	11	11
D	Stress	2	11	13
E	Iron Metabolism/Binding proteins	0	16	16
F	Transcription/Translation	2	14	16
G	Ribosomal	5	12	17
H	Novel/Unknown function	5	15	20
I	Other	3	19	22
	<b>Subtotal of informative sequences</b>	<b>23</b>	<b>109</b>	<b>132</b>
	<b>Milk Protein</b>	<b>30</b>	<b>73</b>	<b>103</b>
	<b>E.coli derived clones</b>	<b>0</b>	<b>33</b>	<b>33</b>
	<b>Uninformative</b>	<b>0</b>	<b>78</b>	<b>78</b>
	<b>Total clone analysis</b>	<b>53</b>	<b>293</b>	<b>346</b>

B



Categories from individual screens

C



Total clones from each category

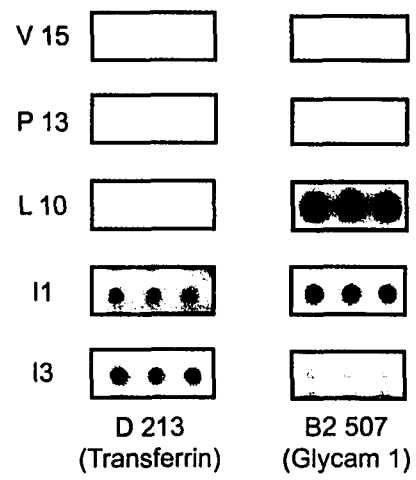
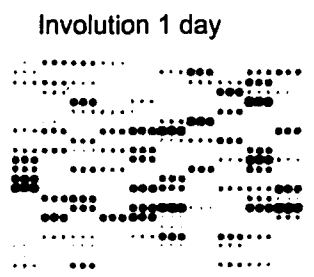
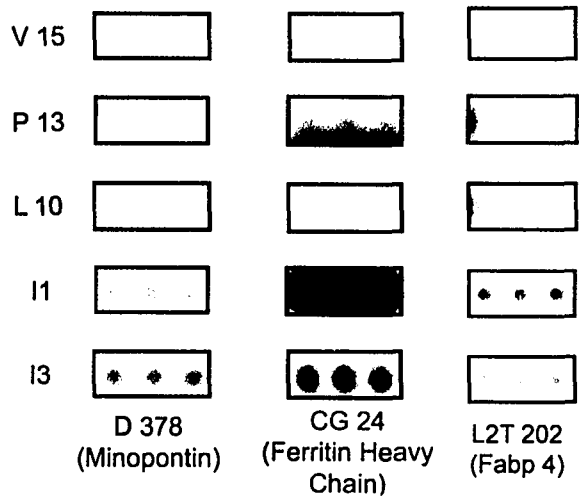
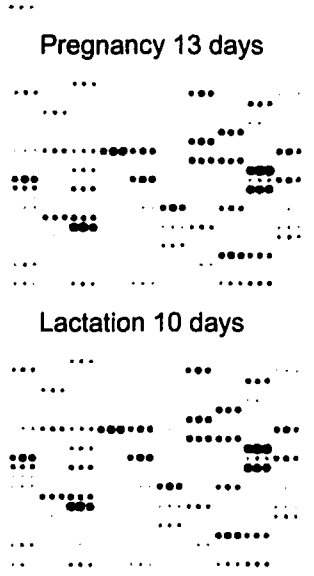
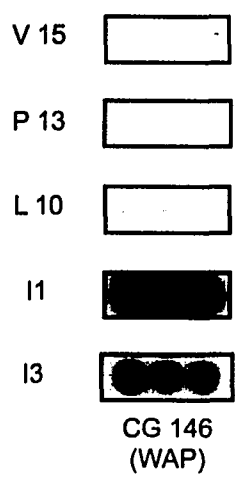
In case the high incidence of clones corresponding to milk proteins was due to the library amplification, I made a second cDNA library from new I1 MG tissue with the intention of working with it in an unamplified state. In total 2685 plaques were isolated from the unamplified library. Each clone was subsequently amplified by PCR. Of the 2685 clone stocks, 1488 produced a single PCR product upon electrophoretic analysis. Macroarrays were created from the PCR products that produced single amplified DNA bands. Differential screening was performed on the macroarrays with radiolabelled PCR amplified cDNA made from RNA isolated from MG from Dams at day 10 lactation (L10) and MG from Dams one day after weaning (I1). In the pilot analysis of 20 apparent differential clones I found a high number of clones corresponding to milk associated proteins (10/20, 50%). As an alternative I reanalyzed the macroarrays using the hybridization patterns for each clone on the arrays with 5 different PCR amplified cDNA probes derived from mRNA isolated from (figure 3.3):

- a) MG from 15 week old virgin animals (V15)
- b) MG from Dams at 13 days pregnancy (P13)
- c) MG from Dams at day 10 lactation (L10)
- d) MG from Dams one day after weaning, Day 1 involution (I1)
- e) MG from Dams three days after weaning, Day 3 involution (I3)

A few clones that gave identical hybridization profiles as a known whey acidic protein (*WAP*) clone on the array were also sequenced. In all cases the clones were found to correspond to the *WAP* gene sequence, thus confirming the reproducibility and consistency of the screen employed. Clones that showed a MG developmental expression profile that was different from *WAP* were further selected for sequencing and subsequent blast analysis.

Application of a 5 way differential screening system identified 293 clones as MG developmental differentially expressed genes over the course of postnatal MG development. 73 of these clones were found to correspond to milk related protein genes (alpha casein, *WAP* etc). With only 33% of the sequenced clones from this screen corresponding to milk associated protein genes, this selection system appears to be more efficient in obtaining non-milk associated factors, than selecting for highly expressed genes (57% milk protein genes; figure 3.2). From the analysis of the 5 way differential

**Figure 3.3 Macroarray Screen:** Mammary macroarrays were created from the I1 cDNA library. Macroarrays were made in 5 duplicates and each macroarray was probed with a different cDNA probe representing 5 developmental stages of the MG postnatal developmental cycle. Differential clones were selected by eye based on the varying profiles. A second selection was done in an attempt to reduce the number of milk associated proteins by looking for profiles that did not conform to the WAP profile. Minimum activity used per hybridization was  $1.6 \times 10^6$  CPM/ml.



selected clones, 33 corresponded to *Escherichia coli* related sequences, and attempts at sequencing 78 of the clones did not give readable DNA sequence. In the end 109 (7% of total number screened) clones from the original 1488 PCR products on the macroarray corresponded to putative MG differentially developmentally expressed genes that were not milk protein genes.

The sequence analysis of all clones isolated in the study is summarized in figure 3.2. Clones were categorized according to the perceived function of the gene that they corresponded to. Between the two major screens (the screen for highly expressed genes, and the 5 way differential screen) a total of 103 clones were identified that corresponded to milk associated protein genes, and a total of 132 clones were identified that corresponded to MG developmentally expressed genes of non-milk protein gene origin. A distribution of the types of genes isolated according to broad gene function is given in figure 3.2. What is evident from these results is that the second screen reduced the number of isolated milk proteins (56% down to 25%) while mostly maintaining the percentage of informative clones (43% compared to 37%). Unfortunately with this screen, the number of novel clones isolated decreased (9.4% down to 4.8%).

The sequence of each non-milk protein associated clone and the corresponding blast analysis results can be found in appendix A. Within the subgroup of 132 non-milk protein gene clones, 20 either do not have sequence similarities to known sequences in the NCBI database, or correspond to expressed sequence tags that do not yet have a known function. In either case I regard these 20 clones as representing novel uncharacterized genes. 22 clones that corresponded to genes that segregated into distinct functional groups but which were the only member of that group were classified under the category “other”. Other groups of clones obtained fell into functional gene categories such as stress related, ribosomal, cell adhesion, protease inhibitors, transcriptional and translational related, iron metabolism, and the Calycin superfamily of genes (figure 3.2). Clones belonging to iron metabolism and the Calycin superfamily of genes will be elaborated on in Chapter 4.

### 3.2.3 Validity of Genes Isolated from the Mammary Gland

To determine if the cDNA clones I identified and sequenced represented genes that had been previously isolated from the MG, I examined the UNIGene database. Out of the list of clones, only 3 clones represent genes (*orm2*, *cox2*, *cox3*) that have not been previously isolated from mouse or human MG. The remainder of the genes isolated from my screen have previously been identified in the MG (though not necessarily during the course of involution). Therefore the screen that I completed on the MG to identify MG expressed genes is consistent with previous studies with the large majority of genes having been previously isolated from MG cDNA libraries.

### 3.2.4. Expression

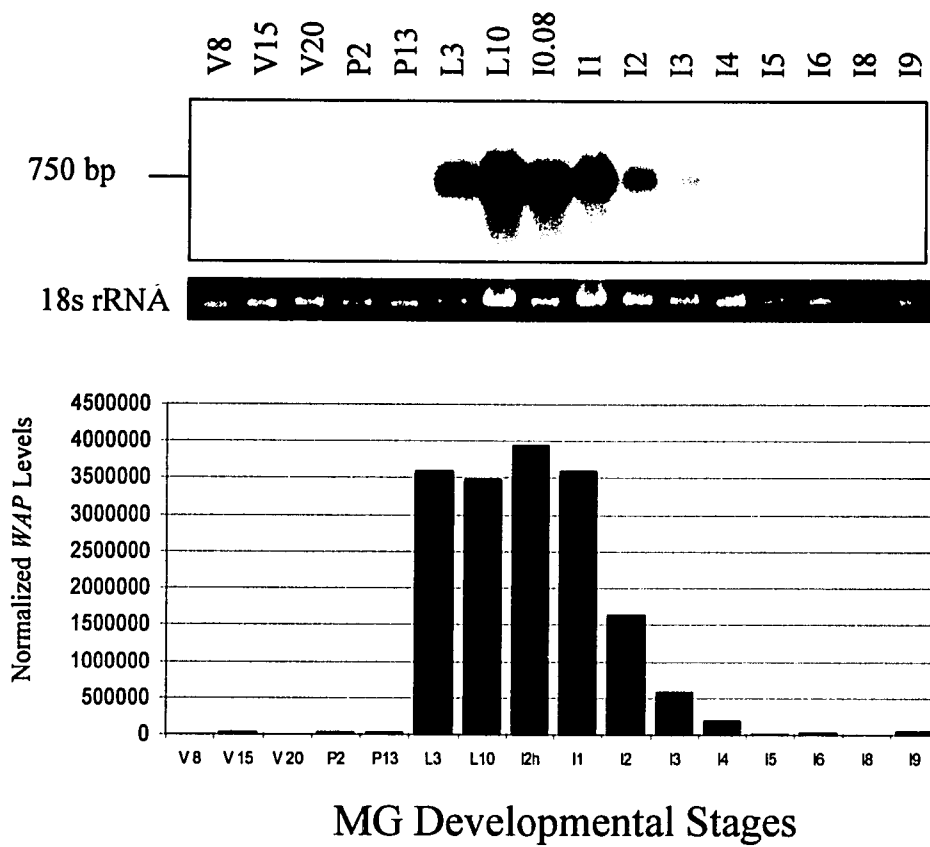
A DNA probe for *WAP* was hybridized to a northern blot to confirm the postnatal developmental profile of the tissues and RNA used in the study (figure 3.4). *WAP* mRNA levels become detectable by L3, and remain high at L10, I 0.08, and I1, but begin to decrease by I2. By mid-late involution (I5-I9) *WAP* mRNA levels return to those observed in the virgin time period. This confirms the profile observed in the results of Burdon *et al.*, 1991 and Lee *et al.*, 1996.

The origin of each clone in the current study is from an I1 MG cDNA library. By definition each clone isolated defines a gene that is expressed in MG one day after weaning, one day after the induction of the involution process. Northern analysis was used to confirm that a portion of these genes are differentially expressed over the period of postnatal MG development. 14 of the northern analyses are shown in this chapter (figures 3.5-3.6). The analysis of clones corresponding to known genes is presented in figure 3.5. The analysis of clones corresponding to novel genes is presented in figure 3.6. The MG developmental northern profile consists of MG RNA samples isolated from V15 or V20, P2, L10, I1, I3, and I9 or I10 animals.

The developmental MG expression profiles of non-*WAP* genes placed on northern blots isolated from the I1 MG cDNA library, revealed a differential expression profile for all of the clones/genes analyzed (figure 3.5 and 3.6). The majority of the genes assayed by northern analysis do not share the same profile as *WAP* (something that was selected for). Three genes (malic enzyme, *glycam1* and *claudin 3*), however, have

**Fig 3.4: *WAP* Northern Expression Profile:** The probe for *WAP* was made from the PCR product produced from the respective cDNA clone. It was labelled with  $\alpha$ -<sup>32</sup>P-dCTP using Invitrogen's Random Primer Labelling Kit. Hybridization was carried out overnight at 65 degrees Celsius. Bands observed on the northern blots were normalized to the 18S rRNA from the gel and processed through densitometry. The results from the normalization can be observed below the northern blot. The intensity of the EtBr stained 18S rRNA band was used as a loading control (Correa-Rotter, 1992).

V: Virgin; P: Pregnancy; L: Lactation; I: Involution



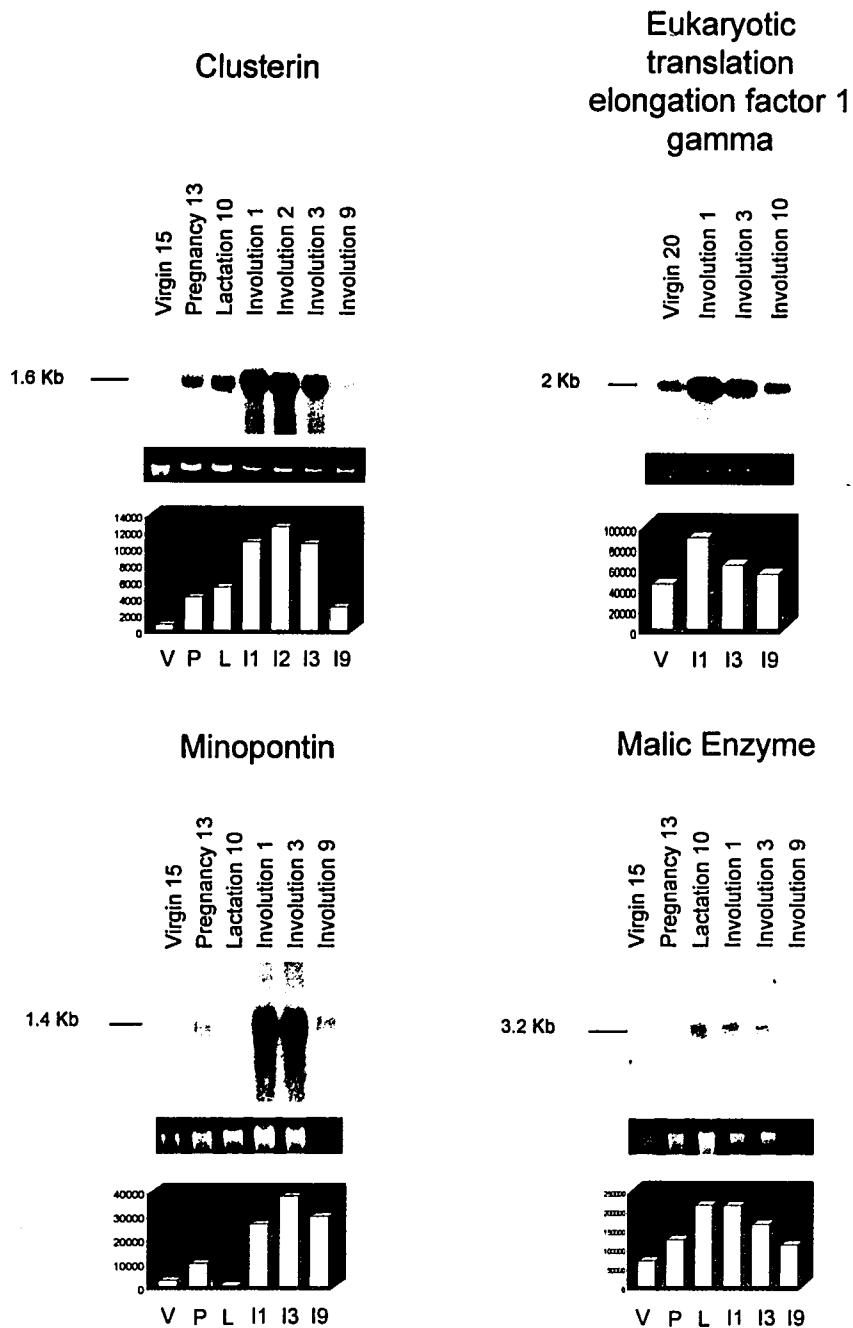
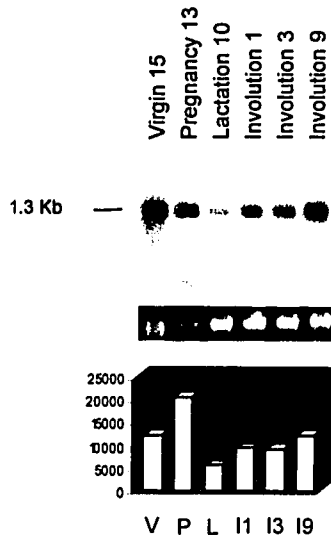
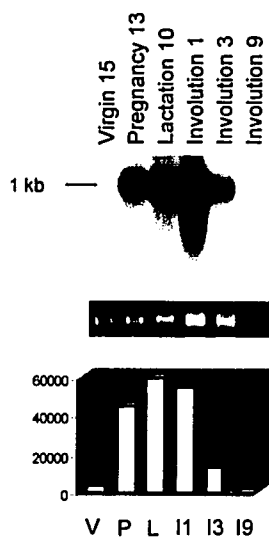


**Figure 3.5: Known Clone Northern Analysis:** Probes were made from the PCR product produced from the respective cDNA clone. They were labelled with  $\alpha$ - $^{32}$ P-dCTP using Invitrogens Random Primer Labelling Kit. Hybridization was carried out overnight at 65 degrees Celsius. Bands observed on the Northern blots were normalized to the 18S rRNA from the gel and processed through densitometry. Northern blots with multiple bands were subjected to densitometry for each band. The intensity of the 18S rRNA band was used as a loading control (Correa-Rotter, 1992).

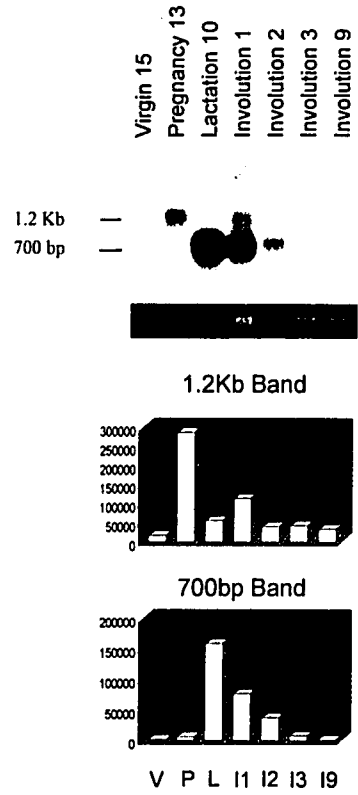
LLRep 3



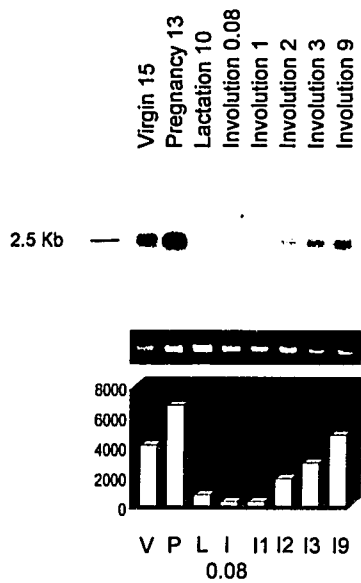
Glycam 1



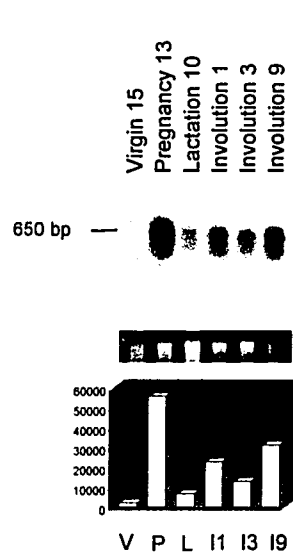
Claudin 3



SPARC



Hemoglobin alpha



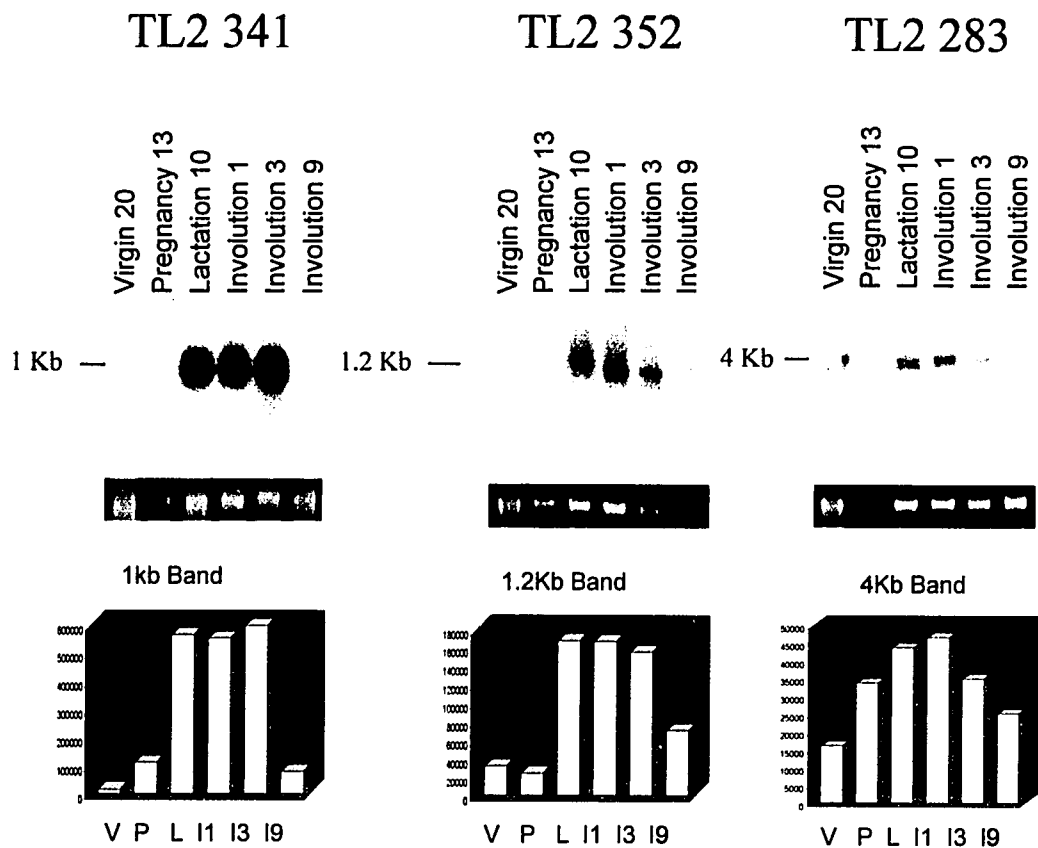
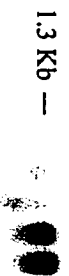


**Figure 3.6: Unknown Northern Analysis:** Probes were made from the PCR product produced from the respective cDNA clone. They were labelled with  $\alpha$ -<sup>32</sup>P-dCTP using Invitrogens Random Primer Labelling Kit. Hybridization was carried out overnight at 65 degrees Celsius. Bands observed on the northern blots were normalized to the 18S rRNA from the gel and processed through densitometry. If multiple bands appeared on the northern, each one was normalized and can be observed in the graphs below the Northern. The results from the normalization can be observed below each respective northern. The intensity of the 18S rRNA band was used as a loading control (Correa-Rotter, 1992).

### TL2 324

Virgin 20  
Pregnancy 13  
Lactation 10  
Involution 1  
Involution 3  
Involution 9



18s rRNA



1.3Kb Band



### TL2 215

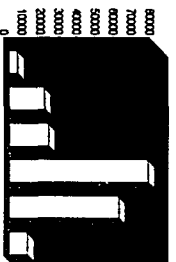
Virgin 15  
Pregnancy 13  
Lactation 10  
Involution 1  
Involution 3  
Involution 9



18s rRNA



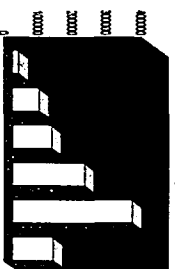
3.8Kb Band



1.9Kb Band



800bp Band



V P L I1 I3 I9

similar profiles to *WAP* with an increase in mRNA levels during lactation, high levels through early involution, after which levels decreased by I2/I3.

Looking at the transition from lactation to involution stages a number of genes show a more pronounced difference in relative mRNA levels between L10 and I2h/I1 than that seen with *WAP*. From the nine known genes examined on northern blots in this chapter, 5 show expression profiles where mRNA levels increase from L10 to I1 (minopontin, clusterin, LLRep3, haemoglobin alpha, claudin 3 (1.2b band)), 3 show a decrease in levels from L10 to I1 (eukaryotic translation elongation factor 1 gamma (*EFl* gamma), *glycam1*, and *sparc*) and one does not change (Malic enzyme)

Gene	L10 Densitometry	I1 Densitometry	I1/ L10	Net change	Ontology
Glycam1	58829.03	53614.2	0.91	D	adhesion
Eef1g	88286.2	61970.26	0.7	D	translation
Sparc	714.20	267.22	0.37	D	stress
Malic enzyme	210778.4	209876.5	0.99	N	other
Minopontin	151.99	26071.18	171. 53	I	other
Clusterin	5205.88	10674.62	2.05	I	stress
LLRep3	5467.39	9353.32	1.71	I	ribosomal
haemoglobin alpha	6453.34	22584.75	3.5	I	iron metabolsim
Claudin3	54863.63	113454	2.06	I	adhesion

**Table 3.1: Difference in Densitometry Values Between L10 and I1 for Known**

**Clones:** The normalized densitometry values were compared between L10 and I1 to exemplify those clones that exhibit a decrease in mRNA levels at the switch, and those that exemplify an increase in mRNA levels at the switch. (D= decrease; I=increase; N=neutral)

The gene expression profiles revealed by northern analysis can be clustered, by eye, into 3 broad profiles according to when the initial induction that leads to the peak level is observed (figure 3.7). The three profiles observed are as follows; Wave 1 genes: Genes that are pregnancy induced (the initial rise in mRNA levels that leads to the most

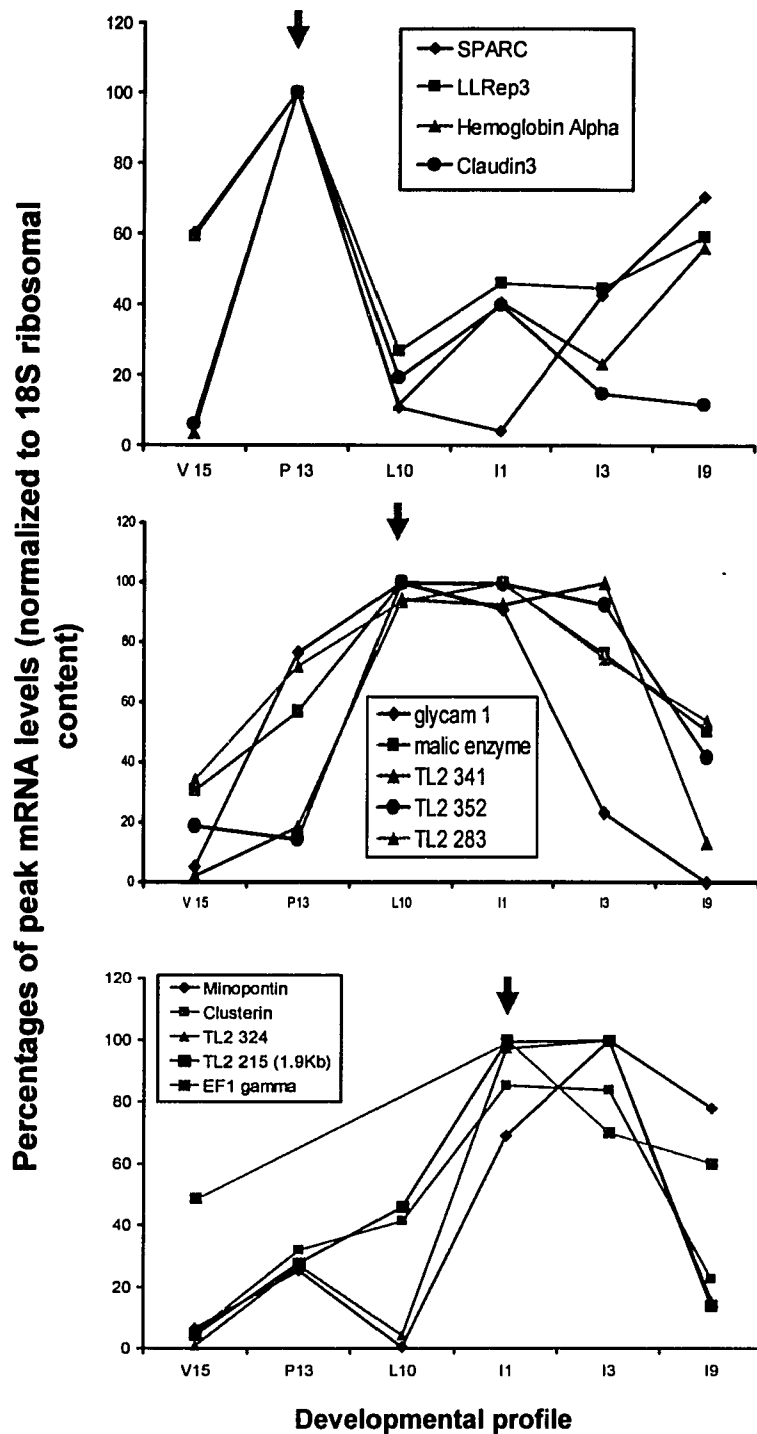
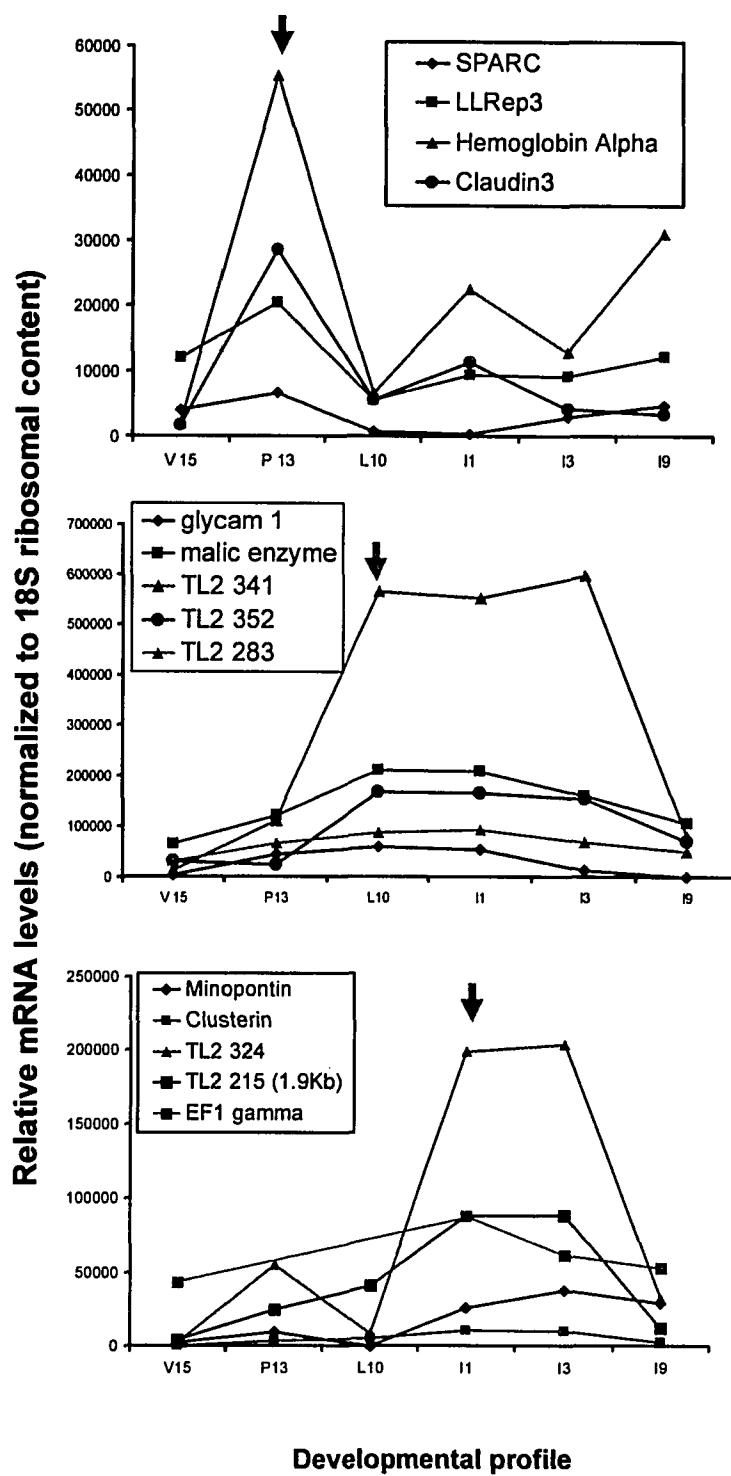


**Figure 3.7 Observing common profiles among the clones placed on northern:** Using the values obtained from the normalized densitometry these graphs were created to demonstrate the common trends that are apparent when looking at the northern profiles of the clones in chapter 3. Each clone was normalized to the developmental stage with the highest level of mRNA detection. Clones were grouped based on common peaks, common points of increased and decrease expression, and common overall profiles. To create the profiles only common developmental stages among all northern profiles were included for the trend analysis. Arrows indicate peak points of mRNA intensity



prominent peak occurs between V15 and P13); Wave 2: Genes that are lactation induced (the initial rise in mRNA levels that leads to the most prominent peak occurs between L3 and L10), and; Wave 3: Genes that are involution induced (the initial rise in mRNA levels that leads to the most prominent peak occurs between L10 and I1). The genes that “peak in pregnancy” are *sparc*, *LLRep3*, and haemoglobin alpha and claudin 3. The second wave of genes that “peak in lactation” are *glycam1*, malic enzyme, TL2 341, TL2 352. The wave 3 genes that “peak in involution” are clusterin, minopontin, TL2 324, TL2 283, TL2 215 (1.9kb), and *EF1* gamma. For the majority of all genes examined in this chapter by northern analyses, mRNA levels fall by late involution (I9) to levels close to those observed at V15 (the virgin period). In the developmental profile examined I9 is quickly approaching a state that is defined as the virgin-like state (few epithelial cells, higher density of stromal cells, and a reappearance of adipocytes). The profiles for iron binding protein genes and the calycin superfamily genes identified in this study are presented in chapter 4. In brief, the majority of the genes in these two gene groups have a similar expression profile to the patterns described above.

### 3.3 DISCUSSION

#### 3.3.1 Effectiveness of the 5 Way Differential Screen

Of the clones screened by the 5 probe differential system roughly 7% were found to be putatively differential in nature. This percentage is higher than what is typically seen in a differential screen of 1% (Guenette *et al.*, 1994; Ishida *et al.*, 1992), but the selection process implemented in my study was much broader as it encompassed an analysis of 5 cDNA probes as opposed to 2. The relative profile of a known *WAP* clone on the arrays was used as a rough guide to help avoid the selection of milk protein genes. This selection was only partially successful. Of the clones identified and that gave analyzable sequence, 33% (73/215) still corresponded to milk associated protein genes. Although, not perfect, the screen was able to reduce the isolation of clones associated with milk production as compared to a screen for purely highly expressed genes or by a L10/I1 differential screen.

The presence of clones with *E.coli* sequence from the screen was unexpected. The mouse MG cDNA library was screened with mouse MG cDNA, which should result in

the isolation of genes expressed in the mouse. I eventually found out from the manufacturer of the vector used (Stratagene) that some of the components in the cloning kit may have had abnormally high levels of bacterial contamination and that bacterial DNA was more than likely incorporated in the cloning procedures. This contamination would be present in the phage library and hybridization with cDNA within the probe that had sequence similarities to *E. coli* genes could lead to their isolation.

A correlation of the selective macroarray results shown in figure 3.3 with their corresponding northern profiles (figure 3.5) suggests that for a good portion of the clones the array results are reflective of the northern results. In some cases however the array profiles and the northern profiles are different (*fabp4*, *WAP*). This result could be due to the fact that I used amplified cDNA as probe for the macroarray screens. Depending on the extent of the amplification of the cDNA the amplification could have altered the actual representation of expressed genes in a given tissue (Ji *et al.*, 2000).

Alternatively, another reason the macroarray screen produced gene profiles that did not match up to their corresponding northern profiles could be due to differences in the nature of hybridization that is occurring in each of the experiments. In the case of the macroarray, a specific DNA sequence is being screened with a probe that is made up of a mixed array of cDNA sequences (a tissue derived cDNA probe). In theory, if a particular gene is a member of a gene family, then more than one “gene” sequence can be hybridizing to it, especially at the reduced stringencies that the array screening is carried out. In the case of a northern analysis you have many possible gene sequences on the blot but you are hybridizing a single gene sequence to it. Although many bands may be detected (in cases where the gene in question is part of a very similar gene family) the transcripts that hybridize and therefore the genes themselves can be differentiated by size. Although the northern profiles of the genes tested in this chapter did not necessarily reflect the profile seen on the macroarray (data not shown), the analysis did reveal that all clones/genes placed on a northern blot showed a differential gene expression profile over the course of MG development. The screening method therefore was successful in identifying those genes that did change their levels of expression over the course of MG development, although the accuracy of the profile could not be assured.

### 3.3.2 Gene Expression

In the further analysis of my clones it became evident that certain groups of genes were more abundant than others. The most pronounced gene groups include genes related to iron metabolism, and genes coding for ribosomal proteins (figure 3.2). Ribosomal protein genes have been previously isolated from a cDNA differential screen and displayed an increase in involution of the MG (Lee *et al.*, 1998). *LLRep3 (Rps2)* has not been analyzed functionally in depth over the course of MG development, but the basic activity of any ribosomal protein suggests that changes in ribosomal protein expression reflects either the requirement for translation, potentially of specific translation, or changes in the translation machinery. The potential roles of iron binding proteins and calycin superfamily during post-natal development are elaborated on in chapter 4.

A high percentage of clones representing novel (uncharacterized) genes were identified in the current study. 20/346 or 6% of the total clones analyzed contained features that categorized them as novel. To better understand a possible role for the unknown genes in the MG, a number of the respective clones were used for northern analysis on MG developmental blots. All of the clones examined showed differential expression over the MG developmental profile, with a high level of mRNA in the period of the profile where there is a switch from lactation to involution (figure 3.6). TL2 341 and TL2 352 could be associated with milk production as they produce similar expression profiles as *WAP*, though they maintain high levels of mRNA in I3, which is typically lower in factors associated with milk (Liu *et al.*, 1995; Bong *et al.*, 2002). Factors that show a high level of mRNA during or after this switch could represent genes with a role involved in the induction of involution or the progression of this event. To specifically define their role during MG development requires additional studies, including a more in-depth sequence analysis, elucidation of potential gene structures from the mouse genome database, and subsequently additional studies to define function.

The switch in expression between L10 and I1/I2h represents the switch from cell proliferation/maintenance to cell death. The difference in genetic expression between these two environments should be reflective of the global events that are occurring in the tissue through this change. Genes involved in metabolism and maintenance of function appear to be prominent before the switch to involution, i.e. in pregnancy and lactation

(malic enzyme, claudin3, glycam1, sparc, *LLRep3*). These genes are known to be down regulated when the system becomes stressed and begins to involute (Clarkson and Watson, 2003). When the MG involutes, genes involved in cell protection and cell death are induced, this would include proteins associated with inflammation, apoptosis, and cell stress (clusterin, minopontin, *eef1g*). These genes are known to underlie roles in alleviating stress by either adding a protective effect or by aiding in controlled cell death (French *et al.*, 1994; Standel *et al.*, 2004; reviewed in Yan *et al.*, 1999). Thus the switch from lactation to involution depicts a switch in genetic expression from milk production to cell protection and death.

### 3.3.3 Gene Profiling

A comparison of the expression profiles of the clones placed on northern blots revealed three distinct patterns (Wave 1 (pregnancy induced), Wave 2 (lactation induced), Wave3 (involution induced) genes (Figure 3.7). Wave 1 genes include sparc, *LLRep3* and hemoglobin alpha, claudin 3. Sparc is a soluble protein involved in tissue development/differentiation (Bradshaw and Sage, 2001) by inducing and organizing connections to ECM proteins such as fibronectin and collagen IV (reviewed by Brekken and Sage, 2001; Puolakkainen *et al.*, 2003). *LLRep3* has been observed to be up regulated in embryogenesis and its expression is dependent on cell growth (Heller *et al.*, 1988). Haemoglobin alpha is a subunit of haemoglobin and is present in high amounts where there is high blood content. During pregnancy there is a massive increase in vascularization throughout the MG (Djonov *et al.*, 2001) and the induction of the genes identified here as Wave 1 genes may contribute to this process. Claudin 3 is involved in the formation of tight junctions between epithelial cells, as development during pregnancy occurs, MEC number increases and so does the number of interactions between cells (Matsuda *et al.*, 2004). These factors identified in Wave 1 correlate to the development of the MG.

Wave 2 (“lactation induced”) genes include glycam1, malic enzyme and three novel genes (TL2 341, TL2 283 and TL2 352). The production of milk is the predominant metabolic activity of the MG during the lactation stage of MG development. Glycam1 has historically been classified as a milk protein (Dowbenko *et al.*, 1993) as it is

present in the membrane of milk globules, but more recent studies suggest that glycamin might also play a role in the immune system by mediating the transfer of blood borne lymphocytes into secondary lymph nodes (Rasmussen *et al.*, 2002). Malic enzyme is required for NADPH production and expression is dependent on levels of carbohydrates in the system, but is also influenced by thyroid hormones (Gonzalez-Manchon *et al.*, 1995). The increase of malic enzyme at lactation could be due to the increased requirement of energy due to the high metabolic activity of the tissue during lactation.

Wave 3 (“involution induced”) genes include clusterin, EF1 gamma and minopontin and two novel genes (TL2 324 and the 1.9Kb band of the TL2 215 clone). Clusterin expression has been previously observed at this stage in MG postnatal development (reviewed in Jones and Jomary, 2002; French *et al.*, 1996) and has been associated with providing a protective effect to neighbouring apoptotic cells (French *et al.*, 1994). Clusterin has also been identified as a potential pro-apoptotic factor showing high levels of expression in the nucleus of cells in apoptotic tissues (Yang *et al.*, 2000). Either one of these functions validates the observed expression of clusterin after the switch from lactation to involution and the removal of expression by late involution. Minopontin (osteopontin) is a factor known to be associated with invasive metastatic growth (Borlak *et al.*, 2005) and has been thought to be expressed in tissues undergoing apoptosis (Rittling and Novick, 1997, Lee *et al.*, 2000). EF1 gamma has yet to be characterized in the MG, but is known to traffic tRNA to the ribosome for translation (Lew *et al.*, 1992). The clustering of the genes identified above indicates a possible coordinate regulation of various genes that is in turn regulated by the switch from one phase to another during MG development. The functions of the genes identified and the stage during MG in which they are highly expressed seem to correlate with the perceived biological needs of the tissue at that specific stage of development.

### **3.3.4 Conclusions**

Through the macro array screen I was able to identify 132 clones that displayed a differential profile over the course of postnatal MG development. Among the most abundant types of genes identified were genes that represented ribosomal protein genes and iron binding/metabolism genes. Northern analysis validated the differential

expression over the course of MG postnatal development for 14 genes selected from my screen. Genes identified here in the current study define 3 groups of genes (3 waves) with distinct expression profiles. 8 known genes of those identified define molecular changes during the L10 to I1 transition period. The results of the current study support my initial hypothesis that differences in the expression of specific subsets of genes may define the change in the tissue environment over the course of MG postnatal development.

## CHAPTER 4 – THE CALYCIN SUPERFAMILY AND IRON METABOLISM GENES

### 4.1 INTRODUCTION

Of the 132 clones identified and that correspond to non-WAP genes; further analysis was done on two subgroups of genes identified, namely genes defining iron binding proteins and those that are members of the Calycin superfamily of genes (Table 4.1).

Group	Gene Name	Accession Number
Iron Metabolism	transferrin ( <i>trf</i> )	NM_133977.1
Iron Metabolism	lactotransferrin ( <i>ltf</i> )	NM_008522.2
Iron Metabolism	ferritin heavy chain ( <i>fth</i> )	BC012314.1
Iron Metabolism	ferritin light chain ( <i>flt</i> )	AK011244.1
The Calycin Superfamily	fatty acid binding protein 4 ( <i>fabp4/afabp</i> )	AK003143
The Calycin Superfamily	fatty acid binding protein 3 ( <i>fabp3/hfabp</i> )	BC002082
The Calycin Superfamily	lipocalin 2 ( <i>lcn2/NGAL/24p3</i> )	X14607
The Calycin Superfamily	orosomuroid 1 ( <i>orm1/AGP</i> )	NM_008768

**Table 4.1 Genes Relating to Iron Metabolism or the Calycin Superfamily:** The gene identity of each clone was identified using the NCBI BLAST analysis (Appendix A). Genes that define either iron metabolism genes or members of the calycin superfamily of genes and identified in my screen are tabulated here. In cases where a given gene has more than one gene symbol, the symbol shaded in grey is the one used for the duration of the thesis.

Under careful scrutiny it was found that these two groups are interrelated, lipocalin 2 (*lcn2*) has iron binding capabilities (Yang *et al.*, 2002, Kaplan, 2002) and orosomuroid 1 (*orm1*) is an acute phase response protein which has anti-inflammatory properties (de Vries *et al.*, 2004; reviewed in Fournier, Medjoubi-N and Porquet, 2000). Lactotransferrin (*ltf*), an iron binding protein, is also capable of performing both functions mentioned above (reviewed in Legrand *et al.*, 2004). Indirectly then members of these two gene groups have a common role in responding to cellular stress. 25 clones of the 132 isolated belong to either of these two categories of genes. In this chapter I will review what is known about these genes in the context of MG biology and function, and

use bio-analysis and meta-analysis approaches to search for any additional common features between these two groups of genes.

#### 4.1.1 The Iron Binding Proteins

Iron is a metal that is required in numerous cellular processes, but can also be extremely toxic to a cell (Halliwell and Gutteridge, 1984; reviewed in Meneghini, 1997). High levels of iron can result in massive tissue and DNA damage; in contrast, extremely low iron levels can result in anemia (reviewed in Arosio *et al.*, 2002; Doreswamy and Muralidhara, 2005). The cell produces numerous factors that can modulate iron levels to meet the metabolic requirements, as well as some that can protect cells from the toxic effects of free iron (Halliwell *et al.*, 1988). It is essential to cell survival that these factors exist since free iron can react with hydrogen peroxide through the Fenton reaction (Figure 4.1) to produce hydroxyl radicals (Casanueva and Viteri, 2003; Held *et al.*, 1996). These radicals can cause single and double stranded DNA breaks. Free iron also has the ability to cause lipid peroxidation that leads to the formation of hydroxyl radicals and aldehydes that can damage DNA (Casanueva and Viteri, 2003). The presence of oxygen free radicals can also result in the production of 8-hydroxy-deoxyguanosine that can cause mutations in DNA by base mispairing during replication (Halliwell and Aruoma, 1991).

Through the differential screens I performed (Chapter 3), clones relating to iron metabolism were identified. Transferrin (*trf*) is a factor that can bind iron molecules outside of the cell and transport them into a cell by binding to the transferrin receptor (*tfr*) on the cell membrane (Monteiro and Winterbourn, 1988; Donovan and Andrews, 2004). This association internalizes diferric *trf*, and once internalized iron is released due to an acidic environment in the endocytic vesicle and used for normal metabolic needs or stored. The *trf* is subsequently returned to the extracellular space to repeat the process (Klausner *et al.*, 1983). Lactotransferrin or lactoferrin (*lft*) binds iron in the same manner as *trf* and has a similar structure to *trf*. The activity of *lft*, however, is more pronounced in stressed environments with high levels of free iron. Typically when levels of free iron are high, *trf* and *tfr* are down-regulated to prevent toxic levels of iron in the cell, whereas *lft* will be up regulated to take iron and sequester it in macrophages (Iyer and



**Figure 4.1: Fenton Reaction:** Ferrous iron salt has the ability to react with hydrogen peroxide and form the hazardous oxygen free radical  $\cdot\text{OH}$ . This radical can then react with other organic molecules in the cell and damage them. This includes DNA which can have double stranded breaks created or insertion of mutation inducing agents such as 8-oxo-guanine. (Henle et al. 1996).

Lonnerdal, 1993; Nuijens *et al.*, 1996). A macrophage is capable of storing large amounts of iron bound in ferritin molecules resulting in a protection for the surrounding cellular environment (Oria *et al.*, 1998). *Ltf* also has the ability to bind siderophore iron as a secondary protective action to prevent its utilization by bacteria (Kanyshkova *et al.*, 2003). Though the mechanism of action is similar for these two factors, the designated role for each is substantially different. By regulating these factors the cell is able to maintain an optimal level of iron to carry out normal cellular activity, without sustaining serious damage. Once inside the cell the free iron can be taken up by ferritin, a large spherical structure composed of numerous ferritin heavy chains (*fth*) and ferritin light chains (*fil*) (Arosio *et al.*, 1978; Boyd *et al.*, 1984) that can sequester the free iron (Monteiro and Winterbourn, 1988). Alternatively the iron can be immediately used in processes such as the electron transport chain, transcription, or oxygen transport (Crichton and Ward, 1995).

#### **4.1.2 The Calycin Superfamily**

There are three main groups of proteins that comprise the calycin superfamily; they are the lipid binding proteins (LBP), the lipocalins and the avidins. Members belonging to this superfamily are grouped based on their similarity in protein physical structure rather than sequence similarity. The hallmark structural feature of these proteins is a  $\beta$ -barrel configuration (figure 4.2) that has a general role in binding hydrophobic molecules. The  $\beta$ -barrel structure is compositionally different among the three subgroups of calycin genes; the LBPs have a 10 stranded  $\beta$ -barrel configuration while the lipocalins and avidins are comprised of 8 strands (Flower *et al.*, 1993; Muller-Fahrnow *et al.*, 1991). In addition the different groups of calycin gene proteins bind to different things. The LBPs have a major role in trafficking of fatty acids, the lipocalins are involved in binding extracellular hydrophobic compounds (LaLonde *et al.*, 1994), and the avidins have a high affinity for factors such as biotin and other related vitamins. Though there is some structural similarity, the relationship of avidins to LBP and lipocalins has been questioned due to weak structural homology between the groups.



**Figure 4.2: Beta Barrel Protein Structure:** The image above depicts the basic structure of the beta barrel formation. Beta sheets are created (usually in anti-parallel orientation) to form a structure that represents a hydrophobic pocket. Above, the beta sheets are arranged in parallel, which is depicted by the direction of the arrows. The sheets above are then tethered together by alpha helices, but this is not always the case. The dotted lines represent hydrogen bonds that aid in the structure of the barrel. In the situation of the LBP, alpha helices form and serve to function almost as a lid to the barrel creating a complete hydrophobic environment that is used to sequester various elements. Typically the calycin superfamily beta barrel structure is created by beta sheets in anti-parallel conformation (reviewed in Flower *et al.*, 2000). The structure was provided by Dr. Oliver Kreylos (2004).

The LBP are classified as being tissue specific proteins, and the different LBPs were initially named based on the tissue from which they were originally isolated. On a genomic level the LBP genes all maintain the same gene structure that consists of 4 exons (Li and Norris, 1997). Two clones were identified in the differential cross screen that had sequence corresponding to the LBP, fatty acid binding protein 3 (*fabp3*) and fatty acid binding protein 4 (*fabp4*). *Fabp3* is also known as heart *fabp* (*hfabp*) since it was initially identified in that tissue, even though it has a broad profile of tissue expression (Paulussen *et al.*, 1989). *Fabp3* has also been identified as being the human form of MG derived growth inhibitor (MDGI) (Phelan *et al.*, 1996). MDGI has been shown to have differentiation properties in the MG and is able to inhibit growth of the MG by restricting proliferation of the epithelial cells (Grosse *et al.*, 1991; Bohmer *et al.*, 1987; Kurtz *et al.*, 1998). *Fabp4* was initially isolated from adipose tissue and as such was named adipose *fabp*. *Fabp4*, unlike *fabp3*, is mainly expressed in adipose tissue alluding to a highly specific role in this tissue (Bernlohr *et al.*, 1984). Both factors have similar roles in that they are responsible for binding with high affinity to long chain fatty acids, but can also bind other molecules with structures similar to fatty acids (Kaikaus *et al.*, 1990). The reason for sequestering these fatty acids is not well known. It has been proposed that the trafficking of these fatty acids by FABP is part of a regulatory pathway mediated by peroxisome proliferator activated receptors, PPAR (Sorof, 1994; van Bilsen, 2002; Schoonjans *et al.*, 1995).

The lipocalins are mostly extracellular factors that have a role in binding hydrophobic compounds such as retinol and pheromones, and transporting them to cells by binding to extracellular receptors and that can internalize these factors for transport to their appropriate target. Three clones isolated from this screen are members of the lipocalin family. These factors are lipocalin 2 (*lcn2*; *NGAL*; *24p3*), orosomuroid 1 (*orm1*) and orosomuroid 2 (*orm2*). *Lcn2* has been characterized as a 25 kDa protein that associates to a matrix metalloproteinase, human neutrophil gelatinase (Kjeldsen *et al.*, 1993; Flower, North and Atwood, 1993). As a protective agent, *lcn2* is part of the acute phase response, the initial protein response to a toxic or damaging agent to the body, and has numerous functions. In the MG it can prevent neutrophils from invading the early involuting MG by forcing the neutrophils to enter apoptosis (Nilsen-Hamilton *et al.* 2003;

Bundgaard *et al.*, 1994). Post involution levels of *lcn2* remain high supporting a protective affect for the MG, possibly by inducing apoptosis in inhabiting neutrophils that are considered to be major contributors of oxygen free radicals. Interestingly *lcn2* has been shown to bind bacterial catechol-type ferric siderophores alluding to a role in an immune response by preventing bacterial growth (Goetz *et al.*, 2002). MG *lcn2* also has the ability to bind iron in a fashion similar to *trf* and can transport this iron into epithelial cells resulting in modulation of iron responsive genes (Yang *et al.*, 2002). Although the levels of iron transport are typically lower, the mechanism of action of *lcn2* is highly similar to both *trf* and *ltf*.

The last two members of the calycin superfamily that were isolated from the screen are *orm1* and *orm2*. Also known as  $\alpha$ -1-acid glycoprotein (AGP) types 1 and 2 respectively, these factors have a role in the acute phase response of the innate immune response (reviewed in Hocheplied *et al.*, 2003). The two genes differ by a stretch of 22 base pairs in the gene structure (Dente, 1987), with a difference in at least 21 amino acids at the protein level (Merritt and Board, 1998). Activity of *orm1* is not only dictated by the level of protein present, but also by the glycosylation patterns on the protein. *Orm1* can be categorized into three forms based on the levels of glycosylation: AGP A; AGP B; AGP C (van Dijk *et al.*, 1995; Bennett and Schmid, 1980; Higai *et al.*, 2005). Patterns of glycosylation of *orm1* are known to be altered during the course of pregnancy and stress in the MG (reviewed in Fournier *et al.*, 2000; van Dijk *et al.*, 1995). *Orm1* was originally identified as a breast cancer glycoprotein (Twining and Brecher, 1977) and its mRNA message has been localized to epithelial cells in MG (Gendler *et al.* 1982). *Orm1* can be up regulated by addition of peroxisome proliferators (PP) (Anderson *et al.*, 1999), and has the ability to prevent superoxide anion formation in the presence of phorbol myristate acetate (Vasson *et al.*, 1994) promoting activity in response to oxidative stress.

In the current chapter I examine the two groups of genes (iron binding proteins and the calycin superfamily) that share a common feature in that members of each group respond to cellular stress. *Ltf*, *trf*, *fth*, and *ftl* are all known to play a role in regulating iron, a source of oxidative stress. *Lcn2*, *ltf* and *orm1* are all thought to be part of an acute stress response. In order to examine if any other similarities exist a more thorough bioinformatic analysis was performed. Because of the known association of PP induced

*orm1* expression, I made a focused examination for evidence of peroxisome proliferator activated receptor (PPAR) mediated transcription for each of the genes in question.

## 4.2 RESULTS

### 4.2.1 Northern Analysis

Genes I identified that relate to iron metabolism and/or the Calycin superfamily display a differential expression over the profile of the MG. These results support the initial screen of the macroarrays in that they do have a differential profile.

### 4.2.2 Northern Analysis of Clones Relating to Iron Metabolism

#### 4.2.2.1 Transferrin

The *trf* PCR product used to probe the MG northern for *trf* transcript levels was 2kb in size and the single pass sequence obtained (appendix A) aligned to bases 698 to 1500 of the *Mus musculus trf* gene. The single band observed on the autorad was present at approximately 2.5kb, which is consistent with the expected transcript size of 2332 bases in UNIGene (Figure 4.3). The levels for *trf* mRNA increased gradually between late pregnancy (P13) and early lactation (L3) and persisted into early involution (I2) after which levels decreased. *Trf* mRNA abundance is significantly lower in I9 (Virgin-like stage). After repeating the northern analysis, a common trend was observed confirming the initial expression profile (figure 4.3). These results confirm the results previously published by Grigor *et al.* (1990).

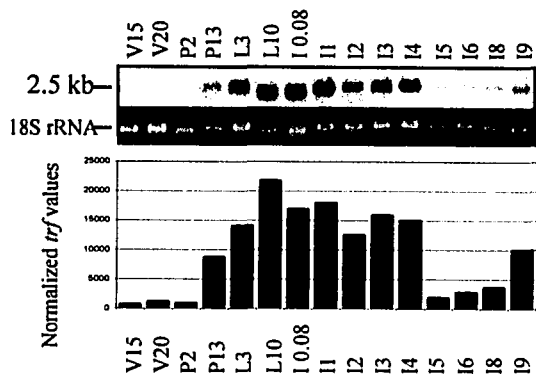
#### 4.2.2.2 Lactotransferrin

The *ltf* PCR product used for probe labeling was approximately 1.1kb and the sequence (appendix A) aligned to bases 1405- 2106 of the *Mus musculus* lactotransferrin transcript. When probed to the MG northern blot a single prominent band was observed at 2.7Kb on the autoradiograph which correlated to the estimated *ltf* transcript size (2744 bases in UNIGene). *Ltf* mRNA levels sharply increased upon progression into the involuting period at I1. A high level of *ltf* mRNA persisted through early involution and rapidly dropped down to levels that are characteristic of the virgin time point at I5 after which they remained constant (Figure 4.3). Levels of mRNA were undetectable during virgin,

**Figure 4.3: *trf* and *lrf* Northern Analysis:** Probes were made from the PCR product produced from the respective cDNA clone. They were labelled with  $\alpha$ -<sup>32</sup>P-dCTP using Invitrogen's Random Primer Labelling Kit. Two sets of mouse tissue were used to create MG Northern profiles and were used to confirm the expression profile for each clone. These are presented under the columns tissue set 1 and tissue set 2 A) The *trf* probe was hybridized to northern created from the RNA of tissue sets 1 and 2. B) The *lrf* probe was hybridized to northern created from the RNA of tissue sets 1 and 2. Bands observed on the northern were normalized to the 18s rRNA from the gel and processed through densitometry. The intensity of the 18S rRNA band was used as a loading control (Correa-Rotter, 1992). V: Virgin; P: Pregnancy; L: Lactation; I: Involution

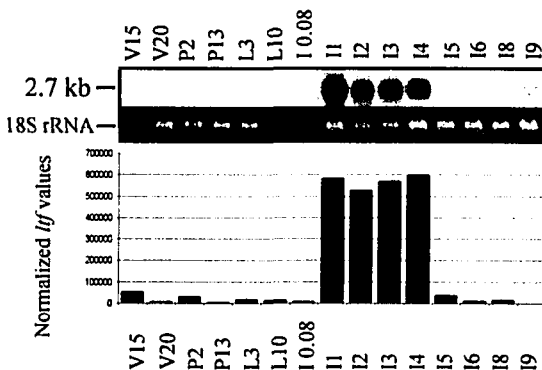
**Transferrin**

Mouse Tissue Set 1

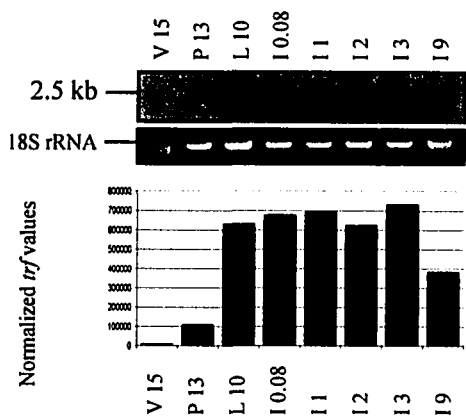


**Lactotransferrin**

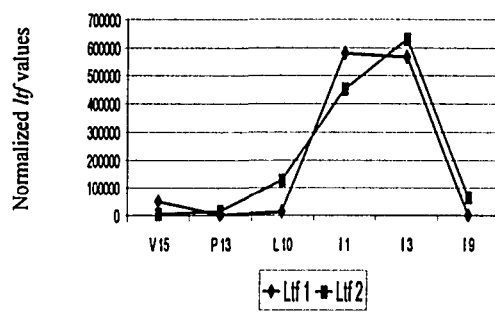
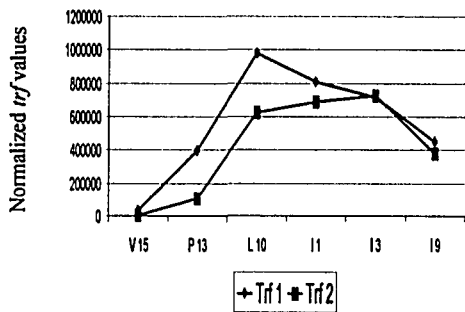
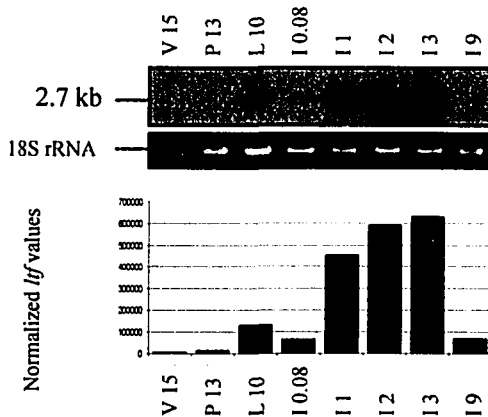
Mouse Tissue Set 1



Mouse Tissue Set 2



Mouse Tissue Set 2



**MG Developmental Stages**

pregnancy, lactation and late involution periods. Northern analyses of MG RNA isolated from a second independent group of animals confirmed the basic trend of *lif* mRNA levels throughout the MG postnatal developmental profile (figure 4.3). These observations support the findings by Lee *et al.* (1996).

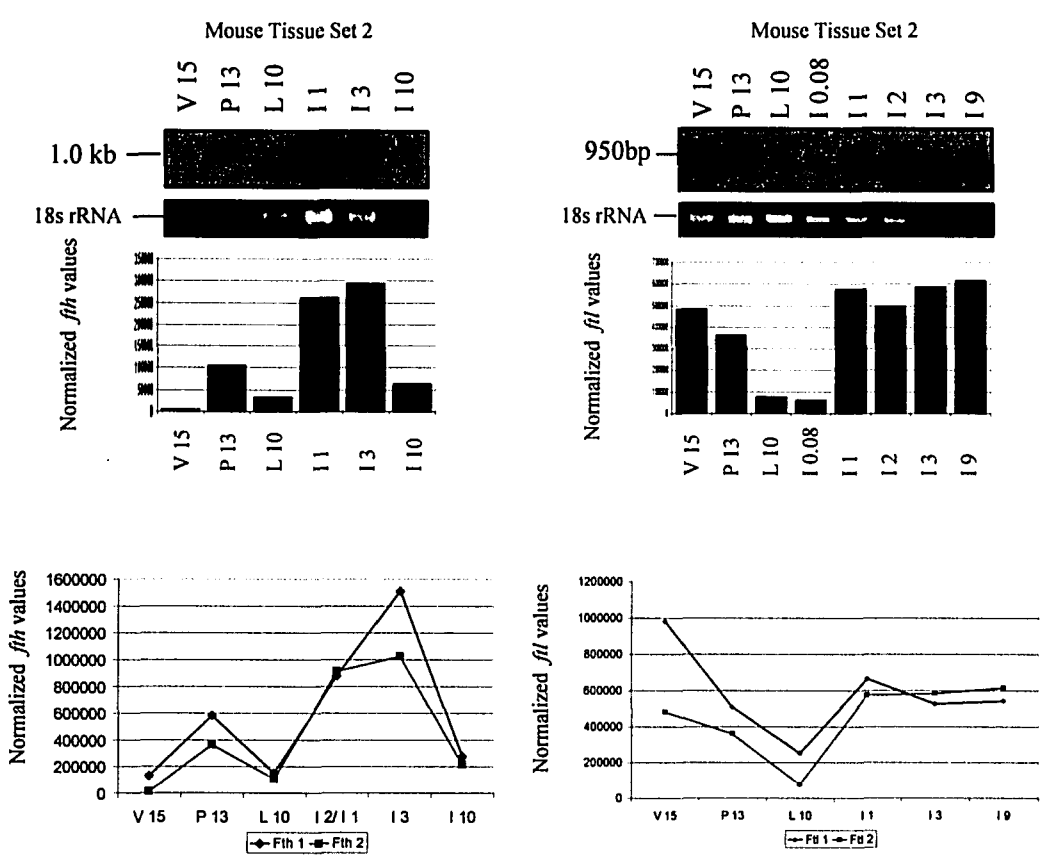
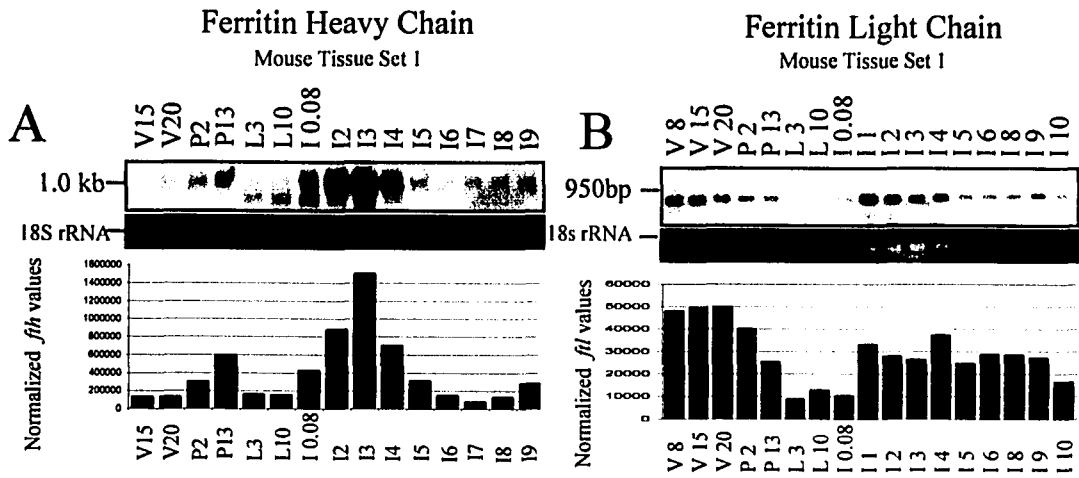
#### 4.2.2.3 Ferritin Light Chain

The *fil* PCR product used for the current study was sized at approximately 720 bases based on gel electrophoresis. When sequenced (appendix A), the fragment aligned to bases 147 to 786 of the *Mus musculus fil* mRNA transcript. Over the course of MG postnatal development *fil* mRNA levels were found to increase during I1 and remain elevated until I4 after which levels decreased to levels similar to those present during the virgin and pregnancy stages of the profile. The single band observed on the northern is approximately 950 bases and correlates to the documented size in the UNIGene database of 924 bases, although this has not been confirmed as the complete mRNA molecule. *Fil* mRNA levels peaked at Virgin 15 and levels decreased throughout pregnancy and reached their lowest levels during MG lactation (L3, L10, and I 0.08). During early involution, levels of *fil* mRNA began to increase. A second peak in levels occurs at I2, after which levels decreased slowly the remainder of the involution period (Figure 4.4). The data observed for *fil* has not been previously reported in the MG during postnatal development.

#### 4.2.2.4 Ferritin Heavy Chain

The *fth* PCR product used to identify *fth* mRNA transcripts on MG northern blots was approximately 750bp in size and the sequence (appendix A) aligned to bases 295 – 845 of the *Mus musculus fth* mRNA transcript (reported to be 866 bases). The most prominent band on the autoradiographs resulting from the northern analysis was approximately 1kb. A second band was observed at approximately 920 bases on the autoradiographs during the lactation period where the 1kb band levels decreased. The 1kb band is still visible during this period but in relatively low levels when compared to the 920 base band. During I0.08 (2hours after weaning) the two bands appear to be present in equal intensity,

**Figure 4.4: *fth* and *ftl* Northern Analysis:** Probes were made from the PCR product produced from the respective cDNA clone. They were labelled with  $\alpha$ -<sup>32</sup>P-dCTP using Invitrogen's Random Primer Labelling Kit. Two sets of mouse tissue were used to create MG northern profiles and were used to confirm the expression profile for each clone. These are presented under the columns tissue set 1 and tissue set 2 A) The *fth* probe was hybridized to northern created from the RNA isolated from mouse tissue sets 1 and 2. B) The *ftl* probe was hybridized to northern created from the RNA isolated from mouse tissue sets 1 and 2. Bands observed on the northern were normalized to the 18S rRNA from the gel and processed through densitometry. The intensity of the 18S rRNA band was used as a loading control (Correa-Rotter, 1992). V: Virgin; P: Pregnancy; L: Lactation; I: Involution



## MG Developmental Stages

and the 1kb band is solely observed after this point. An increase in mRNA abundance is observed at I0.08 which peaked at I3. After I4, levels again decreased to those observed for the virgin period (Figure 4.4). The data obtained for *fth* expression supports the data produced by Lee *et al.* (1996) and follows the common trend observed in figure 4.4. The 900 nucleotide band was not observed by Lee *et al.*, (1996); however resolution of the two bands (which are relatively similar) will rely on the specific electrophoretic conditions used in the experiment. In addition, subtle differences could have arisen through genetic differences in the animals, differences in ages of animals used, or differences in the way animals are cared for (food, water, light) at different institutions.

### **4.2.3 Northern analysis of members of the Calycin superfamily**

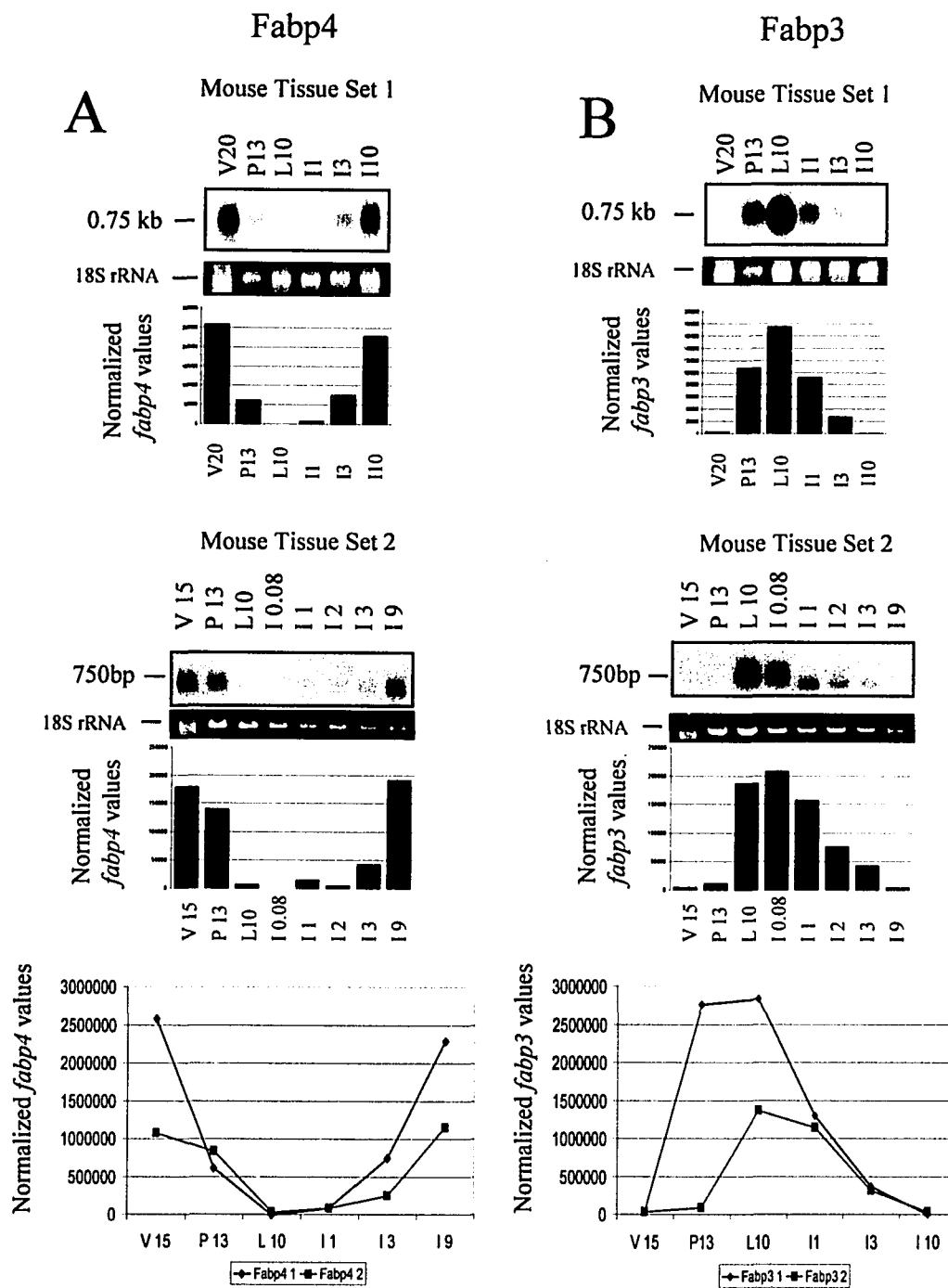
#### **4.2.3.1 Fatty Acid Binding Protein 4**

The *fabp4* PCR product isolated and amplified for probe labeling was approximately 475 bases when analyzed via gel electrophoresis. The sequence (appendix A) obtained from this product aligned to bases 187-620 of the *fabp4* mRNA transcript. The sole band that appeared on the autoradiograph resulting from northern analysis was approximately 750 bases which approximates the expected *fabp4* mRNA transcript size of 635bases from UNIGene. *Fabp4* produced a profile that had a peak in mRNA levels in the virgin (V15) and late involution (I9) periods with a drop in levels through P13, L10, I1 and I3 (Figure 4.5). *Fabp4* mRNA has previously been identified in the virgin MG (Bansal and Medina, 1993), but the finding of *fabp4* mRNA in the restored MG has not been observed before. I repeated the northern analyses on a second set of RNA samples (derived from a second set of animals) and obtained data which confirmed the trend of relative *fabp4* gene expression profiles from the first study (figure 4.5).

#### **4.2.3.2 Fatty Acid Binding Protein 3**

PCR amplification followed by electrophoresis of the clone representing *fabp3* revealed a band that was approximately 650 bp in size and the sequenced PCR product (appendix A) aligned to bases 17-635 of the *fabp3* mRNA transcript. From the northern analysis a single band was detected at approximately 750 bases. This size is consistent with the

**Figure 4.5: *fabp3* and *fabp4* Northern Analysis:** Probes were made from the PCR product produced from the respective cDNA clone. They were labelled with  $\alpha$ -<sup>32</sup>P-dCTP using Invitrogen's Random Primer Labelling Kit. Two sets of mouse tissue were used to create MG northern profiles and were used to confirm the expression profile for each clone. These are presented under the columns tissue set 1 and tissue set 2. A) The probe for *fabp3* was hybridized to the northern created from the RNA isolated from the MG tissue set encompassing the short profile. B) The probe for *fabp4* was hybridized to the northern created from the RNA isolated from the MG tissue set encompassing the short profile. Bands witnessed on the northern were compared and normalized to the 18s rRNA band via densitometry (right of the Northern). The intensity of the 18S rRNA band was used as a loading control (Correa-Rotter, 1992). V: Virgin; P: Pregnancy; L: Lactation; I: Involution



## MG Developmental Stages

expected (669 bases) size of *fabp3* obtained from UNIGene. *Fabp3* mRNA levels were undetectable during the virgin stage examined but became detectable by P13 and peaked at L10/I008. After this, levels decreased by I1 and returned to virgin state levels by I9 (Figure 4.5). The observation of *fabp3* in the MG has been previously identified in the MG during pregnancy and lactation (Treuner *et al.*, 1994) and this supports my findings (figure 4.5), but the complete developmental profile has not previously been determined. The only discrepancy that is apparent in my *fabp3* northern profile data is that high levels of *fabp3* mRNA are observed by P13 in the first data set, whereas high levels were not detected until L10 in the second analysis. Following this initial presence of high mRNA levels the profiles do follow the same trend with a decrease in I3 and minimal levels in I9.

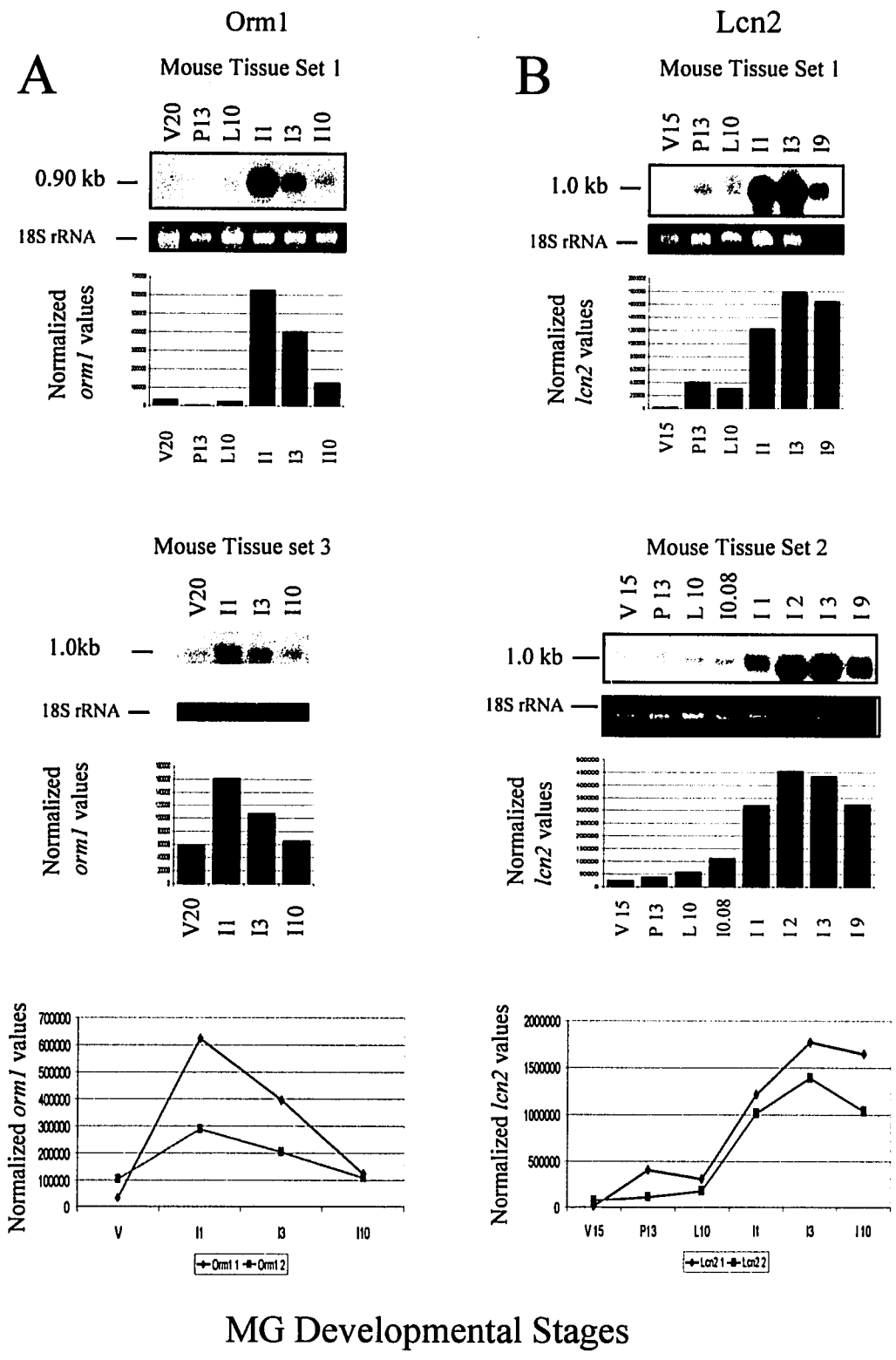
#### 4.2.3.3 Orosomuroid 1

The amplification of the *orm1* PCR product resulted in a band approximately 551 bp in size. When sequenced and analyzed it was found to align to bases 18-548 of the *orm1* mRNA transcript. The documented mRNA transcript size for *orm1* is approximately 768 bases; the single band observed upon northern analysis was approximately 900 bases in size. *Orm1* mRNA levels are barely detectable until L10 where there is a minimal increase, followed by a large increase in levels at I1 and a gradual decrease though involution by I9 (Figure 4.6). *Orm1* has been previously identified in the lactating MG (Clarkson *et al.*, (2004) based on microarray analysis, but nothing has been done to confirm these findings. The results produced here show the first northern profiles of *orm1* over a broad course of MG postnatal development.

#### 4.2.3.4 Lipocalin 2

The size of the *lcn2* PCR product used to probe the MG northern was approximately 780 bases in size. When the PCR product was sequenced it aligned to bases 1-723 of the *Mus musculus lcn2* mRNA transcript. Analysis of *lcn2* on the MG northern revealed a band at approximately 1.0 kb which approximates the expected 868 base mRNA transcript size obtained from UNIGene. Little to barely detectable levels of *lcn2* mRNA were observed in V15, P13 or L10 samples (figure 4.6). *Lcn2* mRNA levels increased by I1 and peaked

**Figure 4.6: *orm1* and *lcn2* Northern Analysis:** Probes were made from the PCR product produced from the respective cDNA clone. They were labelled with  $\alpha$ -<sup>32</sup>P-dCTP using Invitrogen's Random Primer Labelling Kit. Two sets of mouse tissue were used to create MG northern profiles and were used to confirm the expression profile for each clone. These are presented under the columns tissue set 1 and tissue set 2. A third tissue set (tissue set 3) was used to create the short profile observed for *orm1*. A) The probe for *orm1* was hybridized to the northern created from the RNA isolated from the MG tissue sets 1 and 3. B) The probe for *Lcn2* was hybridized to the northern created from the RNA isolated from the MG tissue sets 1 and 2. Bands witnessed on the northern blots were compared and normalized to the 18S rRNA band via densitometry (right of the northern blots). The intensity of the 18S rRNA band was used as a loading control (Correa-Rotter, 1992). C) Graphs represent profile trends between northern blots of the same clone. This confirms the profile of each clone observed in the northern blots. V: Virgin; P: Pregnancy; L: Lactation; I: Involution



at I3, after which high levels were maintained throughout involution. The data observed for *lcn2* is similar to previously published findings (Bong *et al.*, 2002) except that I observed high levels of *lcn2* mRNA during late involution. This finding is in contrast with the work of Bong *et al.* (2002) where mRNA levels taper off by late involution. In support of my results is the finding that my second replicate study confirms the basic trend of the *lcn2* expression profile observed in the initial study, and the fact that an independent study had previously reported that *lcn2* mRNA levels are maintained in the mouse MG after the first pregnancy (D'Cruz *et al.*, 2002).

#### **4.2.4 Multi Tissue Bioinformatic Analysis**

A search of the UNIGene database was made to determine the broad spectrum tissue expression profile for each of the genes analyzed by northern analysis in this chapter. The data was compiled and tabulated in table 4.2. The eleven organs/tissues selected for the bio-analysis were: bone, heart, kidney, liver, MG, pancreas, brain, spleen, muscle, eye, and lung. *trf*, *fil*, and *fth* cDNA have all previously been isolated from each of the tissues mentioned above. *Ltf* cDNA has previously been isolated only from bone, heart, pancreas, MG, brain, spleen, and lung. In contrast, none of the calycin superfamily genes analyzed have been previously identified in all the tissues tissue listed. *Orm1* has been identified in the fewest tissues (3/11); the liver, MG and muscle. *Lcn2* has been identified in brain, kidney, liver, MG and spleen. *Fabp3* has been previously isolated from bone, heart, kidney, liver, MG, brain, muscle and eye. *Fabp4*, the most abundantly expressed calycin member that I studied, has been found in the heart, kidney, liver, MG, brain, pancreas, spleen, muscle, and eye. To summarize, all genes considered in this chapter have been previously isolated from the MG. In general genes relating to iron metabolism are more ubiquitously expressed than those that belong to the calycin family of genes. All data described here was obtained from the ncbi UNIGene database.

#### **4.2.5 Association with PPAR Mediated Transcription**

A very cursory analysis of the literature revealed that several of the genes discussed in the current chapter were under the influence of peroxisome proliferator activated receptors (PPAR) or affected by peroxisome proliferators (PP, chemicals that induce

Tissue/ Clone Identity	Bone	Heart	Kidney	Liver	Mammary gland	Brain	Pancreas	Spleen	Muscle	Eye	Lung
Ftl	X	X	X	X	X	X	X	X	X	X	X
Fth	X	X	X	X	X	X	X	X	X	X	X
Trf	X	X	X	X	X	X	X	X	X	X	X
Ltf	X	X			X	X	X	X			X
Orm1				X	X				X		
Lcn2			X	X	X	X			X	X	
Fabp3	X	X	X	X	X	X			X	X	
Fabp4		X	X	X	X	X	X	X	X	X	

**Table 4.2: Multi-tissue Bioinformatic Characterization of Clones Related to Iron Metabolism and the Calycin Superfamily:** For each clone, the *Mus musculus* gene was used to search UNIGene and identify in which tissues cDNA relating to the subject had previously been isolated. 11 of the major mouse organs were selected for comparison among the 8 clones. The observation that the cDNA of each respective gene had been previously identified in a tissue is indicated by an “X” in the appropriate column.

<http://www.ncbi.nlm.nih.gov/entrez/query.fcgi?db=unigene>

PPAR transcription which have structural homology to fatty acids (Krey *et al.*, 1997). Historically PPARs are factors involved in the increase of peroxisomes in response to PP. However, more recent evidence attributes PPAR mediated transcription to regulate numerous pathways such as fatty acid metabolism, inflammation, glycerol metabolism, angiogenesis and glucose homeostasis (reviewed in Desvergne and Wahli, 1999; Wahli *et al.*, 1995; Latruffe and Vamecq, 1997; Tabernero *et al.*, 2002; Tien *et al.*, 2004; Elangbam *et al.*, 2001; Auboeuf *et al.*, 1997; Auwerx *et al.*, 1996). In the current section I ran a meta-analysis to determine if the genes under consideration in this chapter had the correct recognition promoter elements that could place them under the control of PPARs. This was followed by a more involved literature mining to uncover published evidence that these genes may be under the influence of PPAR control or responsive to PPs. In brief, the meta-analysis revealed the presence of a PPAR responsive element in the majority of the genes under consideration.

The series of events that leads to PPAR mediated transcriptional activation is initiated by the presence of a PP. This PP is then trafficked to the nuclear membrane where it is received by PPAR. PPAR then binds to a secondary factor, retinoid X receptor (RXR) and this heterodimer then binds to the respective peroxisome proliferator response element (PPRE) in the gene to be activated (Kliwer *et al.*, 1992). All three isoforms of PPAR (PPAR $\alpha$ , PPAR $\beta$ , and PPAR $\gamma$ ) have been detected in the MG during the virgin, pregnant and lactation periods in either adipocytes or MG epithelial cells (Gimble *et al.*, 1998). Both PPAR $\alpha$  and PPAR $\gamma$  are at their highest levels during the virgin period after which levels decrease, but PPAR expression has yet to be determined during the involution stage of MG development. The removal of a PPAR interacting factor (PRIP, peroxisome proliferator-activated receptor interacting protein) greatly hinders the metabolic activity of the MG by reducing the number of functional alveoli and the efficiency of the alveolus suggesting that PPAR or the PPAR pathway plays an integral role in MG development (Qi *et al.*, 2004). From the literature search using Entrez PubMed from the NCBI database, documentation associating some of the factors identified in our screen to PPAR and PP was obtained. Though each association is not directly related to the next, the indication that in some manner the majority of the factors are involved with or are regulated by PPAR is interesting.

#### 4.2.5.1 Promoter Analysis for Evidence of a Potential PPAR Interaction

The putative promoter region for each gene isolated in the current study and discussed above was obtained from the NCBI Entrez Gene database. Each promoter (as defined in the text provided for each gene in the NCBI Entrez Gene database) was subjected to ClustalW alignment with the consensus sequence for the PPAR response element (PPRE). In general the putative promoter region ranged from 740 bp to 3000 bp. The consensus PPRE sequence (AGGTCAAAGGTCA) used to identify the binding element is a direct repeat hexamer (DR1) with one base separating the repeats. The DR1 repeat is quite leaky and is also a recognition sequence for RXR (*9-cis*-retinoic acid receptor) homodimers and RXR/RAR (retinoic acid receptor) dimers (Nakshatri and Chambon, 1994). Following ClustalW alignment it was observed that each gene studied in this chapter showed some homology to the consensus sequence in their respective promoter and the alignments with the highest homology (as determined by ClustalW) are illustrated in figure 4.7. The homology of the PPRE sites ranges from 7/13 bases for *orm1* and *fabp4* to 11/13 bases for *trf* and *fabp3*. These sites are probable PPRE sites given the finding that the majority of the genes identified have known associations with PPAR regulation or are PP responsive (discussed below).

The putative PPRE site (GAGTTAGAGACCA) for the *fabp4* gene identified by my search with the consensus PPRE sequence does not coincide with the PPRE established recently (Schachtrup *et al.* (2004). The PPRE sequence established in that study was TCTTACTGGATCAGAGTTCA. The *fabp4* PPRE site defined by Schachtrup encompasses a much larger region of sequence than the consensus sequence mentioned above and was approximately 5000 bp upstream of the start codon. In their PPRE sequence they also included a 5' flanking region of the PPRE. This region (C(A/G)(A/G)A(A/C)CT) was found to be more important with respect PPAR/RXR binding specificity to the promoter region than the PPRE itself (Juge-Aubry *et al.*, 1997). The PPRE identified by Schachtrup *et al.* (2004) was functionally analyzed and was found to interact with PPAR $\gamma$  and weakly with PPAR $\alpha$ . The putative PPRE site identified based on the consensus sequence is much more similar to the PPRE found in *fabp3* and may correspond to an alternative binding site for PPARs.

## A.

PPRE	1	<b>AGGTCAAAGGTCA</b>	13
Trf	-124	<b>AGGTCAAAGAT</b> TG	-112
Lcn2	-600	AG <b>GA</b> CC <b>AA</b> GGCTG	-588
Fabp3	-898	AG <b>CT</b> CAGAG <b>GT</b> CA	-886
Ltf	-671	<b>AA</b> ATCAA <b>AT</b> GTCA	-659
Ftl	-1169	<b>TC</b> CTCAA <b>AG</b> TC <b>A</b>	-1157
Fth	-985	<b>AA</b> CCCAA <b>AG</b> GT <b>TA</b>	-973
Fabp4	-757	GA <b>GT</b> TA <b>GA</b> GA <b>CC</b> CA	-745
Orm1	-99	<b>AA</b> TCCAA <b>CA</b> CC <b>CA</b>	-87

## B.

PPRE	1	<b>CAAACCTAGGTCAAAGGTCA</b>	20
Trf	-4466	<b>CAA</b> AT <b>T</b> GG <b>T</b> TCAGAG <b>GC</b> CC	-4457
Fth	-992	<b>A</b> AG <b>G</b> AC <b>AA</b> AC <b>CC</b> AAAG <b>GT</b> TA	-973
Fabp3	-905	<b>T</b> GG <b>C</b> AC <b>AA</b> GC <b>TC</b> AGAG <b>GT</b> CA	-886
Fabp4	-3381	<b>CC</b> AA <b>AC</b> CA <b>AA</b> CC <b>AA</b> AA <b>CC</b> CA	-3362
Orm1	-4356	<b>CA</b> AT <b>G</b> CTA <b>T</b> AC <b>CC</b> AA <b>AG</b> TC <b>C</b>	-4337
Ftl	-2156	<b>CA</b> AA <b>ACT</b> AA <b>AT</b> TCAG <b>GT</b> CA	-2137
Lcn2	-3414	<b>C</b> AG <b>AG</b> CTA <b>GG</b> TT <b>GG</b> AG <b>CC</b> CA	-3393
Ltf	-2829	<b>CA</b> AG <b>G</b> CTA <b>CG</b> TA <b>GA</b> GA <b>CT</b> CA	-2810

**Figure 4.7: Identification of Putative PPRE in the Promoter Region of Genes Related to Iron Metabolism and the Calycin Superfamily.** A) The promoter regions for each gene were obtained from Entrez Gene and were scanned using ClustalW alignment with the consensus PPRE sequence AGGTCAAAGGTCA to find the best possible alignment between the promoter sequence and the consensus PPRE. Each gene's representative PPRE sequence was then aligned to other putative PPRE to compare the homology. B) For each gene 5000 bases upstream of the start codon (ATG) was scanned with the consensus PPRE sequence including the 5' flanking consensus sequence that is believed to aid in PPAR/RXR recognition. The consensus sequence (sequence that the promoters were aligned to) (grey shading) is indicated at the top of each group of sequences and is depicted by the notation "PPRE". Boxshade was used to view the alignments. The black boxes indicate bases that occur most frequently and bases with a lower frequency are marked by a white box. Each sequences position has been referenced to the start codon for each gene and is indicated by the numbers present bordering the sequences. Upstream sequence was obtained from the mouse genome informatics database. <http://www.informatics.jax.org/>

As a secondary screen I expanded the region upstream of the translational start codon of each gene to 5000 bp and rescreened them for the PPRE consensus sequence containing the 5' flanking consensus sequence (Schachtrup *et al.*, 2004). The best match to the consensus PPRE sequence CAAAATCTAGGTCAAAGGTCA for each gene is presented in figure 4.7B. It is interesting to note that in all cases except for *fabp3* different regions in the upstream region were identified with the extended PPRE sequence than that identified by the (AGGTCAAAGGTCA) sequence alone. In general the overall homology for each extended PPRE region is lower than that of the PPRE sequence alone. The best homology was found in the case of *fil* (16/20) and the lowest degree of similarity of 12/20 in the cases of *ltf*, *lcn2* and *fabp3*. The data suggests that for the genes examined that each gene may have as many as 2 to 3 potential PPRE sites within the promoter region.

#### 4.2.5.2 Iron Binding Proteins and PPAR Mediated Transcription

Of the genes related to iron metabolism *ltf*, *trf*, and *fil* expression was previously found to be affected by PPAR mediated transcription. *Trf* expression is repressed by PPAR in the liver. This mechanism is thought to act not as a direct inhibition by PPAR binding to a PPRE, but an indirect mechanism that prevents HNF-4 (hepatic nuclear factor) from binding to the PRI (proximal region I) element in the *trf* promoter. In this case PPAR binds to the PRI element, thus HNF-4 cannot activate *trf* transcription, and *trf* levels drop causing an eventual decrease of iron transport into cells (Hertz *et al.*, 1996). In the case of the MG, I observed an increase in *trf* levels during lactation, this would correlate to the control mechanism described above since inherent levels of PPARs decrease during lactation (Gimble *et al.*, 1998, Haslam *et al.*, 2000).

Microarray profiling of hepatic gene expression suggests that liver *ltf* levels decrease in response to treatment with a PPAR $\alpha$  specific PP, diethylhexylphthalate (DEHP). In the MG I observed that *ltf* levels increase during late lactation and early involution. Correlating these observations to PPAR levels observed by other groups (Gimble *et al.*, 1998, Haslam *et al.*, 2000) it would appear that increases in *ltf* levels could again be responding to decreases in PPAR levels. Supporting this possibility is the finding that the *ltf* gene does have a putative PPRE (figure 4.7A and B) in its promoter. In

brief PPAR $\alpha$  could be acting as a repressor of *ltf* expression in the MG. Further analysis of *ltf* and *trf* expression, however, in wildtype and PPAR $\alpha$  null mice showed a decrease in expression after PP addition. This suggested that the effect seen may represent a PP mediated effect as opposed to a direct effect by PPAR $\alpha$  (Hasmall et al. 2002). This down-regulation in expression is believed to be responsible for a positive growth effect by preventing the *ltf* inhibition of TNF- $\alpha$ , allowing TNF- $\alpha$  to induce cell proliferation. In the case of the MG this would correlate to the pregnancy and lactation stages of development.

Addition of 15d-PGJ2 (15-deoxy-D12,14-prostaglandin J2), a derivative of arachadonic acid that is a known PP activator of PPAR $\gamma$ , to human monocytic THP-1 cells results in an increase in *fil* mRNA levels. (Jang *et al.*, 1999). Since *fil* and *fh* produce the 2 different subunits that interact to form a single ferritin functional complex, the regulation of *fil* may underlie a corresponding regulation of *fh*. Alternatively an effect that decreases or increases the relative levels of *fil* or *fh* will have an affect on the relative number of functional ferritin complexes that can be assembled. The initial high levels of *fil* MG mRNA during the virgin and pregnancy periods followed by a decrease in mRNA levels during lactation, observed in the current study, follows the published expression profile of PPAR $\alpha$  (Gimble *et al.*, 1998)

#### 4.2.5.3 The Calycin Superfamily and PPAR Mediated Transcription

The Calycin superfamily genes examined in the current study (*fabp3*, *fabp4*, *orm1* and *lcn2*) have published evidence that their expression can be affected by PPAR and/or PP. *Fabp3* and *fabp4* are induced in liver with Wy14,643 a potent activator of PPAR $\alpha$ , as a latent effect following liver *fabp* induction (Motojima, 2000). *Fabp4* mediated transport of fatty acids is directly associated to the PPAR $\gamma$  activity in adipose tissue. PPAR $\gamma$  binds to a PPRE in the promoter of *fabp4* subsequently increasing expression and production of *fabp4*, which in turn positively regulates PPAR $\gamma$  by transporting substrates to PPAR $\gamma$  for activity (Storch and Thumser, 2000; Tontonoz *et al.*, 1995). The result of this may be to aid in the differentiation of the adipose tissue, though the exact result of this interaction is not fully understood. In the case of the MG, adipocytes are predominantly present during virgin or virgin-like states of the tissue and both levels of *fabp4* and PPAR $\gamma$  seem to

correlate with the presence or absence of this cell type in the MG tissue over the course of development. The involvement of *orm1* with PPAR and PP is currently speculative. In a study examining PP induced acute phase protein expression, PP (Wy-14643, a PPAR $\alpha$  activator) treatment of normal livers in rats was found to cause a decrease in *orm1* mRNA levels, while the same treatment in cancerous livers in rats resulted in an increase in *orm1* mRNA levels (Anderson *et al.*, 1999). Lastly *lcn2* expression appears to be selectively induced in murine prolymphoid progenitor cells (FL5.12) exposed to Wy-14643 (PPAR $\alpha$  activator) (Tong *et al.*, 2003). The observation of a putative PPRE in the *lcn2* promoter does coincide with the previous finding of *lcn2* being up-regulated in the presence of PP Wy 14,643 (Tong *et al.*, 2003).

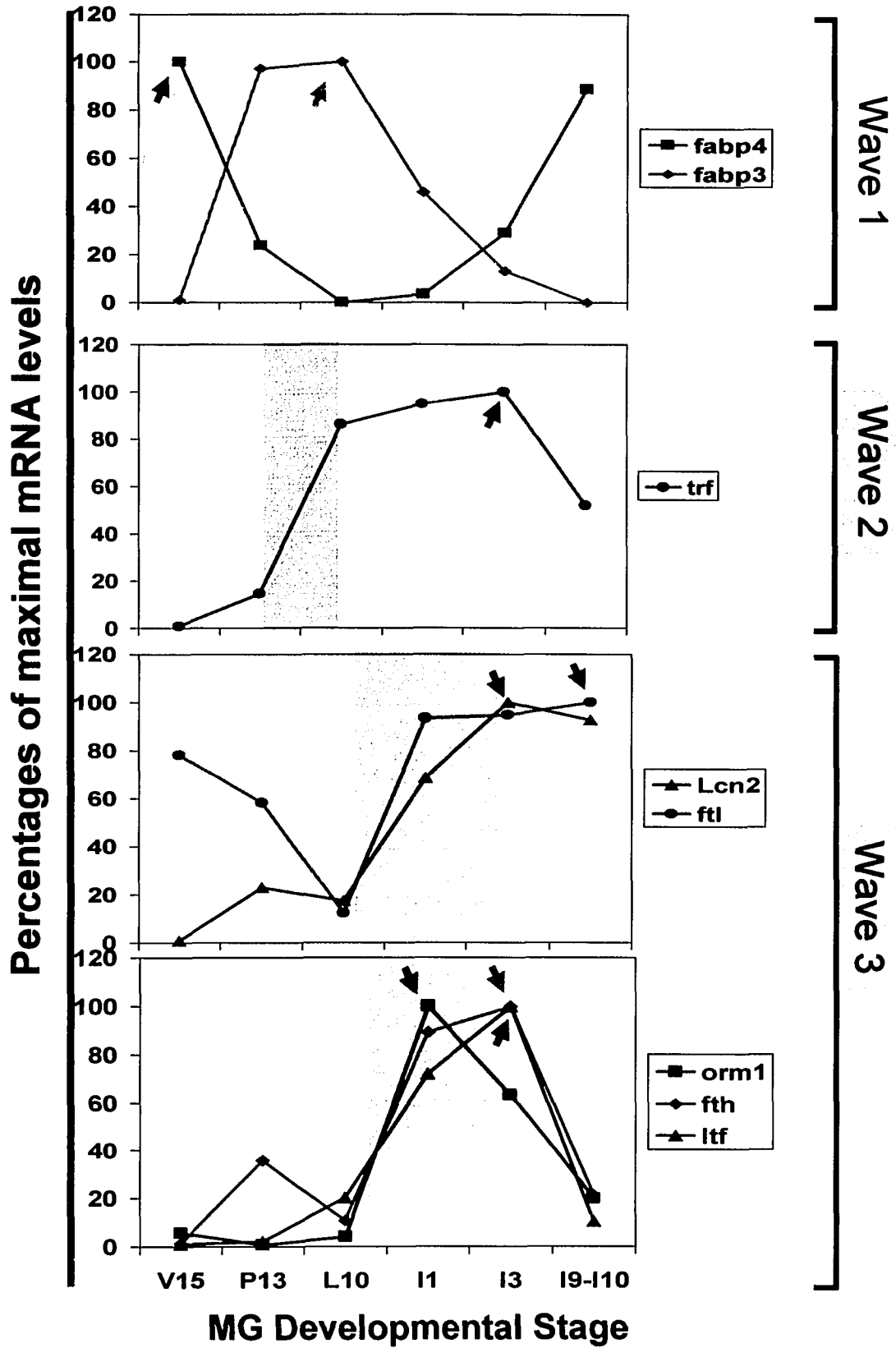
### 4.3 DISCUSSION

Two groups of genes were analyzed in the current chapter, iron binding protein genes and members of the calycin superfamily of genes. Literature mining resulted in the initial realization that members of both gene groups shared a common functional role in responding to cellular stresses (oxidative stress response or an immune response). For most of the genes the most prominent increase in mRNA levels is followed by a decrease by late involution (I9-I10, the virgin-like state).

Upon careful analysis there are actually three waves of gene induction over the course of MG development. A collective summary of the northern data is presented in figure 4.8. *Fabp4* (a marker of adipocytes) and *fabp3* mRNA expression (a marker of MG epithelial cells) define the first wave of changes in gene expression and mark the major switch from a virgin MG (adipocyte cell rich tissue) to a developed MG (epithelial cell rich tissue) back to a virgin like tissue (adipocyte cell rich tissue). The increase in *fabp3* mRNA levels during pregnancy and lactation coincides with the possibility that *fabp3* may be involved in differentiation of the MG and a regulator of MG growth (Yang *et al.*, 1994; Borchers *et al.*, 1997). In hindsight it is not surprising that the PPRE sites that contribute to defining the expression of *fabp3* and *fabp4* are different. The expression profiles between *fabp3* and *fabp4* are inverted, when the expression of one is very high the expression of the other is typically low. Both *fabp3* and *fabp4* can be induced by induction and activation of PPAR $\alpha$  (Motojima, 2000), but increased *fabp4* cellular

**Figure 4.8 Expression Trends for the Calycin Superfamily and Genes Related to Iron Metabolism:** The normalized mRNA values obtained from densitometry are graphed and the profiles of genes related to iron metabolism and the genes related to the Calycin superfamily were grouped based on common expression trends.

V: Virgin (weeks); P: Pregnancy (days); L: Lactation (days); I: Involution (days)



activity has been correlated with increased PPAR $\gamma$  activity in adipocytes. It is possible that the balance of PPAR $\alpha$  and PPAR  $\gamma$  activity controls the drastically different profiles of *fabp4* and *fabp3* that are observed.

In the context of this chapter, the iron metabolism genes and the remaining calycin superfamily genes define wave 2 and wave 3 of changes in gene expression. Within this group, *trf* is the only gene to show its major increase in mRNA levels between P13 and L10 (Wave 2). During pregnancy and lactation the MG is in a state of high metabolic activity, an induction in *trf* is therefore logical since *trf* expression is largely associated with iron metabolism for normal cellular processes. When the mammary gland becomes stressed by the buildup of milk in the alveoli, there is a down regulation of *trf* indicating that the MG has shifted its cellular phenotype.

The wave 3 genes (*lcn2*, *fil*, *orm1*, *fth*, *ltf*) all show marked increases in mRNA levels between L10 and I1 and which remain relatively high during I3. The majority of the mRNA levels for the genes surveyed peaked at I1-I3. The major induction of wave 3 genes encompasses the switch from lactation to involution and defines gene products which have roles in responding to environmental stresses. Expression of these genes marks a change in the physiology of the MG. After weaning there is a build up of milk in the ducts of the MG which causes physical stress that can lead to oxidative stresses to the tissue and set up an environment for bacterial growth and infections. Four of the five genes in wave 3 define products that play a role in regulating free iron levels within the tissue or modulate an immune response or surveillance pathway. *Lcn2*, *ltf*, *fth* and *fil* all have direct roles in the control of free iron. *Lcn2* is believed to mediate the removal of oxygen free radicals (Devireddy *et al.*, 1993; Kjeldsen, 1994) and can traffic iron from the extracellular space into cells using the same endocytic mechanism as *trf* (Yang *et al.*, 2002). In addition *lcn2*, like *ltf*, can bind siderophores produced by bacterial cells that transport iron into bacterial cells for metabolism (Goetz *et al.*, 2002; Braun, 1987; Bullen, 1981). Theoretically, when *lcn2* or *ltf* binds the siderophores, it prevents the iron from being taken up by the bacteria and therefore limits bacterial growth (Flo *et al.*, 2004). Co-coordinately, these two factors could have an important role in the involuting MG by preventing bacterial infection in the static milk (Erickson *et al.*, 2003).

The exact functional role of *orm1* is not fully understood, although it is thought to be regulated by varying degrees of glycosylation of itself as well as the quantity of *orm1* present. *Orm1* is the only gene in the current genes examined that has a sharp peak of mRNA levels at I1, with levels sharply decreasing after this developmental stage. The presence of *orm1* is seen upon induction of the acute phase response as is *lcn2*, and thus is associated with the acute phase response (Williams *et al.*, 1997). *Orm1* has the ability to delay the onset of apoptosis and inflammation in the ischemic kidney (de Vries *et al.*, 2004); therefore the high levels of *orm1* mRNA in early involution in the MG may represent an attempt to delay the progression towards a proteinase dependent state of involution and the progression to the virgin-like state (Daemen *et al.*, 2000). *Orm1* may therefore represent one component that is essential from the switch from a lactating to an involuting MG. A common theme that seems to be inferred by the wave 3 genes, in general, is that changes in specific gene expression observed during the onset of involution and subsequent maintenance of these mRNA levels through early involution may therefore exist to compensate for the destruction of neighbouring cells (Wang, 2001).

There is a subtlety in the expression profiles of wave 3 genes that allow them to be subdivided into two groups, wave 3 genes that show a marked decrease in mRNA levels by I9-I10, the virgin-like state (*orm1*, *fh*, *ltf*) or genes that show only a slight decrease in mRNA levels by I9-I10 relative to the peak levels of expression (*lcn2* and *ftl*). Genes that maintain a very high level of expression relative to levels observed at the virgin stage (V15) are interesting because they indicate that there is a molecular differentiation between the virgin stage and the virgin like stage. The high level of *lcn2* observed through late involution (I9), for example, is thought to provide an anti-cancer protective affect in women who have been pregnant (Devireddy *et al.*, 1993; Kjeldsen, 1994).

It is already documented that fatty acids are ligands that can stimulate PPAR mediated transcription (reviewed in van Bilsen *et al.*, 2002), but a role for PPAR mediated transcription in iron metabolism has not yet been established. The results from my screen identified at least two putative PPRE sites in the promoter region of each gene analyzed in this chapter. As noted above the consensus sequence used for the PPRE

analysis did not pick up the known binding site that is present in the *fabp4* gene. The data therefore suggests that there may be a number of different sites within these genes that govern its potential interactions with PPARs. Although the majority of genes show a increase in where there is a known decrease in PPAR $\alpha$  and PPAR  $\gamma$  levels, and that I have found potential PPRE sites within the promoters of the iron metabolism protein and calycin superfamily genes examined, the mechanism of PPAR interaction with the promoter elements for each of these genes cannot be elucidated. Either a PPAR can directly bind to a PPRE and either positively or negatively regulate gene expression or a PPAR can bind to alternative promoter motifs that then inhibit the binding of other transcription factors that would activate the expression of that gene (Hertz et al., 1996). The information accumulated here relating fatty acids, iron metabolism and the mammary gland although preliminary, may aid in the definition of the events leading into, during and following MG involution.

## CHAPTER 5 - CHARACTERIZATION OF *CITED2* EXPRESSION IN MAMMARY GLAND INVOLUTION

### 5.1 INTRODUCTION

In addition to a direct or differential cDNA library screening approach (chapters 3 and 4) I also initiated a study to use a comparative functional genomics approach to identify a putative molecular component that might be essential to the involution process. In this approach the goal is to identify common changes in gene expression between 2 independent models systems undergoing a common process, involution. In addition to MG involution, other members of the lab also study light-induced retina degeneration (LIRD) in adult rats.

LIRD in rats involves involution of the retina. More specifically, intense green light (1300-1500 lux) induces oxidative stress in the retina, which is followed by the onset of apoptosis (Wong *et al.*, 2003, Wong *et al.*, 2004; Kutty *et al.*, 1995, Organisciak *et al.*, 1989). What drives apoptosis is a change in genetic expression, protein expression and/or a modification of existing proteins (Wylie *et al.*, 1984). The mouse MG is an excellent candidate to compare against the LIRD model. It shares similarities to the retina in that both tissues undergo postnatal development and both tissues responds to external triggers to undergoing involution. Weaning of the pups from the Dam causes a mechanical stress to the MG because of milk engorgement, this coupled with hormonal change induces the process of apoptosis leading to MG involution (Li *et al.*, 1997). In addition the expression of clusterin, a gene that is responsive to stress and a state of active cell death is highly induced in both systems undergoing involution (Wong *et al.*, 2001, Chapter 3). Because we see this similarity in gene expression in both models it is reasonable to hypothesis that both systems may employ similar programs to undergo involution. Thus when a factor shows up-regulation during LIRD a question that arises is if this factor also shares a similar response during MG involution, and vice versa.

One gene that changes its levels of expression over the course of LIRD is CREB binding protein/p300 interacting transactivator with ED rich tail 2 (*cited2*), a member of the CITED family of transcriptional modifiers (Figure 5.1; Maciejko *et al.*, 2005 published abstract). Although *cited2* has been previously reported as an expressed

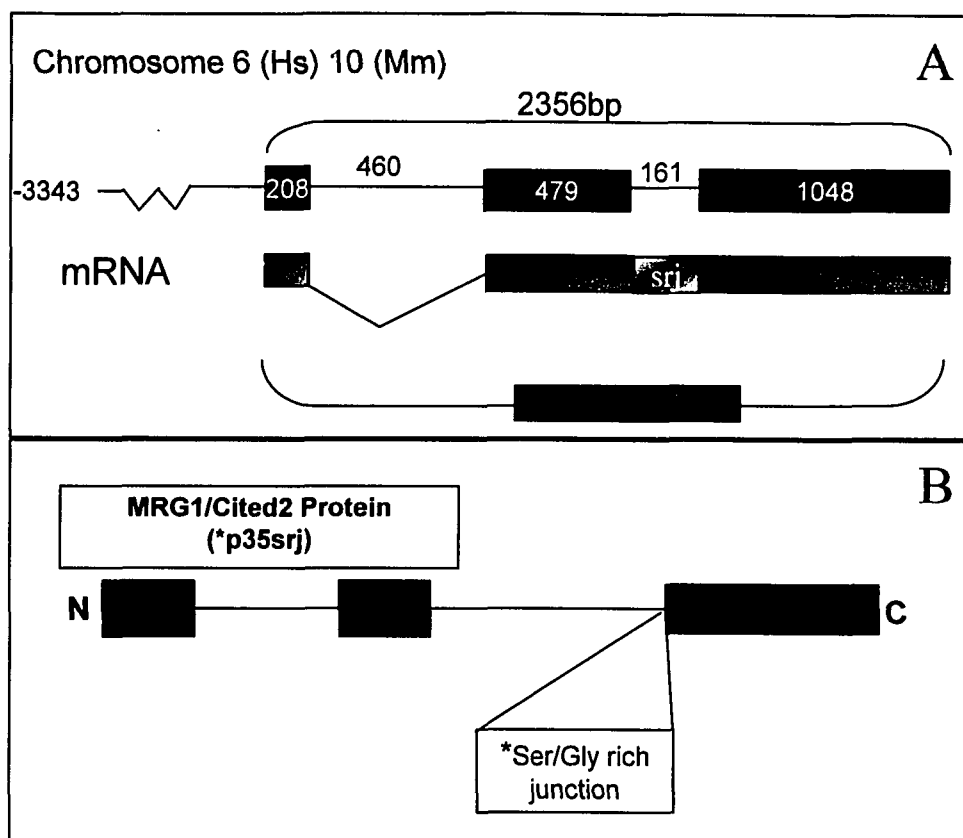


**Figure 5.1: *cited2* Gene and Protein Structure:**

- A) The gene structure of *cited2* consists of three exons and two introns. The first intron has characteristic boundaries, while the second intron does not and is present in the longest alternative transcript of the gene. The main transcript is depicted below the gene, and the second intron is identified by the different colored box. It is this region that is present in the largest splice variant and produces the srj region. This region is absent in the second most common transcript.
- B) The structure of the MRG1 protein is characteristic of the CITED family with the CR2 domain that is responsible for p300/CBP binding. The CR3 domain is evident in CITED 3 and 4 as well. Notice the serine glycine rich region, it is present in the largest splice variant (270 aa) but not in the second observed isoform (213 aa).

sequence tag derived from mouse MG (<http://www.ncbi.nlm.nih.gov/UniGene/clust.cgi?ORG=Mm&CID=272321>), no published reports examining *cited2* expression over the course of MG postnatal development have appeared. There is significant homology at the nucleic acid level between human and mouse gene structure (Figure 5.2) (88.9%, obtained from the NIH Homologene database). The human *cited2* gene spans a region of 2.4kb, and is comprised of 3 exons and 2 introns (Leung *et al.*, 1999). Predicted alternative splicing of the human gene reveals 4 putative products with the respective open reading frame sizes 1939bp (36kDa), 710bp (23.9kDa), 482bp (17.2 kDa), and 450bp (11.6kDa) (Mammalian Gene Collection (MGC) Program Team, 2002). The 36kDa protein and 24kDa protein correspond to products p35srj (Bhattacharya *et al.*, 1999) and Mrg1 (Shioda, 1997) respectively. There are no documented factors that coincide with the smaller sized products, though to date both are now classified as *cited2*. Each putative protein variant harbors exon 2, which is the exon that contains the region coding for the CR2 (conserved region 2) domain and is responsible for interacting with p300/CBP (Figure 5.1) (Braganca *et al.*, 2003; Freedman *et al.*, 2003, Yin *et al.*, 2002; Bhattacharya *et al.*, 1999). The variant known as p35srj is the only product that maintains intron 2 in its coding sequence. The second intron introduces a region that is rich in serine and glycine and is thought to act as a flexible arm in the protein, though the exact benefit of this region is unknown (Leung *et al.*, 1999). Of these 4 possible transcripts the 1939 bp transcript has been consistently observed and the 3 smaller species are thought to be rare products if not artifacts (Bhattacharya not yet published).

Members of the CITED family of genes cannot bind DNA directly, but have the ability to associate with the CH1 (cysteine-histidine rich 1) domain of the p300/CBP (Creb binding protein) complex (Yahata *et al.*, 2001; Freedman *et al.*, 2003) via its ED rich CR2 domain and act as a transcriptional modifier. p300 itself is critical for cardiac and neural development and CBP is involved in angiogenesis, skeletal and cardiac development, neurulation and hematopoietic differentiation (Bamforth *et al.*, 2001). *Cited2* as a transcriptional modifier has the ability to prevent factors such as hypoxia inducible factor 1 subunit alpha (*hif1- $\alpha$* ) from associating with the p300/CBP complex and subsequently hinder expression of genes regulated by these co-activators (Bhattacharya *et al.*, 1999; Yin *et al.*, 2002). *Hif1- $\alpha$*  is the oxygen sensitive component

**Figure 5.2: *cited2* Sequence Alignments:** Alignments were made between the clone our lab isolated and; Top: *Mus musculus Mrg1* mRNA; Bottom: *Homo sapiens p35srj* mRNA. Sequence highlighted in red corresponds to the second intron of the *cited2* gene, indicating the isolated sequence is the largest splice variant. Alignments were completed using the NCBI nucleotide alignment BLAST program.

Isolated:	54	<u>gcggtggcagcaccatgcnccgctcggtnnctcacgtccccgggcaatgctgncgccca</u>	113
Mm Cited2:	803	<u>gcggtggcagcaccatgcccgcctcggtggtcacgtccccgggcaatgctgncgccca</u>	862
Isolated:	114	atgtcatagacactgatttcatcgacgaggaagtgcttatgtccttagtgatagagatgg	173
Mm Cited2:	863	atgtcatagacactgatttcatcgacgaggaagtgcttatgtccttagtgatagaaatgg	922
Isolated:	174	gtttgaccgcatcaaggagctgccagaactctggctgggcaaaatgagtttgatttta	233
Mm Cited2:	923	gtttgaccgcatcaaggagctgccgaactctggctgggcaaaatgagtttgatttta	982
Isolated:	234	tgacggacttcggtgcaaacagcagcccagcagagtcagctggtgactcggttaacctc	293
Mm Cited2:	983	tgacggacttcggtgcaagcagcagcccagcagagtcagctggtgactcggttaacctc	1042
Isolated:	294	gc-ggctgaaagaaatcacct-----ccctgccccaccccccaacttcttcggtgtgaa	347
Mm Cited2:	1043	gcaggcgaaacaaatcacctccccacccccaccccccaacttcttcggtgtgaa	1102
Isolated:	348	tt	349
Mm Cited2:	1103	tt	1104

Hs Cited2:	816	<u>catgccgcctccgtggcccacgtccccgctgcaatgctgcccaccaatgtcatagacac</u>	875
Isolated:	67	<u>catgcnccgctcggtnnctcacgtccccgggcaatgctgncgcccaatgtcatagacac</u>	126
Hs Cited2:	876	tgatttcatcgacgaggaagtcttatgtccttggtgatagaaatgggttggaccgcat	935
Isolated:	127	tgatttcatcgacgaggaagtgcttatgtccttagtgatagagatgggttggaccgcat	186
Hs Cited2:	936	caaggagctgccgaactctggctgggcaaaacgagtttgattttatgacggacttcgt	995
Isolated:	187	caaggagctgccagaactctggctgggcaaaatgagtttgattttatgacggacttcgt	246
Hs Cited2:	996	gtgcaaacagcagcccagcagagtgagctggtgactcg	1033
Isolated:	247	gtgcaaacagcagcccagcagagtcagctggtgactcg	284

of the transcriptional activator *hif1* that ultimately regulates the complex's activity. In environments consisting of low levels of oxygen, *hif1- $\alpha$*  is activated. Through the interaction of *hif1- $\alpha$*  with p300/CBP, genes that are involved in angiogenesis and relief of hypoxic environments, such as vascular endothelial growth factor (*vegfa/vegf*), are up regulated (Bhattacharya *et al.*, 1998). If *cited2* can prevent the interaction of *hif1- $\alpha$*  with p300/CBP, levels of *vegfa* mRNA expression and subsequently protein expression should decrease due to the lack of activation. It has also been found that the promoter region of *cited2* has 3 HRE (hypoxia response elements), which suggest that the gene is regulated by *hif1- $\alpha$*  (Leung *et al.*, 1999; Bhattacharya *et al.*, 1999). If this were true, levels of *cited2* mRNA would eventually rise in the presence of prolonged *hif1* exposure. The competition between *cited2* and *hif1- $\alpha$*  for p300/CBP suggests that *cited2* may act as a negative regulator of *hif1- $\alpha$* /p300/CBP (Freedman *et al.*, 2003). Therefore *cited2* can indirectly mediate numerous pathways via its interaction with p300/CBP, and potentially may have the ability to activate transcription of other genes through its interaction with p300/CBP.

*Cited2* has also been implicated in the regulation of transcription via PPAR $\alpha$  (peroxisome proliferator activated receptor), a known activator of many subsets of genes such as those involved in glycerol metabolism, fatty acid metabolism, glucose homeostasis, inflammation and angiogenesis (Taberner *et al.*, 2002, Tien *et al.*, 2004; reviewed in Desvergne and Wahli, 1999). In a study by Tien, Davis and Heuvel (2004), they discovered the direct interaction of PPAR $\alpha$  with an over-expression of *cited2* resulted in the reduced expression of mRNA for the genes angio-like protein 4 (ANGPTL4), Forkhead C2 (FOXc2), hypoxia inducible factor 1  $\alpha$  (*hif1- $\alpha$* ), and MAPK phosphatase 1 (MPK1). In addition, over expression of *cited2* has been shown to have transforming qualities (Sun *et al.*, 1998). In contrast low levels of *cited2* results in decreased levels of *Bml1/Mel18* mRNA and protein and a subsequent increase in mRNA and protein levels of cell proliferator inhibitors INK $\alpha$ /ARF (Kranc *et al.*, 2003).

The examination of *cited2* mRNA and protein levels in the MG was initiated to answer the question "Is *cited2* expressed during MG involution, a second model that undergoes apoptosis?" To better understand the role of *cited2* in the involuting MG, I looked at *vegfa*, a gene whose function is known to be affected by *cited2* protein. *cited2*

protein indirectly inhibits *hif1- $\alpha$*  activity and results in the down-regulation of *vegfa*. I looked at the mRNA expression of *vegfa* to see if the levels of *vegfa* mRNA decreases with an increase in *cited2* protein. If levels do decrease after an increase in *cited2* protein is observed, then it is possible that the presence of *cited2* may be inhibiting *vegfa* mRNA expression (figures 5.3 and 5.4).

## 5.2 RESULTS

### 5.2.1 mRNA Analysis

#### 5.2.1.1 *Cited2* Northern Analysis

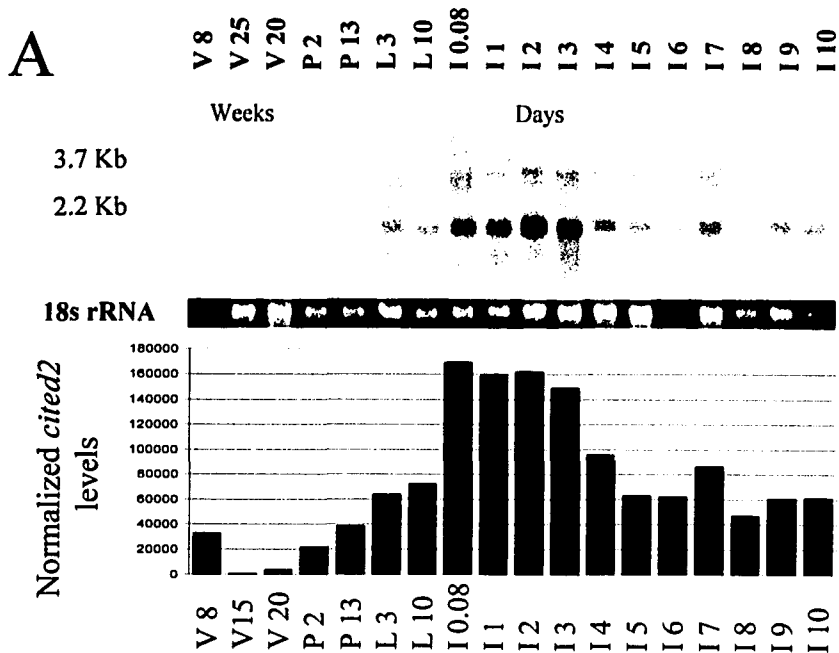
The clone used to probe the northern blots was isolated from a rat cDNA library. The PCR product of the clone was approximately 400 bases in length and aligned to bases 803 to 1103 of the *Mus musculus Mrg1/ p35srj/cited2* mRNA. The predominant mRNA band size that is observed throughout the experiments involving *cited2* is approximately 2.2kb which correlates with the mouse expected transcript size of 1960 bases (NCBI UNIGene). The mRNA expression levels over the profile exhibit increased expression during early involution and a basal level during the virgin and virgin like stages (figure 5.3). We see a moderate increase in mRNA levels during late pregnancy, but the most notable increase of the 2.2kb band intensity is at involution 0.08 (or 2 hours after weaning) and it persists throughout the onset of involution until day 4 where it begins to drop. The larger 3.5kb band follows the same profile as the 2.2kb band, though this band has yet to be documented in the literature (figure 5.3). Confirmation of the *cited2* northern blots were similar in band size and relative intensity, only in 1 northern was there a slight deviation between time points I1 and I3 where it appears that maximal mRNA levels were reversed. This can be more clearly observed in the trend analysis (figure 5.3C).

#### 5.2.1.2 *Vegfa* Northern Analysis

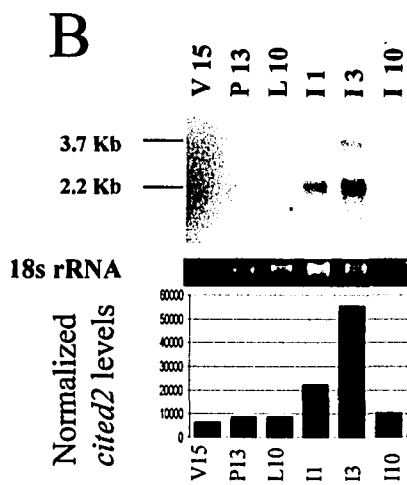
The cDNA clone for mouse *vegfa* was obtained from RESGEN and amplified using PCR. The cloned insert was approximately 1.2kb bases and its sequence aligns to bases 814-1236 of the *Mus musculus vegfa* mRNA. Hybridization of labelled *vegfa* PCR product to the mammary profile revealed an approximate 1.2kb band that first appears at P13. *Vegfa*

**Figure 5.3: *cited2* Northern Expression in the Mammary Gland:** The *cited2* probe was created from the PCR product of the rat *cited2* clone,  $\alpha$ -<sup>32</sup>P-dCTP, and Invitrogen's Random Primer Labelling Kit. A) The probe was hybridized to the Northern created from the RNA of the long profile of MG tissue. Bands were detected and compared to the 18s rRNA for normalization. B) The probe was hybridized to a Northern created with the RNA from the short MG tissue profile. Densitometry was completed using the 18s rRNA band as a loading standard. Calculations were carried out with numbers obtained from Adobe Photoshop 7 analysis. C. The intensities acquired from densitometry were normalized approximately based on pixel resolution of the images. The general trend for each northern is plotted on the line graph selecting common time points.

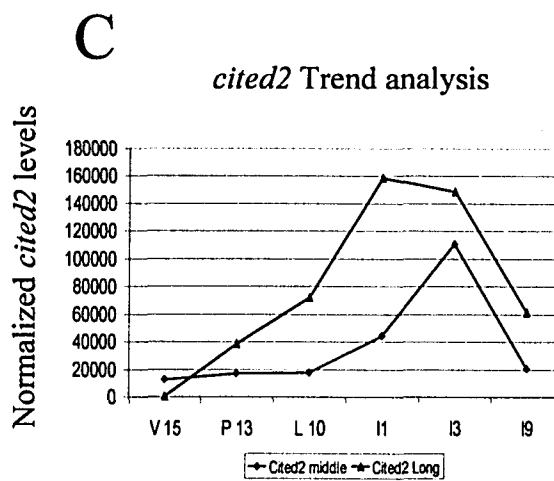
V: Virgin; P: Pregnancy; L: Lactation; I: Involution



MG Developmental Stages



MG Developmental Stages



mRNA levels increases to peak levels at L10 and is present at these levels through early involution I0.08. After the switch to an involuting environment, there is a large decrease in mRNA by I1 and levels taper off to those observed in the virgin period (Figure 5.4).

### **5.2.1.3 Fluorescent *in situ* Analysis of *cited 2***

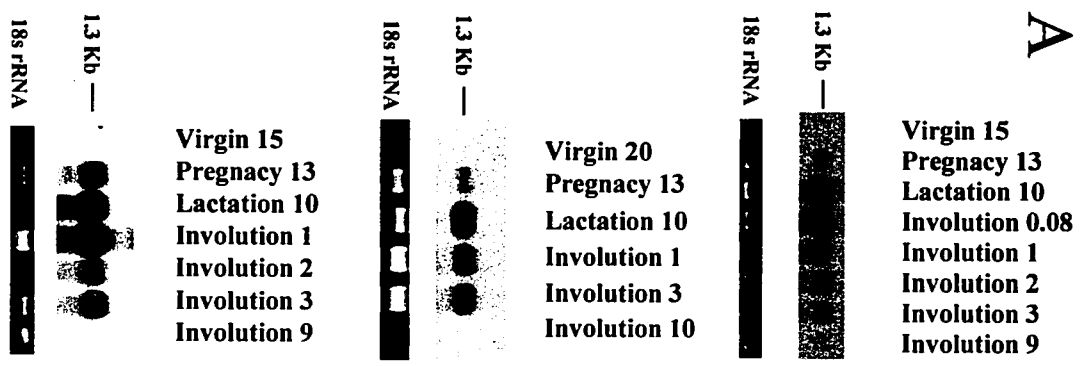
To identify the cellular localization of *cited2* mRNA expression fluorescent *in situ* analysis was attempted. Preliminary trials of *in situ* analysis were executed with whey acidic protein (*WAP*) because the expression pattern and location of this gene is already known. When the experiment was executed with normal conditions, using DIG labelled PCR product described in 2.6.1.2 there was a moderate difference between the RNase treated and untreated samples, though a definite result could not be interpreted due to the high levels of background fluorescence. L10 and I1 Sections subjected to the protocol with the modification of removing both primary and secondary antibodies from the hybridizations revealed fluorescence that was moderately similar to the results obtained in the previous experiment with antibody, but there was more intense fluorescence in the stromal tissue suggesting the results around the alveoli were just background fluorescence (Figure 5.5).

### **5.2.1.4 Radioactive *in situ* Hybridization**

The Myal lab at the University of Manitoba executed the following experiment to determine the location of *cited2* mRNA expression via radioactive *in situ* analysis, which was thought to be more sensitive than the method defined in B.1.3. Prior to the *in situ* I subcloned the PCR product representing the *cited2* recombinant phage into a TA plasmid cloning vector. This was sequence confirmed and the plasmid was sent to the Myal lab for *in situ* hybridization experiments. The plasmid was used to generate S<sup>35</sup> antisense and sense riboprobes. Anti-sense signalling localized *cited2* expression to the alveoli of the MG in the I0 and I2 developmental stages (Figure 5.5). Sense strand was used as a control. The sections hybridized with the sense probe showed minimal radioactivity. H&E staining was completed to provide a visible structure of the MG for reference to the staining witnessed with the antisense probe. The levels of stain in the *in situ* follow the levels of mRNA observed on the northern, where mRNA levels are high during early

**Figure 5.4: *vegfa* Northern Expression in the Mammary Gland:** PCR product obtained from the RESGEN *vegfa* clone was used as a probe in the above short profile Northern. A) Probes were labelled using  $\alpha$ -<sup>32</sup>P-dCTP and Invitrogen's Random Primer Labelling Kit. Trials were completed on three different mouse MG tissue sets above to confirm the Northern profiles. B) Densitometry was completed using the 18s rRNA band as a loading standard. The panels right of the northern represent normalized calculation of the 1.3kb band. Calculations were carried out with numbers obtained from Adobe Photoshop 7 analysis. V: Virgin; P: Pregnancy; L: Lactation; I: Involution

**A**



**B**

Normalized densitometry values

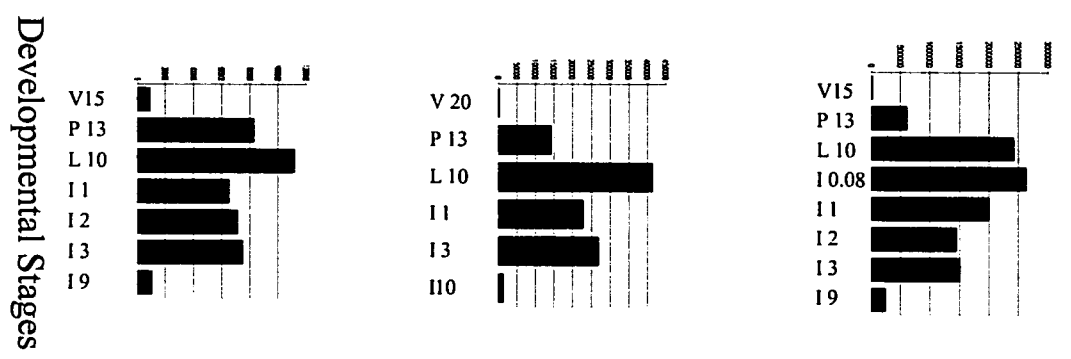
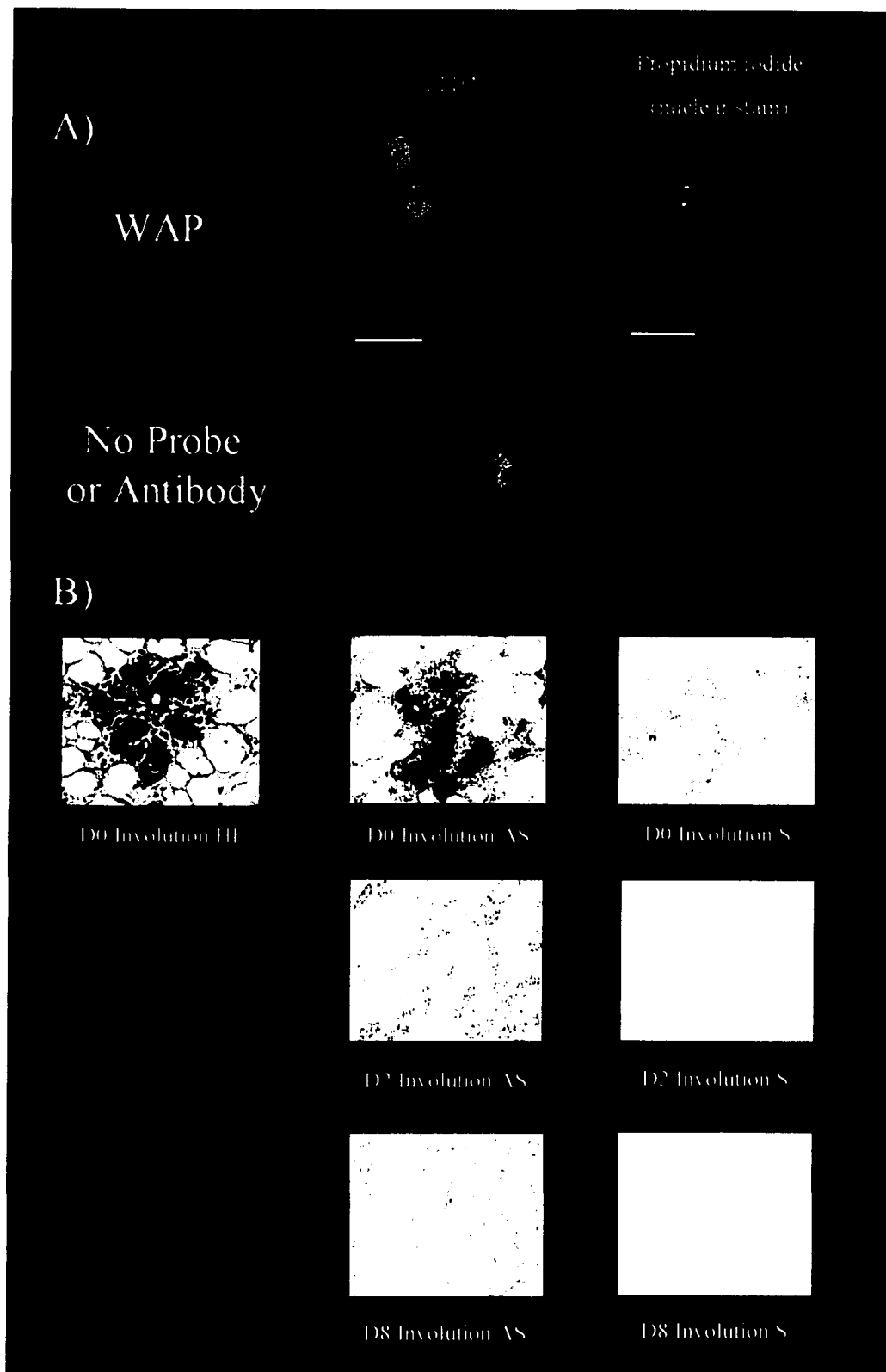


**Figure 5.5: *In situ analysis.*** A) DIG labelled probes were created using Invitrogen's DIG labelling kit. Whey acid protein PCR product was used for the reaction. Probes were hybridized to Lactation day 10 sections as a control. Anti-DIG antibodies conjugated to FITC were utilized for detection. Propidium iodide was used as a nuclear stain. B) Radiolabelled riboprobes were used in the reaction. Tissue sections were extracted from an involuting mammary gland 0,2 and 8 days after weaning (I0, I2 and I8 respectively). Anti-sense (AS) and sense (S) probes were used in the experiments. *In situ* analysis was executed by the Myal lab at the University of Manitoba.



involution and decrease in late involution (I8). In fully developed MG *In situ* analysis localized *cited2* mRNA expression to the alveoli of the MG. From the images it appears that the mRNA is localized to the cells lining the alveolus, the epithelial cells and myoepithelial cells. The alveoli consist of mainly epithelial cells and few myoepithelial cells in close proximity to the epithelial cells; therefore due to the low resolution of the microscope the exact location could not be discriminated.

## **5.2.2 Protein Analysis of *cited2***

### **5.2.2.1 Competition Assay**

The *cited2* antibody produced by Covance (Princeton, NJ) through the Windber Research Institute was designed to a peptide created from the sequence Shioda (Shioda *et al.*, 1997) used to create his *cited2* antibody. To determine if the band on the western was specific to the antibody, the peptide used to raise the primary antibody was incubated with the antibody before immuno-hybridization (the competed antibody). The competed antibody and the un-competed antibody were immuno-hybridized to test strip westerns comprising of only total protein from the P13 and L10 MG and processed accordingly. A 22 kDa protein, the size expected for *cited2*, was detected. The western that was incubated with the competed antibody showed highly reduced levels of antigen detection compared to the western that was incubated with the uncompleted antibody thus demonstrating that the antibody was specific for the protein it was intended for (Figure 5.6).

### **5.2.2.2 Western Analysis**

Protein isolated from the MG tissue used for RNA isolation for northern analysis, were purified for western analysis. Blots obtained from these experiments were blocked, incubated with the *cited2* antibody and processed accordingly. A protein of approximately 22 kDa was detected on the western blot. Protein levels were undetectable in the virgin (V15) and pregnancy (P13) developmental stages. Upon the switch to lactation (L10) the protein levels of *cited2* increased dramatically. These levels persisted through late lactation and early involution (I1, I2, and I3) and decreased dramatically by mid to late involution. Expression was absent in late involution (I9) as it was in virgin (V15) (Figure 5.7).

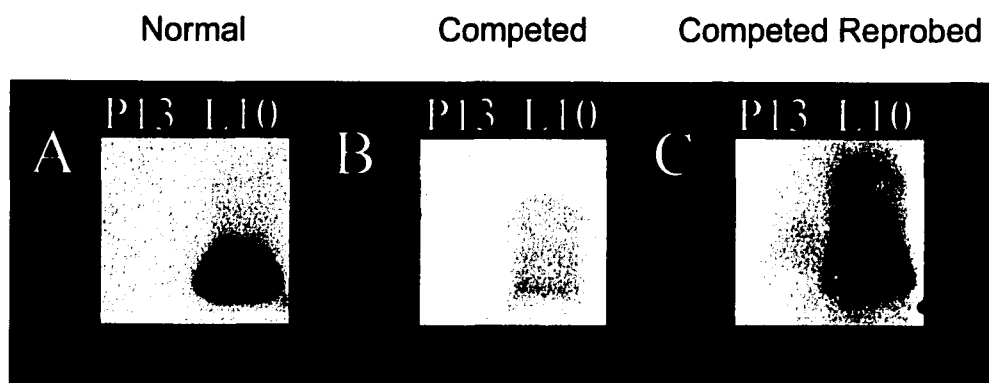


**Figure 5.6: *cited2* Antibody Competition Assay:**

Test western strips consisting of P13 and L10 Mammary Gland Proteins were probed with *cited2* antibody created in conjunction with Windber Research Institute. A) Test strip probed with anti-*cited2* antibody in a 1:5000 dilution. B) Test strip probed with solution containing a 1:5000 dilution of the anti-*cited2* antibody, but was previously incubated for one hour before hybridization with 10 $\mu$ g of the peptide used to create the antibody. C) Test strip originally incubated with the competition solution from B, but probed with un-competed anti-*cited2* antibody in a 1:5000 dilution.

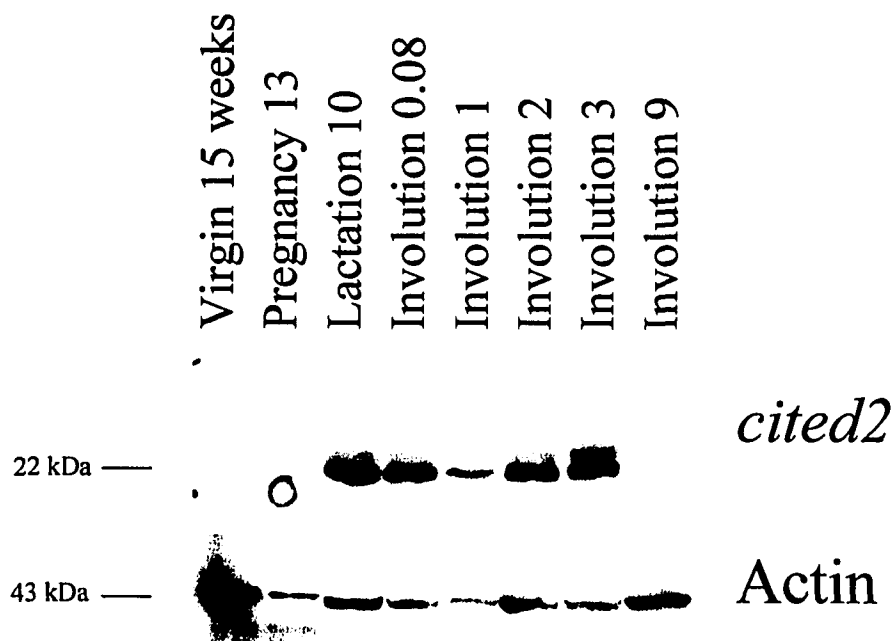


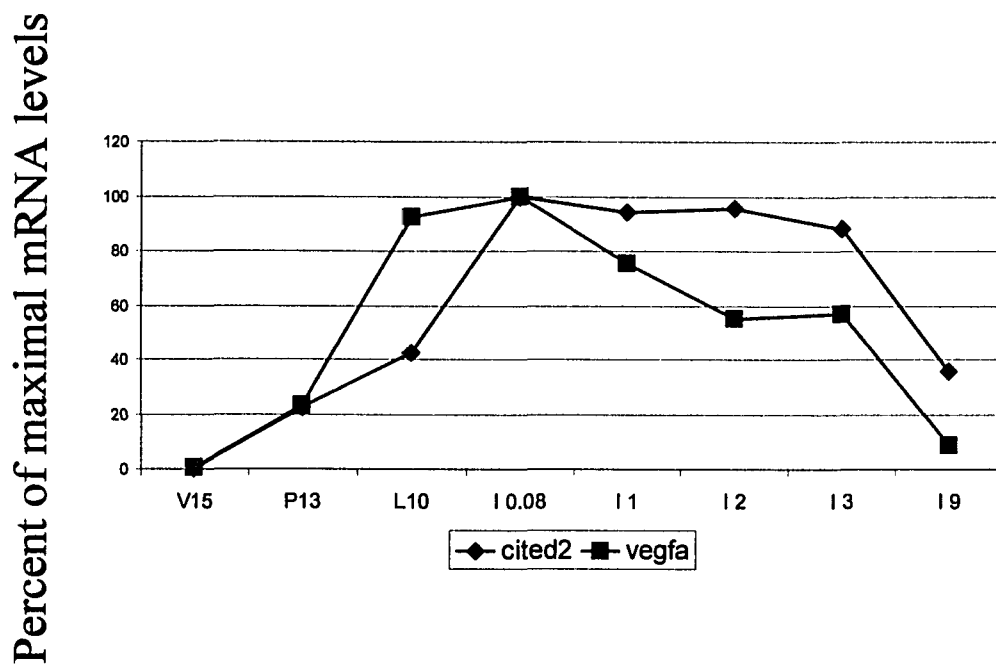
**Figure 5.7: Western Analysis of *cited2/Mrg1*** : Antibodies were made to the same peptide sequence as used by Shioda *et al.* (1996). Secondary antibodies were conjugated with horseradish peroxidase (HRP) and detected with ECL detection kit from Amersham Biosciences. Depending on whether the anti-body used was from Shioda or whether the anti-body we had created was used, the dilution ranged from 1:500 to 1:10000 respectively. In this western the primary antibody dilution used was 1:10000. The same Western blot was stripped and reprobred with anti-actin (Stressgen) antibody (1:1000 primary antibody dilution) as a control for protein loading.

### 5.2.3 *Cited2* and a Possible Role in PPAR Mediated Transcription

To examine the possibility of a common transcription regulatory pathway I completed a bioinformatics analysis and literature mining of *cited2* and PPAR. Until recently no known association between *cited2* protein and any PPAR had been uncovered. In 2003 Tien *et al.* discovered a direct interaction between *cited2* and PPAR $\alpha$ . In an attempt to identify novel PPAR interacting factors they isolated *cited2*. The interaction between the 2 was direct and independent of any cofactors or PP. *Cited2* did aid in the PPAR $\alpha$  and PPAR $\gamma$  mediated transcriptional regulation pathways, but did not show any affect on PPAR $\delta/\beta$  mediated transcription. Unfortunately levels of PPAR have not been examined in the involuting MG; therefore no direct correlation can be discerned between *cited2* and PPAR activity in the MG.

### 5.2.4 Isolation of PPRE in Upstream Sequence of Factors Involved with *cited2*

To identify if there are any putative PPRE sites in the upstream regions of *cited2*, *hif1- $\alpha$* , and *vegfa*, I scanned the promoters and an additional 5kb upstream of the transcription start sites. The methodology is the same as in 4.2.5.1. From the clustalW results there is evidence of putative PPRE in each gene with homology exceeding 50% in each case for both the scan of the promoter region and the scan of the 5kb upstream of the transcription start site (figure 5.8 A and B). The scan of the *cited2* gene produced 2 potential PPRE, though the homology to the PPRE at -4063 bases was higher with 70% homology opposed to the 61% homology of the PPRE scan lacking the 5' flanking consensus sequence. *Hif1- $\alpha$*  contains a PPRE with the highest homology out of all the genes examined in this chapter with an 80% match from the scan of the 5kb upstream sequence. *Vegfa* contains a putative PPRE that has the highest homology in the scan with the promoter region and the PPRE without the 5' flanking consensus (figure 5.8 A). When the scan was completed on the 5kb upstream DNA sequence and with the probe containing the 5' flanking consensus sequence, it produced the lowest match, compared to *cited2* and *hif1- $\alpha$* , with only 12/20 or 60% (figure 5.8 B).



## Developmental stages

**Figure 5.9: *vegfa* and *cited2* mRNA comparison:** The normalized densitometry values for *cited2* and *vegfa* mRNA were compared to exemplify a relation between the expression profiles of the two genes. Levels were obtained by dividing the normalized densitometry values by the highest value for that gene. Note that with the increase of *cited2* mRNA levels, there is a subsequent decrease in *vegfa* mRNA levels.

### 5.3 DISCUSSION

The profile of the *cited2* band observed from the northern analysis peaked in early involution (I1-I3), the period dictating the switch in activity of the MG, and decreased in levels by mid to late involution, a period in which the MG has almost reset itself into a virgin-like state. The northern that was made from a different set of MG tissue produced a profile similar to the previously mentioned northern when probed with *cited2*. The general trend where an increase in expression from virgin to early involution and a decrease into late involution is observed (figure 5.3), but the exact period of induction varies. In both cases the peak level of expression encompasses the time where there is a switch from a lactating gland to an involuting one and that levels decrease after I3. The results obtained from the *in situ* analysis, localization of *cited2* mRNA to MG epithelial cells is logical, as the epithelial cells that comprise the alveolus are the most metabolically active cells in the MG during the periods of lactation and involution. Secondly it is these cells that undergo the most apoptosis during involution (Boudreau *et al.*, 1995); therefore *cited2* may play an important role in the involution of the MG.

Western analysis was used to determine whether the *cited2* protein was present at the same time as the mRNA during the MG postnatal developmental cycle. Although the mRNA levels are induced moderately during late pregnancy, we do not detect the presence of the protein until early lactation. The peak in *cited2* mRNA during early involution is synchronous with the high levels of *cited2* during early involution. At the mRNA level, *cited2* is induced during early lactation and peaks at I2/I3; the protein is expressed in late involution and is maintained until the *cited2* mRNA levels begin to decrease (I4). It is after I3 that the protein levels drop and are minimal by I9. The levels of the protein expression and the mRNA expression do correlate and are present throughout the switch from lactation to involution. The delay in translation of a protein is not unheard of especially in factors that are required for temporal transitions (Charlesworth *et al.*, 2000). The half-life of *cited2* is extremely short, approximately 20mins, which may tie in with the delay of *cited2* translation. This short half life also allows for exquisite control of *cited2* activity (Bhattacharya *et al.*, 1998).

*Cited2* is a nuclear protein (Sun *et al.*, 1998), this fact with the observation that *cited2* mRNA and protein levels are high at the onset of involution in the northern and

westerns alludes to a possible role for *cited2* as a regulator of gene expression participating in the transition from lactation to involution. This is also supported by the previous information from Sun *et al.* (1998) indicating that *cited2* has transforming capabilities and is a transcriptional co-activator. Unfortunately the direct affect of *cited2* on gene expression has yet to be examined, though it has been implicated in the regulation of angiogenesis via inhibiting *hif1- $\alpha$*  from binding to p300/CBP.

To examine if *cited2* had a direct affect on the angiogenic pathway I looked at the expression of *vegfa*. The *vegfa* northern results lead me to conclude that *vegfa* mRNA levels are elevated during pregnancy and lactation, but decreased during the induction of involution. *Vegfa* is involved in vascularization and the presence of the mRNA during pregnancy correlates to the requirements of vascularization for cell growth and differentiation of the MG at this time. When the MG enters lactation and proceeds into involution the requirement for vascularization is removed (reviewed by Djonov, Andres and Ziemiecki, 2001). Therefore the levels of factors involved with angiogenesis of the gland should be removed and this appears to be the case with *vegfa*. Although the mRNA levels depict this, the protein levels were not obtained and therefore a role for *vegfa* on a protein and functional level cannot be concretely stated. It has been observed that *vegfa* protein is present in human MEC during pregnancy and lactation (Nishimura *et al.*, 2002). Therefore it is possible that *vegfa* is affected by the increase in *cited2* expression. Previous knowledge of the inhibition of *hif1- $\alpha$* , the regulator of *vegfa*, by *cited2* suggests that it may be partake in the inhibition of angiogenesis, and subsequently the reduction in the supply of oxygen to the MG, by preventing angiogenic factors from being transcribed (reviewed in Mazure *et al.*, 2004). This mechanism may be present in the MG system given that there are large levels of *cited2* mRNA and protein during late lactation at a time where levels of *vegfa* mRNA start to decrease (figure 5.9). This regulation is obtained through the interaction of the CR2 domain of *cited2* and the CH1 domain of the p300/CBP complex; *cited2* prevents *hif1- $\alpha$*  from binding to p300/CBP through this interaction (de Guzman *et al.*, 2003). Through the interaction of *hif1- $\alpha$*  with p300/CBP genes that are involved in angiogenesis such as *vegfa* are up regulated. If *cited2* prevents this interaction, levels of *vegfa* mRNA and subsequently protein expression should

A)

PPRE	1	<b>A G G T C A A A G G T C A</b>	13
Cited2	-1157	<b>G G A T C A A G G G C A A</b>	-1145
Hif1a	-172	<b>G A G C C G G A G C T C A</b>	-160
Vegfa	-748	<b>A A G C C A G G G G T C A</b>	-736

B)

PPRE	1	<b>C A A A A C T A G G T C A A A G G T C A</b>	20
Cited2	-4063	<b>A G A A A T G A G G A C A A G G G C C A</b>	-4044
Hif1a	-3118	<b>G C C A A T T A G G T C A A A G G T C A</b>	-2999
Vegfa	-2421	<b>C A A G G G T G G G T T A G A G G T G G</b>	-2402

**Figure 5.8 : Identification of PPRE in the Promoter Region of Genes Involved with *cited2*.**

A) The promoter regions for each gene were obtained from Entrez Gene and were scanned using ClustalW alignment with the consensus PPRE sequence AGGTCAAAGGTCA to find the best possible alignment between the promoter sequence and the consensus PPRE. Each gene's representative PPRE sequence was then aligned to other putative PPRE to compare the homology.

B) For each gene, 5000 bases upstream of the start codon (ATG) was scanned with the consensus PPRE sequence including the 5' flanking consensus sequence that is believed to aid in PPAR/RXR recognition. The consensus sequence (sequence that the promoters were aligned to) (grey boxes) is indicated at the top of each group of sequences and is depicted by the notation "PPRE". Boxshade was used to view the alignments. The black boxes indicate bases that occur most frequently and bases with a lower frequency are marked by a white box. Each sequences position has been referenced to the start codon for each gene and is indicated by the numbers present bordering the sequences. Upstream sequence was obtained from the mouse genome informatics database. <http://www.informatics.jax.org/>

decrease due to the lack of activation (Freedman *et al.*, 2003). Therefore *cited2* may be involved in the regulation of *vegfa* mRNA expression in the MG. In contrast the noted difference in mRNA levels of *cited2* and *vegfa* fluctuate after the period of proteinase dependent involution, with levels of *cited2* always exceeding *vegfa*. The differential levels at I3 however are quite small and this suggests that other mechanisms that regulate and require *vegfa* and *cited2* must also be in place.

The evidence of *cited2* acting as a co-regulator of PPAR $\alpha$  adds a new element to the presence of a PPAR mediated transcriptional regulatory pathway in the MG. The fact that *cited2* does contain a putative PPRE and interacts with PPAR $\alpha$  provides strong evidence that *cited2* may play a role in PPAR mediated transcription. The evidence of a strong PPRE in the *hif1- $\alpha$*  promoter region suggests that it is possible that *cited2* may regulate *hif1- $\alpha$*  and *vegfa* through a PPAR pathway. The regulation of *vegfa* through a PPAR mediated pathway is supported by the previous evidence of a PPAR $\gamma$  induced up-regulation of transcription of *vegfa* (Jozkowicz *et al.*, 2000; Yamakawa *et al.*, 2000; reviewed in Josko and Mazurek, 2004). This is further solidified by the observation of a PPRE in the promoter region of *vegfa* (figure 5.8). Conversely, PPAR $\alpha$  can inhibit the transcription of *vegfa*-receptor 2 via an association with the transcriptional regulator Sp1 (Meissner *et al.*, 2004), indicating a secondary method of angiogenic regulation through a PPAR mediated pathway. Whether PPAR $\alpha$  can regulate *vegfa* expression is not yet known, but it could introduce a possible method of exquisite regulation of the *vegfa* gene by counteracting the affects of PPAR $\gamma$ .

These observations compiled with the evidence of the involvement in the regulation of numerous factors from chapter 4, emphasizes an even more cohesive finding in the selection and screen of the macroarrays. Potentially, *cited2* may be involved in the regulation of these factors, but expressional analysis specifically looking at these affect of these genes from *cited2* over-expression would have to be completed to solidify this hypothesis.

The evidence obtained in regards to the expression pattern of *cited2* and the location of the mRNA and protein lead to the idea that *cited2* may function as a regulator of various pathways involved in the switch of the MG from lactation to involution. In addition to the possible inhibition of *vegfa* by *cited2*, it may also have an affect in the

system via an association with p300/CBP and PPAR $\alpha$  in up-regulating other subsets of genes, such as those involved in cell proliferation, or those involved in protection from the stressed environment. It can be further postulated that *cited2* may even act to regulate genes such as *fabp3*, *ltf*, *trf*, *fil*, and *lcn2* through an interaction with PPAR $\alpha$ . To develop the idea that *vegfa* is affected by *cited2* protein, localization of *vegfa* mRNA would be critical to determine if they exist in the same cells. As well protein levels of *vegfa* would also be beneficial in the development of this interaction as it is necessary to see if the protein levels decrease concomitantly with the mRNA. To elaborate on the function of *cited2*, over-expression of *cited2* in a cell culture system and the subsequent cDNA produced would have to be compared to a culture exhibiting un-induced expression. Through this a comparison may be made and possible factors up regulated by *cited2* could be determined. The exact role of *cited2* at this point cannot be elucidated based on the results obtained, but a requirement for *cited2* during the switch from lactation to involution is quite evident. Ultimately to develop the idea of a common PPAR mediated transcriptional regulation, the genes mentioned here need to be further scrutinized in the presence of various PPAR and in the absence of *cited2*.

## CHAPTER 6 – CONCLUSIONS

My work over the last few years has been reasonably productive and has/will give rise to a number of primary author and co-authored manuscripts (Table 6.1). The objective of my thesis was to identify differentially expressed genes over the course of the MG postnatal developmental profile with an emphasis on the switch from a lactating state to an involuting state. The shift between L10 to I1 has never been the focus of study in MG development, though much work has been done defining the Lactation stage, and the transition between proteinase independent to proteinase dependent involution. In total 17 genes, examined in the current study by northern analysis, were found to either increase or decrease between the stages of L10 and I1.

From the macro array screens I was able to identify 132 clones that had differential expression profiles over the course of postnatal MG development. Among the most abundant types of genes identified were genes that represented ribosomal protein genes and iron binding/metabolism genes. Examination of the literature lead to the realization that two of the gene groups (iron binding/metabolism genes and calycin superfamily genes) shared common features that allowed me to join them into a larger group. Select gene members in both groups have documented roles in iron metabolism and in an immune response to changes in the tissue environment. In total 25 of the 132 clones fall into this supergene category. The results of the current study therefore support my initial hypothesis that differences in the expression of specific subsets of genes may define the change in the tissue environment over the course of MG postnatal development. In the case of the supergene family it is thought that they would serve to help protect or attempt to protect the tissue environment in the face of high levels of active cell death.

Northern analysis validated the differential expression over the course of MG postnatal development for 22 genes selected from my screen. Based on the gene expression profiles obtained I observed three major patterns of gene expression based on when the initial increase leading to peak values occurs (genes in which the initial increase in mRNA levels leading to peak levels occurred between V15 and P13; genes in which the initial increase occurred between P13 and L10; genes in which the initial increase

occurred between L10 and I1). All genes that fell in the iron binding/metabolism and calycin genes were found to have a PPRE element that could be controlled by PPAR

Publication (manuscript or abstract)	Contribution	Data in the paper appears in part or whole in Chapter
<b>Maciejko BD</b> , Sprague D, Wilton B, Cheung H, Hesselson D, Kirk J, Scott K, Hucaluk C, Clark R, Caceres L, Kelln R, Clark W, Weaver WM, Myal Y, Chrenek MA, Wong P. (2001). Identification and characterization of genes involved in early mouse mammary gland involution. <i>Mol Biol Cell</i> 12: 2294	Verified all the data, made the presentation and presented it at the international meeting	3
Wong P, Ziesel A, Erickson T, Chrenek M, Patterson M, Gaultier, Wilton B, Block M, Stepczynski J, McDonald B, <b>Maciejko B</b> , Gee C, Lam V, Ng D, Kelln R, Lagali P, Grewal R, Sprague D, Organisciak D, Ayyagari R, Myal Y. (2004). Applying meta-bio-data and array analyses to understand disease states. <i>TIBETS</i> 1:102-117.	Contributed the MG data, read and edited the manuscript.	1 and 5
<b>Maciejko B</b> , Erickson T <sup>†</sup> , †, Gee C, Lam V, Ng D, Blanchard A, Myal Y, Chrenek M, Wong P. (+co-first authors). (2004). Identification of mammary gland differential expressed genes in breast cancer tissues. <i>TIBETS</i> 1:1-14.	Provided the data and did a significant part of the writing of this manuscript	4
<b>Maciejko BD</b> , Chambers M, Blanchard A, Darrow R, Myal Y, Organisciak DT, Wong P. (2005). Expression of Cited2, a gene isolated from a light induced retinal degeneration cDNA library, in the degenerating retina and the involuting mammary gland. <i>Invest. Ophthalmol. Vis. Sci.</i> 2005 46: E-Abstract 3082.	Provided significant amounts of data. Made the presentation and presented it at the international meeting.	5
<b>Maciejko BD</b> , Blanchard A, Chrenek MA, Somiari S, Weaver VM, Myal Y, Wong P. (2005). Cited2 is induced over the course of mouse mammary gland development. (in prep).	Provided the data and did significant portions of the writing.	5

**Table 6.1: Contributions to published manuscripts or abstracts**

factors in their respective promoter regions. Indirectly these patterns seem to conform with a reported down regulation of PPAR $\alpha$  and PPAR $\gamma$ , though the direct mechanism of

transcriptional control is not fully understood. The correlation of PPAR mediated transcription to the factors examined from the screen described in this thesis may indicate an involvement of PPAR mediated transcription in the switch between different stages of the MG. Unfortunately the presence of various PPAR in the involuting MG has not been well examined, and only minor analysis has been completed in the developing MG and in the cancerous environment (Gimble et al., 1998). Ultimately more than just PPAR control is occurring to be able to explain the presentation of 3 waves of gene expression.

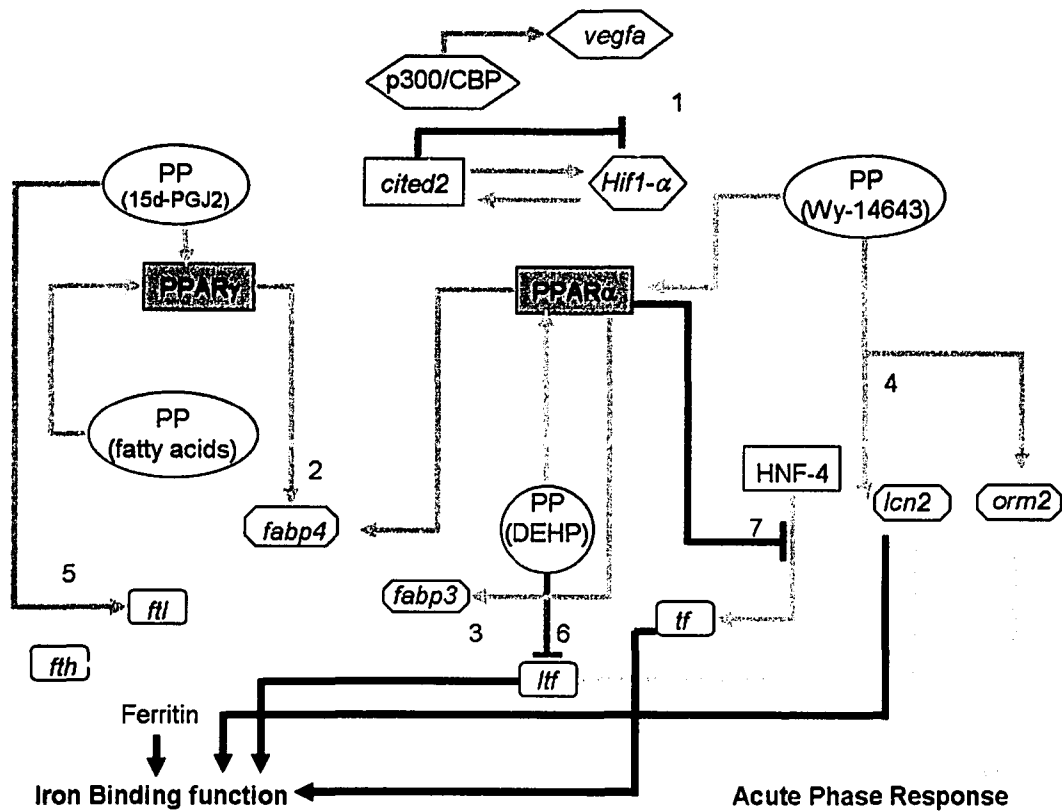
In a parallel series of studies, that adapted a functional genomics approach to identify a putative molecular component that might be essential to the involution process, lead to the examination of *cited2* expression over the course of MG development. We had identified *cited2* as a light-inducible gene in a retinal system (LIRD) induced to undergo retinal degeneration. *Cited2* had not been previously studied in MG development and is a transcription mediator that interacts with the transactivator CBP/p300. Interestingly, *cited2* protein has recently been found to physically interact with PPAR $\alpha$ . Analyses of *cited2* through northern, western and *in situ* experiments imply high levels of *cited2* during late lactation and early involution. In the LIRD model system *cited2* is induced by a light-mediated oxidative stress, suggesting that MG during lactation and involution may be under a state of oxidative stress. Potentially *cited2* may be part of the induction of PPAR mediated transcription, which may be responsible for the regulation of subsets of genes analyzed above, or the activation of other mechanisms in the MG during stress.

The subsets of genes analyzed above may be involved in the onset of controlled tissue involution due to the nature of the MG at the developmental stages analyzed. A speculative overview of the regulation by PPAR interactions with each of the genes from chapters 4 and 5 and the subsequent effect in MG involution can be observed in figure 6.1. The data at this point is suggestive; nothing can be concretely stated at this point as the sets of experiments carried out in this thesis are merely starting points to the characterization of subsets of genes that may be involved in the alleviation of stress in the MG during involution. Realistically the network of genes and proteins involved in this process is much more complex, diverse, and elegant and as such requires much more work to fully elucidate the system.

## Figure 6.1: A hypothetical Model

The focus of this thesis has been the identification of subsets of genes that share associations with the postnatal development of the mouse MG. Subsequently iron binding genes, calycin super family genes, and *Cited2* were further characterized and found to share a common association with PPAR and PPs.

*Cited2* can act as a transcriptional co-activator by interacting with PPAR-alpha and PPAR-gamma, and can also act as a co-repressor by inhibiting the *hif1- $\alpha$*  interaction with p300/CBP (1). This inhibition of *hif1- $\alpha$*  subsequently down regulates *vegfa* expression, a factor involved with angiogenesis. This down-regulation can be associated with the lack of cell growth during involution and the removal of the requirement of vascularization (Djonov *et al.*, 2001). The activating abilities of *cited2* with PPAR may work in numerous ways. Activation with PPAR-alpha could result in the increased activity of *fabp4* and *fabp3* increasing fatty acid metabolism. The increase in *fabp4* activity results in adipogenesis during the virgin and virgin like periods (Rival *et al.*, 2004) (2). Subsequently the activation of *fabp4* results in the transport of fatty acid ligands (PP) to PPAR $\gamma$  for further activation (Tontonoz *et al.*, 1995). The activation of *fabp3* activity is believed to be involved in differentiation of the MG during late pregnancy and lactation as it represses the proliferation of the gland and promotes differentiation (3) (Yang *et al.*, 1994; Clark *et al.*, 2000). As such the increased expression in late pregnancy and lactation correlates to the previously determined role. The increase in activity of *orm1* and *lcn2* is induced by the presence of PPAR-alpha activator Wy-14643 has only been observed in cancerous cells, but at the same time has been observed to inhibit *orm1* expression in normal cell lines (4) (Gupta *et al.*, 2001; Anderson *et al.*, 1999). In the normal involuting MG, the role of *lcn2* and *orm1* are believed to be involved in an anti-inflammatory response to the stress on the system by preventing neutrophils from invading the gland (kjeldsen *et al.*, 2000; Daemen *et al.*, 2000; de Vries *et al.*, 2004). This has been shown to be independent of PPAR-alpha, but has yet to be confirmed. The activating effect of *cited2* on PPAR gamma may also be involved in activating activity of *fabp4* and an increase in transcription of *fil* (5). *Fih* (the cooperative subunit to the ferritin molecule) has been previously observed to be induced after the switch to involution (Lee *et al.*, 1996). *Fih* has been observed to have an inhibitory effect to apoptosis. There is an increase in *fih* levels HeLa cells induced to enter apoptosis via TNF- $\alpha$  (Cozzi *et al.*, 2003). Therefore the presence of ferritin during involution may be a result of cells trying to avoid apoptosis, which is why levels of *fih* decrease after early involution where the system can no longer resurrect. *Fih* was also observed to increase in oxidative stressed HeLa cells (Guzzo *et al.*, 1994) and as such may be induced in the involuting MG to prevent oxidative damage, possibly by sequestering free iron (Arosio and Levi, 2002). How iron is introduced into milk of the MG is unknown, but it is believed that iron in the milk is most likely extracted via transferrin receptors during lactation to be used by the MG (Sigman and Lonnerdale, 1990). Therefore the coordinate increase in *fil* and *fih* during involution may be involved in reducing cellular free iron levels thusly preventing oxidative stress during involution. The association of PPAR alpha and *cited2* may also have a negative effect on the expression of *lzf* (6) and *trf* as it has been shown that an increase in PPAR-alpha activity results in a decrease of *lzf* expression and by inhibiting HNF-4 from binding the promoter of *tf* prevents transcription from the *tf* gene (Hertz *et al.*, 1996) (7). Although the levels of PPAR-alpha are unknown during early involution, the presence of these factors may indicate the absence of PPAR in the involuting MG. *Tf* may have a second role in the MG besides that of general iron metabolism. By increasing the defense mechanisms by inducing cytokine production, *tf* may benefit the entire gland (Ryu *et al.*, 1998). The presence of *lzf* in the MG is required for bacteriostatic properties in the milk preventing growth of fungi such as *Candida albicans* and other bacteria (Morrill *et al.*, 2003). Through these properties it can provide a protective effect to the offspring and during early involution it may aid in bacteriostatic and anti-inflammatory properties (reviewed in Dorea, 2000; Lee *et al.*, 1996; Nickerson, 1989). Together these factors may act through a common transcriptional pathway that mediates expression of these genes through activation and repression during specific stages in MG post-natal development. Though these separate pieces of information are potentially associated, this is purely a speculative theory describing the interplay among the factors analyzed in my thesis.



**Iron Binding function**  
 During Involution these factors maintain the free iron levels in the cell and the tissue to control bacterial growth, to maintain normal metabolism, to sequester free iron that enters the system, to limit the toxicity of free iron, to maintain potential levels of oxidative stress.

**Acute Phase Response Anti-inflammatory**  
 In an active cell death environment it is important that an immune response does not occur in order to preserve the integrity of the tissue.

- Activates transcription of gene
- Competitively inhibits binding of factor
- Inhibits transcription (subsequent reduction in mRNA)
- PPAR is activated by ligands (PP)
- Associates with factor for subsequent activity
- Transcription factor    □ Receptor    □ PP

## Citations

- Anderson, S.P., Cattley, R.C., and Corton, J.C. (1999) Hepatic expression of acute-phase protein genes during carcinogenesis induced by peroxisome proliferators. *Mol Carcinog* **26**: 226-238.
- Arosio, P., Adelman, T.G., and Drysdale, J.W. (1978) On ferritin heterogeneity. Further evidence for heteropolymers. *J Biol Chem* **253**: 4451-4458.
- Arosio, P., and Levi, S. (2002) Ferritin, iron homeostasis, and oxidative damage. *Free Radic Biol Med* **33**: 457-463.
- Auboeuf, D., Rieusset, J., Fajas, L., Vallier, P., Frering, V., Riou, J.P., Staels, B., Auwerx, J., Laville, M., and Vidal, H. (1997) Tissue distribution and quantification of the expression of mRNAs of peroxisome proliferator-activated receptors and liver X receptor-alpha in humans: no alteration in adipose tissue of obese and NIDDM patients. *Diabetes* **46**: 1319-1327.
- Auwerx, J., Schoonjans, K., Fruchart, J.C., and Staels, B. (1996) Regulation of triglyceride metabolism by PPARs: fibrates and thiazolidinediones have distinct effects. *J Atheroscler Thromb* **3**: 81-89.
- Baik, M.G., Lee, M.J., and Choi, Y.J. (1998) Gene expression during involution of mammary gland (review). *Int J Mol Med* **2**: 39-44.
- Bamforth, S.D., Braganca, J., Eloranta, J.J., Murdoch, J.N., Marques, F.I., Kranc, K.R., Farza, H., Henderson, D.J., Hurst, H.C., and Bhattacharya, S. (2001) Cardiac malformations, adrenal agenesis, neural crest defects and exencephaly in mice lacking Cited2, a new Tfap2 co-activator. *Nat Genet* **29**: 469-474.
- Bansal, M.P., and Medina, D. (1993) Expression of fatty acid-binding proteins in the developing mouse mammary gland. *Biochem Biophys Res Commun* **191**: 61-69.
- Bennett, M., and Schmid, K. (1980) Immunosuppression by human plasma alpha 1-acid glycoprotein: importance of the carbohydrate moiety. *Proc Natl Acad Sci U S A* **77**: 6109-6113.
- Berger, J., Albet, S., Bentejac, M., Netik, A., Holzinger, A., Roscher, A.A., Bugaut, M., and Forss-Petter, S. (1999) The four murine peroxisomal ABC-transporter genes differ in constitutive, inducible and developmental expression. *Eur J Biochem* **265**: 719-727.
- Bernlohr, D.A., Angus, C.W., Lane, M.D., Bolanowski, M.A., and Kelly, T.J., Jr. (1984) Expression of specific mRNAs during adipose differentiation: identification of an mRNA encoding a homologue of myelin P2 protein. *Proc Natl Acad Sci U S A* **81**: 5468-5472.

- Bhattacharya, S., Michels, C.L., Leung, M.K., Arany, Z.P., Kung, A.L., and Livingston, D.M. (1999) Functional role of p35srj, a novel p300/CBP binding protein, during transactivation by HIF-1. *Genes Dev* **13**: 64-75.
- Bohmer, F.D., Sun, Q., Pepperle, M., Muller, T., Eriksson, U., Wang, J.L., and Grosse, R. (1987) Antibodies against mammary derived growth inhibitor (MDGI) react with a fibroblast growth inhibitor and with heart fatty acid binding protein. *Biochem Biophys Res Commun* **148**: 1425-1431.
- Bong, J.J., Seol, M.B., Kim, H.H., Han, O., Back, K., and Baik, M. (2004) The 24p3 gene is induced during involution of the mammary gland and induces apoptosis of mammary epithelial cells. *Mol Cells* **17**: 29-34.
- Borchers, T., Hohoff, C., Buhlmann, C., and Spener, F. (1997) Heart-type fatty acid binding protein - involvement in growth inhibition and differentiation. *Prostaglandins Leukot Essent Fatty Acids* **57**: 77-84.
- Borlak, J., Meier, T., Halter, R., Spanel, R., and Spanel-Borowski, K. (2005) Epidermal growth factor-induced hepatocellular carcinoma: gene expression profiles in precursor lesions, early stage and solitary tumours. *Oncogene* **24**: 1809-1819.
- Boudreau, N., Sympton, C.J., Werb, Z., and Bissell, M.J. (1995) Suppression of ICE and apoptosis in mammary epithelial cells by extracellular matrix. *Science* **267**: 891-893.
- Boyd, D., Jain, S.K., Crampton, J., Barrett, K.J., and Drysdale, J. (1984) Isolation and characterization of a cDNA clone for human ferritin heavy chain. *Proc Natl Acad Sci U S A* **81**: 4751-4755.
- Bradshaw, A.D., and Sage, E.H. (2001) SPARC, a matricellular protein that functions in cellular differentiation and tissue response to injury. *J Clin Invest* **107**: 1049-1054.
- Braganca, J., Eloranta, J.J., Bamforth, S.D., Ibbitt, J.C., Hurst, H.C., and Bhattacharya, S. (2003) Physical and functional interactions among AP-2 transcription factors, p300/CREB-binding protein, and CITED2. *J Biol Chem* **278**: 16021-16029.
- Braun, V. (1997) Avoidance of iron toxicity through regulation of bacterial iron transport. *Biol Chem* **378**: 779-786.
- Brekken, R.A., Puolakkainen, P., Graves, D.C., Workman, G., Lubkin, S.R., and Sage, E.H. (2003) Enhanced growth of tumors in SPARC null mice is associated with changes in the ECM. *J Clin Invest* **111**: 487-495.
- Brisken, C., Ayyannan, A., Nguyen, C., Heineman, A., Reinhardt, F., Tan, J., Dey, S.K., Dotto, G.P., and Weinberg, R.A. (2002) IGF-2 is a mediator of prolactin-induced morphogenesis in the breast. *Dev Cell* **3**: 877-887.

- Bullen, J.J. (1981) The significance of iron in infection. *Rev Infect Dis* **3**: 1127-1138.
- Bundgaard, J.R., Sengelov, H., Borregaard, N., and Kjeldsen, L. (1994) Molecular cloning and expression of a cDNA encoding NGAL: a lipocalin expressed in human neutrophils. *Biochem Biophys Res Commun* **202**: 1468-1475.
- Casanueva, E., and Viteri, F.E. (2003) Iron and oxidative stress in pregnancy. *J Nutr* **133**: 1700S-1708S.
- Charlesworth, A., Welk, J., and MacNicol, A.M. (2000) The temporal control of Wee1 mRNA translation during *Xenopus* oocyte maturation is regulated by cytoplasmic polyadenylation elements within the 3'-untranslated region. *Dev Biol* **227**: 706-719.
- Chrenek, M.A., Wong, P., and Weaver, V.M. (2001) Tumour-stromal interactions. Integrins and cell adhesions as modulators of mammary cell survival and transformation. *Breast Cancer Res* **3**: 224-229.
- Clarkson, R.W., and Watson, C.J. (2003) Microarray analysis of the involution switch. *J Mammary Gland Biol Neoplasia* **8**: 309-319.
- Clarkson, R.W., Wayland, M.T., Lee, J., Freeman, T., and Watson, C.J. (2004) Gene expression profiling of mammary gland development reveals putative roles for death receptors and immune mediators in post-lactational regression. *Breast Cancer Res* **6**: R92-109.
- Correa-Rotter, R., Mariash, C.N., and Rosenberg, M.E. (1992) Loading and transfer control for Northern hybridization. *Biotechniques* **12**: 154-158.
- Crichton, R.R., and Ward, R.J. (1995) Iron species in iron homeostasis and toxicity. *Analyst* **120**: 693-697.
- D'Cruz, C.M., Moody, S.E., Master, S.R., Hartman, J.L., Keiper, E.A., Imielinski, M.B., Cox, J.D., Wang, J.Y., Ha, S.I., Keister, B.A., and Chodosh, L.A. (2002) Persistent parity-induced changes in growth factors, TGF-beta3, and differentiation in the rodent mammary gland. *Mol Endocrinol* **16**: 2034-2051.
- Daemen, M.A., Heemskerk, V.H., van't Veer, C., Denecker, G., Wolfs, T.G., Vandenabeele, P., and Buurman, W.A. (2000) Functional protection by acute phase proteins alpha(1)-acid glycoprotein and alpha(1)-antitrypsin against ischemia/reperfusion injury by preventing apoptosis and inflammation. *Circulation* **102**: 1420-1426.
- De Guzman, R.N., Martinez-Yamout, M.A., Dyson, H.J., and Wright, P.E. (2004) Interaction of the TAZ1 domain of the CREB-binding protein with the activation domain of CITED2: regulation by competition between intrinsically unstructured ligands for non-identical binding sites. *J Biol Chem* **279**: 3042-3049.

- de Vries, B., Walter, S.J., Wolfs, T.G., Hochepped, T., Rabina, J., Heeringa, P., Parkkinen, J., Libert, C., and Buurman, W.A. (2004) Exogenous alpha-1-acid glycoprotein protects against renal ischemia-reperfusion injury by inhibition of inflammation and apoptosis. *Transplantation* **78**: 1116-1124.
- Dente, L., Pizza, M.G., Metspalu, A., and Cortese, R. (1987) Structure and expression of the genes coding for human alpha 1-acid glycoprotein. *Embo J* **6**: 2289-2296.
- Desvergne, B., and Wahli, W. (1999) Peroxisome proliferator-activated receptors: nuclear control of metabolism. *Endocr Rev* **20**: 649-688.
- Devireddy, L.R., Teodoro, J.G., Richard, F.A., and Green, M.R. (2001) Induction of apoptosis by a secreted lipocalin that is transcriptionally regulated by IL-3 deprivation. *Science* **293**: 829-834.
- Djonov, V., Andres, A.C., and Ziemiecki, A. (2001) Vascular remodelling during the normal and malignant life cycle of the mammary gland. *Microsc Res Tech* **52**: 182-189.
- Donovan, A., and Andrews, N.C. (2004) The molecular regulation of iron metabolism. *Hematol J* **5**: 373-380.
- Doreswamy, K., and Muralidhara (2005) Genotoxic consequences associated with oxidative damage in testis of mice subjected to iron intoxication. *Toxicology* **206**: 169-178.
- Dowbenko, D., Kikuta, A., Fennie, C., Gillett, N., and Lasky, L.A. (1993) Glycosylation-dependent cell adhesion molecule 1 (GlyCAM 1) mucin is expressed by lactating mammary gland epithelial cells and is present in milk. *J Clin Invest* **92**: 952-960.
- Elangbam, C.S., Tyler, R.D., and Lightfoot, R.M. (2001) Peroxisome proliferator-activated receptors in atherosclerosis and inflammation--an update. *Toxicol Pathol* **29**: 224-231.
- Flo, T.H., Smith, K.D., Sato, S., Rodriguez, D.J., Holmes, M.A., Strong, R.K., Akira, S., and Aderem, A. (2004) Lipocalin 2 mediates an innate immune response to bacterial infection by sequestering iron. *Nature* **432**: 917-921.
- Flower, D.R. (1993) Structural relationship of streptavidin to the calycin protein superfamily. *FEBS Lett* **333**: 99-102.
- Flower, D.R., North, A.C., and Attwood, T.K. (1993) Structure and sequence relationships in the lipocalins and related proteins. *Protein Sci* **2**: 753-761.
- Fournier, T., Medjoubi, N.N., and Porquet, D. (2000) Alpha-1-acid glycoprotein. *Biochim Biophys Acta* **1482**: 157-171.

- Freedman, S.J., Sun, Z.Y., Kung, A.L., France, D.S., Wagner, G., and Eck, M.J. (2003) Structural basis for negative regulation of hypoxia-inducible factor-1alpha by CITED2. *Nat Struct Biol* **10**: 504-512.
- French, L.E., Wohlwend, A., Sappino, A.P., Tschopp, J., and Schifferli, J.A. (1994) Human clusterin gene expression is confined to surviving cells during in vitro programmed cell death. *J Clin Invest* **93**: 877-884.
- French, L.E., Soriano, J.V., Montesano, R., and Pepper, M.S. (1996) Modulation of clusterin gene expression in the rat mammary gland during pregnancy, lactation, and involution. *Biol Reprod* **55**: 1213-1220.
- Furth, P.A. (1999) Introduction: mammary gland involution and apoptosis of mammary epithelial cells. *J Mammary Gland Biol Neoplasia* **4**: 123-127.
- Gendler, S.J., Dermer, G.B., Silverman, L.M., and Tokes, Z.A. (1982) Synthesis of alpha 1-antichymotrypsin and alpha 1-acid glycoprotein by human breast epithelial cells. *Cancer Res* **42**: 4567-4573.
- Gimble, J.M., Pighetti, G.M., Lerner, M.R., Wu, X., Lightfoot, S.A., Brackett, D.J., Darcy, K., and Hollingsworth, A.B. (1998) Expression of peroxisome proliferator activated receptor mRNA in normal and tumorigenic rodent mammary glands. *Biochem Biophys Res Commun* **253**: 813-817.
- Goetz, D.H., Holmes, M.A., Borregaard, N., Bluhm, M.E., Raymond, K.N., and Strong, R.K. (2002) The neutrophil lipocalin NGAL is a bacteriostatic agent that interferes with siderophore-mediated iron acquisition. *Mol Cell* **10**: 1033-1043.
- Gonzalez-Manchon, C., Ferrer, M., Ayuso, M.S., and Parrilla, R. (1995) Cloning, sequencing and functional expression of a cDNA encoding a NADP-dependent malic enzyme from human liver. *Gene* **159**: 255-260.
- Grigor, M.R., McDonald, F.J., Latta, N., Richardson, C.L., and Tate, W.P. (1990) Transferrin-gene expression in the rat mammary gland. Independence of maternal iron status. *Biochem J* **267**: 815-819.
- Grosse, R., Boehmer, F.D., Langen, P., Kurtz, A., Lehmann, W., Mieth, M., and Wallukat, G. (1991) Purification, biological assay, and immunoassay of mammary-derived growth inhibitor. *Methods Enzymol* **198**: 425-440.
- Halliwell, B., and Gutteridge, J.M. (1984) Role of iron in oxygen radical reactions. *Methods Enzymol* **105**: 47-56.
- Halliwell, B., Aruoma, O.I., Wasil, M., and Gutteridge, J.M. (1988) The resistance of transferrin, lactoferrin and caeruloplasmin to oxidative damage. *Biochem J* **256**: 311-312.

- Halliwell, B., and Aruoma, O.I. (1991) DNA damage by oxygen-derived species. Its mechanism and measurement in mammalian systems. *FEBS Lett* **281**: 9-19.
- Hasmall, S., Orphanides, G., James, N., Pennie, W., Hedley, K., Soames, A., Kimber, I., and Roberts, R. (2002) Downregulation of lactoferrin by PPAR $\alpha$  ligands: role in perturbation of hepatocyte proliferation and apoptosis. *Toxicol Sci* **68**: 304-313.
- Hebbard, L., Steffen, A., Zawadzki, V., Fieber, C., Howells, N., Moll, J., Ponta, H., Hofmann, M., and Sleeman, J. (2000) CD44 expression and regulation during mammary gland development and function. *J Cell Sci* **113** (Pt 14): 2619-2630.
- Held, K.D., Sylvester, F.C., Hopcia, K.L., and Biaglow, J.E. (1996) Role of Fenton chemistry in thiol-induced toxicity and apoptosis. *Radiat Res* **145**: 542-553.
- Heller, D.L., Gianola, K.M., and Leinwand, L.A. (1988) A highly conserved mouse gene with a propensity to form pseudogenes in mammals. *Mol Cell Biol* **8**: 2797-2803.
- Hertz, R., Seckbach, M., Zakin, M.M., and Bar-Tana, J. (1996) Transcriptional suppression of the transferrin gene by hypolipidemic peroxisome proliferators. *J Biol Chem* **271**: 218-224.
- Higai, K., Aoki, Y., Azuma, Y., and Matsumoto, K. (2005) Glycosylation of site-specific glycans of alpha(1)-acid glycoprotein and alterations in acute and chronic inflammation. *Biochim Biophys Acta*.
- Hochepped, T., Berger, F.G., Baumann, H., and Libert, C. (2003) Alpha(1)-acid glycoprotein: an acute phase protein with inflammatory and immunomodulating properties. *Cytokine Growth Factor Rev* **14**: 25-34.
- Hovey, R.C., Trott, J.F., and Vonderhaar, B.K. (2002) Establishing a framework for the functional mammary gland: from endocrinology to morphology. *J Mammary Gland Biol Neoplasia* **7**: 17-38.
- Iyer, S., and Lonnerdal, B. (1993) Lactoferrin, lactoferrin receptors and iron metabolism. *Eur J Clin Nutr* **47**: 232-241.
- Jang, M.K., Choi, M.S., and Park, Y.B. (1999) Regulation of ferritin light chain gene expression by oxidized low-density lipoproteins in human monocytic THP-1 cells. *Biochem Biophys Res Commun* **265**: 577-583.
- Ji, W., Cai, L., Wright, M.B., Walker, G., Salgam, P., Vater, A., and Lindpaintner, K. (2000) Preservation of gene expression ratios among multiple complex cDNAs after PCR amplification: application to differential gene expression studies. *J Struct Funct Genomics* **1**: 1-7.
- Jin, H.S., Umemura, S., Iwasaka, T., and Osamura, R.Y. (2000) Alterations of myoepithelial cells in the rat mammary gland during pregnancy, lactation and involution, and after estradiol treatment. *Pathol Int* **50**: 384-391.

- Jones, J.L., and Walker, R.A. (1999) Integrins: a role as cell signalling molecules. *Mol Pathol* **52**: 208-213.
- Jones, S.E., and Jomary, C. (2002) Clusterin. *Int J Biochem Cell Biol* **34**: 427-431.
- Josko, J., and Mazurek, M. (2004) Transcription factors having impact on vascular endothelial growth factor (VEGF) gene expression in angiogenesis. *Med Sci Monit* **10**: RA89-98.
- Jozkowicz, A., Dulak, J., Piatkowska, E., Placha, W., and Dembinska-Kiec, A. (2000) Ligands of peroxisome proliferator-activated receptor-gamma increase the generation of vascular endothelial growth factor in vascular smooth muscle cells and in macrophages. *Acta Biochim Pol* **47**: 1147-1157.
- Juge-Aubry, C., Pernin, A., Favez, T., Burger, A.G., Wahli, W., Meier, C.A., and Desvergne, B. (1997) DNA binding properties of peroxisome proliferator-activated receptor subtypes on various natural peroxisome proliferator response elements. Importance of the 5'-flanking region. *J Biol Chem* **272**: 25252-25259.
- Kaikaus, R.M., Bass, N.M., and Ockner, R.K. (1990) Functions of fatty acid binding proteins. *Experientia* **46**: 617-630.
- Kane, R., Finlay, D., Lamb, T., and Martin, F. (2000) Transcription factor NF 1 expression in involuting mammary gland. *Adv Exp Med Biol* **480**: 117-122.
- Kanyshkova, T.G., Babina, S.E., Semenov, D.V., Isaeva, N., Vlassov, A.V., Neustroev, K.N., Kul'minskaya, A.A., Buneva, V.N., and Nevinsky, G.A. (2003) Multiple enzymic activities of human milk lactoferrin. *Eur J Biochem* **270**: 3353-3361.
- Kaplan, J. (2002) Mechanisms of cellular iron acquisition: another iron in the fire. *Cell* **111**: 603-606.
- Kjeldsen, L., Johnsen, A.H., Sengelov, H., and Borregaard, N. (1993) Isolation and primary structure of NGAL, a novel protein associated with human neutrophil gelatinase. *J Biol Chem* **268**: 10425-10432.
- Kjeldsen, L., Bainton, D.F., Sengelov, H., and Borregaard, N. (1994) Identification of neutrophil gelatinase-associated lipocalin as a novel matrix protein of specific granules in human neutrophils. *Blood* **83**: 799-807.
- Klausner, R.D., Ashwell, G., van Renswoude, J., Harford, J.B., and Bridges, K.R. (1983) Binding of apotransferrin to K562 cells: explanation of the transferrin cycle. *Proc Natl Acad Sci U S A* **80**: 2263-2266.
- Kliwer, S.A., Umesono, K., Noonan, D.J., Heyman, R.A., and Evans, R.M. (1992) Convergence of 9-cis retinoic acid and peroxisome proliferator signalling pathways through heterodimer formation of their receptors. *Nature* **358**: 771-774.

- Kranc, K.R., Bamforth, S.D., Braganca, J., Norbury, C., van Lohuizen, M., and Bhattacharya, S. (2003) Transcriptional coactivator Cited2 induces Bmi1 and Mel18 and controls fibroblast proliferation via Ink4a/ARF. *Mol Cell Biol* **23**: 7658-7666.
- Krey, G., Braissant, O., L'Horset, F., Kalkhoven, E., Perroud, M., Parker, M.G., and Wahli, W. (1997) Fatty acids, eicosanoids, and hypolipidemic agents identified as ligands of peroxisome proliferator-activated receptors by coactivator-dependent receptor ligand assay. *Mol Endocrinol* **11**: 779-791.
- Kumar, R., Vadlamudi, R.K., and Adam, L. (2000) Apoptosis in mammary gland and cancer. *Endocr Relat Cancer* **7**: 257-269.
- Kurtz, A., Spitzer, E., Zschesche, W., Wellstein, A., and Grosse, R. (1998) Local control of mammary gland differentiation: mammary-derived growth inhibitor and pleiotrophin. *Biochem Soc Symp* **63**: 51-69.
- Kutty, R.K., Kutty, G., Wiggert, B., Chader, G.J., Darrow, R.M., and Organisciak, D.T. (1995) Induction of heme oxygenase 1 in the retina by intense visible light: suppression by the antioxidant dimethylthiourea. *Proc Natl Acad Sci U S A* **92**: 1177-1181.
- LaLonde, J.M., Bernlohr, D.A., and Banaszak, L.J. (1994) The up-and-down beta-barrel proteins. *Faseb J* **8**: 1240-1247.
- Latruffe, N., and Vamecq, J. (1997) Peroxisome proliferators and peroxisome proliferator activated receptors (PPARs) as regulators of lipid metabolism. *Biochimie* **79**: 81-94.
- Lee, M., Kim, H., Jeon, D., Hwang, I., Choi, B., Myung, K., Kim, H., Choi, Y., Paik, S., and Baik, M. (1996) Iron metabolism-related genes and mitochondrial genes are induced during involution of mouse mammary gland. *Biochem Biophys Res Commun* **224**: 164-168.
- Lee, M., Hwang, I., Choi, Y., and Baik, M. (1998) Sequence of a cDNA encoding mouse ribosomal protein S14. *Biosci Biotechnol Biochem* **62**: 573-574.
- Lee, M., Na, S., Jeon, D., Kim, H., Choi, Y., and Baik, M. (2000) Induction of osteopontin gene expression during mammary gland involution and effects of glucocorticoid on its expression in mammary epithelial cells. *Biosci Biotechnol Biochem* **64**: 2225-2228.
- Lefcourt, A.M., and Akers, R.M. (1983) Is oxytocin really necessary for efficient milk removal in dairy cows? *J Dairy Sci* **66**: 2251-2259.
- Legrand, D., Elass, E., Pierce, A., and Mazurier, J. (2004) Lactoferrin and host defence: an overview of its immuno-modulating and anti-inflammatory properties. *Biometals* **17**: 225-229.

- Lemkin, P.F., Thornwall, G.C., Walton, K.D., and Hennighausen, L. (2000) The microarray explorer tool for data mining of cDNA microarrays: application for the mammary gland. *Nucleic Acids Res* **28**: 4452-4459.
- Leung, M.K., Jones, T., Michels, C.L., Livingston, D.M., and Bhattacharya, S. (1999) Molecular cloning and chromosomal localization of the human CITED2 gene encoding p35srj/Mrg1. *Genomics* **61**: 307-313.
- Li, M., Liu, X., Robinson, G., Bar-Peled, U., Wagner, K.U., Young, W.S., Hennighausen, L., and Furth, P.A. (1997) Mammary-derived signals activate programmed cell death during the first stage of mammary gland involution. *Proc Natl Acad Sci US A* **94**: 3425-3430.
- Liu, X., Robinson, G.W., Gouilleux, F., Groner, B., and Hennighausen, L. (1995) Cloning and expression of Stat5 and an additional homologue (Stat5b) involved in prolactin signal transduction in mouse mammary tissue. *Proc Natl Acad Sci US A* **92**: 8831-8835.
- Lund, L.R., Romer, J., Thomasset, N., Solberg, H., Pyke, C., Bissell, M.J., Dano, K., and Werb, Z. (1996) Two distinct phases of apoptosis in mammary gland involution: proteinase-independent and -dependent pathways. *Development* **122**: 181-193.
- Marti, A., Jehn, B., Costello, E., Keon, N., Ke, G., Martin, F., and Jaggi, R. (1994) Protein kinase A and AP-1 (c-Fos/JunD) are induced during apoptosis of mouse mammary epithelial cells. *Oncogene* **9**: 1213-1223.
- Marti, A., Lazar, H., Ritter, P., and Jaggi, R. (1999) Transcription factor activities and gene expression during mouse mammary gland involution. *J Mammary Gland Biol Neoplasia* **4**: 145-152.
- Master, S.R., Hartman, J.L., D'Cruz, C.M., Moody, S.E., Keiper, E.A., Ha, S.I., Cox, J.D., Belka, G.K., and Chodosh, L.A. (2002) Functional microarray analysis of mammary organogenesis reveals a developmental role in adaptive thermogenesis. *Mol Endocrinol* **16**: 1185-1203.
- Mather, I.H., and Keenan, T.W. (1998) The cell biology of milk secretion: historical notes. Introduction. *J Mammary Gland Biol Neoplasia* **3**: 227-232.
- Mazure, N.M., Brahimi-Horn, M.C., Berta, M.A., Benizri, E., Bilton, R.L., Dayan, F., Ginouves, A., Berra, E., and Pouyssegur, J. (2004) HIF-1: master and commander of the hypoxic world. A pharmacological approach to its regulation by siRNAs. *Biochem Pharmacol* **68**: 971-980.
- Meissner, M., Stein, M., Urbich, C., Reisinger, K., Suske, G., Staels, B., Kaufmann, R., and Gille, J. (2004) PPARalpha activators inhibit vascular endothelial growth factor receptor-2 expression by repressing Sp1-dependent DNA binding and transactivation. *Circ Res* **94**: 324-332.

- Meneghini, R. (1997) Iron homeostasis, oxidative stress, and DNA damage. *Free Radic Biol Med* **23**: 783-792.
- Merritt, C.M., and Board, P.G. (1988) Structure and characterisation of a duplicated human alpha 1 acid glycoprotein gene. *Gene* **66**: 97-106.
- Motojima, K. (2000) Differential effects of PPARalpha activators on induction of ectopic expression of tissue-specific fatty acid binding protein genes in the mouse liver. *Int J Biochem Cell Biol* **32**: 1085-1092.
- Motojima, K. (2000) PPAR-mediated diverse responses in various tissues of mouse. *Cell Biochem Biophys* **32 Spring**: 205-211.
- Muller-Fahrnow, A., Egner, U., Jones, T.A., Rudel, H., Spener, F., and Saenger, W. (1991) Three-dimensional structure of fatty-acid-binding protein from bovine heart. *Eur J Biochem* **199**: 271-276.
- Neve, R., Chang, C.H., Scott, G.K., Wong, A., Friis, R.R., Hynes, N.E., and Benz, C.C. (1998) The epithelium-specific ets transcription factor ESX is associated with mammary gland development and involution. *Faseb J* **12**: 1541-1550.
- Nguyen, A.V., and Pollard, J.W. (2000) Transforming growth factor beta3 induces cell death during the first stage of mammary gland involution. *Development* **127**: 3107-3118.
- Nilsen-Hamilton, M., Liu, Q., Ryon, J., Bendickson, L., Lepont, P., and Chang, Q. (2003) Tissue involution and the acute phase response. *Ann N Y Acad Sci* **995**: 94-108.
- Nishimura, S., Maeno, N., Matsuo, K., Nakajima, T., Kitajima, I., Saito, H., and Maruyama, I. (2002) Human lactiferous mammary gland cells produce vascular endothelial growth factor (VEGF) and express the VEGF receptors, Flt-1 AND KDR/Flk-1. *Cytokine* **18**: 191-198.
- Nuijens, J.H., van Berkel, P.H., and Schanbacher, F.L. (1996) Structure and biological actions of lactoferrin. *J Mammary Gland Biol Neoplasia* **1**: 285-295.
- Organisciak, D.T., Jiang, Y.L., Wang, H.M., Pickford, M., and Blanks, J.C. (1989) Retinal light damage in rats exposed to intermittent light. Comparison with continuous light exposure. *Invest Ophthalmol Vis Sci* **30**: 795-805.
- Oria, R., Alvarez-Hernandez, X., Liceaga, J., and Brock, J.H. (1988) Uptake and handling of iron from transferrin, lactoferrin and immune complexes by a macrophage cell line. *Biochem J* **252**: 221-225.
- Paape, M.J., Lilius, E.M., Wiitanen, P.A., Kontio, M.P., and Miller, R.H. (1996) Intramammary defense against infections induced by *Escherichia coli* in cows. *Am J Vet Res* **57**: 477-482.

- Paulussen, R.J., Geelen, M.J., Beynen, A.C., and Veerkamp, J.H. (1989) Immunochemical quantitation of fatty-acid-binding proteins. I. Tissue and intracellular distribution, postnatal development and influence of physiological conditions on rat heart and liver FABP. *Biochim Biophys Acta* **1001**: 201-209.
- Phelan, C.M., Larsson, C., Baird, S., Futreal, P.A., Ruttledge, M.H., Morgan, K., Tonin, P., Hung, H., Korneluk, R.G., Pollak, M.N., and Narod, S.A. (1996) The human mammary-derived growth inhibitor (MDGI) gene: genomic structure and mutation analysis in human breast tumors. *Genomics* **34**: 63-68.
- Prince, J.M., Klinowska, T.C., Marshman, E., Lowe, E.T., Mayer, U., Miner, J., Aberdam, D., Vestweber, D., Gusterson, B., and Streuli, C.H. (2002) Cell-matrix interactions during development and apoptosis of the mouse mammary gland in vivo. *Dev Dyn* **223**: 497-516.
- Puolakkainen, P., Bradshaw, A.D., Kyriakides, T.R., Reed, M., Brekken, R., Wight, T., Bornstein, P., Ratner, B., and Sage, E.H. (2003) Compromised production of extracellular matrix in mice lacking secreted protein, acidic and rich in cysteine (SPARC) leads to a reduced foreign body reaction to implanted biomaterials. *Am J Pathol* **162**: 627-635.
- Qi, C., Kashireddy, P., Zhu, Y.T., Rao, S.M., and Zhu, Y.J. (2004) Null mutation of peroxisome proliferator-activated receptor-interacting protein in mammary glands causes defective mammapoiesis. *J Biol Chem* **279**: 33696-33701.
- Quarrie, L.H., Addey, C.V., and Wilde, C.J. (1995) Apoptosis in lactating and involuting mouse mammary tissue demonstrated by nick-end DNA labelling. *Cell Tissue Res* **281**: 413-419.
- Rasmussen, L.K., Johnsen, L.B., Petersen, T.E., and Sorensen, E.S. (2002) Human GlyCAM-1 mRNA is expressed in the mammary gland as splicing variants and encodes various aberrant truncated proteins. *Immunol Lett* **83**: 73-75.
- Richert, M.M., Schwertfeger, K.L., Ryder, J.W., and Anderson, S.M. (2000) An atlas of mouse mammary gland development. *J Mammary Gland Biol Neoplasia* **5**: 227-241.
- Rittling, S.R., and Novick, K.E. (1997) Osteopontin expression in mammary gland development and tumorigenesis. *Cell Growth Differ* **8**: 1061-1069.
- Rudolph, M.C., McManaman, J.L., Hunter, L., Phang, T., and Neville, M.C. (2003) Functional development of the mammary gland: use of expression profiling and trajectory clustering to reveal changes in gene expression during pregnancy, lactation, and involution. *J Mammary Gland Biol Neoplasia* **8**: 287-307.
- Satoh, K., Ginsburg, E., and Vonderhaar, B.K. (2004) Msx-1 and Msx-2 in mammary gland development. *J Mammary Gland Biol Neoplasia* **9**: 195-205.

- Schachtrup, C., Emmler, T., Bleck, B., Sandqvist, A., and Spener, F. (2004) Functional analysis of peroxisome-proliferator-responsive element motifs in genes of fatty acid-binding proteins. *Biochem J* **382**: 239-245.
- Schoonjans, K., Staels, B., and Auwerx, J. (1996) The peroxisome proliferator activated receptors (PPARS) and their effects on lipid metabolism and adipocyte differentiation. *Biochim Biophys Acta* **1302**: 93-109.
- Shioda, T., Fenner, M.H., and Isselbacher, K.J. (1997) MSG1 and its related protein MRG1 share a transcription activating domain. *Gene* **204**: 235-241.
- Sorof, S. (1994) Modulation of mitogenesis by liver fatty acid binding protein. *Cancer Metastasis Rev* **13**: 317-336.
- Stein, T., Morris, J.S., Davies, C.R., Weber-Hall, S.J., Duffy, M.A., Heath, V.J., Bell, A.K., Ferrier, R.K., Sandilands, G.P., and Gusterson, B.A. (2004) Involution of the mouse mammary gland is associated with an immune cascade and an acute-phase response, involving LBP, CD14 and STAT3. *Breast Cancer Res* **6**: R75-91.
- Storch, J., and Thumser, A.E. (2000) The fatty acid transport function of fatty acid-binding proteins. *Biochim Biophys Acta* **1486**: 28-44.
- Strange, R., Li, F., Saurer, S., Burkhardt, A., and Friis, R.R. (1992) Apoptotic cell death and tissue remodelling during mouse mammary gland involution. *Development* **115**: 49-58.
- Sun, H.B., Zhu, Y.X., Yin, T., Sledge, G., and Yang, Y.C. (1998) MRG1, the product of a melanocyte-specific gene related gene, is a cytokine-inducible transcription factor with transformation activity. *Proc Natl Acad Sci U S A* **95**: 13555-13560.
- Taberero, A., Schoonjans, K., Jesel, L., Carpusca, I., Auwerx, J., and Andriantsitohaina, R. (2002) Activation of the peroxisome proliferator-activated receptor alpha protects against myocardial ischaemic injury and improves endothelial vasodilatation. *BMC Pharmacol* **2**: 10.
- Thompson, C.B. (1995) Apoptosis in the pathogenesis and treatment of disease. *Science* **267**: 1456-1462.
- Tien, E.S., Davis, J.W., and Vanden Heuvel, J.P. (2004) Identification of the CREB-binding protein/p300-interacting protein CITED2 as a peroxisome proliferator-activated receptor alpha coregulator. *J Biol Chem* **279**: 24053-24063.
- Tong, Z., Wu, X., and Kehrer, J.P. (2003) Increased expression of the lipocalin 24p3 as an apoptotic mechanism for MK886. *Biochem J* **372**: 203-210.
- Tontonoz, P., Hu, E., and Spiegelman, B.M. (1995) Regulation of adipocyte gene expression and differentiation by peroxisome proliferator activated receptor gamma. *Curr Opin Genet Dev* **5**: 571-576.

- Treuner, M., Kozak, C.A., Gallahan, D., Grosse, R., and Muller, T. (1994) Cloning and characterization of the mouse gene encoding mammary-derived growth inhibitor/heart-fatty acid-binding protein. *Gene* **147**: 237-242.
- Twining, S.S., and Brecher, A.S. (1977a) Identification of alpha1-acid glycoprotein, alpha2-macroglobulin and antithrombin III as components of normal and malignant human tissues. *Clin Chim Acta* **75**: 143-148.
- van Bilsen, M., van der Vusse, G.J., Gilde, A.J., Lindhout, M., and van der Lee, K.A. (2002) Peroxisome proliferator-activated receptors: lipid binding proteins controlling gene expression. *Mol Cell Biochem* **239**: 131-138.
- van Dijk, W. (1995) alpha 1-Acid glycoprotein. A natural occurring anti-inflammatory molecule? *Adv Exp Med Biol* **376**: 223-229.
- van Dijk, W., Havenaar, E.C., and Brinkman-van der Linden, E.C. (1995) Alpha 1-acid glycoprotein (orosomucoïd): pathophysiological changes in glycosylation in relation to its function. *Glycoconj J* **12**: 227-233.
- Vasson, M.P., Roch-Arveiller, M., Couderc, R., Baguet, J.C., and Raichvarg, D. (1994) Effects of alpha-1 acid glycoprotein on human polymorphonuclear neutrophils: influence of glycan microheterogeneity. *Clin Chim Acta* **224**: 65-71.
- Wahli, W., Braissant, O., and Desvergne, B. (1995) Peroxisome proliferator activated receptors: transcriptional regulators of adipogenesis, lipid metabolism and more. *Chem Biol* **2**: 261-266.
- Wang, H., and Hurley, W.L. (1998) Identification of lactoferrin complexes in bovine mammary secretions during mammary gland involution. *J Dairy Sci* **81**: 1896-1903.
- Williams, J.P., Weiser, M.R., Pechet, T.T., Kobzik, L., Moore, F.D., Jr., and Hechtman, H.B. (1997) alpha 1-Acid glycoprotein reduces local and remote injuries after intestinal ischemia in the rat. *Am J Physiol* **273**: G1031-1035.
- Wong, P., Ulyanova, T., Organisciak, D.T., Bennett, S., Lakins, J., Arnold, J.M., Kutty, R.K., Tenniswood, M., vanVeen, T., Darrow, R.M., and Chader, G. (2001) Expression of multiple forms of clusterin during light-induced retinal degeneration. *Curr Eye Res* **23**: 157-165.
- Yahata, T., Shao, W., Endoh, H., Hur, J., Coser, K.R., Sun, H., Ueda, Y., Kato, S., Isselbacher, K.J., Brown, M., and Shioda, T. (2001) Selective coactivation of estrogen-dependent transcription by CITED1 CBP/p300-binding protein. *Genes Dev* **15**: 2598-2612.
- Yamakawa, K., Hosoi, M., Koyama, H., Tanaka, S., Fukumoto, S., Morii, H., and Nishizawa, Y. (2000) Peroxisome proliferator-activated receptor-gamma agonists

- increase vascular endothelial growth factor expression in human vascular smooth muscle cells. *Biochem Biophys Res Commun* **271**: 571-574.
- Yan, Q., and Sage, E.H. (1999) SPARC, a matricellular glycoprotein with important biological functions. *J Histochem Cytochem* **47**: 1495-1506.
- Yang, C.R., Leskov, K., Hosley-Eberlein, K., Criswell, T., Pink, J.J., Kinsella, T.J., and Boothman, D.A. (2000) Nuclear clusterin/XIP8, an x-ray-induced Ku70-binding protein that signals cell death. *Proc Natl Acad Sci U S A* **97**: 5907-5912.
- Yang, D.C., Wang, F., Elliott, R.L., and Head, J.F. (2001) Expression of transferrin receptor and ferritin H-chain mRNA are associated with clinical and histopathological prognostic indicators in breast cancer. *Anticancer Res* **21**: 541-549.
- Yang, J., Goetz, D., Li, J.Y., Wang, W., Mori, K., Setlik, D., Du, T., Erdjument-Bromage, H., Tempst, P., Strong, R., and Barasch, J. (2002) An iron delivery pathway mediated by a lipocalin. *Mol Cell* **10**: 1045-1056.
- Yang, Y., Spitzer, E., Kenney, N., Zschiesche, W., Li, M., Kromminga, A., Muller, T., Spener, F., Lezius, A., Veerkamp, J.H., and et al. (1994) Members of the fatty acid binding protein family are differentiation factors for the mammary gland. *J Cell Biol* **127**: 1097-1109.
- Yin, Z., Haynie, J., Yang, X., Han, B., Kiatchosakun, S., Restivo, J., Yuan, S., Prabhakar, N.R., Herrup, K., Conlon, R.A., Hoit, B.D., Watanabe, M., and Yang, Y.C. (2002) The essential role of Cited2, a negative regulator for HIF-1 alpha, in heart development and neurulation. *Proc Natl Acad Sci U S A* **99**: 10488-10493.
- Zhao, F.Q., Zheng, Y., Dong, B., and Oka, T. (2004) Cloning, genomic organization, expression, and effect on beta-casein promoter activity of a novel isoform of the mouse Oct-1 transcription factor. *Gene* **326**: 175-187.

Category/ Clone ID#		Identity	Accession	Score	E-Value	mRNA length
Novel/Unknown function						
B2 254	GCGGNCGAGCTGNCTGAGACGGCACGAGGAAAAATCACGGNGGTTTAAATAATAGCGCCACGTTTCAGTATAATAAGCTCCACCCCTGTCTGTGCGGGACATGGCCAGCAGGCCAGGAGGACAGGTGGAGCCAGCGTCCGATGCTGCACGGTCTGAGAATTGCCCTTGGAGTGGTTAGTACAGATGGATGGGGACAGGCCAGGACCCCAAGCACACAGGTCAGTCAGGGCCTTGACACACTGGTTCGGTTACACAGCTCCGGGAGCATCTGAGTGGGGGCCGGTACCCAATTTCGCCCTATATCTGCTCTATACAGC	Mus musculus RIKEN cDNA 1810010G06 gene	BC042772.1	490	e-136	partial cds Length = 2295
C 140-2	GCAATCCNGATCATGTGTGCTGTGATGGTGNNGCTCTGGGAATCATCTNNGCNCCTGTCCCTCCAATCTANACTTTACCTCAGTGTNTNCCATCTGNGGAGAATCTGGCTACCCATTTGTAGGAGCTTTGTTTTGGCCATCTCTGGAATTCTGTCTATTGTACAGAAAAAGATGACTAAGCCTTTGGTTACACAGCAGCCTAGCCCTGAGCATCTGAGTGCCTCTCTGCTCTTACAGGCATCGCTATTCTCTGTCTGTGCTGCTTTAGAGCCTGCCTTGCAGCAATGTAAGCTGGCTTTACACAACCTAGACACAACCCAAGATGCTTATCATTCTTTAGCCCTGAGCCATTAAACAGCTGCTTCTGTGGCCAAAGCTGCTCTGACTGGAGCTTTTACTGATGCTAATCAGCAGTGTGTGGAGCTGGCCTGGCTGTCTCACTGCCACACTGTGGTGGAAACAGAGCTCCTCTGCTTTCTCTGGGAATGTGATTTTCTGTCTCAGAACTCAAAGAATAAATCCAGTGTATCTTCAGAGTCACTTTGTAAACCCTACATATGAAAACATATTGACTTNCNTCAGAATTAGTAGAGGTATATAGCANAAAAATCTGTCTAACATGATTTAGAAAAACCANTTACTGTGTGACAACAATGCTTAATATCTTAATCTAATGTGNTTTGGNTAATCANAAACNTNAAACATANAACCTGGNTGGTTCATANCCGNCCTTGATTGGCGTCAGNCAAACNNACCTGTAATCCATTGTGNTGGCAAGATCCAATTTTTTCAAAAANGAGATNTTC	Mus musculus membrane-spanning 4-domains, subfamily A, member 6D (Ms4a6d), mRNA	AK004295.1	1237	0	1351
C 230	CACGAGGCCTTAGTCTACAGTGCCTGCTCTTTTACCGGTACCACCTCACCTCACTTCAGGAGGGCAAGGCATTATACC CATCAGGCAAGCGGTCAAGATTGCAGCCTGTGCCAGTGTCTGGCTTCCACTCTCCACATGTGTGCACCCTAGCTTGGCCAGCCCTTAGTCTGACTGTGGGGCCAAAGCGCTTGCACCTCCGCTTTCATCTCTGGGACTGGGATGAGTGCCCTAGCTCTCATCTCTTTTCTGCTTTTGTGCTCCTTGCAGCTTGGCTCAGCGGCATCCCTACCAGTGGCCAGGGGTTCAATGGCTGGGACAAGGGCTCCAGAACCACCTCTGTAGCCACCACGACCAGAAAGGCTAAGGTCTTTATGCTGGATATTAAGTTTAGCGGCCAGTTCCTGGGCGGGAAAAATAAATAATTCAGCATTGTTNAA	Mus musculus chromosome 19 clone RP24-179M18	AK013256.1	876	0	163878
C 282	CCCTGNTGAATTCGGCAGGAGGGCACATTAGCCGGCTGATTTTCTTGCATGCATGTATTGAAATGACTCATGTTGCATTACGCTTTACCTCAGCTCTTGTAGCCAAGAGCCTGGTCCGTGTCTTGGAAAACAGTAACCAAGTTACCGTTCTCAATGCTGTACATTGTGTCGGGCAGCTTACCCACAGATTGAATGGCGACTAATGAGCACTTGGGTTTGGTGCCGTG CCTTGCCTCTGTCTGTGGTGGTGTGTGACTGTGTGGCCATGCTTGCAGACAGAAGGGTCTCGAGGTGCCATGG ATACCATCTGAGCTTCCCTGTCTCAGTCTGCTAGTTAGCATACCATCTGGGAAACACATTTAAATGGTATTTGTGTTGCTATATGATTTTAGGTGTTAGGTGTTTGTGTTTTTATTTTTGGTCTATTTCCTGTTTTCTATTATGTGTCATC AAAAAATTTCTAAACAGAAATTGAAATGCTTGTCTTGCATGAGGGCTGCTCTAAGGCCCTAAGTAACATCGAGTCAAAACAGCTTTAACAGNTAACAAATGAACTGACATTTTCAGACATCTGTCATGCAGGAGCCATTGGAGCCTG CTGTAGACATTCCAGCAGATGCCACNAATGCAGGTCAAGATGTGTGTAGCCTGNTGGTTTNGTCTANATTTGGGTACCA	Mouse DNA sequence from clone RP23-395B22, chromosome 11	AL645615.14	1291	0	196812
C 47	CCNTGAATCAGNNTCGANAGAGGGCCGAGTCCAATCCAAGTGTGGGGGAGGAGANNCTCCCTTGGCACAGTCTGATGAGGAGGACGGGGATGACGGAGGGGCAGANCTGGACCCTGCAGTAGCAGTGGGCCNCGTACAGACTGACCA GCCCGGCTGTTCTCCATGAAAGGAGACCTAGGCCCAGCAGAGCCTGGAGAAGACCTGACACTTCTTACTTACAGC ACCAAAGGGAGGGAAAGGATGGTGGATGGTGTGCCCTGAGAGTTAGCTCCCTGCTTTACCGCTAACGCTATCCTGCT GCCACGGCCCCACAGTCTTTTCTCTGAGGTAGGACTTCCAAGTGAAGCTGAGAGGTGAGGTGGGACAAGACGGCA GCTGCTTCTTATGTCCTCTGCCCCAGATGATCTGTGTCTTCCACAGAGTCTCCTAAGCCAGTGTCTCTGAGG GGATGTTCTGAGGAGTCCACTTCCAGTTATCTGCTCTATAAGTCTTTTGGGAACAGGATATGGTATAAATAATA	Mus musculus DNA segment, Chr 2, Brigham & Women's Genetics 0891 expressed (D2Bwg0891e)	XM_130592.3	940	0	1031
CH-10	CACGAGGGGCCCATCTTCCCTTGGAGACTCTGCCCTAGGAGCCAAAGTGGCCGGAAGAAGAGAAATGCGCAGGCTGA AGCGGAAGAGAAGAAAGATGAGGCAGAGGTCCAAGTAAGCCAGCCCGTGCACCTACGACGCCCTGCAGGACAGAA GTGAGGGATGCTGAGGGCCGGGACAGCTATCGGACTGTGTGCTGCCATCGGTAATGAGTCTCAGTAGACCTGGAA CGTCACCTCGCCCGGATCGCCTGGAGAAATGACCCCTTTCTTACAACCAAACAGTCCCTCTGCCCTGGACCCCG GCACTCTGGACTAGCTGTCTCTTGTGGCCAAGTGTAGCTCGTGTACAATAAACCCCTCTTGCAGTCACTGAGAA	Mus musculus 10 days embryo cDNA, RIKEN full-length enriched library,	AK019178	745	0	384

CH-17	CGGCACGAGGATCNGTCCNGGATACANCAGCAGGATNANCTACTCAACAGCCTGGTCTTCTGCTCCCTNTTCCTGN TAGTCTGCNTGNNCGGTTCTGGCATTNNTTNTGAAGNNTTCCAAGGGNCTGTAGACNTGNNTNACCCTGCNCT GANATNATGNAANCNGNCTNNAAGATNTAAACNAATNNTTCCNTGTCANGGNAACTATTATNNNNCCANCGGGGT CCCNNGNNGTNTGNCNTGCGGNTANNATCNGNGNNTNNNNNAGATAACNTTCTCNANTNNTNCGGAAAAAGNNAACA GGACTNCNTGGNTGANCNAGAAGNCNACANNNTGGTCCANGNAAAAACCNAAATNACNACAGANCTCCTGNA CNNACTGNCAAATANTNNTNCTCCTATGACNACAAAAGCGNCTCINTACTCTACCGGTGGGGTCTGTTCTNCN TATCNAGGAACANTCNGATNCTCTNTGNNGCAACATAGNATACCNCTGTGTNTATNCCACATAGNTCTCATATT NGNATTCNCAAGCNTTACTTAATGCTTAAAGACGAGAAGTANTACTNNTGNACTGGGAAATGGNAATAACAANA AATTGAAANTGGNAGGGGGCCCCNNAACCCNATTCNCCGGGGGGGGGGT	novel	n/a	n/a	n/a	n/a
DS-A2	GCTGNACCCGNGTCTGAAGGAATTCGGCAGCAGGCTCGTGCCGAATTCGGCAGCAGGCGCCACGCTGGTCTCA GAACTTCCAGGACATCAGGCTTTCAATTTGATCCCTTCTCCCCAAAGTACCCAATGCCACCTGAGTCAGGCATCAGC TCCTTGGGGAGATCTGCAGACCTGCCCTCAGAGGACGTAGGCTTAGAGTTCTGGGCAGCTTGGGGCTAGCCTGG GTGAGGGGTCTGTCTGGGTGAGAGGTTGGCTGCAGTGACTGCCCTGAGAGCCCTGGAGGCGTCTCAGGCCCA GCCATCGAGCCAGGGATGTCAGACCCAAAGCCAGCAGTACTAGTCCAGCAGCTTCCCTCCAGGGCTCCACTGCCT TCATCACCTGAACCCATCCCTCCAGCCCACTTCTCCCTTAGTGTACCTTCCCTTCTGCTGATATCTTGGCCTAGGT GGGGCCACAGTGAAGTAGGTGAGGCTGGGGCTGGACCCTTTAGATATCCAGGACTCTGGGTCACTATATGGCCC AAATCTGAGCCTGCTTATCCTANGGGTTCAAATTCGCAAGCATNCTGGGAAGATTCGAGTTTCTTATGTGGG GGCAGTCTCTTCTGTTGGGACANCATATACCCTCTGTAAGGCAAGCGAATCATTTCAACTCTCANGTATTGAGA AATGTGCTTACTTTGCAAGCAATGGGTGGTTCATNAATATTNAGTTGTCAAAAAAAAAAAAAAAAAAANTANGGGGG GANNAGNACGNGNCCNACACAAGAATTCGGCAGCAGGCTCGTGCCGAATNCGGCACGAGGAGAGTGTCTGA	Mus musculus 8 days embryo cDNA, RIKEN full-length enriched library, clone:5730427C23, full insert sequence	AK017603	1277	0	2391
KS-13	CATCGCAGCTTCAACAAGATCTGAATGTCCGAAAGAGTGTGNTTATGTGTGTGAGGACCTGCTGAGATTAAGAC TGAGACTCTGCAAN GGGGGGG	Mus musculus 8 days embryo cDNA, RIKEN full-length enriched library, clone:5730435B20, full insert sequence	AK017616	184	0	1589
L2T-136	TCTGCAGGAATTCGGCAGCAGGCCAGACTTGGTGTCTGTGTGGGAGAAGGATGAGGTGCCCTAAGCTGTGCCCA GCAGGGCCAGGGGAAGGTGCCAGCCAAAGCTGCCAGCCACCCGGTCCCTAGCTTCGCTTCCACCGTG AGCATTGGTACTGGCTTTTGTGATATTTAGGAACCCCTGCGTTTTTCTATCTTATCTGTGTGATAATCTTTTCATGTTTT CTAGAGCAAAAGACAAGCAGTACTCTTCTATCGCAATACCAGGTGTGACTAGGAAGAGCAGTATTTTATGGAGCAT TTACAAGTTATATTTTTAAAAAAAAAAATCAAAAACATGTGGGATGAGTGTAGAGGGAGGAGCGTGGGTGTGCCAGG GCTTTGTCTGTGTGACAGGTGGCGTCCCAAGCCATGTGATCTCTGAGGAGGTGGCTCCTGTCTGGTCTTCTCTT GATGACCCAGAAGAAACCTTAGCACCGGGCGGCCACTTGTCTGGCTGCTCCAGCAGATGTAGGACAGCCAGAG AGAATGGAGTCCCTTCTGNCCTGNCCTGTACCTTCCAGAGCCAACCGCATNCTCCTCAGGCAGGGACTTCCCTTAC CAGTGGTAGAGCCCTCAAGGGCCAAAAAGANCTGCTTGGTGGCGGGTCCANGCAANAAAAACATTTGTGACATCTTAT TCTGGTCTATGGCATTAAATGGTGGCTTTCAAAAAGAGTTAAATAAAGTGTNCAAGC	Mus musculus 8 days embryo cDNA, RIKEN full-length enriched library, clone:5730435B20, full insert sequence	XM_134599	706	0	1776
L2T-283	AGAGCGTCCGGCAGGACAGCGCAGGGATGANCCANNGCATGGTGGGCATGAACATGAACATGGGGATGTGGC CTCGGGGATGGGCTTGTGGGCACCATGGGAATGGGCATGCCAGCATGCCATGCCCTTCTGGAACGTGCAACCC AANCAAGATGCCCTTGGCAACTTTGCCAACTTTAGCAAATAAAGGTTGTAACGGAGCGAGTGGAAAGAAGACTCTGT AACTGCAATAGGTGATGTTGGGATGGAAGATGCTAAGCAGTTCCTTTNCTTTTATCANNTAATTAATAACCCACATN AAGAACCNAAGGCGNGGTGTTCAANAAGCGATGCAAGAGCCTTCANATNANGTAGTCAGGATCGGTTTCCCANT GAANATACNCTCCAATGGGGTGGGGTGNNGANANCTCTCTGGGTGANANANCCATGTNACANCATAATCTGNG GGANGANTGGCACAAATNNGGCTGANTGTGTGTGNTCANNCNTTATANTCTTCTCCNCGAGGAANTTGANTTTTCT TGNCCCTCAATCNCNTGNCATGANTGGGTCTGNTCCNTTANTAACNATCTCAAGTCCNTAGATGAAATCATTAAAGTT GGNTNATCANNTTTTATAAAAATATATTTTTGTCCAAAAAAGGCATACATATGTATTATGGCTAAATCACANGTN ACTGGATGTGTGCTTTTCCNNAANTCCACCAGNCTGCNAACACCATNAGTTNCTGGATTGANCCTTCCC CNNAGATCCCGGNTCTGCAGGAATTCGGCAGGAGATAATGTTGAATTTCTGTAAATAAATCTGATTGCAATCCAA CACTGAGTTGCTGGGCTGGCTAAGCCACTGCTGCGTCTCTGTGGAGGGTCCGGCCTTGTGAGTTGAAGCGAAC TGGAAATGTAGCCCTGCAGCTGACGTGTCTCACTCTGTAAGATGTGTACGGTACTGGCAGAAAAGTCTTTTTAAAA GCCATAGATAGGCTTTTCTTGTCTTAGCTGTAATAACACATCTAGTTTGGTCCCTCAAGAGCTGTGTTCTGTCTG TCACCTGTGACTGGCCCCATGTCTACCATCTGGCCCTTGTCACTCTGTCCCCCTGGTCTTTTGGAGTTGTGAC ACGGATCTGAAATGGATGTGTTCTTGCAGCGAATAAGATTGTAAGATTAATTCAGCTATCCAGTTTTCTAACGT AGCTCTAAGGTCCTCATTGCTGTTGTGATAATTGATACATAGCTCATTGGAACGTTGTGCATACATTTATTCAGATGA AATTATGTTTGCACCGTCTATTAATATCTCGATTAATTTAAAAAAGGGGGGGCCGGTACCCAATTCGCCCT	Mus musculus 8 days embryo cDNA, RIKEN full-length enriched library, clone:5730435B20, full insert sequence	BC004080	946	0	2943
L2T-324	CNNAGATCCCGGNTCTGCAGGAATTCGGCAGGAGATAATGTTGAATTTCTGTAAATAAATCTGATTGCAATCCAA CACTGAGTTGCTGGGCTGGCTAAGCCACTGCTGCGTCTCTGTGGAGGGTCCGGCCTTGTGAGTTGAAGCGAAC TGGAAATGTAGCCCTGCAGCTGACGTGTCTCACTCTGTAAGATGTGTACGGTACTGGCAGAAAAGTCTTTTTAAAA GCCATAGATAGGCTTTTCTTGTCTTAGCTGTAATAACACATCTAGTTTGGTCCCTCAAGAGCTGTGTTCTGTCTG TCACCTGTGACTGGCCCCATGTCTACCATCTGGCCCTTGTCACTCTGTCCCCCTGGTCTTTTGGAGTTGTGAC ACGGATCTGAAATGGATGTGTTCTTGCAGCGAATAAGATTGTAAGATTAATTCAGCTATCCAGTTTTCTAACGT AGCTCTAAGGTCCTCATTGCTGTTGTGATAATTGATACATAGCTCATTGGAACGTTGTGCATACATTTATTCAGATGA AATTATGTTTGCACCGTCTATTAATATCTCGATTAATTTAAAAAAGGGGGGGCCGGTACCCAATTCGCCCT	Mus musculus 8 days embryo cDNA, RIKEN full-length enriched library, clone:5730435B20, full insert sequence	NM_029362	1073	0	1080

L2T-341	CCGGNTCTGCAGGAATTCGGCAGGAGGAGGACGTTAAGACACCTTCTCCTCATGAAGGCACTTCTTGACTCTTGGGTTCCTGGCATCTTGGGTAGCTGCAGGAGAGCAGCCATTGAGAGGTTGAATGTCCGGCTGACCCCTTCCCATGTCAGGAGCTGTGTACCGGAGACGAATCTGTCCCGAGGGCACAATGCTGCAGCAGAGGGTGTGGCCATGCCCTGCCCGGAGACATCGAGGGAGGGCCGGGATGGTCAATGTCCAGAAATCCTGGTAGGCCCTGTGATTGTCCAGTGCATGATGGATGAGAAGTGTCAATCCGGGGAAAGGTGCTGTAAGTCAGGCTGCGGCCGCTTCTGCATCCAGGACTCCAGCCCTCCAACAGCTCAAAGACTCCAACCTGACTGATGGCTTAAATTTAAACTGGAGGCTCAAGCCCTAGCTGACCCGATTTGCTTGGAGCTCCAGGAAGCCAGGAAGGGGTGACATCCTGGGGCTTGTGACACTCCCTGGAGTATCAGGCCCTTTCCTCTGTATCTACTGCTACTTGCATGTAGCATGNAACTGCCCTGGTGTGGCGCTTCTTTCCCAATAAAATGCTGGCATGANCCTCTTGTCTGTACTGTGTAGGCATCACTGANGCAGGAGACCCAGTAGTCTTCCTGTNCATGGATTNGGNNGTGTGAAATCTATGGACAAATNAAAATGGCCCTTCTTTAAAA	Mus musculus RIKEN cDNA 1700015L13 gene (1700015L13Rik)	AK007299	985	0	608
L2T-352	TCACTATTNCTACCCTTGATGATGTGNTGANCGACATTCGCCGNATCANCACNTTTTTCGCTGCCGCTGCTGGTGGATCGGGATACGGTTNAGTTCTTCGGNCTTTAACGTGGCCGCCACCGTGAATCNANGATTAANCCGGTCCGGCAGGATTGCTATTGAAGATCAGGTTGGTGCAGAACGCTGCGGTATCGTCCGAATAAAGCGATGCTCGAAAGAAAGCATGGTGGATCGGATCCNGCGGNGGTGGATGCNAAAACCGATCCTGATTTGTGATCATGGCCGNCACCGATGCTCTGGCGGTAGAGGGGCCGGTANCCAATTCNCCCTATANTGAGTCGTATTACANGCCCGCNGC	Mus musculus RIKEN cDNA 1110018B13 gene (1110018B13Rik), mRNA	NM_025369	1225	0	672
L2T-363	ACGGTACGGCAGGAGGATCGTTAATCTTTATTGTGTATGAACAAATGCACACAGCAGCAAGTACAAGCAGACCATGAACCTTAGACCAATGGGAGGAGCAGGGACTGAGCACTCAACGCTTACTGCTTCTACCAAGGTGCGAGCAAGCAGCTCTAGAAAAGTGCCTGGGACGGACGCAGGTTTACAAAATGGTACAGGGAGCAACAGGGTACAGCAGAGCACAAAAGTGCACAGGCATTGCCAAGCCACCGCCATCGGATTATGGAGACCCAGGGGCTCACAGGTATTCTGGCTTCTAAAGAGAATGCAGACATTTTTATTTATGTGGAACTCTCAATTTTAAATCTGGCACCCAATTAATAGAACAAAAGAAATACAGGGCCCTAATAAAACACAGAGCCAGATGGCTGGGGATGGGGAGAGGGCCAGCCCTGTGACATATTAAGCCACCTATTACCGGTACTTAAGTTGGTCCATTTAACCCGTGAGAATGTACTCACTCTCTACGGTTAAGAAAGTCTGGCTCAANACAAAAGGAAACATCAAGGTTGAGANCTGGGTCCNACAGAAGCCCTGGGGCTGGTGGAGTGNAGCTTCTATTGTGGATCTAAGCAGAANGCACTTAATGGGATCTGGGTGCCAAAACCNNAATATNTGTCTCCTCAATGNAGTCTCGGCCATACANAATCATGGGCTAATGTGTCAACTTCAGCACAAAGGCTCAGTCNTAGGAANATCNTGCGATCATATCAGCTATCATACGCCACCCAGGGGGCCGTACCATTC	Mus musculus, fatso, clone MGC:18317 IMAGE:4237261, mRNA, complete cds	BC022222	906	0	3524
L2T-422	ATNACAGGATTCGGCAGGAGGCTCTCTCCTTGGTAGAAATGTCTGGACGCTTCTGTACGTTTCGCAAGTTGTCTTCGCTGATCGGTGAGACTTCGAGCAGTTAGGATGCCCGCTGGAAGCCGAAGCCGCACTTCCCGGGTACTCCTCCGGCCAGCCGGCCCTCAGATGAGGGCTGCTCCCGAAGAGCACCTGCAGCTCAGCCTCCAGCAGCAGCTGCGCCATCTGCAGTTGGCTCACCTGCCCTGCGCCCCGGCAGCCAGGCCATGATGGCCAGATGGCTACCACCAGCCGGCCGGTGTGGCTGTGGGCTCTGCAGTGGGACACACCCTGGGTACGCCATCACTGGGGGCTTACAGCGGAGGTGGCAGTGTAGCCCCAAAGCCGACATCACTTACCAGGAGCCTCAGGGAGCCAGCTGCAGAACCAGCAGTCTTTTGGACCTTGCTCTAGAGATCAAGCAGTTTCTGGAGTGTGCTCAGAACCAGAGCGATGTCAAGCTCTGTGAGGGCTTCAACGAGGTGTGCGGCAGTGCAGGATTGCAAAATGGTTAATGTAATCAAGAAATCAAGCTGAAGAGATGTAACATTGGTTCTGTATAATGATAGTACAAGTGTGGACCTTATATTCTAACAGTTCATTGNNTTGGAAATGGCCGTGAAAGAATTNACTGTGGATGTTACTGAGGNTGATGATGTTGTTATGGGAATGTGGCTCCTGGATGTGTTGTGATGTAGTTAAAAAATAATGGTATCTGAAAAAATAAATAATCGGGGGGGCCGG	Mus musculus coiled-coil-helix-coiled-coil-helix domain containing 2 (Chchd2), mRNA	AK003399	1239	0	745
L2T-460	GTCCCGGNCAGAATTCGGCACAGGCTGCCATCTCTGAAGTATTCCATTTAGGATGCCAGGCAGAGTGCAAATGAAACCCAGAACTTGAAGATGCTCAAGATTCCTCAATGTCCTAAATCACAGCCATATGTTAGTGAACCTTAGGAAAAGCAATGAATTTATCTATTTGCTCACTGTGAATTTAGGAAAAGCAATGAATTTATGCCTGTCTTTATGAACAGCTTTGACTTTGGACTATGCTTTGCAATCCAAGATCATGACTTGGCCATCTTATAAGCAGGAACCTTAGAAGTCTCAGAACAAGGACAAGTGGGACCAGCTCAACCTGGTGGTTTGTGGATTAGCTGGGCATGCCCTCTTTGCTGTCACTTTTGTGCATAAAGTATGGAGGGCCGACATGCTCTGGGATGCTTGGATGGAAGAAAAGATGCTCTGGCCTGCTTCCCTCTTTGTTGAAAGAACANITGGCTGTGGCACTGCTCTGGCTTCTCTTCACTTACTCCACTTTTGNCTGCAGGAAATTCACCTGTTAGGCCCTACTTCTGTTGGGAGGATTTTGTAGAGTGTCAAGATTAGCAGACTATATACTTGTATGCCTAAAAGTGNACTATTANCTGTTNACCAGTTAATNCAAATTTTTATTTAAAAAATAAATAAACCAGGGGGGGCCCG	Mus musculus hypothetical protein A230016E22, mRNA (cDNA clone IMAGE:5011290), partial cds	BC029706	1154	0	1589

VL-258	ANAAAAAGNITTTGAATGTNACTGCCCCAACAGAAGTGGGGGNTCCTGAGAGCCAACAGCATTGGTCTCTACAAGTGTG AACITTTGTGAATTTTNCANTAATACTTTTCTGACCTANGGNAGNATGTGATCCTGAAACACAAGCGCAGTACTCG AATGTGTGTGCGGGTGTGAAGGAAAGCTTCTACCAACATGCTTCTCAITGAAACACGCCAACTCCATGAAGAAGAC CCCTACATCTGTAAGTACTGTGATTACAAGACTGTGATCTTTGAGAACCCTAGCCAGCCACATTGCAGACACGCCACTT AGCCAGCCACTTTACTGGTGTGAGCAGTGTGACGTGCAGTTCCTCAAGCAGTGAAGTCTACCTGCACCTCCAGGA GCATAGCCGTGATGAGCAGNACCTGTGCCACNTTCTGTGANACAGAGACAGGGGACCCCTGAGGACTTGCACAGCCA CGTTGTCAACNAGCAGCCTCNCAGACTGATTGAGCTGAGTGAACAAGTGTGGCANTGGTGGCCATGGGCAGTGCAGC CTTTTAAAGCAAGATCCCTTTGACAAATGTAATAATTNCTTCTGTGTCAAGTATGTGGNTTTCGGAGCCAGACTTAC NACAAATGTCAACAGACAGCTGGCTATCGAGCATACNAAAATATTCCTCATGTTGGATGACTGNGGGAAAGGNCCT TTCCAGCATGTTGGANTATTGCAAGCNTCTAAATTCACATCTATCTGANGGATTTNCTTNTGCCAATNTTGTGAATATNC ACNNGGACAAATTGNCGATCTTACATCNTNTAGATTTGANGCATTGACTGACTNCCCTATAATGTGTGNGTGTGAT CCGTCCGGCTNTNNGAATTCAGGCACGAGGCTTCCCTNCAGACTCCTGGCCCATGAGAGCGAAGATGGCGGAAGA AGAGAATGCTGCAGGCTGAAGCGCAAGTAGAATGACAAGATGAGGCAGAGGTCCAACGTAAGCCAGCCCGCTGCAC CTACGATCGCTGCAGGAGCAGAAGTGAAGGATGCTGAGGGCCGGGACAAAGCTATCGGACTGTGTGCTGCCATCG GTAATGAGTCTCAGTAGACTTGAACGTCACCTGCGCCGATCGCTGGAGAAATGACCGCTTTCTTACACCAA ACAGTCCCTCTGCCCTGGACCCCGGCAGCTCTGGACTAGCTCTGTTCTTGTGGCCAAAGTGTAGCTCGTGTACAAT	Homo sapiens zinc finger protein ANC_2H01, mRNA	BC042660.1	1239	0	1202
HC-2	CCGTCCGGCTNTNNGAATTCAGGCACGAGGCTTCCCTNCAGACTCCTGGCCCATGAGAGCGAAGATGGCGGAAGA AGAGAATGCTGCAGGCTGAAGCGCAAGTAGAATGACAAGATGAGGCAGAGGTCCAACGTAAGCCAGCCCGCTGCAC CTACGATCGCTGCAGGAGCAGAAGTGAAGGATGCTGAGGGCCGGGACAAAGCTATCGGACTGTGTGCTGCCATCG GTAATGAGTCTCAGTAGACTTGAACGTCACCTGCGCCGATCGCTGGAGAAATGACCGCTTTCTTACACCAA ACAGTCCCTCTGCCCTGGACCCCGGCAGCTCTGGACTAGCTCTGTTCTTGTGGCCAAAGTGTAGCTCGTGTACAAT	Mus Musculus Pale Ear Mutant HPS1	BX649236.1	1199	0	1371
Senators	AAAAGAATTTGGTCTCCNCANNTGCCGAATTCGGCAGCAGGCACTCAAGCTNTATTTCAACGCCTTCTGGACTTTCNCCG TATATAAACCCATGNATGACTTCTGAAATACGACTTCTCCAGACCATGTGATGATTGGAGGCCTGCTCCTGGTGG TGGCTTTGGCCAGGGGGTGTGCTCATGGATGANAGAAGAAAGAGTGGTAACACACAGATCCCTCCCTCCCTG GCTGAGGCACAGGGCCCTGGCCTGGTTGAGGGCAGAGTCAACAACTGCCGGCGTGTGTGTCTCTCCCTCC CCTCCCTTGGTAAAGGCACAGATGTTTTGAGAAGTATTTGACAGACCTGAAAATTGGAGATAAAAATCTTTGAAAT AGTCTGGAGTCTTACTGTCCAGGGCTGGCGAGCTGGATGGTCACTCCTAGCCAAGGCTTGGAGGANACAGCGTG CTGGGCTGTGGCTCATTCTCCTGTCTCCGAGTNCCTTTGGGGAAGTCCGACTGAGCTGATTTTTATCATTCAA GCAGTTTTCCCTTCTTAGTTNGAGTTCACATCCTTAGCTCAAACCTAAATGACTTAGGATAGTNCACCAACNCAA ACGGTTAAACCTCCAGTCAANAATCTACAGTGGNCCCATNGGTTCTGCCCTGTATTNATAGGATCAGTGAAAATGT TANAAAACCAAGTCAANAACAGTACAGTATTGGNAAGGGGGTNTTCTGNTGCCCA	Mus musculus, surfeit gene 4, clone MGC:6155 IMAGE:3582114, mRNA, complete cds	BC027352.1	1132	0	2781
20						
Iron Metabolism/ Binding proteins						
B2 515	GAACGNACAGGGAGTCCCTTACATGCTGTGATCCCGAAGCAGAAATGACAAGAAGAGGCCATCTGGGAGCTTC TCCGCCAGTTTCAGGAGAAGTTTGGAAAAAACAAGCATCGGGATTCCAGCTCTTGCCTCCCCCTGGGACAGAAG GACCTGCTGTTCAAGGAGTCTGCCATTGGCTTTGTGAGGGTTCGCCAGAAGGTAGATGATAGGGCTTACCTGACCTT CAGCTACACCACATCCATACAGAACCCTGAATAAAAAGCAGCAGGATGTGATAGCCTCAAAGGCCCGGGTACATGTT GTGCCGTGGCAGTGAAGGAGAAGCGCAAGTGTGATCAGTGAACAGAGCAAGCAGAGGCAGGGTCACTGCATCT CATTCCCCACCAGGAAGACTGCATTTGCGCAATCATGAAGGGAGATGCTGATGCCATGAGCCTGGATGGAGGCTAT ATCTACACTGCGGGCAAGTCCGGTGTAGTTCCAGTCTTGGCAGAGAACCAGAAATCTCCAAAAGCAATGGCTTGG TTGTGTGAACAGACCAGTGAAGGGTACCTTGTGTAGCAGCAGTTAGAAGAGAAGATGCTGGCTTACCTGGAGCT CTTTGAGAGGCAAGAAGTCTGCCACACTGCCCTGGACAGGACCGCAGGCTGGAACATCCCATGGCCCTGCTTGT AACAGACCAGATCTGCAATTAATGAGTCTTAGCCAAAGCTGTGCCCTGGTGTGACCCAATCAATCTCTGTGCCCTGT GTTTGGTGTGAAAGGTGAGACATGTGCTCCACAGCAAAGAATACAGNTACCTGGGCTTAGGGTTG	Mus musculus lactotransferrin (Ltf)	NM_008522.2	1320	0	2744
C 113	GAATTCGGCAGGAGGGAAGAAACCATGGTGTCTTCTGGGGAAGACAAAAGCAACATCAAGGCTGCTGGGGGAAGA TTGGTGGCCATGGTGTGCTGAATATGGAGCTGAAGCCCTGGAAGGATGTTTGTACTACCTCCACCACCAAGACCTAC TTCCCTCACTTTGATGTAAGCCACGGCTCTGCCAGGTCAAGGGTCAAGGNAAGAAGTCCCGATGCTTGGCCAA TGCTGCAGGCCACTCGATGACCTGCCCGCTGCCCTGTCTGCTCTGAGCGACCTGCATGCCACAAAGTGCCTGTG GATCCCGTCAACTTCAAGCTCCTGAGCCACTGCCTGTGCTGACCTTGGTGAAGCCACCACCCTGCCGATTTACACCC CGGGTGCATGCCCTCTGGACAAATTCCTTGCTCTGTGAGCACCCTGCTGACTCCAAGTACCGTTAAGCTGCCT TCTGCCGGGCTTGCCTTCTGGCCATGCCCTTCTTCTCCCTTGACCTGTACTCTTGGTCTTTGAATAAAGCCTGA	Mus musculus, similar to hemoglobin alpha, adult chain 1, clone	BC043020.1	1008	0	569

C 16	<p>ATTCCGGCAGGAGGTGGCCAGTGAGGAGAAGCGCAAGTGTGATCAGTGGAAACAGAGCAAGCAGAGGCCAGGGTCCAC            CTGCATCTCATTCCCACCACGGAAGACTGCATTGTCCGAATCATGAAGGGAGATGCTGATGCCATGAGCCTGGATG            GAGGCTATATCTTACACTGCGGGCAAGTGCCGTTAGTTCAGTCTTGGCAGAGAACCAGAAATCCTCCAAAAGCAAT            GGCTTGGATTGTGTGAACAGACAGCAGTGGAAAGGGTACCTTGTCTGTAGCAGCAGTTAGAAGAGAAGATGCTGGCTTCCAC            CTGGAGCTCTTTGAGAGGCAAGAAGTCTGCCACACTGCCGTGGACAGGACCGCAGGCTGGAACATCCCATGGGC            CTGCTTGCCTAACAGACCAGATCCTGCAAATTAATGAGTCTTTAGCCAAAGCTGTGCCCTGGTGTGACCCCAA            TCCAATCTCTGTGCCCTGTGTAATGGTGATGAGAAGGGTGAGAACAAGTGTGCTCCCAACAGCAAAGAGAGATACCA            AGGCTACACTGGGGCTTAAAGTGTCTGGCTGAGAAGGCAGGAAATGTCATTTTGAAGGACTCCACTGCTTTC            AGAATACTGACGGGAAGAACACTGAAGAGTGGGCTANGAECTTAAGCTGAAGGACTTTGAGCTTTTGTGCTTGATGA            CACCGGAAACTGTGACTGAGGTTANAACCTGACACTACCATAACCAACATCTGTATGCTCGACAANAAGTGAANCC            TTCACAGTGTGCTGACACNGTCAATGGAAAATGAANAGTGCAGAAATTTGCTCCNTTAAACAAACTTTGCAGAAAT            GATTTGCAANCCNNAACCTCAATTTGGAAAGTCTTANACANCTANNGCNCCTCGACTGTTTACANANCNAAAACT            CGATTTCNCGCCGACNCTCCCNCTAGAAAANNINCTNNNAAAAAAGAAAAAAGAAAAAAG</p>	Mus musculus lactotransferrin (Lif)	NM_008522.2	1334	0	2744
C 24	<p>CAACNTGGACNANGGAACCTTGGCAAATACTTCTCCACCAATCTCATGAGGAGAGGGAGCATGCCGAGAACTGAT            GAAGCTGCAGAACCAGCGAGGTGGNCGAATCTTCTCGCAGGATATAAAGAANACAGACCTGATGACTGGGAGAGC            GGGCTGAATGCAATGGAGTGTGCACCTGCACTTGGAAAAGAGTGTGAATCAGTCACTACTGGAAGTGCACAACTGGC            TACTGACAAGAATGATCCCACTTATGTGACTTCAATTGAGACGTATTATCTGAGTGAACAGGTGAAATCCATTAAGAA            CTGGGTGACCACGTGACCAACTTACGCAAGATGGTGCCCTGAAGCTGGCATGGCAGAAATATCTTTGACAAGCA            CACCTGGGACACGGTGTGAGAGCTAAGTGACTTCCCAAAGCCACGTGACTTTACTGGTCACTGAGGCACTGCA            TGCATGTGAGGCTGCCCTCATCTTTCTATAANTNGACCACAAACATCTGCTTAAGTCTTTAATTTGACCATTCTTC</p>	Mus musculus ferritin heavy chain, mRNA (cDNA clone MGC:19422 IMAGE:3488821)	BC012314.1	1068	0	860
C 278	<p>GAGAAANTGATGAAGTGCAGAACCAGCGAGGTGGCCGNATCTTCTGCAAGATATAAAGAACCACANCCCCNATN            ACTGGGNGAGCGGGCTGTATGCAANGNCCNCCCGCCNNTCNCGCGCANGGTGNCACCAANGGGGNGCNG            GGACCGNNAACGCTNNCNGGNGTNNNGC</p>	Mus musculus ferritin heavy chain 1 (Fth1)	BC012314.1	299	e-78	866
C 85	<p>TNCNNGANCCCGNTGNNGCAGGAATTCGGCAGCAGGTTACCTGGAGCTCTTTGAGAGGCAAGAAGTCTGCCACA            CTGCCGTGGACAGGACCGCAGGCTGGAACATCCCATGGCCCTGCTTGTCTAACAGACAGATCCTGCAAAATTAAT            GAGTTCCTTAGCCAAAGCTGTGCCCTGGTGTGCTGACCCCAAATCCAATCTGTGCTTGTATTGGTGATGAGAAG            GGTGAGAACAAAGTGTCTCCCAACAGCAAAGAGATACCAAGGCTACACTGGGGCTTTAAGGTGTCTGGCTGAGAA            GGCAGGAAATGTTGCATTTTGAAGGACTCCACTGTCTTGCAGAATACTGACGGGAAGAACACTGAAGAGTGGGCTA            GGAACCTAAAGCTGAAGGACTTTGAGCTTTTGTGCCCTTGATGACACCCGGAACCTGTGACTGAGGCTAAGAACTGC            CACCTAGCCATAGCCCAAACCATGCTGTAGTGTCTCGGACAGACAAGGTGGAAGTCTTCAGCAGGTGCTGCTTGA            CCAACAGGTTCAAGTTGGGAGAAATGGACAGAGGTGTCAGGAGAGTTTTGNCTGTTCCAGTAAACCAAAAACCT            TCTGTCAATGACAACACTGAGTGTCTGGCCAAGATNCCGGCAAAAACACATCGGAGAAGTATCTGGGAAAAGGAG            TACGTCAATACGANGANGCCTGAANCAATGCTCCAAGCTCCCAAATTCCTGGGAAGCCTTNGCTTTTTCTTACC            CAGTGNAAAAACTTGAGCAAATACANAACCTTCCAAGGAANTTTTCAATCCCGNANCCACNGGCCCGGGGNC            TTCAAAACCAATCTGGGTCTCCCCCTCCCTGGGNGTCTTAAAGGTNMAAATAAATGAANNATAANNGTTCGNCT</p>	Mus musculus lactotransferrin, mRNA (cDNA clone IMAGE:3485548)	BC009662.1	1310	0	1751
D 213	<p>GNCNGCGGAATTCGGCACGAGGCGGTGGGGATGTGGCCTTTGTCAAGCACACAACCATATTGAGGCTTGGCCGGA            GAAGGCTGACAGGGACCAATATAAAGTGTCTGCTTGAATACCCGCAAGCCAGTGGATCAGTATGAGGATTGCT            ACCTGGCTCGGATCCCTTCTCATGTGTTGTGGCTCGAAAAACAATGCAAGGAAGACTTGCATCTGGGAGATTCTCA            AAGTGGCACAGGAACACTTTGGCAAAGGCAAAATCAAAGACTTCCAAGTGTTCAGCTCTCCTTTGGGAAAGACTGC            TGTTTAAAGATTCTGCCTTTGGGCTGTTAAGGGTCCCCCAAGGATGGACTACAGGCTGTACCTTGGCCATAACTAT            GTCACCTGCCATTCGGAATCAGCANGAAGGCGTGTGCCGGAGGGCTGCATGCACAACCTGCCAGTGAAGTGGTGTG            CNCTGAGTCACTGGAGAGAACAAGTGTGACGAGTGGAGCATCATCAGTGAAGGAAAGATAGAGTGTGAGTCAAGC            ANAGACCACTGANGACTGCAATGAAAAGATTGTAAACGNAGAAGCGGACNCCANGACTTTGGGANNAGGACATGC            CTACATTGCAGGCCANTGTGGTCTTAGTGCCTGTATGGCAGAGTATTACNAGAGCTCNAATTTGTGCCATCCATT            ACAACANGTANCTTNCCTAAANGGTATTTNCCGNGGCTNGTGGTGAAGGCNCGGAACCTANACATCACCTGGAAA            CCACCTGAANGGCGNAAAANTCNTGCCAACTGGGGTANANNGAACCCGCTGGTTGGAACATTCTTNNGGGCTGTGCT</p>	Mus musculus transferrin (Trf),	NM_133977.1	1207	0	2345

D 252	GCACGANGTCTCAAAGTGGCACAGGAACACTTTGGCAAAGGCAATCAAAGACTTCCAAGTGTTTTCTCTCCTCTT GGGAAAGACTGCTGTTAAAGATTCTGCCTTTGGGCTGTTAAGGGTCCCCCAAGGATGGACTACAGGCTGTACCT TGCCATAACTATGCACTGCCATTCGGAATCAGCAGGAAGGGCTGTGCCGGNGGGCTGCATCGACAACTCGCCA GTGAAGTGGTGTGCACCTGAGTCACTGGAGAGAACCAAGTGTGACGAGTGGANCATCATCAGTGAGGGAAAGATAG AGTGTGAGTCAGCANAGACCCTGAGGACTGCATTGANAAGATTGTGAACGGAGAACCCGACCCCATGACTTTGGAT GGAGGACATGCCTACATNGCAGGCCAGTGTGNNTACTGCTGTGCATGCCAGAGTACTACCAGAAGCTCAATTGT GCCANCCNTCACNACAANGTATCTTNCCTAAAGGNTATTATGCCCGTGGCTGTNGCTGAANGGCATTTCNACNNT TACCTCCACTTGGNACCAACTGAAAAGCAACNAACNCCTGCCAAACTGNGGTATACAGNAACNGTTNGTNGCAA ACCTCCCTATGNGGCATGCTNGTACAACAAGGATCNAACCACNTGCNAATCCGCTGAACCTTNTTCAGNNCAAGGCTN GCCGCTCCCGGTATNNACAAAATTCACCCCTCTGTGACCTGGGNTTCGN	Mus musculus transferrin (Trf	BC018573.1	825	0	2345
L2T-100	GGAGNAACTTATAGAAAAGATGAAGGCAGACTGACATGCATGCCTCAGTGACCAGTAAAGTACAGTGGCTTT GGGGAAGTCAGNTTAGCTCTCATCACCGTGTCCCAGGGTGTGCTTGTCAAAGAGATATTCTGCCATGCCAGCTTCAG GGGCACCCTATCTTGCCTAAGTGGTGCACGTGGTCAACCAGTCTTTAATGGATTTACCTGTCTACTCAGATAATACG TCTCAATGAAGTCACATAAGTGGGGATCATTCTTGTGACAGTCCAGTGTGTGACAGTCCAGTAGTGACTGATTCAACT CTTTTCCAAGTGCAGTGCACACTCCAATTCAGTTCAGCCGCTCTCCAGTGCATCAGGGTCTGTTTCTTTATATCCTGC AGGAAGATTCGGNACCTCGCTGGTTCGACGTCNATCAGTTTTCTCGGCATGCTCCCTCTCCTCATGAGATTG	Mus musculus, Similar to ferritin heavy chain, clone IMAGE:3968914, mRNA	BC011096	878	0	887
L2T 167	AACCCNTTGGAAAAGAAATCGGCTATNCGTATATGACANNATGCACAGTCTCTTCGGGGTGTAGCTCCTACTCCGGATCA ATTTGACCTCTCAGATTGACAGAAATATTCCACCAGGTGGAAGTGCCTGTGAACCGCCTGGTCAACTTGCACCTG CGGGCCTCCTACACCTACCTCTCTCTGGGCTCTTTTGTATCGGGATGACGTGGCTCTGGAGGGCGTANGCCACTT TTCGCCGAATTGGCCGAGGAGAAAGCCGAGGGCCGCGGAGCGTCTCCTCGAGTTTCAAGAACGATCGCCGGGGCCG TGCACCTTTCAGGATGTGCAGAAGCCATCTCAAGATGAATGGGGTAAACCCAGGAGGCCATGGAAGCTGCCTTGG CCATGGAGANAACCTGAATCAGGCCCTCTGGATGTCATGCCCTGGTCTGCCCCGCGGACCCCTATCTGTG GACTTCTGGAAANCCACTATCTGNATAAGGAGGTGNANCTCATCAAGGAANATGGGAACCATCTGACCAAANCTC CGCAGGGTGGCGGGGCACAACCAAGCCAAACTGGNGCGCCCAAGGGTCTCTGGCCGAGANTATTTCTTNNACCGC TTNCTCTCCAAGCACNACTAGGAGGCCCTGTTCCTTCCAANGGGCTCCCNCTCTGNTCTNACCAGNCCCGCCNG GACCTNCATTGTGTAAGTCTANGCCACTAGCANTTNNACCCCGGANCTTTAACNTNTGCCANTCAAATANA	Mus musculus 10 days embryo whole body cDNA, RIKEN full-length enriched library, clone:2600017112 ferritin light chain 1, full insert sequence	AK011244.1	979	0	924
L2T-221	CGGCAGAGGGCCGCTTCGAGCCTGAGCCCTTTCACACTTCGTCTTCCGCCCTCCAGCGTCCGCCACCCGCGCCTCG CCCCGCCGCCACCATGACCACCGCGTCTCCCTCGCAAGTGCGCCAGAATACCACCAGGACGCGGAGGCTGCCAT CAACCGCCAGATCAACCTGGAGTGTATGCCTCCTACGCTATCTGTCTATGTCTTGTATTTTGACCCGAGATGATGTG GCTCTGAAGAACTTTGCCAAATACTTTCACCAATCTCATGAGGAGAGGGAGCATGCCGAGAAAATGATGAAGCTG CAGAACCAGCGAGGTGGCCGAATCTCCTGCAAGGATATAAAGAAACCAAGCCGTGATGACTGGGAGAGCGGGCTGA ATGCAATGGAGTGTGCACCTTGGAAAAGAGTGTGAATCAGTCACTACTGGAAGTGCACAACTGGCTACTGACA AGAATGATCCCCACTTATGTGACTTCATTGAGACGTATTATCTGAGTGAACAGGTGAAATCCATTAAGAACTGGGTGA CCACGTGACCAACTTACGCAAGATGGGTGCCCTGAAGCTGGCATGGCAGAATATCTTTGACAAGCACACCCTGG GACACGGTATGAGAGCTAAGCTGACTCCCCAAAGCCACGTGACTTTACTGGTCACTGAGGCAGTGCATGCATGTC AGGCTGNTTCATCTTTTCTATAAGTTGCACCAAACATCTGCTAAGTTCCTTAATTTGACCATTTCTCAAATAAGA ATTTTGGTACCAAAAAAAAAAAAAA	Mus musculus ferritin heavy chain, mRNA (cDNA clone MGC:19422 IMAGE:3488821), complete cds	BC012314	1538	0	860
L2T-429	GCCTCTNATAGTTCTANAGCGNCGGCACGAGGCTACACTGGGCTTAAAGTGTCTGGCTGAGAAGGCAGGAAATGT TGCAITTTTGAAGGACTCCACTGTCTTGCAGAACTACTGACGGGAAGAACACTGAAGAGTGGGCTAGGAACCTAAAGCT GAAGGACTTTGAGCTTTTGTGCCCTTGTGACACCCGGAACCTGTGACTGAGGCTAAGAAGTCCACCTAGCCATAG CCCCAAACCATGCTGATGTCTCGGACAGACAAGGTGGAAGTCTTCANAGAGTGTCTTGGACCAACAGTTCAG TTTGGGAGAAATGGACAGAGGTGCCAGGANAGTTTGCCTGTTCCAGTCTAAACCAAAACCTTCTGTTCAATGAC AACACTGAGTGTCTGGCAAGATCCCCGGGCAAAACCATCGGAGAAGTATCTGNGAAAGGAGTACGTCATAGCGAC CGANCGCTGAAGCAGTGTCCAGCTCCCACTCCTGGAAGCCTGCGCTTNTCTTACCAGTGAAGCACTGAGCAA ATAGCAGAACCTCCAGGAAGTCTCATCCCGAGCCACGGTCCGGGGGCTTCAGACCATCTGGTCTCCTCACTCC CTGCTGTCACCTTAGGTAGAAATANAATGAAGTANTGTTGANNTTCTCGTCAAAAAAAAAAAAAAAAAA	Mus musculus lactotransferrin, mRNA (cDNA clone IMAGE:3485548), partial cds	BC009662	1221	0	1751

L2T-435	GCAGAATTGGGCACGAGGCCGCGCCTCGCCCCGCCACCATGACCACCGCGTCTCCCTCGCAAGTGGCCAGA ACTACCACCAGGACGGGAGGCTGCCATCAACCGCCAGATCAACCTGGAGTTGTATGCCTCCTACGTCTATCTGTCT ATGTCTTGTTATTTTGACCAGATGATGTGGCTCTGAAGAACTTTGCCAAATACTTTCTCCACCAATCTCATGAGGAGA GGGAGCATGCCGAGAACTGATGAAGCTGCAGAACCAGCGAGGTGGCCGAATCTTCTGCAGGATATAAAGAAACC AGACCGTGATGACTGGGAGAGCGGGCTGAATGCAATGGAGTGTCACTGCACCTGGAAAAGAGTGAATCAGTCA CTACTGGAAGTGCACAAACTGGCTACTGACAAGAATGATCCCACCTTATGTGACTTCATTGAGACGTATTATCTGAGTG AACAGGTGAAATCCATTAAGAAGCTGGTGACCACGTGACCACTTACGCAAGATGGGTGCCCTGAAGCTGGCATGGCA GAATATCTCTTTGACAAGCACACCTGGGGACACGGTGAATGAAAGCTAAGCTGACTTCCCCAAGCCACGTGACTTTACT GGTCACTGAGCAGTGCATGCATGTCAGGCTGCCTCATCTTTCTATNAGTGNACCAAACATCTGCTTAGTTCTTAATTG	Mus musculus, Similar to ferritin heavy chain, clone MGC:19422 IMAGE:3488821, mRNA, complete cds	BC012314	1178	0	860
L2T-454	ANCNTGATCACTANCTTCTAGAGTGNITTCGGCACGAGGAGGACGCGGAGGCTGCCATCAACCGCCAGATCAACCTG GAGTTGTATGCCCTCCTACGTCTATCTGTCTATGTCTTGTTATTTTGACCGAGATGATGTGGCTCTGAAGAAGTTGCCA AATACTTTCTCCACCAATCTCATGAGGAGAGGGAGCATGCCGAGAACTGATGAAGCTGCAGAACCAGCGAGGTGGC CGAATCTTCTGCAGGATATAAAGAAACCAGACCGTGATGACTGGGAGAGCGGGCTGAATGCAATGGAGTGTCACT GCACCTGGAAAAGAGTGTGAATCAGTCACTACTGGAAGTGCACAACTGGCTACTGACAAGAATGATCCCACCTTATG TGACTTCATTGAGACGTATTATCTGAGTGAACAGGTGAAATCCATTAAGAAGCTGGGTGACCACGTGACCAACTTACG CAAGATGGGTGCCCTGAAGCTGGCATGGCAGAATATCTCTTTGACAAGCACACCCTGGGACACGGTGATGAGAGCT AAGCTGACTTCCCCAAGCCACGTGACTTTACTGGTCACTGAGCGAGTGCATGCATGTCAGGCTGNCTTCATCTTTT CTATAAGTTGCANCAAAAACATCTGCTTAAGTTCCTTAATTNGTACCATTTCTTCAAATAAAGAATTTT	Mus musculus ferritin heavy chain, mRNA (cDNA clone MGC:19422 IMAGE:3488821), complete cds	BC012314	1241	0	860

L2T-403	GGCTNNTNATNACNGGANCGGCACGAGGGNCATANTCNGGANAAAAAGGTGCTCTCTGGNGAAGANAAAAGCAA NATCAAAGNTGACTGGGGGAANATANGTGGTNAANGTGCTGNATATGNAGCTGAGNGANCGGGCANNGATNTTGGC NATNNTCNCCNCCACCAATAACCACTTCCCTCANATCATCTATANACGGGTNTGNCCANGGNATANGTCANNNTA TNAANNNGTCCNNTTNCNNTGNAATNATGCANGACNCCNGCAAAGATNNGTNNGNAGANCTGANCNATCTGACNGA ACTNGTGGCCNCTCAGNCGCNTGNGNGTNCCTGCAACNNAACAACTCCTANNTCCANTGACTGCTGGTGAANTC TGTTAANNACCACCTNCGNGATNTGANCCCNNTNCNNAAGCCGCTCTGGANANAAATCCTANCCCTNTGATCN CCGGGNCCTGGTCCCNAANAACNNAATGACTNCTNTGGNGCTTGANTGCTNAAGCATGNCCTCTNTTNTGCC TTGAAAATAAACCTCTTGGGNTTTTNGANAAAGCCCCACTAGG	Mus musculus hemoglobin alpha, adult chain 1 (Hba-1), mRNA	NM_008218	62	1e-6	564
L2T-407	AAGGATNCGGCAGAGGACAGACTCAGGAAGAAACCATGGTGCTCTCTGGGGAAGACAAAAGCAACATCAAGGCTG CCTGGGGGAAGATGGTGGCCATGGTCTGAATATGGAGCTGAAGCCCTGGAAGGATGTTTGTAGCTTCCCACC ACCAAGACCTACTTCCCTCACTTTGATGTAAGCCACGGCTCTGCCAGGTCAGGGTCACGGCAAGAAGGTCGCCGA TGCTCTGGCCAATGCTGCAGGCCACCTCGATGACCTGCCGGTGCCCTGTCTGCTCTGAGCGACCTGCATGCCAC AAGCTGCGTGTGGATCCCCTCAACTCAAGCTCCTGAGCCACTGCCTGCTGGTACCTGGCTAGCCACCACCTGC CGATTCACCCCCGGGTCATGCCTCTCTGGACAAATTCCTTGCCTCTGTGAGCACCGTGCTGACCTCCAAGTACC GTAAGCTGCCTTCTGGGGTGTCTCTGGCCATGCCCTTCTCTCCCTTGCACCTGACCTCTTGGCTTTGATA AAAGCCTGAGTAGGAAGAAAAAAGAAAAAAGAAAAAAGAAAAAAGAAAAAAGAAAAAAGAAAAAAGAAAAAAG	Mus musculus similar to data source:MGD, source key:MGI:96021, evidence:ISS-hemoglobin, beta adult major chain-putative (LOC192803)	XM_109189	1003	0	564
16						
Calycin Superfamily						
B1 56	TGCNGCAGGAATTCGGCACGAGGCTAAGCATGGCACTGCACATGATTTGTATGGTGGAGCCCTCTGCCGCTGT GGAAGCTCAGAACCAGAACATGTCAACATCACCATAGGCGACCCTATCACCATGAGACCCTGAGCTGGCTCTCTG ACAAATGGTTTTTCAATGGTGGCGCTGTCTAAACCTGATTACCGGCAGGAAATCAAAGACGCAGATGGTATTTTT TAACCTTACCCCCAACTTGATAAATGACACGATGGAGCTTCGAGAGTATCACACCATAGATGACCAGTGTGCTATAAC TCCACTCATCTAGGAATCCAGAGAGAGAATGGACCCCTCCTCAAGTATGATAGGAGGAGTAAAAATCTTTCAGACCTG ATAGTCTTGAAGATGCATGGGCCTTCATGCTTGCCTTGAAGTATGAGAAGAACGGGGACTGTCCTCAAT GCAAAAAGGCCAGATATCACCCGGAGCTGCGGGAAAGTATTCAGAAAGGCTGTCACACACGTGGGCATGGATGAAT CAGAAATCATATTTGTTGGACTGGAAAAAGGATTAGGTGCAGTACAGCAGGGAGAAGCNGCAGCTTGAAGTGGAGAAG GAGAACAGAAAGATNCTGGAGGAANGGCCAGGCATGAATCAGCTCTCTGAACTCCGANGGNTGGTCCACANGCT CCACAAAANCCANCCCTCTGTGCACCTTGGATTCTGTCTGCCCCAATNAAAGGTTTGTGACACAGTCAAAAAA	Mus musculus orosomucoid 2 (Orm2)	NM_011016.1	1229	0	739
CH-14	TGCCGAATTCGGCACGAGGCTGAGTGCCTCAGCATGGCGCTGCACACGGTTCTTATCATATTGAGCCCTCTGCCGA TGTTGGAAGCTCAGAACCAGAACATGCCAACTTACCATAGGCGAACCTATCACCATGAGACCCTGAGCTGGCTC TCTGACAAATGGTTTTTTCATGGGTGCAGCTTTCAGAAAACCTCAGTACAGGCAGGCAATCAAACAATGCAGAGTGAA TTNNGTTACCTTACCACCACTTGATAAACGACACAATAGAGCTTCCGGAGTCTCAAACAATAGGTGACCAGTGTGTC TATAACTCCACCCTAGGATTCAGAGAGAAAATGGACCTTCTCCAAGTATGAAGGAGGAGTAGAAAACCTTTGCC CACCTTATAGTCTGAGGAAACATGGGCCCTCATGCTTGCCTTTCACCTCAAGGATGAGAAGAAACGGGGACTGTC CCTCTATGCCAAAAGGCCAGATATCACCCGGAGCTGCGGGAAAGTATTCAGAAGGCTGTACACACGTGGGCATG	Mus musculus orosomucoid 1 (Orm1),	NM_008768	1019	0	768

D 25	GAGGCCTAAGCATGGCACTGCACATGATTCTTGTCTATGGTGGCCTCCTGCCGCTGTTGGAAGCTCAGAACCAGAA CATGTCAACATCACCATAGCCGACCTATCACCATGAGACCCTGAGCTGGCTCTCTGACAAATGGTTTTTCATTGGT GGGGCTGTCTAAACCCTGATTACCAGCCAGGAAATCAAAGACGCCAGATGGTATTTTTAACCTTACCCCAACTGT ATAATGACACGATGGAGCTTCCAGAGTATCACACCATAGATGACCACCTGTGTCTATAACTCCACTCATCTAGGAATC CAGAGAGAGAATGGACCCTCTCCAAGTATGTAGGAGGAGTAAAAATCTTGCAGACCTGATAGTCTTGAAGATGCAT GGGGCTTATGCTTGCCTTGGACTTGAAGGATGAGAAGAAACGGGGACTGTCCTCAATGCAAAAAGCCAGATAT CACCCCGGAGCTCGGGGAAGTATCCAGAAGGCTGTCACACACGTGGGCATGGATGAATCAGAAATCATATTTGTTG ACTGGA AAAAGGATAGGTGCGAGTCAGCAGGAGAAGCAGCAGCTTGAAGTGGAGAAGGACCAAGAAGATCCTGA GGAAGGCCAGGCATGAACTCAGCTCTCTGAACTCCGAGGGCTGTCACAGGCTCACAAACCCACCCCTCCTGTG CACTTTGATTCTGTCTGCCACAATAAAGTTTGGTGCACACAGTCAAAAAAAAAAAAAAAAAAAT	Mus musculus orosomucoid 2 (Orm2)	NM_011016.1	1431	0	719
DH-B4	CGAGGCCTCCAGCACATCAGACCTAGTAGCTGTGGAAACCATGGCCCTGAGTGTCTGTCTGGGCCCTTGCCT GCTTGGGGTCTGCAGAGCCAGGCCAGGACTCAACTCAGAACTTGATCCCTGCCCATCTCTGTCTACTGTCCCCC TGCAGCCAGACTTCCGGAGCGATCAGTCCGGGGCAGGTGGTACGTTGTGGCCCTGGCAGGCAATCGGGTCCAGA AAAAAACAGAAAGGCAGCTTACGATGTACAGCACCATCTATGAGCTACAAGAGAACAATAGTACAATGTACCTCCA TCCTGGTCAGGGACCAGGACCAGGGCTGTCGCTACTGGATCAGAACATTTGTTCCAAGCTCCAGGGCTGGCCAGTTC ACTCTGGGAAATATGCACAGGTATCCTCAGGTACAGAGCTACAATGTGCAAGTGGCCACCACGACTACAACAGT CGCCATGGTATTTTTCCGAAAGACTTCTGAAAACAAGCAATACTCAAATACCCTGTATGGAAGAACCAAGGAGCTG TCCCCTGAACTGAAGGAACGTTTTACCCGCTTTGCCAAGTCTCTGGGCCCAAGGACGACAACATCATCTTCTGT CCCACCGAACAATGCATTGACAACGAATGGGTGGTGTGAGTGTGGCTGACTGGGATGCCAAANACCAATGGTTGAG CGCTGCCGTCTGTCTGNCACTCCATCTTCTGTTGCCAGANAGCCNCTGGGTGNCACAGCACATACCAGGACAT	Mouse SV-40 induced 24p3 mRNA	X14607	1304	0	853
DS-A7	GCAACNGNGCCNCAACCCGNGCTGCAGGAATTCGGCACGAGGCCTCGTGCCGAATTCGGCACGAGGGGAAGGC TGTCACACACGTGGGCATGGATGAATCAGAAATCATATTTGTGCACTGGAAAAAGGATAGGTGCGGTGAGCAGGAGA AGAAGCAGCTTGAAGTTGGGGAAGGAGACCAAGAAAGATCCTGAGGAAGGCCAGGCATGAACTCAGCTCTCTGAACT CCGAGGGCTGTCCACAGGCTCACAAACCCACCCCTCCTGTGCACTTTGATTCTGTCTCTGCCACAATAAAGGTTG CGCATATCTCAAAAAAAAAAAAAAAAAAAT	Mus musculus orosomucoid 1 (Orm1),	NM_008768.1	492	e-137	768
DS-N7	CGGCACGAGGCCTCGTGCCGAATTCGGCACGAGGCCGATGTTGGAAGCTCAGAACCCAGAACATGCCTTCTCACC ATAGGCAGAACCTATCACCATGAGACCCTGAGCTGGCTCTCTGACAAATGGTTTTTCATGGTGCAGCTTTCAGAAAA CTCGAGTACAGGCAGGCAATTCAAACAATGCAAGTGAATTTTTTACCTTACCACCAACTTGATAAACGACACAATAG AGCTTCGGGAGTCTCAACAATAGGTGACCAGTGTGTCTATAACTCCACCCATCTAGGATCCAGAGAGAAAAATGGGA CCTTCTCCAAGTATGAAGGAGGAGTGAACCTTTGCCACCTTATAGTGTGAGGAAACATGGGGCCTTCATGCTTG CCTTTGACCTCAAGGATGAGAAGAAACGGGGACTGTCCCTCTATGCCAAAAGGGCAGATATCACCCGGAGTGCG	ORM1	NM_008768.1	914	0	768
L2T-202	GGTNGCCGAGAATCGGCACGAGGGGGATTGGTCCACCATCCGGTCAGAGAGTACTTTTTAAAAACCCGAGATTTCC TTCAAACCTGGGCGTGAATTCGATGAAATCACCAGCAGACAGGAAGGTGAAGAGCATATAACCTAGATGGCGG GGCCCTGGTGCAGGTGCAGAAGTGGGATGAAAGTCGACCACAATAAAGAGAAAAACGAGATGTTGACAAGCTGGTG GTGGAATGTGTTATGAAAGGCGTACTTCCACAAGATTTATGAAAGGCATGAGCCAAAGGAAGAGGCCTGGATGG AAATTTGCATCAACACTACAATAGTCAGTCGGATTTATTGTTTTTTTTAAAGATATGATTTTCCACTAATAAGCAAGCA ATTAATTTTTCTGAAGATGCATTTTATTGGATATGGTTATGTTAATAAAAAACCTTTTTAGACTTAAAAAAAAAAAA AAAAA	Mus musculus 18 days embryo whole body cDNA, RIKEN full-length enriched library, clone:1100001A08:fatty acid bindingprotein 4, adipocyte, full insert sequence	AK003143	807	0	638
L2T-294	ATAGTNAGAGCGTTCGGCACGAGGGGAGAACAATAGCTACAATGTACCTCCATCCTGGTCAGGGACCAGGACCAGG GCTGTGCTACTGGATCAGAAACATTTGTTCCAAGCTCCAGGGCTGGCCAGTTCACCTGCGGAAATATGCACAGGTAT CCTCAGGTACAGAGCTACAATGTCAAGTGGCCACCACGGACTACAACAGTTCCCATGTTATTTTCCGAAAGACT TCTGAAAAACAAGCAACTCTCAAATACCCTGTATGGAAGAACAAGGAGCTGTCCCTGAACTGAAGGAACGTTTC ACCCGCTTTGCCAAGTCTCTGGCCCTCAAGGACGACAACATCATCTTCTGTGCCACCAGCAATGCATTGACACA TGAATGGGTGGTGTGCTGACTGGGATGCGCAGAGACCAATGGTTACAGGCCTGCCTGTCTGTCTGCCACT CCATCTTCTGTTGCCAGAGACCACCTGGCTGCCCCACCAGCCACCATACCAAGGAGCATCTGGAGCCTCTCTT ATTTGGCCAGCACTCCCATCCACTGTCTTAACACCACCAATGGCGTCCCTTTCTGTCTGAATAAATACATGCCCCC	Mus musculus lipocalin 2 (Lcn2), mRNA	XM_130171	1178	0	911





L2T-371	TCCTNATNAAAGGTTCCGGCACGAGGAAACAACGGTCGCGCCAAAAGGGCCGNGGNCATGTGCAGCCATTGCGTG CACGAACTGCGCCCGGTGCGTGCCCAAGGATAAGGCCATCAAGAAGTTTGTCACTCGGAACATTGTANAAGCCGCTG CTGTGAGGACATATCTGAAGCAAGCGTCTTCGACGCCTACGTGCTTCCCAAGCTCTATGTCAAGCTGNATTATTGCG TGAGCTGTGCCATCCATAGCAAGGTTGTTAGGAATCGATCCCGCAGGCCCCGGAAGACCACACCCACCACG ATTCANACCTGCTGGCGCTGCACCTCGACCTCCACCAAGCCCATGTAAGAGGCCGTTTTGTAAGGACGGAAGGAA AATTACCCTGGAAAAATAAATGGAAGTTGTACTTTAAAGGGGGGGCCCGTACCCAATNCGCCCTATAGTGAGTCG	Mus musculus, Similar to ribosomal protein S26, clone MGC:46874 IMAGE:4987659, mRNA, complete cds	BC036987	757	0	453
L2T-374	CTNGACTAGATCGGCACAGGAAACAACGGTCGCGCCAAAAGGGCCGCGCCATGTGCAGCCATTGCGTGACGGA ACTGCGCCCGGTGCGTGCCCAAGGATAAGGCCATCAAGAAGTTTGTCACTCGGAACATTGTAGAAGCCGCTGCTGTC AGGGACATATCTGAAGCAAGCGTCTTCGACGCCTACGTGCTTCCCAAGCTCTATGTCAAGCTGCATTATTGCGTGAGC TGTGCCATCCATAGCAAGGTTGTTAGGAATCGATCCCGCAGGCCCCGGAAGACCACACCCACCACGATTCA GACCTGTGGCGCTGCACCTCGACCTCCACCAAGCCCATGTAAGAGGCCGTTTTGTAAGGAGGGAAGGAAATTAC CCTGGAAAAATAAATGGAAGTTGTACTTTAAAGGGGGGGCCCGTACCCAATNCGCCCTATAGTGAGTCGATTAC	Mus musculus ribosomal protein S26, mRNA (cDNA clone MGC:46874 IMAGE:4987659)	BC036987.1	793	0	453
L2T-376	GNGTCTTNATNACNGGTANGCAGATGAAACAACCTGTCGCGCCAAAAGGGTCCGNGGGCATGTGCAGACCCATCC NCTGTACGAACTGCGCCCGGTGCGTGCCCAATNTATAATTGNCATCAANAATANTGTGCGGNGGGAACATTGTNGA AGCCCGCTGCNTGTCAANNACCATATCTGAAGNAAGCGTCTTCGACGCCTACGTGCTCCCAAGCTCTATGTCAAGCT GCATTATTGCGTGAGCTGTGNATCCNTAGCAAGNNGTNAGGAATCGATCCCNAGGCCCGGAAGGANCGAACA CNCCCACCACCTAGTCAGACCTGCTGGNGCTGCACCTCGACCTCCACCAAGNCCATNTAANAAGGTCGNTTTGTT AAGGACGGANAAGAAAATNACCCTGGAAAAATAAACANGGAAGTTGTCNTTCTNAAANGGGGGCCCGNGTNACC	Mus musculus, Similar to ribosomal protein S26, clone MGC:46874 IMAGE:4987659, mRNA, complete cds	BC036987	281	0	453
L2T-427	ATNCGGCACGAGGCNTGNNCNCATGCGNAAAGCTCGCATGAGTACAANATTCGGCNCNACCCTGATTACCCGTCATG GCCGAGGAAGGNATATGTGNTGAGAGCGTGAATGGACGTNAAGACTGNTTACAANANGTGNNGNNGACCAGCC TCATCCCATATGGNCTAGCANGTGGCATAACGCAAGCTGCCAAANCCCTTATAACAANCGCCAAGNCCATCTGTGTG CTCGCNTCCAACNGTGATGANCCCATGTATGTCANNCTGGTGGAGGCACCTTTGTGCTNGAGCACCAANTCAACCTGA TNAACGTTGNTGACGACAAAANANTATG	Mus musculus ribosomal protein S12, mRNA (cDNA clone MGC:19264 IMAGE:3986648), complete cds	BC018362	272	0	937
L2T-64	CGCAGANGTCTATNGAGAGNCGNATNACAAGAGGAGGGGCTGAGGTGAGAGCATGAGGTTGTCNCTGGNTGNCG CTATCTCCACGGNCGCTACCGCCGCTGGGCCTGGGTCGGGAGTCCCGCATCCATCTGCTGCCGAACCTTGCT CACGGGCTAGTTCCGCCACGAACGCATCGAGGGCAGATGGGCACCGCGGACGAGATGAGGGGCTACCGGGAGAA GCTCATCGATTATGGAAGCTGGGCACACCAACGAACGAGCCATGCGTATGCGTACTTCTGGCTCACAGAGAAGG ACTTGATCCCAAAGCTGTTAAAGTGTAGCGCTCGGTTCCAAGGTCAGAATGGGAACACACAAGAATGCTACAGA TCCCGAATCGGAAGGAGCAAGATCGGGCCAAGATGGCGGTGATAGAAATAAAGGGAACACTCCCTCCCTCGCCT CTGCGCTCACAGAGCAGCAACCTTACTCTCTAAACCAGTCTCCTGGGACTGCAGCAGGACCTGCACCATAACCA GGACGCAAGCCTCCACAGCTCCTGTACAGTTCAAACACCAAAAGACTTAACTGGAGCTGNAGAGTGGTGCATTAGGTG TGGTGCCCGTGTCTGGGTCTTGGAGCTCGTGTAGTGTGTGAGGCCCTGGGAANNTAGCATNGTAAANCCCCCTCA TAATNGAGACCAGAACTCCCTGCTGACTCACACGATCCTCNTGNACAG	Mus musculus mitochondrial ribosomal protein L17 (Mrpl17)	NM_025301	1247	0	891
17						
Cell Adhesion						
B2 507	TNGNNACCCGGTTGTGAAGGAATTCGGCACGAGGCTGACCTTGTTCAGTGCCACCATGAAATTCCTACTGTCCTG CTATTGTGAGTCTTGCTGCCACCTCTCTTGCTCTCCTGCCGCTGGGTCCAAAGATGAACCTTCAAATGAAGACTCAGCCC ACAGATGCCATTCAGCTGCCAGTCCACTCCACCAGCTACACCAGTGAGGAGACTTCCAGTAAGGACCTTTC CAAGGAGCCTTCCATCTTCAGAGAAGAGCTGATTTCCAAAGATAATGTGGTGATAGAATCACCAGCCAGAGAATCA AGAGGCCCAGGATGGGCTCAGGAGCGGGTCATCTCAGCTGGAAGAGACCACAAGACCACCACCTCAGCTGGTATG AGCCAGGGAAGAAGGAAGATGCTTTGGAGGTGCAACCACCTCAGAGGAAAATCGACCAAGTCAAGCCAGACAGT GGAGGAAGAACTGGGTAATAATTGAAGGATTTGTAAGTGGTGCAGAAGACATAATCTCTGGTGCCAGTCTGATCAC GAAGTCATGAAGACAAAAACCTAACCACTAAGTCCCATGCTAGGTGGTGCCTTCATCAGCCACACTCTGNTCATCT GGACCANCANCTCTCAGTCTGGCCTTGATGCTTACATTAAAGTATTGCAACCTAAAAGGGGGGGNCCGGGTAC	Mus musculus glycosylation dependent cell adhesion molecule 1 (Glycam1)	IXM_128312.2	690	0	625

B2 524	TCNCCAATGAAGACTCAGCCACAGATGCCATTCCAGTCCAGTCCAGTCCACTCCACCAGCTACACCAGTGGGAGA GTACTTCCAGTAAGGACCTTTCCAAGGAGCCTTCCATCTTCAGAGAAGAGCTGATTTCCAAGATAATGTGGTGATAG AATCTACCAAGCCAGAGAATCAAGAGGCCAGGATGGGCTCAGGAGCGGGTCACTCAGCTGGAGAGACCACAAG ACCCACCACCTCAGCTGCAACCACCTCAGAGGAAAAATCTGACCAAGTCAAGCCAGACAGTGGAGGAAGAACTGGGTA AAATAATTGAAGGATTTGTAAGTGGTGCAGAAGACATAATCTCTGGTCCAGTCCGATCAGCAAGTGCATGAAGACAAA AACACCTAACCTAAGTCCCATGCTAGTGGTGCCTTCATCAGCCACATTTCTGCTCATCTGACCACCACCTCTCAGT CTGCCCTTTGATGCTTACATTAAGTATTGCAACCTAAAAAATAAAAAAAAAAAAAAAAAANCCGNNCCNNGGGCCAAAT CTTGNAGCCCGGGGGTCCNTTTTTTAAANGNCCNCCCGGGGGGACCCCNNTTNGTCCCTTTANGGG	Mus musculus glycosylation dependent cell adhesion molecule 1 (Glycam1), mRNA	XM_128312.2	985	0	625
C 132	CNCNGACACNNGTTAGAAGGAATTCNNACGANGTTTTNTATTGCACAGTGTTCCTTAAATGAGAGACAACTGACCT CATAAGCAGTTTCCCTCTTGCTGGGTGCAACTGACCATCACCTCTACCACATCAGGGACCCAGGGGTGAGGGAG GGGACCTAGCCATCTTGGGGAGAGAGCAGGGGCCAATGCAAACTGGTCTGGCGGCTCTGATGGCCTGCTGAGCCT CTCCAGGGGTANGAAGCTCTTGATCCTCGCTTGATAGCAGANTATGAACCTTTCTGGACAAAATGGACAGGAT TCTGGCCTCCACCTTCCAGCTTCTCCAGGGTGGGGGTCAAGTCTGGGTATGGCAATCAGGAAGATACTGGC CCATATTTGTTGTGGAGGGACTGGCTANAGACCTGTNAAGCANAAGCAGCCTGGGGCCTCGTGCCCAATTCGGCA CGAGGAGAGAGANACAGACAGAGANACNNAGANNANAGAGNNANAGAGANAGAGAGAGANANNANAGACAGAC ACAGANAGAGATAGAGANNANANANAGCACCNCNCCNCCATCNCNNTCTTTAGTCTGCNAACAACCATN CTCNACCNCNCCNCCACTCCAGNNGCNCNCCGNNCCNCCACNCACNTACACNNTCTNCCNCCAGCCTCNC	Mus musculus biglycan, mRNA (cDNA clone MGC:60404 IMAGE:30061850),	BC052857.1	733	0	2376
C 136	AGAATTCGGCAGGAGGTTACACTTTAAAACTTTTTATATAAAAACTCATTGTTTTTAAAGCATTAANTAAGAG AAAGAAGAGAGAAAAGATACAGAGCAGAAGATATGCCCTTAGTAGTATTGGTGGGAGGGTAGGATTTTTGGTTTG CTGAAATTGAATGTTTGTGTTTTATAATGAAAAGGAAAACAAAACAACAAAACAAAAGTAAAGGTCCCC AAAGCCCATGGCTATTCTATTACCACACCCACCAGAGAAGAGAGCACCAGGAAGAGCAGGAAGAGGACAAAGAGAA CCAAAACCAGAGGCAGATAGATGTGGGTGGGGGAGGCTCCCTGTGCAGTGTACTCTGAGGGTACAGAGAGCAC ANAGTCTCTTTTNGCCAGAAAAGGGAAACGGGACTAGGAAGAAATGGGAAGGAATCAANGGTTGGGGGGAGGGGGT GACTGCAATGTATAACAAAAGGAGTGGTGGGCTGTGCACTTTTCTCCTACCCCATAGCCTCAATATCTTAACGGGA ACNNGACAAGAGGGATAACGAATTCCTCACTTGCCTTCGCAATTAGAGCCTTTAAGAATTCACGGGA	Mus musculus catenin src, mRNA (cDNA clone MGC:54774 IMAGE:6309010),	BC046589.1	958	0	5435
C 150	NCTGAACCCGGGCTGCAGGAATCGGCACGAGGCTGACCTTGTCCAGTGCCACCATGAAATTCCTCACTGTCTGCT ATTTGTAGTCTTGTGCCACCTCTCTTGTCTCTCTGCTGGTCCAAGATGAACCTCAAATGAAGACTCAGCCAC AGATGCCATTCCAGCTGCCAGTCCACTCCACCAGCTACACCAGTGGAGAGTACTTCCAGTAAGGACCTTTCCA AGGAGCCTTCCATCTTCAGAGAAGAGCTGATTTCCAAGATAATGTGGTGATAGAATCTACCAAGCCAGAGAATCAAG AGGCCAGGATGGGCTCAGGAGCGGGTCACTCAGCTGGAAGAGACCACAAGACCCACCCTCAGCTGCAACCAC CTCAGAGGAAAATCTGACCAAGTCAAGCCAGACAGTGGAGGAAGAACTGGGTAATAATGAAGGATTTGTAAGT GTGCAGAAGACATAATCTCTGTGTCAGTGCATCAGCAAGTCAAGACAAAACACCTAACCTAAGTCCCAGT CTAGGTGGTGCCTTATCAGCCACATTCTGCTCATCTGANACCACCTCTCAGTCTGGCCTTTGATGCTTACATTAAG	Mus musculus glycosylation dependent cell adhesion molecule 1(Glycam1)	XM_128312.2	1146	0	625
C 238	TCTTGACCCGGGCTGCAGGAATTCGGCAGGAGGCTTCAGAGAAGAGCTGATTTCCAAGATAATGTGGTGATAGAAT CTACCAAGCCAGAGAATCAAGAGGCCAGGATGGGCTCAGGAGCGGGTCACTCAGCTGGAAGAGACCACAAGACC CACCACCTCAGCTGCAACCACCTCAGAGGAAAATCTGACCAAGTCAAGCCAGACAGTGGAGGAAGAACTGGGTA TAATTGAAGGATTTGTAAGTGGTGCAGAAGACATAATCTCTGGTCCAGTCTGATCAGCAAGTCAAGACAAAAAC ACCTAACCTAAGTCCCATGCTAGGTGGTGCCTTATCAGCCACATTTCTGCTCATCTGACCACCACCTCTCAGTCTG CCCTTTGATGCTTACATTAAGTATTGCAACCTAAAAAATAAAAAAAAAAAAAA	Mus musculus, Similar to Glycosylation dependent cell adhesion molecule 1, clone IMAGE:4039244	BC031931.1	767	0	2095
C 288	GAGCAAGGCTGGGAGGAATTCGGCAGGAGGCTGACCTTGTCCAGTGCCACCATGAAATTCCTCACTGTCTGCTA TTTGTGAGTCTTGTGCCACCTCTCTTGTCTCTCTGCTGGTCCAAGATGAACCTCAAATGAAGACTCAGCCACA GATGCCATTCCAGTCCAGTCCACTCCACCAGCTACACCAGTGGAGAGTACTTCCAGTAAGGACCTTTCCAA GGAGCCTTCCATCTCAGAGAAGAGCTGATTTCCAAGATAATGTGGTGATAGAATCTACCAAGCCAGAGAATCAAGA GGCCAGGATGGGCTCAGGAGCGGGTCACTCAGCTGGAAGAGACCACAAGACCCACCACCTCAGCTGCAACCACC TCAGAGGAAAATCTGACCAAGTCAAGCCAGACAGTGGAGGAAGAACTGGGTAATAATAATGAAGGATTTGTAAGTGGT GCAGAAGACATAATCTCTGGTCCAGTCTGATCAGCAAGTCAAGACAAAACACCTAACCTAAGTCCATGCT AGGTGGTGCCTTATCAGCCACATTCTGCTCATCTGACCACCACCTCTCAGTCTGGCCTTTGATGCTTACATTAAG	Mus musculus glycosylation dependent cell adhesion molecule 1 (Glycam1)	XM_128312.2	1150	0	625

L2T-299	CTACNTCTAGNTNAGCTGCGTACGGCAGGAGCTGANNNTGTTCCAGTCCACCATGAAATTCCTCACTGTCCTGCTATTTGTCACTCTTGTGCCACCTCTCTTTGCTCTCCTGCTGGGTCCAAAGATGAACITCAAATGAANACTCAGCCCACAGATGCCATTCAGNTGCCAGTCCANTCCACCAGCTACACCAGTGAGGAGAGTACTTCCAGTAAGGACCTTCCAAGGAGCCTCCATCTTCAGAGAAGAGCTGATTTCCAAGATAATGTGGTGATAGAATCTACCAAGCCAGAGAATCANGAGGNCCAGGATGGGCTCAGGAGCGGGTCACTCTCAGCTGGAACAGACCACAAGACCCACCACCTCAGGNNGAACCANCTCAGAGGAAAACTGACCAAGTCAAGCCAGACAGTGGAGGAAGAACTGGTAAAAATAATNGAANGATNTGTA ACTGGTGACAANACNTAATCTCTGGTGCCAGNCGTATCACGAAGTCATGAAGACAANNGANCTAACCACTAAGTCCCATGCTAGGNNGTCCATCAGCCAAATTCGCTCATCTGACCACCACCTCTCAGTCTGCCCTTTNGATGTCTTAC	Mus musculus glycosylation dependent cell adhesion molecule 1 (Glycam1), mRNA	XM_128312	987	0	625
L2T-321	CCACTAGTCTAGAGCGTCGGCAGGAGACTGACCTTGTCCAGTGCCACCATGAAATTCCTCACTGTCCTGCTATTTGTCAGTCTTGTGCCACCTCTCTTGTCTCCTGCCTGGTCCAAAGATGAACITCAAATGAAGACTCAGCCCACAGATGCCATTCCAGTGGCCAGTCCACTCCACCAGCTACACCAGTGAGGAGAGTACTTCCAGTAAGGACCTTCCAAGGAGCCCTCCATCTTCAGAGAAGAGCTGATTTCCAAGATAATGTGGTGATAGAATCTACCAAGCCAGAGAATCAGAGGCCAGGATGGGCTCAGGAGCGGTCATCTCAGCTGGAAGAGACCACAAGACCCACCACCTCAGCTGCAACCACCTCAGGAAAACTGACCAAGTCAAGCCAGACAGTGGAGGAAGAACTGGGTAATAATAATGAAGGATTTGTAAGTGGTGCAGAAAGACATAATCTCTGGTGCCAGTGTATCACGAAGTCATGAAGACAAAAACACCTAACCACTAAGTCCCATGCTAGGTGGCTTCATCAGCCACATTCGCTCATCTGACCACCACCTCTCAGTCTGCCCTTTGATGTCTTACATTAAGTAT	Mus musculus glycosylation dependent cell adhesion molecule 1 (Glycam1), mRNA	XM_128312	1193	0	625
L2T-423	AGGGAAAGATGAACITTTGTTCCAGTGACANCATGAAATTCCTCACTGTCCTGCTATTTGTGAGTCTTGTGCCANCTCTCTTGTCTCCTGCCTGGGTCCAAAGATGAACITCAAATGAAGACTCAGCCCACAGATGCCATNCCAGTGGCCAGTCACTCCACCAGTACCCCAAGTGGAGAGTACTNCCANTAAAGGACCTTCCAAGGAGCCTCCATCTTCAGAGAAGAGCTGATTCCAAAGATAATGTGNTGATANACTCTACCAAGNCACANAATCCNGAGGNCCAGGATGGGCTCAGGAGCGGTCATCTCAGTGGCANAGACNNAAGACCCACCACCTCCGNGACAACCAC	Mus musculus glycosylation dependent cell adhesion molecule 1 (Glycam1), mRNA	XM_128312	529	e-148	625
C 328	AGNGTGACCAAGCTTGCCTACAAGACGAGAGCGGCCAAGGTCCAAGATCACCATCTGGCGGGAGTGCITTTCTGTTGGCGGCTCTGCTCACCTTAGTACCGGTGCTCTGGTCCGCCAACACCATCATCAGGGTATTTCTATAACCCGTTGGTGCCCGAGGCCAGAAAGCGGGAGATGGGAGCTGGGTTGTACGTGGGCTGGGCTGCCGCCCGCTGCAGTTGCTAGGGGGCCCTTGTGTGTTGCTCCTGCCACCAGCGCCGACAAAGTATGCACCACCAAGATCCTTATTCTGCGCCCGGATCCACCGCCCTGGCACCGGTTACCGGCACCGCTACGACCGNAAGGACTACGCTGAGGGGCGGGGTGCACGCA GACCGTACCCTACCCTACCAGCAGTGCATGAACCCACCCGTTCCAGCGTGCAGCCCTCNCNTNGACACCACC CCCAACCTTCCAGATGGTGACAGACGACACAGTTCTGCTTGCTAAGNTTGAAAAAGGACAGGACAGGCTGGCATCTCCCCCTTTNCTNCGGGTTGGNCAACNTGAACNCCGGGNCCTAGGNANCTGTCCAGCCCATGGNCAAAAAAACCTCNCCTTCCCAANAAANTGGGGTNGNNNTNCCACNNGNACCTCTTCCCCCCCC	Mus musculus claudin 3 (Cldn3)	NM_009902.2	805	0	1260
11						
Transcription /Translation						
B1 75	CAAGGAAGTCAGCACCTACATTAAGAAAATGGCTACAANCCTGACACAGTAGCATTGTGCCAATTTCTGGTTGGATGGTGACAACATGCTGGAGCCAAGTGTAAATGCTTGGTTCAAGGGATGGAAAGTCAACCCGCAAGATGGCAGT GCCAGTGGCACCAAGCTGCTGGAAGCTTTGGATTGTATCTACCACCAACTCGTCCAAGTACCAAGCCCTGGGACT GCGCCCTCCAGGATGTCTATAAAATGGAGGCATTGGCACTGTCCCTGTGGGCCAGTGGAGACTGGTGTCTCAAGC CTGGCATGGTGGTTACCTTTGCTCCAGTCAATGTAACAACGAAGTCAAGTCTGTTGAAATGCACCATGAAGCTTTGA GTGAAGCTCTCTGGGACAATGTGGGCTTCAATGTAAGAAGCTGTCCGTTCAAGATGTTAGACGAGGCAATGTT GCTGGTGACAGCAAAAAACGACCCCAATGGAAGCAGCTGGCTTCACTGCTCAGGTGATTATCCTGAACCATCCAGG CCAATCAGTGTGGTACGCTCCTGTTCTGGATTGTACACAGCCACATAGCATGCAAGTTTGTGAGCTTAAAGA AAAGATCGATGCTTTCTGGTAAGAAGCTGGAAGATGGCCAAAGTTCCTGAAGTCTGGCATGCTGCATTGTTGATTG GTCCTGGCAAGCATGTTGTTGAAGCTTCTGCTANCTCACTGTCNTTGTCTGTGNATAAGCNACGTGTGGTGTATCAACTNGGACANAAGTGTGGAGCTGCAATCCAGNTGCANAAN	Mus musculus, Similar to eukaryotic translation elongation factor 1 alpha 1, clone IMAGE:3488648	BC003969.1	1306	0	1722





Sabres	NCCCTCGGNCCAAGGCCNNNCACTCANAAANANNCAATTNCNCAAAGNCACTNGGNCTATCCTACCGNAGGTTNC CCGNCTCTATNNTCACANITTTTTAACTTGTACATACTAGGGGCTGTTTTCCNNNTCAAACCTGCCATCCANGCTGT CACAGGCAANCGAGCACANCTCCGCGCCAAAGCTAACTAATTTGCTAATCACCATNGATTCTCCAAAATGTGTGGA GATTNGGCTGGACAGTNACCATCAGAGTGNATGTACCATTGAGTNAANCAANATANAAAACCTGCCAAGTTGTGT GGCAAGTNACTAGTTCTGAAATACCTTGCAAGATACCGATATTCAAGCTGTTGACATACTCGTTGCCTACTTTAAACAAC TGTCAGAAAACGTGATGGGGTAANGAGGTACTTTCTAAAATCGTNCATAGACTCTGTAAAANGCAANATAAANTA	Mus musculus, Similar to eukaryotic translation initiation factor 2, subunit 2 (beta, 38kD ).	BC003848	502	e-139	2327
L2T-181	CCTGGGACGCAGNATCGGCACGAGGCTCAGTTGTAAGTGTGTATAATGACTGTCTGNTCTTAATGGCTCCATAA ATGACTAGTTGCTATTCAAAACATATTTTTGTGATTTGAAGATGGGGAAGGAAAACACTAAATGACAATTTGAGAAAAGG TGTATTGTTCCAAATTCGACTGGAGGGGAGAGGCTTTGCAGTGAGATCGTTGATAAGTTACTGCAAAAGTAGCCAC TAGTTTATTA AAAACCAAACTGTACAGATTAATAAACCTTTCCACAATATTCAGTTTTCTAACTCCTTGTGGCGTACAG TGTATGTTTTCTACTCATACATATTTAATTTCTTTAACCTCTGCTATTTATGCTCCACAAGTAAAATGACTTAGACTG GTCACTGTATTGCCCTTATTAAGATGCTGATATTAATTTTACAGTTTATTATCTATGCAATGGTAAATGATAAACAT TTTGTGTACCTTTGCAATATGTGTGTTACTGGGTTTACTTCGGATTGATTTCTTTCTGAATAGGGTGTCTTCATATGGAA ACCTCACATTACATCATTATATTTGGTGGTCTACATGTGATTAGAGCTTTTATACATTTCTGTATATTTTTATTAATGTAA GACTTTGCTTCTATAATGTTAGAGGAAGGTAGCTCACACATGATTTATAATTTAGTCACATTACATTAATTTTAGATT	Mus musculus RAB18, member RAS oncogene family (Rab18)	NM_181070.2	1267	0	2257
C 50	TATCTGCTGSCATACAGACCAGTTTTAGGACTGGTAATCCAACAGGGACTTACCAGAACGGTTATGATAGCACTAGC AATATGGAAGTAATGTTGCAATATGCACAATGGTATGAACCAACAGGCATATGCATATCCTGCTACCGCAGCTGCTG CGCCTATGATTGGCTATCCCATGCCAACAGGGTATTCTCAATAAGACTTTAGAAGTATATGTAATGTCTGTTTNTCATA ATTGCTCTTATATTGTGTGNATCAGACAAGATAGTTATTTAAGAAACATGGGAAATGCAGAAATGACTGCAGTGCAG CAGTAATTATGGTGCACTTTTTTCGCTATTAAGTTGGATATTTCTACTTCTGAAACATTTTANGTTTTTTGNCTAAA ATGCAGCGTGTNNCAAGTACTGTCGTGATTCAATACATAATAAGCATGCTGGCCTCCATAANATTTGAG	Mus musculus adult retina cDNA, RIKEN full-length enriched library, clone:A930106P08 product:DEAD (aspartate- glutamate-alanine-aspartate) box polypeptide 5	AK044792.1	1415	0	2329
16						
Protein Inhibitors						
B2 597	GCTNGAGGAATTCGGCACGAGGTGAAGCTCTAGANGAAANGNANTGGCAGTGTCTTACCCCTGTGCCATAAAGCTG GAATAGCACAAATGGCGTACTGTTCCAGGANACACCNAACTCAAGTACCAAGCGCTTNGTCCATGGCCGGCAGCCCAA CCATGTGTGGCTCCAGGATANATGGGGAGATAGACTGGACTGACAGGACCAGGGCCAGTCTCAGGGAGGNTGGGCT NGGGCTCAATCCANCATGAGCAGGCTCCCTAGCTGTTGAANGATCCATGGGTCCANGCACTGACCACCTGAAGGT GTNNGNCATTTCTGTGCTCTGAGGCCACNGACCATGCANANACNAGGACAAGACGTCCATTGTGCATCAACTTCATCC TTGAGGGCTGGCAGGTGGATGTCTGGGTTCTGTTGGTAACTGGGTACCTGCAAAAAGAGCTNTAGGACACTTTGCTCA TTAAAGCATCCCTTTGGATGCNAGGAAGCATTNNAGGAACAGTGGCTANAATNCTCCANATAGGTTTGGGAATGNAN ATNACTTGGACCCTGATTTAAANGAAAANGTAAAAGTGGAAA	Mus musculus adult male colon cDNA, RIKEN full- length enriched library, clone:9030416B16 product:similar to PROTEASOME INHIBITOR PI31 SUBUNIT (HPI31) [Homo sapiens]	AK078867.1	896	0	3236
C 15a	NCNNTNAGTGCCGCACAGTCTTTGTTCTGGTAGCTTTGATTTTCATGACAATGACTACTGCCTGGGCTGTGCTAACCC CCAAAGAAAAACCTGGCGCTTGTCTAAGCCGCCCCACGCAGTTTTGGAACCTGTGATGAACGATGCACAGGAGAT GGATCGTGTCTGGCAACATGAAGTGTGAGCAATGGCTGTGGTCATGCCCTGCAAACTCCTGTCTTTTAAACCATGT GGAAGATGGATCTTTATAAGCAGGACTGATGGCTAGCCCCAGAAGATTTTTTGAACCTACAGACCCCATGCTGGCT CCTCCTTAGACCTAGAATTGCATCTTGGAAAGAGGAAGATCTATACTGTGGTGACAGCTTCTAACGTTTGTGTCTA	M.musculus mRNA for WDNM1 protein	X93037.1	749	0	424

C 94	GNGNNTNGTGTCCCATNACATNTNCAGGAAATCGNAACNAGGCAGCCACAGTCTTTGTTCTGGTAGCTTTGATTTTCA TGACAATGACTACTGCCTGGGTCTCTGTCTAACCCCAAAGAAAAACCTGGCGCTTGCTCTAAGCCGCCCCACGCAG TTTTGGAACTTGTGATGAACGATGCACAGGAGATGGATCGTGTCTGGCAACATGAAGTGTGCAGCAATGGCTGTG GTCATGCCTGCAAACTCCTGTCTTTAACCATGTGGAAGATGGATCTTTATAAGCAGGACTGATGGCTAGCCCCAGA AGATTTTTTGAACCTACAGACCCCATGCTTGGCTCCTCCTAGACCTAGAATTGCATCCTTGGAAAGAGGAAGATCTAT ACTGTGGTGACAGCTTCTAACGTGTTTGTGTCTAAAATAAACTATCCTTAGCATCCTNNANAANAACCACAAACAA	Mus musculus extracellular proteinase inhibitor (Expi), mRNA	NM_007969.1	743	0	424
DS-A10	TGAAGACAGCCACAGTCTTGTCTGGTGGCTTGTGATCACTGTGGGGATGAACACTACCTATGTAGTGTCTGCCCCA AAGAATTTGAAAACTGGAGCTTGCCCAAGCCTTACCAGAAAAGTGTGGAATTTGTGTGATCAATGCTCAGGAG ATGGATCCTGCCCTGGCAACATGAAGTGTGTAGCAATAGCTGTGGTCATGTCTGCAAACTCCTGTCTTTAAATGG TTGACAGCCATGTGGAAGATGGATTCAATCTTCATAAACATGAATGATGGCCAGCCCCAGAAGATTTCTTGAATTC CAGAGCCTGTGCTTGGCTACTTCTAGCCCTAGAATTGCATTCCTGGACAAGGAAGATCTATATTGGTGTGACAATGC CCTAATATGCTGTGTCCAAAATAAACTACCCTTAGCATTAAA	Similar to Rat WDNM1 mRNA fragment from nonmetastatic mammary adenocarcinoma, Mus musculus, Similar to extracellular proteinase inhibitor, clone MGC:6000, mRNA, complete cds	X13309	212	0	429
L2T-322b	TGCACACGAGGGTCTGGTATCTTTGATTTTCATGACAATGANNCTGCCTGGGCTCTGTCTAACCCCAAAGAAAAAC CTGGCGCTTGTCCATAATTCNTCCCAACGAGTTTTGGAACCTGNGNNGAACGATGCACAGGAGATGGATCGTGTCT TGGCAACATGAAGTGTGCAGCAATGGCTGTGGTCATGCCTGCAAACTCCTGTCTTTAAACCATGTGGAAGATGGAT CTTTATAAGCAGGACTGATGGCTAGCCCCAGAAGATTTTTTGAACCTACAGACCCCATGCTTGGCTCCTCCTTAGAC CTAGAATTGCATCCTTGGAAAGAGGAAGATCTATACTGTGGTGACAGCTTCTAACGTGTTTGTGTCTAAAATAAACTAT	M.musculus mRNA for WDNM1 protein	X93037.1	642	0	424
L2T-430	TTGGCAGCAGGCCACAGTCTTGTCTGGTAGCTTTGATTTTCATGACAATGACTACTGCCTGGGCTCTGTCTAACCC CAAAGAAAAACCTGGCGCTTGTCTAAGCCGCCCCACGCAGTTTTGGAACCTGTGATGAACGATGCACAGGAGAT GGATCGTGTCTGGCAACATGAAGTGTGCAGCAATGGCTGTGGTCATGCCTGCAAACTCCTGTCTTTAAACCATGT GGAAGATGGATCTTTATAAGCAGGACTGATGGCTAGCCCCAGAAGATTTTTTGAACCTACAGACCCCATGCTTGGCT CCTCCTTAGACCTAGAATTGCATCCTTGGAAAGAGGAAGATCTATACTGTGGTGACAGCTTCTAACGTGTTTGTGTCTA AAATAAACTATCCTTAGCATCCTTAAAAAAAAAAAAAAAAAAAAAAAAAAAAA	Mus musculus extracellular proteinase inhibitor (Expi),I49390 WDNM1 protein, mRNA	NM_007969	753	0	424
DS-A6	CCCGTCCNCTGTNNTGAATCTGGCACGAGCCCTCNNTGCNGAATCTGGCACNAGGGACAGCCACAGGTCTTGT GTNCTGGATAGCTTTGAGTTTGTGATGACAAGTACTACTGCCTGGTGTCTGTCTAACCCCAAAGAAAAACCTGGCG CTTGTCTCAAGCCGCCCCACGCAGTTTTGGAACCTGTGATGAACGATGCACAGGAGATGGATCGTGTCTGGCAA CATGAAGTGTGCAGCAATGGCTGTGGTCATGCCTGCAAACTCCTGTCTTTAAACCATGTGGAAGATGGATCTTTAT AAGCAGGACTGATGGCTAGCCCCAGAAGATTTTTTGAACCTACAGACCCCATGCTTGGCTCCTCCTTAGACCTAGAA TTGCATCCTTGGAAAGAGGAAGATCTATACTGTGGTGACAGCTTCTAACGTGTTTGTGTCTAAAATAAACTATCCTTAG	M.musculus mRNA for WDNM1 protein	X93037.1	642	0	424
L2T-292	CTCTATAATNNGAGCGTCGGAACGAGGTTTTGAANATGAATGGACTNCCNTATTAGATAACAATGTGTATGTTAGCC CTTGCTAAAGATGTCTTGATGNCCAGGTGGTGTCTCCGAAGCTCTGTTGAGCCTGCTGCCTCCTCCCTTATNTCCTG GGGCNCAGCGCACGTGCTCTTCTATNGTCACCTTANCATGNNCTGGTGCCCTTNCCTTCTGCTCTTCA CTAGGGCTCCGGTGTGGCCGGCTCCTCACCTCCTGTGCTTCTGACGGTAAGGANTCCTGCTTCTGCTTCGCCGGCT GNTCTCANCCTGGCTACGGCTCCGACTTCGGATTCCCGATTTCTGTGACACCTTTTNCCTCTGGACTGTGCCGNT GGNTTCTGGATGTCGGTCAAGCAGAAATGGACCCACATGCTATTCTCCCGAAGCTCTTGTGNTTGNAAACCTTA ATNTNNTCTGGCNANTCCCTGTCANTGTGACTGCTGGAAGTTCNTCGTAAANCATGTNCTTATGCTGTCCCTCTTA	Mus musculus CBF1 interacting corepressor (Cir- pending), mRNA.	NM_025854	813	0	1857
8						

Other						
C 77	<p>TGAACACTGNTTGAANAGAATGGNACGAGGCAAGGAGCACCCACTNGGTGACAGGCCAGTGCCTCTGATCTTGTGAC</p> <p>GTGATGNTNCCAGGGCTCTGCACAATAAGCTCTCTGGCTAGCCACCACCCTCTTGAGCAGGGCCTGTACTCCAGA</p> <p>TACTGCCTCTGCCCGGATCAAGCGCTCCATATTTTAGACAAATTGGGAAGAGAGAGGGCTGAGCAGCTCAGGGGTGG</p> <p>CCCTGACTGCGTGTCAAGTGTATCTTGGACTGCGATCCACACCAGCACACAGCAGCAGCATAACTCTTGGAGGTG</p> <p>CCTTTAGAAGCAACCTGTCAGGCCAAACCCTCAAGTAAACACCAGAATATCTTAAGTTCCCAATAATTCTGACAC</p> <p>TCATCAGCCAAGCTGCTGCCCTCAATAAATCCACTGTACCCTTTCAANAAAAA</p>	Mus musculus B lymphocyte B cells CRL-1669 BCL1 Clone 13.20-3B3 cDNA,RIKEN full-length enriched library, clone:G430003E02 product:NIMA (never in mitosis gene a)-related expressed kinase 6,	AK089919.1	739	0	3129
C 130	<p>TTCCGGCACGAGGTCCAAGTCCATGACCATTAACTGGAGCCCTTTTCAGCCCTCCTTCTAACATCAGGTCTAGTAATATG</p> <p>ATTTCACTATAATTC AATTACACTATTAACCTTGGCCTACTCACC AATATCCTCACAATATATCAATGATGACGAGACG</p> <p>TAATTCGTGAAGGAACCTACCAAGGCCACCACACTCCTATTGTACAAAAAGGACTACGATATGGTATAATTTCTAATTCAT</p> <p>CGTCTCGGAAGTATTTTTCTTTGCAGGATTCTCTGAGCGTTCTATCATTCTAGCCTCGTACCAACACATGATCTAGGA</p> <p>GGCTGCTGACCTCCAACAGGAATTCACCACTTAACCTCTAGAAGTCCACTACTTAATACTTCAGTACTTCTAGCAT</p> <p>CAGGTGTTCAATTACATGAGCTCATCATAGCCTATAGAAGGTA AACGAAACCACATAAATCAAGCCCTACTAATTAC</p> <p>CATTATACTAGGACTTTACTTCACCATCCTCCAAGCTTCAAGAATACTTTGAAACATCATTCTCCATTTTCAGATGGGTATC</p> <p>TATGGGTTCTACATTTCTCATGGGCTTACTGGATTCCATGGGACTCCATGTAATTTATGGGATCAACATTCCTTATTGG</p> <p>TTTGGCTACTACGAACAATAAAATTTCACTTCACATCAAAACATTCACCTTCNGATTTGAAGGCCGCNGCATGGACT</p> <p>GGACATTTTTGGTANAACGTAGCTGGACTTTTTCTATACGNTCTCCATTTATTGGATGAGGATCTTTAGGGGGGGG</p> <p>GCCCGGGAACCCAATTCGNCCTATAGTGGGNCCTTTAAAAA</p>	Mus musculus BAC clone RP23-8J15 from chromosome 1 with homology to mitochondrial Cox3 subunit	AC116997.3	1207	0	190712
L2T-277	<p>GGGCNGAGCTGCTGAGACGGCAGAGGCCCTCGTCCCGAATGGCTCTGCTGGCGAACCTGGACCAAGGGGAGAAC</p> <p>GTGGACTAAGTGGACCTCCAGGACTTCCAGGTATTCTGTGTCAGCTGGGAAAGAAAGGTCCCTCTGGGAAGCAGGG</p> <p>GAACATAGGACCTCAAGGCAAACAGGCTCTAAAGGAGAGGCTGGGCCCAAAGGAGAAGTAGGTGCTCCTGGCATG</p> <p>CAAGGATCTACAGGGGCAAAGGCTCCACAGGCCCAAGGGAGAAAGAGGTGCCCTGGTGTGCAAGGAGCCCCA</p> <p>GGGAATGCTGGAGCAGCAGGACCTGCCGGACCTGCCGGTCCACAGGGAGCTCCAGGTTCCAGGGGGCCCCCAGG</p> <p>ACTCAAGGGGACAGAGGTGTTCTCGGAGACAGAGGAATCAAAGGTGAAAGCGGGCTTCCAGACAGTGTCTGCTG</p> <p>AGGCAGCAGATGGAGGCCTTAAAGGAAAACACAGCGTCTAGAGGTTGCCTTCTCCACTATCAGAAAGCTGCATT</p> <p>GTTCCCTGATGGCCGAAGTGTGGAGACAAGATCTCAGGACAGCAGACTCGAAAAGCCTTTTGAGGATGCCCAGG</p> <p>AGATGTGCAACAGGCTGGAGGACAGCTGGCCTCCACAGTCTGCTACTGAGAATGTGCCATACAGCAACTCATC</p> <p>ACAGCCCAACAAGGCTGNTTCTGATTTGACAGATNTGGCACAAGGCCANTTCACTACCCACAGGAGACCCTGTT</p> <p>TTTTCTATTTGGTCCAGGGAGCCACACATGTGGACAANATGNTGAGATCTCACATGGCATGATATAGNTTTGAACACCTN</p>	Mus musculus surfactant associated protein D (Sftpd), Mma	NM_009160.1	1318	0	1288
L2T-401	<p>CCCGGNTTGCAGGAATTCGGCAGCAGGTGGGCTTCTACCCTGCTGACATCACCCTGACCTGGCAGTTGAATGGGGA</p> <p>GGAGCTGACCCAGGACATGGAGCTTGTGGAGACCAGGCCCTGCAGGGGATGGAACCTTCCAGAAGTGGGCATCTGTG</p> <p>GTGGTGCCTCTGGGAAGGAGCAGTATTACACATGCCATGTGTACCATCAGGGGCTGCCTAAGCCCCCACCCTGAG</p> <p>ATGGGAGCCTCCTCCTCCGCTGTCTCAACACGGTAATCATTGCTGTCTGGTTGTCCTTGGAGCTGCAATAGTCAC</p> <p>TGGAGCTGTGGTGGCTTTTGTGATGATGAGGAGGAGAAACACAGGTGGAAGGAGGGGACTATGCTCTGGCTCCA</p> <p>GGCTCCACAGCCTCTGATCTGTCTCTCCAGATTGTAAGTGATGGTTCATGACCTCATTCTCTAGCGTGAAGACAG</p> <p>CTGCCTGGAGTGGACTTGGTGACAGACAATGTCTTCTATATCTCTGTGACATCCAGAGCCCTCAGTTCTTTTGT</p> <p>CAAGTGTCTGATGTTCCCTGTGAGCCTATGGACTCAATGTGAAGAAGTGTGGAGCCAGTCCAAACCCTCCACANCA</p> <p>GAACTGTCCCTGCACTGCTGTCTTCCCTCCACAGCCAANCCTGCTGGTTCAGCCAAACACTGGAGGGACATTTG</p> <p>NAGCCTGTGAGCTNCATGCTAACCTGAACTGCAACTCCTCACTCCACACTGANAATAATAATTTGAATGTAACCTTGA</p>	Mus musculus histocompatibility 2, K region, mRNA (cDNA clone MGC:7052 IMAGE:3156482), complete cds	BC011306	1419	0	1345

L2T-59	ACATCCCACACATGAACACAACAATCCTGGTGAATAACCTAACTACAGTTGGAAATCTAACTGGCTTTAAAGGA AAAGAGAGCCTGCCGTCTCTTTGTGGTTGCCATTTATATAGATGATATATTAGCTTTGGTCTGTTATGCTTTGGAA TGCTTAGTGCAAGCCCTGGTTGCCCCAGAGACCCAAGTGATGTTATGTGACCTTGACCCTAAGTTACTTCTGGTTGGT GAATAAAGATGCCTGCAGTCGATAGCTGGGCAGGAGAGACCAGGGTGGGGTTTAGGGTTCCTGAGCTTGGGGTTGT AAGAGAAGCACCAGGAGGGCGAGAAGGTGAAGGGAGGAGGAAGCGGGCGTGGATTGGGTGAGTTGTGGAATGATG GCTATGTGGGTGGCTAATTGGAGTTAAGAGCAGCCAGATGGAACATGAGGAATTAGATGATGGCTTACTGGCTG GGGAGTAGGCATACTAGTGTAGAGGATAGATATCTGCCAGCTCTTGCTGATTAAGGCTTGTTAT	Mus musculus major histocompatibility locus class III regions Hsc70t gene, partial cds; smRNP, G7A, NG23, MutS homolog, CLCP, NG24, NG25, and NG26 genes, complete cds; and unknown genes	AF109905	1039	0	135545
L2T 215	AANCNNTGGANANGAANATCAATATTNTCCTGCCTTTGTGGCCAGGGGGGTGAGGGTGTGGCCAAANTATTTACAGG TCACNTAAAAATCCATTGTGNTNNATTACCTCATAACTACGACANANGNGGGTNTAAAATAAACTCTACACAAA CCTTGACAAACTTAATCCTAGAGACTGGCACAGACTTACTTGGTCCCTTCCCTTGGCCCTATTNAGAACTGAGAA TACTCCCTCTTGATTCGGTTTTAATCTTTTAAGATCCTTATGGGGCTCTATGCCATCACTGCTTAAATAATGTGT TTAACCCCTATGTTGTTANTANTGATCTATATGTTAANTTCCAAGGCTTNCAGGTGGTGCANAAAACGCTCGGTAC ANACTGGCCTACNGNCAACGAGCCAGGTNCCCAANGGACATCNCACCANTTCCGGCCAGAGATCTGATCTACGT ACACCTGCNTCCTGCCTGANACCCTCCAAGCCTCCANTAAAAGGGTCCCTGNCCT	Mouse major histocompatibility complex region containing the Q region	MHC322F1	430	e-117	159179
L2T-50	GCGGNACGAGGCTGGCTCGGGACCCCGCGCCGCTGCGCTCCGAGAAGACCTCAAGCAGCGCCGGAGCTTTGA ACAAAGAGTGGAAAGATGCCGGCTCATCCGGGAGCAGCACCCACCAAGATCCCAAGTATTATAGAGCGATACAAGG GGGAGAAGCAGCTGCCCGTCTGGACAAGACCAAGTTCCTGGTGCCTGACCAGTGAACATGAGCGAGCTCATCAA GATAATCAGACGGCGCTTGACAGCTCAATGCTAACCAAGCCTTCTTCCCTGGTGAATGGGCACAGCATGGTGAAGT TGCCCACTCCCATCTCCGAAGTGTACGAGAGTGAAGAGATGAAGACGGCTTCTGTACATGGTTTATGCCTGCCAG GAGACATTCGGGACAGCAATGGCTGTGAAGACTCCAACAAAGCCAAATGTTGTTAAGCCCTTACCAGGCAAAAAG GGATGTTACCAGCGGACGCTGGACGGCTCACCACCCACAGATGAGAAGCTAGGCACCCACATAGGGTATTAGGAAC TGTTTCATCAGCCAGAAACTGAGCTCCATGCAAGTGCCTCAGNTTGGAAACTCGTCTAACTAGGCTATTTNGTGTTT	Mus musculus microtubule-associated protein 1 light chain 3 Map1 lc3	NM_026160	1197	0	1711
D 378	CAACTTCGANAGAAGGGACNGAGGTTAAGTCTACGACTGGCCAGGGGGNGNTGAACAGTATCCTGATGCCACAGA TGACGACCTCACCTCTCACATGNNTTANCGGTGAGTCTAAGGAGTCCCTNNGGNGTNNCCCTGCTNCCCAGCTTC TGAACATGCCCTCTGATCAGGACAACAACGGAAAGGGCAGCCATGAGTCAAGTCAGCTGGATGAACCAAGTCTGGAA ACACACAGACTTGAGCATTCCAAGAGAGCCAGGAGAGTGCCGATCAGTCGGATGTGATCGATAGTCAAGCAAGTTC CAAAGCCAGCCTGGAACATCAGAGCCACAAGTTCACAGCCACAAGGACAAGCTAGTCTAGACCCTAAGAGTAAGG AAGATGATAGGTATCTGAAATCCGAATTTCTCATGAATTAGAGAGTTCATCTTCTGAGGTCAACTAAGAANAGGCAA AAACACAGTTCCTTACTTTGCATTTACTAAAAACCAGAAAAAGTGTAGTGAGGGTNAAGCACGAATACTAAGTCTCA TTTCTCAGTTCAGTGGATATATGNTGTAGAGAAAGAGAGTAATATTNTGGGCTCTTAGCTNACTCTNGTTGTGTCAT GCACACNCCGTTGTAACCAAAGCTTCTGCCTTNGCTTCTGTTCTTCTGTACAANAATGCANACNGCCACNGCA TTTNAANGATTGTAATNCNNGCTTGAATANAATGNATGTANAANCNAGCAA	Mouse mRNA for minopontin	X13986.1	1025	0	1328
C 213	CTCTTGAACCCGGGCTGCAGGAATTCGGCACGAGGGGAAATTAAGTGCCTGAGGAGCCAGGTGGGTGGCCAGGTCA GTGTGGAGGTGGATTCCACTCCCGGTGTCGACCTAGCCAAGATCCTGAGTGAGATGAGAAGTCAGTATGAGATCATG GCCGAGAAGAACCAGGATGCTGAAGCCACCTACCTTGTCTGGATTGAGGAGCTGAACACCCAGGTGCGCGTCC ACTCTGAGCAGATCCAGATAAGCAAGACCGAAGTCCAGGACCTTCCAGGACCCCTCAGGGCCCTTGAAGTGAAGT CAGTCCAGCTCAGCATGAAAGTGCCTGGAAGGCACGCTGGCAGAGCAGGAGGCCCTTATGGAGTCCAGCTGT CACAGATCCAGAGCGTATCAGCGTTTTGAAGCCAGCTGAGCGACGTGCGTGCCGACATAGAGCGCCAGAACCA GGAGTATAAGCAGCTCATGGACATCAAGTCCAGGCTGGAGCAGGAGATGCCACCTACCCGAGCCTGCTGGAGGGC CAGGAAGCCCACTACAACAATCTGCCACCCCAAGGCATCTGAGCTACCAGCGAGACTCCCTGGGAAGGGGNC TGACTGGGGTGATAAAGTTACTCTAACCTCCCTCGACTTGTCAATAAACTATCCTCCAAGG	Mus musculus keratin complex 1, acidic, gene 19, mRNA (cDNA clone MGC:25344 IMAGE:2655016)	BC034561.1	1193	0	1382

C 53	CTTCTGANCNNTCTANNAGAATNCGGCACGAGGCTGCATGGCCAAACACACTTGTCTTGTCTCACAAACCAGAG CAAAAAGGGGTGCCTACTGGTTTCGTTCTGCCCATCCGGGACATCCGTGCCAGCGTTGGGGCAGGTTTCTGTATCC TTTAGTAGGAACGATGAGCACAATGCCTGGACTCCCTACGGGCCCTGTTTTATGATATTGATTTGGATCCTGAAAC GGAACAAGTGAATGGATTGTTTTAAGCAGATCTCCATCTCCAAGAGGCCACTGTGCCGGCCAGTGTCTGTTCAGGC CCACTGAAGAAGTGTGCAGAAGTCTTGAAGTCTGTCCCGCCCTGAAGAGCTTCAGAAATAGTGGGAGTTCCCTA AAGCCTTTCATAGCCTTAATTCATGTATGTATAAATTAACATAAATCATGTCTATTTACATAGTGAAGGTCCAGAATAA ATGAATAAATTTTGCTAAAAAAAAAAAAAAAAAAAA	Mus musculus methylenetetrahydrofolate dehydrogenase (NADP+dependent), methylenetetrahydrofolate cyclohydrolase, formyltetrahydrofolate synthase (Mthfd1),	NM_138745.1	892	0	3159
L2T-150	CNCTGCACCGGGTGCANGAATTCGGGCACGAGGCTGCGCACTGGCCGCAGCATCAAGGGTTACACTCTGCCTCCG CACTGCTCCCGTGGAGAGCCCGTGCAGTGGAGAAGCTGTCGGTGGAACTCTCAACAGCCTGACGGCCGAGTTCA AGGGCAAGTACTACCTCTGAAGAGCATGACGGAGCAGGAACAGCAGCAGCTCATTGATGACCATTCTCTTTGAC AAGCCCGTGTACCTCTGCTGCTGGCCTAGGCATGGCCCGAGACTGGCCCGATGCCCGTGGCATCTGGCAACACG ACAACAAAAGCTTCCCTGTGTGGTGAACGAGGAGGACACCTCCGCGTGATCTCATGGAGAAGGGAGGCAATATG AAGGAGGTTTTCCGCCGCTTCTGCGTGGCCCTGCAGAAGATTGAGGAGATCTCAAGAAGGCTGGTCACCCCTCAT GTGGAACGAGCACCTGGGTACGTGCTCACCTGCCCTCCAANCTGGGCACCGGGCTGCGCGGAGGCCTGCACGT GAAGCTGGCGAACCTGAGCAAGCANCCAAAGTTTGAAGAGATTCTCACTCGCCTTCGTCTGCAGAAGCGCGGCACA NGTGGCGTTGACACGGCTGCGGTGGCCGCGTTCGACATCTCAACGNCCGATCGGNTGGGGCTCATTCCGAA GTTCAACAAGGTGCAGCTTGGTGGTGGATGGCCCTGAAACTTATGGTGGGANATGGGAN	Mus musculus creatine kinase, muscle (Ckm),	NM_007710.1	1206	0	1415
L2T-151	GCGGTTGAGCGCNGAGACGGCAGGGTGCACATGCAACCGCAGTGCCTTTTGANNTGATCTCACCCAGAAGCATG AATTCACACCTAACATTCTTAATAACCACCTGTTCTAAAAAAAAATAATNNTAGTATTTCTAGTATGAATTCAGTG AGGAAGAAATAGATGGAAAAATAGCGATAGAGAACAGTGGCTCACTGAGCATATTAGACTCAGAATCTCAGCACTCCT ACTTTTCAGGCTGAGTTACAAATACTACAGAAGTATGGGCCCATGCTATGTATCCGGGTATGGAGGAGTATGGGGAC CTTACCACACTTAAAGTAAAACACAGTTAACATCATTGTAGATCTCAAAAAGTGAATTCATAATGTGTTTTACTTCAA TAATACCAGCGATAATCCATCACTCGTTAAAAATTTGCCACTACCAAGTTTGCCTGGTTTTAGTCACTATAAAACACA CCCATGAAGCCAGGTGTTTTAAAAATGTTTATCCAGCATTTAAATTTCTTCTATAAAGATGGTTTTCTTTGCCAAAG TAGAGCCATTTATTTTTATTTACTACTTTAATCTTNGCATGCCTATTA AAAACAAAACNAACAAACAAAAAANCA AAAACGGCAACAAACAAAAAACTGTGTGAGGTGCTTTGGAGTNGGAGGCTGGGATGTCTGGTTCTGGAACAGGA AGGAGGGATGTCACACTGANNCAGAGCTGCTTTGTCCAGAAAACATAAGACGATGCANTGANANAANAAAAANANA	Mus musculus carbonic anhydrase III gene, exon 7 and complete cds	AF294988.1	1047	0	1426
L2T-322	CTCTCACCACNAGTTCNNAAGGATTCGGCAGGAGGTTNCTGNTAGNTCTNNTCTNATGANANGGACTACTGCCTGNC CTCTGTCTAANCCCATAGANAANCTGNTNCTAGTNTNANANCGCCACGCAGANNCGCAACNAGGGATNANNGA TGCAGAGGANATGGNTCGAGCTCTGNATCATGANNTGATNANANTTTGGCTGNGNTCANGCCTGNGAACCTCCTGT NNTNTATCATGTGNANATGGATCTNTATAANCAGNNCTGATGGCTATGCCACNAGATNNCCTGGANNCTANTNNN NCCATGNTTGGNTCCTCTTNGACCTAAANTNGNATNCTGNNATATGNANATNATAACGNTNNTGACANGTNCCTAA CGTGTGTTGTCTAAAATGGTTATCCTATCATATCCTGATCCAAANCAAGATAAGANTCCTGGGGCCANCCGNACNNN NGTTCNCNGTANCCANTACTTTTAAACCTGTNATAACAGCTTTATAATATTGAAAACCTTAGTGCTTAAAAA	Mus musculus cathepsin L (Ctsl), mRNA	NM_009984	76	e-10	1374
L2T-180	GAATACGGNACGAGGCACACTCGCTTAGTGTGCTGGACCTTGGGGGAGACCTGGCTGGAGCTTGTCCAGCTGTT CTGTTCTGTGGTTCCACCTGGGTTCAAGATTGCTGCCCTCTGCCTGTCTGAAGGAGGCCAAGGCCACCCAGTAC ACGAGGCTGCCTTCAAGGCCCTACTGGTTAATAGTCTGATGAGTGGATTGCTTGTCTGCCGCCCTTTGCTGTG TGGGCAGTACTCTGAAGCAGGCAATGGGCTTAGGATCCCTCCAGAAAACCTGCTCTGACCCAGACCCATCACCCA GCTTGGGGATGGCACCACGTTCTACTGCCCTCCAACCTCTGGCCTGGCAAAGGCCGAAGGTGAGCAGGAAGGAGC AAGAGGACAGAAGCAAACATGAACCTGGGGGTTACCTAGGGCTTGACCCGCCCTCTGGGAAGGCATGCCTC AGCCTGGGGTAGAGGTAGGATGACTGACTGTTTTGGCTGGCCTCTGCTGCCCTCATCTGGGCTANGCAGCTGGG AGCCAAAGTTGAAATACAAATAAAGTTGTTTTGGCCCTGAAAAAACAACAC	Mus musculus cathepsin D (Ctsd), mRNA	NM_009983	1106	0	1979

C 72	<p>GCCCGGNTCTGCAGGAATTCGGCACGAGGTGATCTTGCAATACATTTGCTGAATAAGATGAAGATTATGGTGGTTAA  GGACGTTGNAAGAGAAGACATTGAATTCATCTGTAAGACAATTGGAACCAACCCAGTTGCTCACATTGACCAGTTCAC  TGCTGACATGCTGGGTTCTGCTGAGTTAGCAGAGGAAGTCAGTTAAATGGTTCTGGAACCAATTCAGATTACAGG  TTGTACAAGCCAGGGAAAACAGTTACAATTGCTGACGTGGTTCTAACAACTGGTGATTGAAGAAGCTGAGCCCTC  CATTGATGATGCTCTCTGTGTCATCCGATGCTTAGTAAAGAAAAGAGCTCTATTGCAGGAGGTGGTCTCCAGAAAT  AGAGCTGGCCCTCAGACTGACAGAGTACTCCGAACACTGAGTGGTATGGAGTCTACTGTGTTCTGCTTTCCGG  ATGCTATGGAAGTCATTCATCTACACTAGCTGAAAATGCTGGCTGAATCCATTCTACAGTAACAGAGCTAAGAAA  CCGCCATGCCAAGGANAAAAACTACAGGCATNACTGTCCGAAAGGGTGGGATCTCCAACATTTTGGGAGGAAATG  GTTGTTACGCTCTGTTGGTGGTCAGNCATGCTTTGANCTTNCACACTGAAACTGNGCGGACCTTCNGGAAAATCG  ATGATNNGGNAATNCCAAAACCTCNGGANTAAANGCTTGNITGCCNGGCNTCATTATGGCCAAAAANTANNGGGGG  CTCNGAATNNAAGGCNNAACCCCTNGNCCNTGGCTCNGGNANACTNNAANANNTTTTGGGGCATTGGNNTTNC  CANNNTGGCNATTTGGTTNNAAACTNGTNTTNGAANCANNTTNACTNAAAAACCANTCAAATNCNTGNGNTTTNC  AHCNHCNNAAAAAAASAAAAA</p>	Mus musculus chaperonin subunit 4 (delta) (Cct4) mRNA, or Mus musculus ES cells cDNA, RIKEN	NM_009837.1	1162	0	1966
C 179	<p>GTTCTCGCTCCTGGACGTCCGNTTCTCNTGNANNAGNCACTGGGAGGAAGNTGAGAACAGGAGAGAACTCTNC  TGCCCGGGACCGCGACCGGGCGGAACCCGGGACCGANTCGCTTGGCGGCNCTGACCGAGATCGAGCAGTCC  CTGGATCCCTAAGGAGGAGGCGCTCAGCGGAGGCGCTTGTGACAGNAGAACAGAGATGGCATCAGTAGATTTCAA  NACCTATGTGNACAGGCTCAGAGCTGACAGGAAATTTGCAATGTCTATTACAGACTATGGATAAGCGGCNTC  GGCTGCTGNCCGCTGTACATGGGCACAGNCACTTTNANTATGGAATGGANATGCTGTTCCANNGACCANAATCCTT  NAGTGANTTTTNGAGGATGTNGCCCTTCCAGTGAGTTCNAAANTCAGCNATGGTNGAACTGCCAGTCTGTCATN  GATGAACCTTCNACCNANCGCAGANCAGTGTGATCTGGTCTCNGTGGNACANCTGAANTTTGAAGGNNNGCAAAC  CCGNGACTTTTCANCCNGAANTCAANCTNNGNCTGGNCCNNGGCGTCAACCANGNACCCGCGTGC</p>	Mus musculus NTF2-related export protein NXT1 (NXT1) mRNA, complete	AF156958.2	567	e-158	644
C 182	<p>CACCATGCCACTGCCCGTGTGTGCCGCGTCAGTCATGCCGAAGCAGAGTCTCCGTTGGACATGACCTGTGAGGGC  TGTGCTGAAGCCGCTCCAGAGTCCCAACAAGCTGGGAGGAGTGGAGTTCAACATTGACCTGCCCAACAAGAAGGT  CTGCATCGACTCTGAGCACAGCTCAGACACCCTGCTGGCAACCCTCAACAAAAACAGGAAAGGCTGTTTCTACCTTG  GCCCCAAGTAGCCAGGACCTGGGCGAGTCTTCCGGATATAAATGAAGAGGCAGGCTGTTGATCTGGTCTCCCG  GCAGATCTGGAACACCAACTGCTCAGTCCAGTCCAGCCAGCCATGGAGTTCCTGCCCAGACAGGCCTTCCCGCT  GGCTCCCTGCAAGCTTCCATGTAATAAAGTCAAGCTGAGTTTGTGAAAAAAAAAAAAAAAAA</p>	Mus musculus copper transport protein Atox1 (ATOX1) mRNA, complete	AF004591.1	839	0	432
L2T-297	<p>CTACTCCTAGTCTNGAGNCTCGGCACGAGGGCAAGATCATCTGAAAAGGATTTGGCTCCCCCTCCCGAGGAGTGT  CTTCAGCTTATCAGCAGAGCCACCCAGGTGTTCCGAGAACAGTACATTCTCAAGCAGGACCTGGCCAAGGAGGAGAT  TCAGCGGAGGGTCAAATTTATGTGACCAAAAGAGGAAACAANTCGAAGATCTCAATTACTGTGAGAGGAAAGGAA  AAGTCTCCGGAAATGGCTGAGCGCTTAGCTGACAAATATGAGGAAGCCAAAGAAAAACAAGAATATCATGAACA  GGATGAAAAAAGTGCTTACAGTTTTTATGCTCAGTCCAGTCTCTCTGACAGTGAGAGAGACATGAAGAAAGAGT  TACAGCTGATACCTGATCAACTGCCACATCTAGGCAACGCCATCAACACAGTTACTATGAAAAAAGATTATCAACAGC  GGAAGATGAAAAAAGTGTGAGTCTCAGAAACCCACCATTACTCTCAGTGCCTACCANCGGAAGTGCATGCAGNCC  ATCCTGAAAGAAGAGGGTGAACNCATAANGGAAATGGTGAAGCAATCAATGACATCCGAAATCATGCACTTCTGA  NACCACCTGGAATGAACATAANTTGAAGGCTGTAACAACAACANGGANCACTGTNTAATTTATAAAGGAGCATNTTGG  ATAAGATTCCGGTGTGTTATTCCTTTGATTCTTTNGTATNATTCCTGGTAAATAAATNANTATCCAATAAGTTGATA  AATTTNTTNAAAACAAAAAATAA</p>	Mus musculus nucleoporin, mRNA (cDNA clone MGC:41381 IMAGE:1379673), complete cds	NM_172394	1271	0	2418
C 148	<p>GGGAAGAGTNGGCACGAGGAGACGCCACATCCCTATTATAGAAGAGTAATAAATTTCCATGATCACACACTAATAA  TTGTTTTCTAATTAGTCTTATGCTCTATATCATCTCGCTAATATTAAACAACAACTAACACATACAAGCACAATA  GATGCACAAGAAGTTGAAACCTTTGAACTATTCTACCAGCTGTAATCCITATCATAATTTGCTCTCCCTCTCTACGCAT  TCTATATAATAGACGAAATCAACACCCCGTATTAACCGTTAAACCAATAGGGCAACCAATGATACTGAAGCTACGAA  TATACTGACTATGAAGACCTATGCTTTGATTATATATAATCCAAACAACGACCTAAACCTGGTGAAGTACGACTGC  TAGAAGTTGATAACCGAGTCTGTTGCAATAGAACTCCCAATCCGATATTAATTTATCTGAAGACGCTCCCTCACTC  ATGAGCAGTCCCTCCCTAGGACTTAAAATGATGCCATCCAGGCGGACTAAATCAAGCAACAGTAACATCAAAACCG  ACCAGGGTTATTCTATGGCCAAATGCTCTGAAATTTGTGGATCTAACCATAGCTTTATGCCATTGGCTTAGAAAT  GGTTCACATAAATATTCGAAAACCTGATCTGNTCAATAATTTAAT</p>	Mus musculus cytochrome c oxidase subunit II (Cox2) Mma	JAF378830	1158	0	725

KS-11	AATCNGTNCACGAGAACCTACCAAGGGGCANCACTCCTATTGTNCAAAAAGGACTACGATATGGTTTTTTCTATT ATCGTCTCGGAAGTATTTTTCTNTGCAAGGATTCTTCTGAGCGTTCTATCATTCTAGCCTCGTACCAACACATGATCTAG GAGGCTGCTGACCTCCAACAGGAATTTCCACCTTAACCTCTAGAAGTCCCACTACTTAATACTTCAGTACTTCTAGC ATCAGGTGTTTCAATTACATGAGCTCATATAGCCTTATAGAAGGTAACGAAACCATATAATCAAGCCTACTAATT ACCATTATACTAGGACTTTACTTCACCATCCTCCAAGCTTCAAGAACTTTGAAACATCATTCTCCATTTGATGGTAT CTATGGTTCTACATTCTCATGGCTACTGGATTCATGGACTCCATGTAATTATTGGATCAACATTCCTTATTGTTGCC TACTACGACAACATAAAATTTCACTTCACATCAAAACATCACTTCGGATTGAAGCCGACGATGATACTGACATTTGTA GACGTAGTCTGACTTTTCTATACGCTCCATTATTGATGAGGATCTTAAAAAAAAAAAAAAAAAAAA	Mus musculus domesticus mitochondrial DNA, complete genome	AB042432	1090	0	16300
HC-12	CTTCGCACGTGCCGAATTCGGCACGAGGGGCAAGATGTCGGCGCCGCTGACCTTCCGNNTTTTGTGACTCTCCCC AGGGCNGCACGGGTTNCGGGTTCAAGTGTGCCGAGCGGGGAAAGATCACGCATACCGGCCAGGTGTATGAT GAAAAAGACTACAGGAGGGTTCGTTTTGTAGATCGTCAGAAAGAGGTGAATGAGAACTTTGCCATTGATTTGATAGCA CAACAGCCTGTGAATGAGGTGGAGCACCGCATCATAGCCTGCGATGGAGCGGTGGTGCCTGGGCCACCCCAAG GTGTACATAAACTGGACAAAAGAAACAAAACGGGGACATGTGGCTACTGCGGCCGTCAGTTCAAGCAGCACCATCA CTAGTGTGGGCTGTGCTGCTGCTGACTCCTATGGAACATCTCCACGCTGGGTGTTCTGTGTGAGGCCACTGCT CTGTGAATGGTGCCTTGTGTTGAATAAAGGATGCTCCACCATGAAAAANAACCAC	Rattus norvegicus NADH ubiquinone oxidoreductase subunit (IP13) gene	RATIP13A	470	e-130	3093
C 304	CACGAGGAACCCCTGGCCCTGCTGAGATACTCGGGTGTGNGNGTGAGTGTAGCCTGGGCAGTGAGAAGGGCTGCAG GAGGGTCTTGAGACGGGGCCCTGGGAACCCACCTCTGAGANGGGGGCAGATGCCAGACAGTGGTCCCGAGA CAAGCTCAGGCTCCATGAAGATCACCTGCTCTAATGTCCTGTGTTAGTTCGGAGGACTGAGAGCTCATGGCATGA GTAATAACATCTCTAATGCCACTCTTCTATCAGATATTAATAATGTAAATTACCAAAACCATCTCTGAGAAAAA CCAAGCCTTTCCAGGTGGTATTAATTTACTGGACACGTTGATAATGGCATGACTAGAAACAGCCTTAACTCCTAAGCT CAGTTCAAGAACATCTGTGTATCTAGAGACTCCTGACTTTGAAGTGTCTTAAAGCCTGTGTGGTTTGGCGCGGG CANCTCTGTACAGTGTGCTCCTTSAAGGTGAGGGTGCAGAAGCTTTCAGGTGTGAGCTAAAAGGGTACAGACTTCT AATGACAACCTGTGACTAACGGTTTCTCAGTGTAGTTATTTGAGAAAGATTGAGAAATTTCTATCTTTCTGTATGTTT CATGTTGTCAGGTAGTTGTAATGAATGATTTACCTATGCNAAAGATTTATTANAGCCTAGAGAAATATGAAAAA AAAAAAAAAAAC	Mus musculus 13 days embryo male testis cDNA, RIKEN full length enriched library, clone:6030481D21 product:malic enzyme, supernatant, full insert sequence	AK077968.1	1172	0	3112
22						
Stress						
C 82	GCGGATGANCGCTGAGACGGCACGAGGGGAGCGCAGGCCAACAGCCATGGCGNGGAAGGAGGAATGAAGTGT GTCAAGTTTTTGTCTACGTTCTCCTGCTGGCCTTCTGCGCCTGTGCAAGTGGGATNGATCGCCATTGGTGTAGCGGTT CAGGTTGTCTTGAAGCAGGCCATTACCCATGAGACTACTGCTGGCTCGCTGTTGCCCTGTGGTTCATCATTGCAAGTGGG TGCCCTCCTCTTCTGGTGGCCTTTGTGGGCTGCTGTGGGGCCTGCAAGGAGAACTACTGTCTCATGATTACATTTGC CATCTTCTGTCTTATCATGCTTGTGGAGGTGGCTGTGGCCATTGCTGGCTATGTGTTTAGAGACCAGGTGAAGTC AGAGTTTAATAAAAAGCTTCCAGCAGCAGATGCAGAATTACCTTAAAGACAACAAAACAGCCACTATTTTGGACAAATG CAGAAAGAAAATAACTGCTGTGGAGCTTCTAACTACACAGACTGGGAAAACATCCCGGCATGGCCAAGGACAGAGT CCCCGATTCTGCTGCATCAACATAACTGTGGGCTGTGGGAATGATTTCAAGGAATCCACTATCCATACCCAGGGCTG CGTGGAGACTATAGCAATATGGCTAAGGAAGAACAATACTGCTGGTGGCTGCAGCGGCCCTGGGCATTGCTTTGTGGA GGTCTTGGGAATATCTTCTCCTGCTGTCTGGTGAAGTATCGAAGTGGCTATGAGTATGAGGTTGGGGCGGTTGT CTTTCATGATGATCTCAGTTTCAATTAACGATATTTCAAC	Mus musculus Cd63 antigen, mRNA (cDNA clone MGC:7123 IMAGE:3157993)	BC008108.1	1386	0	878
L2T-266	GAGTTCCGGCACGAGGGTCTGTTTCTCACTACCACACCAAAATCACTAGAGTACACTGGTTCAGAGAGCAGAA TCATGTTGGCCTTGGCTAAATTCAAAATGCTGTCTTTACTTTGGTATATGTTGAGGGCTTTTCATAATTTAAAGTGTGT TCTGTTAGCAAGGCAAAAATATGAGTCTTAATTTCTACAGGCAAAAATATGCAAAGGAGCCAAAACGTAAACCCAGCA TTTGGGATGGTGAAGACTGGAAGCTAATCCTCATTGNATTCACAAAGTCNNTTATNCAANNTCNGGACAT	Mus musculus CD24a antigen (Cd24a), mRNA	NM_009846	478	e-132	1800
L2T-267	GAGTTCCGGCACGAGGGTCTGTTTCTCACTACCACACCAAAATCACTAGAGTACACTGGTTCAGAGAGCAGAA TCATGTTGGCCTTGGCTNATTTCAAATGCTGNCTTTACTGGGGTATATGTNGAGGGCTTTTCATAANNTAAANTGTG TTCTGTTNGCNAGGCAAAAATNTGAGTCTTAATNCTACACGCNAAATATGCAAAGGAGNCGAAACTGTAAACCCAAAC ATTTCCGATCTTCAAGTACTGCAANCTAATCTCATGCAATTCNCAAGTCTTGC	Mus musculus CD24a antigen (Cd24a), mRNA	NM_009846	281	0	1800

HC17	TATCAAANGAATTCGGCACTAGGCCCGCTTGGTCCGCAGGGNTCATGTCTCCCTCCCACTATGGGCCCTCCGAGCTT CCANTTNCATGTTCCAGCCTTTCTTGGNGATGATCCACCAGGCTCAACAGGCCATGGATGTCAGCTCCACAGCCCA GCCTTCCAGTTCACAGCTGGATTCTTAAGAGAAGGTGAAGATGACCGCACTGTGTGCAAGGAGATCCGCCGCAA CTCCACAGGATGCCTGAAGATGAAGGGCCAGTGTGAAAAGTGCCAGGAGATCTCGTCTGTGGACTGTTCAACCAACA ATCCTGCCAGGCTAACCTGCGCCAGGAGCTGAACGACTCGCTCCAGGTGGCCGAGAGGCTGACAGAGCAGTACAA GGAGCTGCTCAGTCTCCAGTCGAAGATGCTCAACACCTCATCCTGCTGGAGCAGCTGAACGACCAGTTCAACT GGGTGTCAGCTGGCTAACCTCACACAGGGCGAAGACAAGTACTACCTTCGGGTCTCCACCCTGACCACCCATTCT CTGACTCANAGGTCCTCCCTCCCGTGTCACTTGAAGTGGTGGTGAACCTGTTTGACTCTGAACCCATCACAGTGGTG TTACCANAAAAAGTCTTAAGGATAACCCTAAGTTTATGGACACAGNGGGGGAAAAGNGCTNAAGGAATACCCAG GAAAGCCNGNCGGAATGAGATAAAAAACNTNCCTCTATATTTAGGANTGCTGGGAGGGAATCCCNCTCCCCAG GGGGGTGCNACCCCNAAAACCCATTTTTAGGGGANTGGCCACCAAANGCNGCCTTCNCNGGNTTGTAAAAAT CCNCTGNGCCCNNGGAAANNNTNCCNCCANNANCCAAAAACCCNGNAAAAGGAAAAAAAAAAAAAAAA	Mus musculus sulfated glycoprotein-2 isoform 2 mRNA	AF248058	1070	0	1374
L2T-124	GCGCCACACCGGATCNCNCTTCCNACTAGNTCGGNACGAGGAATATATCCCCATCCCCCACACAGTTTAAA TATATATTTGGTGAAGCTGTGGTACACATTAAATGTTTCAAATGCAATCTAAGATGCAATAAATAGAGTACCTTGA TAGTTTGAAGGAATCTCANNTCTTGCAGCTGTGTTTGAAGGTGAATTAAGCAATATTTTCAAACGTGGATTTAG CTATCCATTGCTCTGAAGAGTCTTTTCAATGTTTCAAAGATGTGCTTTGTGCTGAAGATTGTGTGCCGTTCTCT GTGCTTCCAACTATCACTGAAGTCTTCTACCTGATTGATCTGCCAAGGATTATAGTTTGCCTTAACTTCAGAGTATTTT ATCTTCCATTTTATTTAATTTGNTCTTTTCTTTTCTTCAAGATAATGTTTANATATGNTATTGGGGAAAAACNCTAN ATTTCTGTCAAAAAAATGAATGTTACTGGAATTCAAGTAANCAACTCTCCATTGAATATCAACTGGGGGATATACTT ATTANAATGTATGCTCANAAAGATGGTTCTGGTTAAATATATGAAGTTACCATTACTGAATNCTAATATGGATTAAAA GCTCCNCTAATATTTTAAAAAAAAAAAAAAAAAAAA	Mus musculus 12 days embryo embryonic body between diaphragm region and neck cDNA, RIKEN full-length enriched library, clone:9430025L12 product:cullin 3, full insert sequence	AK034695	640	0	1152
M-38	GAGGCTCTTCTGCGCCCTGCCTGCCTGCCTGCCTGCCTGCCTGTGCCCAGAGTTCACAGCATCATGAGGCCTGGA TCTTCTTCTCCTTGGCTGGCCGGGAGGGCCCTGGCAGCCCTCAGCAGACTGAAGTGTGCTGAGGAGATAGTGA GGAGGAAACCGTGGTGGAGGAGACAGGGGTACCTGTGGGTGCCAACCCAGTCCAGGTGGAATGGGAGAAATTTGA GGACGGTGCAGAGGAAACGGTGCAGGAGGTGGTGGCTGACAACCCCTGCCAAGCCATCTTGCAAACATGGCAAG GTGTGTGAGCTGGACGAGCAACACCCCATGTGTGTGCCAGGACCCACCAGCTGCCCTGCTCCATTGGCG AGTTTGAGAAGGTATGCAGCAATGACAACAAGACCTTCGACTTCTTCCGCACTTCTTGGCACCAGTGCACCCCTGC AGGGCACCAAGAAGGGCCACAAGCTCCACCTGGACTACATCGGACCATGCAAAATACATCGCCCTGCCTGGATTCC	Mus musculus secreted acidic cysteine rich glycoprotein (Sparc),	NM_009242	1007	0	2079
L2T-14	TGAGCGCTGGACGGCAGCCTAAGTGAGCATCATTTGTGAGAATTTTGTAGTCAAGTGTGTTGAACAATTATTGTTTT CTAAGCTTCATGTTGACTTCTCTGATGCGTAGAAAAAGTGTCTAAGCTGGCTGAGGTTAAGCCGCTGTCACTACTGAA ATGCTAAGAATTTTCTCTTTTCCCGTAGTGTAGAGGGTAGGGTGTGGGCAGAAGCCGTGTAGCACATCTGTAGTA TTGTGTGTATGCTTAGAACAGCGTAGACCGGATGGGAGGATGGACTAGGCCAATCCCTCCCACTGGTGGATG TGAAGAGGTCAAGTAGGAAGGCACAGGAGGGTCAACACTGTACAGCAGTGCATGCAGACATCTAGGAGAAGAC ATGGCAGTGTCTTCTCAGTGTCTTCCCTTAACTGAGCTCTGCTCACAGACAGCTAGAATAGATTTTAACTGAAAC AGAAACCTAAATGAATTAACCTGGTCTTCCCTTGGTAAGCAGACTTAAATATCTGTATAGTACATGCAAGTGGAA AATTTGGGAATGCGTGTCTGTAATACATACCGGAAGGGCTACTATTACCTTTTTCTTACCATTATACTTACCTAATGG AAACGAGCTTGTTTTAACTATCAGAACAATTTTTGTAAGGTGCTGCAAAGACAGTTGAAGTTTTTATTACCAATCCCC AATAAACAGGTGTTCAAAGGGGGCCGGTACCAATTCCGCTATAGT	Mus musculus, p53 apoptosis effector related to Pmp22, clone MGC:18961 IMAGE:3985702	BC021772.1	1354	0	1849
L2T-260	CTGGGACGCACNAGGGCCATCGGCTGCAGGAACCTATCAGNGAGACTCTGGATGCTTATGTCATCAACTGGCCCTG GTTACGCTGGTCTGGAGGAGGACGGCACCTGGTGGAGNACAGGAGATTTCTTCAGACCTTAAGGGACAACACG CATTTTCATGATCTTGGAAAAGGACAGAATGGACACCGGGTAGTAAGTATGTCCAGTCTGCAAGCAACCAAGAAA TCGGGAATAGCCAGAGTCACTTCCGACCTATACAGGCTGAACCCCAAGGACTTCTCGGCTGTCTCAATGTCAAAGC CAGGATGTACGAGATGACTCGGTGCTTACGACATCCGATGCACAAGCTTCAAGGCCGTGTTAAGGAATCTGCTGA GGTTTATGCTTATGCTGCACAGATGACGGGACAGTTCCTGGTCTATCGGGGCACATACATGCTCCGAGTACTGGCC GATACAGAAGAGCAGCCATCCCCAAGCCTAGCACCAAGGCTGGTTCATGTAACAGGGCCACAGCTACAGAGGCC CAGGGACCCTGCTCTCTGTTATAGGCTGTGGGATGCCAGGGGAAGGAATGGGGCTTGGGGTGGTACCAGTGC AGGGCTGAGTAGCAGGATCTGCAAGGAAGCGGCAGAGGGCTTTAAGCGCTTAGGAANGGATCAACAGCGAG TGTGTGGAACTGCTGGATACAATCAGTCTTGGATCCTTACTACTGGATAAACAGTCCCTG	Mus musculus cell death-inducing DNA fragmentation factor, alpha subunit-like effector A (Cidea)	NM_007702.1	1166	0	1114

L2T-265	CTATCAGAGCGTTTCGGCACCAGGAGGNCCTGGGAAGACNAACACCCCTGGGAAGCCAGGGNTAGGAAGATGGTCTC CAAAACANGGTGAGCAGCACCCCTGAGGAAACATCTGACATTGACTGACTTCTGGNGTCCATCACAGGTGCACCCACG ANACACCCACACACAACGTGCNCACAACTAGAAATGTGCATTCAATTCACCCTGTCTGGGAACAGATTGGATTGGA CNAAAACTTATCNGNTNTTATGATTTGNAATTGANNTAAATTGGACATCANGAAANCACTGGGTNTGANCNCATTAAG TNNGGGNCCTTNGNNTNCNTNATAAGTTNCANCNGNCNCNGNAAGGGAACCTCNCNGNTCTAANAATCNTTCTTAT GGNACTGGTCTNTGNTTGGNCCTAAACNTGGCANAATAANAANTGNNTATTTGAACNGGGGTACACACAGGANTCC NGTGTNGANACAGGGANTCTGTGTTCCNTTGGATGNGAGCCGGGAATGAACNTANAAGGNAANNTGTTAATCCCC CNAAAAATGTGGNTGTGTGCNAAACCCACTCTGTGTTGNTAAGAAATGTGTTTTGAACCGANTTATTTCCAANCCA	Mus musculus transforming growth factor, beta receptor II (Tgfr2), transcript variant 1, mRNA	NM_009371	488	e-135	4702
L2T-158	CGNCACGAGGCTNANTTNGNCNTTGGAGANAATGNCAAGAAGNGGGNCCGACTGACGAGAAGGTGGAACGGGTG CGCAGAGCCACCTGAATGATCTTGAAAACATCGTTCCCTTTCTCGGGTNGGCCTCCTGTACTCCCTGAGTGGACC ACATCTCTCAGAGCCCTCATGCATTCAGAATCTTTGTAGGTGCTCGGATCTACCACACCACTTCTACTTACTGACTCCC CTTCTCAGCCAAACAGGGGCTGGCATTTTTTGTGGCTATGGAGTTACTTTGTCAATGGCTTACAGGCTGCTAAGG AGCAGACTGTACTTGTAAAGAGAATTGTGATCTTACCCTTCTAATTGATTCTTTTAAAAAAGAATTCTATATTTTTCAG TGGATCANACTTTCTGAGGTTTTAATGCGTGAAGGAGCAGAGAATAGGAATCAGGGAAAATTCAGTTAAAAGA CTAGCATCAGTAGGCTCTATCTTTGTATTTGGGTTAGAAATTTAATAATAATCAGCCTTAACTATGTTGTCTANCTCCT AAAGTACTTTGTTATAAAGCTTGTATTCATCATAATTTGTTACATTTGTCTATTTCTACGGTGCATCTATAAAGAGT GCACACNCCTATGGGAAACCTAGGTTCAATTATAGCTGAAGTAGACACCTGAATTTACAACATTACAATGAAAAA AAAAA	Mus musculus adult male cerebellum cDNA, RIKEN full-length enriched library, clone: 150002K10 product: microsomal glutathione S-transferase 1	AK005122.1	1098	0	944
L2T-147	TCGANCACTTGATCACTAGNTTCTAGAGGGNTTCGGCACCAGGGCAGCATGTGAAAGCTAAAACAAGTAGCCCTCTA GTCATTTCTTTTCCAGCCAGATAAAAAGGAGCTTCAATATATGTGACTTGATTTTTTACTTCACTCAGCTGAGCTG CTGTTTCTTCTCATGTAATATTGTACTGGTGTGTATAGAAGAAGCTGGTAAGAGTGCCTCTTCATAAATAAGCA ATTGCAGTGTGTCATGCAAAATTAATAAATTTAAATTTGCCTGATTCTATTTTGAATAAGGAGAAACAATCTTTCTAA GCAGTATGGAGGAAGACTAGTGCCTTGTGCATTTTGGTATATTTGAGTTCATGTTCCACAATGTCAATCCCTTGACA CAGTTGGGTTTCTCATAAGTATCCTAGTTCATGTACATCCGAATGCTAACTAATACTGTGTTAAGTTTCGTGTTGCAAG	Mus musculus myotrophin (Mtpn)	NM_008098.1	852	0	3863
B2 529	GGACCTNACGAGGTGGACNCGAAGCAGATAAGGAAGTCNGTGATGATGAGGCTGAAGAAAAGGAAGAGAAGAGG AAGAAAAGAAATNAGAAGAAAAGGAGTCTGATGATAACNTGAAATAGAAGATGTTGGCTCTGATGAAGAAGAGGAG GAGAAGAAGGATGGTGACAAGAAGAAAAGAAAGATAAAGGAAAAGTACATTGATCAAGAAGAACTCAACAAAAACA AAGCCGATTTGGACGAGAAATCCTGATGACATCACTAATGAGGAATAGGAGATTTCAACAAGAGCTTAACTAACGAT TGGGAAGAACACTTGGCAGTAAAGCATTCTGTTGAAGGACAATTAGAATTCGGGGCCCTCTTTTTGTCCCAAGAC GCCTCCTTTGATCTGTTTGAACAGAAAAGAAAAGAACACATCAAGTTGTATGTTCCGAGAGTTTTATCATGGA TAACTGTGAGGAATTAATCCCTGAGTATCTGAAATTTCAATAGAGGGGTAGTGGATTCTGAGGATCTCCCTCAAATATT TCCCGTGAATGCTGCAACAAAGTAAAATTCTGAAAGTTATCAGAAAAGAAATTTGGTCAAGAAATGCTTAGAATATTTA CTGAAGTAGCAGAAGATAAAGAGAAGTCAAAAAAGTTTTATGAGCAGTTCTCAAAAAATATAAAGCTTGGAAATTCACGA GGACTCTCAGAATCGGAAGAAGCTTTCAGAGCTGTGCGGTAATCACTGCTCTGGGACAGATGGTTCTCTGAGGA CTCTGTACAGATGANGAACCAAACCTCTTTTATCCAGNNGACAGGACGGGTGNTCTN	Mus musculus heat shock protein 1, alpha, mRNA (cDNA clone IMAGE:6816250)	BC049124.1	1096	0	2869
L2T-32	GTGGNACGAGGCCAGTACTCGCCCTGTTTTCAGTGGCTGGGTGTCTGCTGCGCACCATGGCCGCAAAAGGAAAA GTGGGTACCAGAGGGAAGAAACAGATATTTGAAGAGAACAAGAACTCTCAAGTTTTACCTCCGGATCATACTGGGA GCCAACGCCATCTACTGCCTTGTAACTTGGTCTTCTTCTATTCTCTGCCTCATTCTGGGCTGGATGGCCCTGGGC TTTAGCTTGGCCGTGACGGGGCCAGCTACCACCTCTATGAGCTCGATGGCTCGGGCATCTCTCTGAGGATGGGTC CTTGATGGATGGTGGCATGGACCTCAACATGGAGCAGGGCATGGCAGAGCACCTTAAGGATGTGATCCTACTGACAC CCATTGTTCAAGTGTCACTGCTTCTCCCTCTACATCTGGTCTTCTGGCTTCTGGCTCCAGGCGGGGCCCTTTACC TTTTGTGGTAACAGTGTGGGCCCTGGTTACAGCAGACAGTGGAGCCCTGCACCANAGCTCAATGAGAAACGA CNACGCCGACAGGAGCGGNGGACAGATGAAAAGGTTATANCATCCTTAACTGAGGCTGTAGGCTGCTGCGCACTGNT TGGCTCTGTTATGCTGCNTGGCCCATGCCTGGGCACTGAGGGACTAGTTNAGGGCCAAANCACTGGATTATANG	Mus musculus RIKEN cDNA 1700006C06 gene (1700006C06Rik) Homologue to HSPC171	NM_025486.1	1273	0	757
13						

Reproduced with permission of the copyright owner. Further reproduction prohibited without permission.

## Appendix B - RECIPES

### *Antibody Buffer*

	(10X)	(10X)
NaCl	81.8 g	8.1 g
Tris-base	12.1 g	1.2 g
Tween 20	3 ml	0.3 ml
ddH <sub>2</sub> O	to 1 liter	to 100 ml

pH to 7.4 with HCl

Dilute 10X antibody buffer and add skim milk powder to 1% final concentration before use.

### *Blocking Buffer for westerns*

TBS (Tris-buffered saline).....	200 ml
NP-40 detergent .....	100 $\mu$ l
Skim milk powder    10 g	

### *Coomassie Blue Staining Solution*

0.1 % Coomassie R-250.....	0.5 gm
40% Methanol.....	200 ml
10% acetic acid .....	50 ml
ddH <sub>2</sub> O.....	250 ml
total volume .....	500 ml

### *Coomassie Blue Destaining Solution*

40% methanol .....	400 ml
10% acetic acid .....	100 ml
ddH <sub>2</sub> O.....	500 ml
total volume .....	1000 ml

**LB – 1 L**

tryptone (1%) .....10 g

yeast extract (0.5%) .....5 g

NaCl (1%) .....10 g

Shake until the solutes have dissolved. Adjust the pH to 7.0 with 5 N NaOH.

Adjust the volume of the solution to 1 L with water.

for plates add agar (1.5 %).....15 g

Sterilize by autoclaving for 20 min on liquid cycle.

For LB-AMP add ampicillin solution to 100 mg/L after autoclaving and cooling.

For LB-AMP-X-gal-IPTG add ampicillin solution to 100 mg/L, X-gal dissolved in N,N-dimethylformamide (20 mg/ml stock) to 40 mg/L, IPTG (0.2 g/ml stock) to 0.5 mM.

**NZY – 1 L**

NaCl (0.5%) .....5 g

yeast extract (0.5%) .....5 g

MgSO<sub>4</sub>·7H<sub>2</sub>O (0.2%) .....2 g

NZ amine (casein hydrolysate) (1%) .....10 g

Shake until the solutes have dissolved.

Adjust the pH to 7.5 with 5 N NaOH.

Adjust the volume of the solution to 1 L with water.

For plates add agar (1.5 %).....15 g

For top agarose add agarose (0.7%).....7 g

Sterilize by autoclaving for 20 min on liquid cycle

**Phosphate Buffered Saline (PBS)-10X**

NaCl.....80g

KCl.....2g

Na<sub>2</sub>HPO<sub>4</sub>.....14.4gKH<sub>2</sub> PO<sub>4</sub>.....2.2gDissolve in 800ml ddH<sub>2</sub>O and pH to 7.4 with HCl.

Top up volume to 1L

**10X PCR buffer – 100 ml**

1 M KCl .....	50 ml
1 M Tris buffer (pH 8.3) .....	20 ml
1 M MgCl <sub>2</sub> .....	5 ml
2% gelatin .....	5 ml
sterile deionized water .....	20 ml

**5X Protein Loading Buffer – 10 ml**

1 M Tris buffer (pH 6.8) .....	3.5 ml
glycerol .....	3 ml
SDS .....	1 g
Dithiothreitol (DTT) .....	0.93 g
Bromophenol blue.....	1.2 mg

Add water to 10 ml.

**Protein Gel Running Buffer [5X] pH 8.3**

Tris Base .....	15 g
Glycine.....	72 g
SDS .....	5 g
ddH <sub>2</sub> O .....	to 1 liter

Check pH, should be around 8.3-8.6

*Make two litres of 1X running buffer at a time.*

*For [1X] running buffer : mix 200 ml [5X] buffer with 800 ml ddH<sub>2</sub>O*

**[2X] sample loading buffer (Laemelli buffer)**

<u>stock</u>	<u>volume needed in master mix</u>
ddH <sub>2</sub> O	10 ml
0.5 M Tris pH 6.8	2.5 ml
Glycerol	2.0 ml
10% SDS (10 g SDS/100ml ddH <sub>2</sub> O)	4.0 ml
1.0% bromophenol blue (1 g bromophenol blue/100 ml ddH <sub>2</sub> O)	0.5 ml
β-mercaptoethanol (add this just prior to use)	1.0 ml
Total volume	20 ml

**SM buffer – 1 L**

NaCl .....5.8 g  
 MgSO<sub>4</sub>-7H<sub>2</sub>O .....2 g  
 1 M Tris buffer (pH 7.5) ..... 50 ml

add water to 1 L

**10% Separating Gel (0.375 M Tris, pH 8.8) (40 ml)**

for protein gels

<u>Solution</u>	<u>stock solns</u>	<u>amt required</u>
ddH <sub>2</sub> O		16.0 ml
1.5M Tris-HCl pH 8.8	90.83 g/500ml ddH <sub>2</sub> O titrate with HCl	10.0 ml
20% SDS	20g/100ml ddH <sub>2</sub> O	0.2 ml
acrylamide/ <i>bis</i> -acrylamide	30% / 0.8% w/v	13.2 ml
Total volume		~40 ml

**4% Stacking Gel (0.125 M Tris, pH 6.8) (30 ml)**

for protein gels

<u>Solution</u>	<u>stock solns</u>	<u>amt required</u>
ddH <sub>2</sub> O		
18.3 ml		
0.5M Tris-HCl, pH 6.8	30.28g/500ml ddH <sub>2</sub> O, titrate with HCl	7.5 ml
20% SDS		0.15 ml
acrylamide/ <i>bis</i> -acrylamide	(30%/0.8% w/v)	4.02 ml
Total volume		~30 ml

**20X SSC – 1 L**

NaCl .....175.3 g  
 Na<sub>3</sub>Citrate.....88.2 g

Add water to 800 ml.

Adjust pH to 7.0 with a few drops 10 N NaOH.

Add water to 1 L.

***TBE – 1 L (5X solution)***

Tris base.....54 g  
Boric acid.....27.5 g  
0.5 M EDTA, pH 8.0 .....20 ml

Add water to 1 L.  
Working concentration = 0.5X

***Transfer buffer for westerns***

Tris-Base.....6.06 g  
glycine.....28.8 g  
methanol..... 400 ml  
water..... 1400 ml

pH to 8.1-8.4. Add water to 2 L. Store at 4°C.  
For a single transfer box you should make 2 litres